



**Fakultät für Medizin
Institut für Virologie**



Development of a thermostable, therapeutic vaccine against chronic hepatitis B

Julia Sacherl

Vollständiger Abdruck der von der Fakultät für Medizin der Technischen Universität München zur Erlangung des akademischen Grades eines

Doktors der Naturwissenschaften (Dr. rer. nat.)

genehmigten Dissertation.

Vorsitzender: Prof. Dr. Jürgen Ruland

Prüfende(r) der Dissertation:

1. Prof. Dr. Ulrike Protzer
2. Prof. Dr. Jörg Durner

Die Dissertation wurde am 17.02.2021 bei der Technischen Universität München eingereicht und durch die Fakultät für Medizin am 13.07.2021 angenommen.

Table of contents

Abstract	1
Zusammenfassung	3
Abbreviations	5
1 Introduction	8
1.1 The hepatitis B virus	8
1.1.1 Classification of HBV	8
1.1.2 Structure of HBV particles.....	9
1.1.3 Pathogenesis of HBV infection	13
1.1.4 Prophylaxis and available treatment options for chronic hepatitis B.....	14
1.2 Therapeutic vaccination as a potential treatment option of chronic hepatitis B.....	15
1.2.1 Heterologous protein prime/MVA vector boost vaccination strategy.....	17
1.2.2 HBsAg and HBcAg as vaccine components	18
1.2.3 MVA as vaccine vector	18
1.3 Solving the cold chain problem	20
1.3.1 WHO recommendations	20
1.3.2 Various drying methods for pharmaceutical products.....	21
1.3.3 Stabilizing excipients	23
1.4 Aim of the study	25
2 Results	27
2.1 Characterization of vaccine components.....	27
2.1.1 Generation of MVA-S/C	27
2.1.2 Characterization of MVA-S/C.....	32
2.1.3 Comparison of antigens from different manufacturers.....	33
2.1.4 Optimal storage conditions for HBV antigens.....	37
2.2 Loss of antigen integrity and MVA-S/C infectivity after a storage at higher temperatures over time	38
2.3 Impact of lyophilization on vaccine components <i>in vitro</i>	40
2.3.1 MVA-S/C	41
2.3.2 Antigens	41
2.3.3 Impact of storage time after reconstitution on TherVacB vaccine.....	43
2.4 Selection of most suitable stabilization formulation	45

2.4.1	Initial selection of SAAF variants for stabilization of HBcAg	45
2.4.2	Selection of most suitable SAAF for stabilization of HBsAg	47
2.4.3	Selection of most suitable SAAF stabilizing the combination of HBcAg and HBsAg	51
2.4.4	Final selection of most suitable SAAF for TherVacB vaccine in HBV-naïve mice.....	53
2.5	Detailed analysis of vaccine components during storage at 25 °C or 40 °C <i>in vitro</i>	57
2.5.1	Successful achievement of WHO CTC guideline	57
2.5.2	Maintenance of antigen integrity and MVA-S/C infectivity after formulation with SAAF during storage at 25 °C and 40 °C up to 3 months.....	59
2.5.3	Preservation of antigen integrity and MVA-S/C infectivity after SAAF-stabilization during long-term storage at 25 °C for up to 12 months.....	64
2.5.4	SAAF improves integrity of single antigens despite exposure to 25 °C or 40 °C	67
2.6	SAAF-stabilized vaccine induces immune response in different hepatitis B mouse models.....	71
2.6.1	Stabilized and heat-exposed vaccine induces an immune response in HBV-naïve mice after 1 and 3 months of storage period	71
2.6.2	Stabilized and heat-exposed vaccine maintains efficacy in persistent HBV replication mouse model.....	75
2.6.3	One-year RT-exposed vaccine induces immune response in persistent HBV replication mouse model.....	79
2.7	TherVacB adjuvant, c-di-AMP, remains stable despite storage at higher temperatures.....	84
3	Discussion.....	86
3.1	Effective stabilization of TherVacB vaccine components <i>in vitro</i>	86
3.2	Influence of lyophilization on vaccine components.....	90
3.3	Efficacy of SAAF-stabilized vaccine <i>in vivo</i>	92
3.4	Future perspectives of thermostable TherVacB and implications for other vaccines	98
3.5	Summary and conclusion.....	99
4	Materials and Methods.....	100
4.1	Materials	100
4.1.1	Antigens	100
4.1.2	Viral vectors.....	100
4.1.3	Cell lines and bacterial strains	100

4.1.4	Primers	101
4.1.5	Antibodies.....	101
4.1.6	Peptides	103
4.1.7	Enzymes.....	104
4.1.8	Plasmids and Markers	104
4.1.9	Kits	104
4.1.10	Mouse strains	105
4.1.11	Cell culture media	105
4.1.12	Buffers and solutions	105
4.1.13	Chemicals and reagents	107
4.1.14	Consumables.....	109
4.1.15	Laboratory equipment.....	110
4.1.16	Software	112
4.2	Methods.....	113
4.2.1	Cell culture	113
4.2.2	Generation of MVA-S/C	113
4.2.3	Amplification of MVA-S/C.....	113
4.2.4	Determination of MVA-S/C titer by TCID ₅₀	114
4.2.5	Determination of MVA-S/C titer by plaque assay	115
4.2.6	Infection assay.....	115
4.2.7	HBeAg and HBsAg measurements of <i>in vitro</i> samples	115
4.2.8	Purification of viral DNA.....	115
4.2.9	Polymerase chain reaction.....	116
4.2.10	Agarose gel electrophoresis	116
4.2.11	Sequencing	116
4.2.12	Determination of DNA, RNA or protein concentrations.....	116
4.2.13	Production of recombinant single-chain variable fragment C8	117
4.2.14	Production and purification of 5F9 antibody	117
4.2.15	Stabilization, lyophilization, temperature exposure and reconstitution.....	118
4.2.16	Sandwich enzyme linked immunosorbent assay	119
4.2.17	Native agarose gel electrophoresis.....	119
4.2.18	Transmission electron microscopy.....	120
4.2.19	Dynamic light scattering.....	120
4.2.20	Size exclusion-high performance liquid chromatography	120

4.2.21	Sodium dodecyl sulphate polyacrylamide gel electrophoresis and Western blot analysis	120
4.2.22	Determination of biological activity of c-di-AMP	121
4.2.23	Mouse experiments	121
4.2.23.1	Ethical statement.....	122
4.2.23.2	Mice and AAV-HBV transduction.....	122
4.2.23.3	Heterologous protein prime/MVA boost vaccination strategy.....	122
4.2.23.4	Blood withdrawal	122
4.2.23.5	Dissection and organ removal	122
4.2.23.6	Isolation of splenocytes	123
4.2.23.7	Isolation of liver associated lymphocytes.....	123
4.2.23.8	Intracellular cytokine staining	123
4.2.23.9	Serological analysis.....	124
4.2.24	Statistical analysis	124
5	Figures and Tables	125
5.1	Figures.....	125
5.2	Tables.....	126
6	References.....	128
7	Publications and Meetings	142
8	Acknowledgments	144

Abstract

With more than 257 million chronically infected people, hepatitis B virus (HBV) infection is one of the major challenges for global health. Despite the availability of a prophylactic vaccine, around 887 000 people die every year from HBV-associated liver diseases. Since current antiviral treatment options for chronic hepatitis B rarely cure HBV, new therapies are urgently needed. Therapeutic vaccination represents a promising approach, as it aims to induce HBV-specific B- and T-cell responses which enable the hosts' immune system to control the virus. Therefore, a heterologous protein prime/modified vaccinia virus Ankara (MVA) boost therapeutic vaccine, termed TherVacB, has recently been developed by our Institute. TherVacB proved to efficiently break HBV-specific immune tolerance in chronic hepatitis B mouse models. However, application of such a vaccine worldwide is a major challenge, as many vaccines require continuous cooling during transport and storage to maintain their efficacy. This is an important logistic and financial hurdle especially in areas with high outdoor temperatures. To prevent loss of vaccine efficacy due to environmental influences, the aim of this thesis was to develop a lyophilized, thermostable form of the TherVacB vaccine.

In the first set of experiments, a viral vector for TherVacB booster immunization, MVA-S/C, which simultaneously expresses HBV small surface (S) and core proteins, was generated. The vector showed the typical MVA morphology and grew at a speed similar to MVA wild-type. In addition, the most suitable manufacturers of HBV core antigen (HBcAg), Riga, and HBV surface antigen (HBsAg), Biovac, for TherVacB priming were selected. These two antigens demonstrated a remarkable purity and integrity during *in vitro* characterization experiments. However, significant loss of antigen integrity and MVA-S/C infectivity was observed after storage at higher temperatures (25 °C up to 40 °C), to some extent already after 24 h onwards, which substantiated the necessity of a cold chain to maintain TherVacB potency.

To achieve thermostability of TherVacB components, lyophilization after addition of stabilizing amino acid-based formulations (SAAF) from LEUKOCARE was performed. Out of approximately 50 formulations tested *in vitro*, one single SAAF proved to be efficient at stabilizing all three TherVacB components during lyophilization and subsequent storage at 40 °C/45 °C for up to 1 month and was therefore selected for detailed characterization *in vitro* and *in vivo*. Using single HBcAg and HBsAg during the lyophilization process, the SAAF-stabilization did not entirely protect the antigens from a loss of integrity. By combining the SAAF-formulated antigens, however, the negative effect of lyophilization was completely prevented.

A comprehensive *in vitro* analysis demonstrated very good thermostability of the SAAF-stabilized vaccine components which allowed to fulfill the WHO controlled temperature chain (CTC) requirements (exposure at 40 °C for 3 days). In addition, the SAAF-formulated and lyophilized vaccine maintained antigen integrity as well as MVA-S/C infectivity even after a temperature challenge for 3 months at 25 °C or 40 °C or 12 months at 25 °C. In contrast, non-stabilized vaccine components showed significant loss of vaccine integrity after heat-exposure at each time point examined.

Finally, first proof of concept experiments were performed in HBV-naïve mice and mice infected with adeno-associated virus vector carrying the HBV genome (AAV-HBV) representing chronic HBV infection. The results demonstrated that TherVacB formulated with SAAF was safe, well-tolerated and highly immunogenic. The SAAF-stabilized vaccine induced high-titer HBV-specific antibodies as well as strong HBV core- and HBV S-specific T-cell responses even when the vaccine components were exposed to 25 °C or 40 °C for 3 months. The non-stabilized vaccine, in contrast, failed to induce T-cell responses after stressing at the same conditions. Even after 12 months of storage at room temperature, the SAAF-stabilized therapeutic vaccine broke HBV-specific immune tolerance and was able to suppress HBV in AAV-HBV infected mice.

In conclusion, the results of this thesis demonstrate the successful generation of a highly functional, thermostable and immunogenic therapeutic vaccine against chronic hepatitis B. The excellent thermostability of TherVacB allows its transport and storage outside a continuous cold chain. These findings could be a major step towards global vaccine application in the near future, especially in countries with high outdoor temperatures.

Zusammenfassung

Mit mehr als 257 Millionen chronisch infizierter Menschen stellt die Hepatitis-B-Virus (HBV) Infektion eine der größten Herausforderungen für die globale Gesundheit dar. Trotz dem Vorhandensein eines prophylaktischen Impfstoffs, sterben jedes Jahr ca. 887 000 Menschen an HBV-assoziierten Lebererkrankungen. Da die derzeitigen antiviralen Behandlungsoptionen für chronische Hepatitis B das HBV nur selten heilen, werden neue Therapien dringend benötigt. Die therapeutische Impfung stellt einen vielversprechenden Ansatz dar, da sie darauf abzielt, HBV-spezifische B- und T-Zell-Antworten zu induzieren, die das Immunsystem des Wirts in die Lage versetzen, das Virus zu kontrollieren. Aus diesem Grund wurde an unserem Institut kürzlich ein heterologer therapeutischer Impfstoff mit einem Protein-Prime/modifiziertes Vaccinia Virus Ankara (MVA) Boost entwickelt, der TherVacB genannt wird. TherVacB hat bewiesen, dass er die HBV-spezifische Immuntoleranz in chronisch infizierten Mausmodellen effizient durchbrechen kann. Die weltweite Anwendung eines solchen Impfstoffs ist jedoch eine große Herausforderung, da viele Impfstoffe eine kontinuierliche Kühlung während des Transports und der Lagerung benötigen, um ihre Wirksamkeit aufrechtzuerhalten. Dies ist insbesondere in Gebieten mit hohen Außentemperaturen eine große logistische und finanzielle Hürde. Um den Verlust der Impfstoffwirksamkeit durch Umwelteinflüsse zu verhindern, war das Ziel dieser Dissertation eine lyophilisierte, thermostabile Form des TherVacB Impfstoffs zu entwickeln.

In der ersten Reihe von Experimenten wurde ein viraler Vektor, MVA-S/C, für die TherVacB Booster-Immunsierung generiert, der gleichzeitig das kleine Oberflächenprotein (S) und das Coreprotein von HBV exprimiert. Der Vektor zeigte die typische Morphologie des MVA und wuchs mit einer ähnlichen Geschwindigkeit wie der MVA-Wildtyp. Darüber hinaus wurden die am besten geeigneten Hersteller des HBV-Coreantigens (HBcAg), Riga, und des HBV-Oberflächenantigens (HBsAg), Biovac, für das TherVacB-Priming ausgewählt. Diese zwei Antigene zeigten während den *in vitro* Charakterisierungsexperimenten eine bemerkenswerte Reinheit und Integrität. Allerdings wurde ein signifikanter Verlust der Antigenintegrität und der Infektiosität des MVA-S/C nach einer Lagerung bei erhöhten Temperaturen (25 °C bis 40 °C) beobachtet, teilweise sogar bereits nach 24 h, was die Notwendigkeit einer Kühlkette zur Aufrechterhaltung der Wirksamkeit des TherVacB untermauert.

Um die Thermostabilität der TherVacB-Komponenten zu erreichen, wurde eine Lyophilisierung nach Zugabe von stabilisierenden Aminosäure-basierten Formulierungen (SAAFs) von LEUKOCARE durchgeführt. Von ca. 50 *in vitro* getesteten Formulierungen erwies sich eine einzige SAAF bei der Stabilisierung aller drei TherVacB-Komponenten, während der Lyophilisierung und der anschließenden Lagerung bei 40 °C/45 °C für bis zu 1 Monat als effizient und wurde daher für eine detaillierte Charakterisierung *in vitro* und *in vivo* ausgewählt. Bei der Verwendung von einzelnen HBcAg und HBsAg während des Lyophilisierungsprozesses, konnte die SAAF-Stabilisierung die Antigene nicht vollständig vor einem Integritätsverlust schützen. Durch die Kombination der SAAF-formulierten Antigene konnte jedoch der negative Effekt der Lyophilisierung vollständig verhindert werden.

Eine umfassende *in vitro*-Analyse zeigte eine sehr gute Thermostabilität der SAAF-stabilisierten Impfstoffkomponenten, die es ermöglichte die Anforderungen der kontrollierten Temperaturkette (CTC) der WHO zu erfüllen (Exposition bei 40 °C für 3 Tage). Darüber hinaus behielt der SAAF-formulierte und lyophilisierte Impfstoff die Antigenintegrität sowie die MVA-S/C-Infektiosität auch nach einer Temperaturbelastung von 3 Monaten bei 25 °C oder 40 °C oder 12 Monate bei 25 °C bei. Im Gegensatz dazu zeigten nicht stabilisierte Impfstoffkomponenten einen signifikanten Verlust der Impfstoffintegrität nach Hitze-Exposition zu jedem untersuchten Zeitpunkt.

Letztendlich wurden erste Experimente zum Nachweis der Wirksamkeit in HBV-naiven Mäusen und in Mäusen, die mit einem Adeno-assoziierten Virusvektor, der das HBV-Genom (AAV-HBV) trägt, infiziert waren und eine chronische HBV-Infektion repräsentieren, durchgeführt. Die Ergebnisse zeigten, dass der mit SAAF-formulierte TherVacB sicher, gut verträglich und hoch immunogen war. Der SAAF-stabilisierte Impfstoff induzierte hochtitrige HBV-spezifische Antikörper sowie eine starke HBV-Core- und HBV-S-spezifische T-Zell-Antwort selbst wenn die Impfstoffkomponenten 3 Monate lang bei 25 °C oder 40 °C gelagert wurden. Der nicht stabilisierte Impfstoff hingegen induzierte keine T-Zell-Antwort nach einer Stressung unter den gleichen Bedingungen. Selbst nach einer 12-monatigen Lagerung bei Raumtemperatur konnte der SAAF-stabilisierte therapeutische Impfstoff die HBV-spezifische Immuntoleranz brechen und war in der Lage, HBV in AAV-HBV-infizierten Mäusen zu unterdrücken.

Zusammenfassend zeigen die Ergebnisse dieser Dissertation die erfolgreiche Generierung eines hochfunktionalen, thermostabilen und immunogenen therapeutischen Impfstoffs gegen chronische Hepatitis B. Die ausgezeichnete Thermostabilität von TherVaB erlaubt dessen Transport und dessen Lagerung außerhalb einer kontinuierlichen Kühlkette. Diese Erkenntnisse könnten in naher Zukunft einen wesentlichen Schritt in Richtung einer weltweiten Impfstoffversorgung sein, insbesondere in Ländern mit hohen Außentemperaturen.

Abbreviations

°C	Degree Celsius
µg	microgram
µL	microliter
a.R.	after reconstitution
AAV	adeno-associated virus
ALT	alanine aminotransferase
anti-HBc	antibodies against hepatitis B virus core protein
anti-HBs	antibodies against hepatitis B virus surface protein
BHK-21	baby hamster kidney fibroblast 21
bp	base pair
cccDNA	covalently closed circular DNA
c-di-AMP	bis-(3',5')-cyclic dimeric adenosine monophosphate
CEF	chicken embryo fibroblast
CPE	cytophatic effect
CTC	controlled temperature chain
Ctrl	control
CV	column volume
CVA	Chorioallantois vaccinia virus Ankara
D (i 0.5)	mean size, where 50 % of all particles is smaller than the measured one
Del	deletion
DF-1	chicken fibroblast cell line
DLS	dynamic light scattering
DMEM	Dulbecco's Modified Eagle Medium
DNA	deoxyribonucleic acid
<i>E. coli</i>	<i>Escherichia coli</i>
e.g.	for example (Latin: <i>exempli gratia</i>)
ECTC	extended controlled temperature condition
ELISA	Enzyme linked immunosorbent assay
EMA	European Medicines Agency
EPI	Expanded Program on Immunization
ER	endoplasmatic reticulum
F1.1	stabilizing amino acid-based formulation 1.1
FACS	fluorescence-activated cell sorting
FasL	Fas ligand
FDA	Food and Drug Administration
g	gram
GMP	good manufacturing practise
GRAS	generally recognized as safe
h	hour
H ₂ O	water
HBc	hepatitis B virus core protein

HBcAg	hepatitis B virus core antigen
HBsAg	hepatitis B virus surface antigen
HBV	hepatitis B virus
HBx	hepatitis B virus x protein
Heb	HeberNasvac®
HEK	human embryonic kidney
HERMES	Highly Extensible Resource for Modelling Event-Driven Supply Chains
HIV	human immunodeficiency virus
HRP	horseradish peroxidase
HSV	herpes simplex virus
i.m.	intramuscular
i.p.	intraperitoneal
i.v.	intravenous
ICH	International Council for Harmonisation of Technical Requirements for Pharmaceuticals for Human Use
ICS	intracellular cytokine staining
IFN- α	interferon-alpha
IFN- γ	interferon-gamma
IgG	immunoglobulin G
IgM	immunoglobulin M
IRF	interferon regulatory factors
ISG	interferon stimulated genes
IU	international unit
kb	kilobase
kDa	kilodalton
KO	knockout
L	litre
L protein	large hepatitis B virus surface protein
LALs	liver associated lymphocytes
M	Molar
M protein	middle hepatitis B virus surface protein
mg	milligram
min	minutes
mL	millilitre
MOI	multiplicity of infection
mRNA	messenger RNA
MVA	Modified vaccinia virus Ankara
MVA-C	Modified vaccinia virus Ankara expressing HBV core protein
MVA-S	Modified vaccinia virus Ankara expressing HBV S protein
MVA-S/C	Modified vaccinia virus Ankara expressing HBV core and S protein
MVA-WT	MVA wild-type
NAGE	native agarose gel electrophoresis
ng	nanogram

NK	natural killer
nm	nanometer
ns	not significant
NTCP	sodium taurocholate cotransporting polypeptide
NUCs	nucleos(t)ide analogues
OD	optical density
ORF	overlapping open reading frame
P2A	porcine teschovirus-1 2A
PCR	polymerase chain reaction
PEG	polyethylene glycol
PFU	plaque forming units
pgDNA	pregenomic DNA
rcDNA	relaxed-circular DNA
RH	relative humidity
RNA	ribonucleic acid
RNase	ribonuclease
RPMI	Roswell Park Memorial Institute
RT	room temperature
S protein, HBs(S)	small hepatitis B virus surface protein
s.c.	subcutaneous
SAAF	stabilizing amino acid-based formulation
scFv	single chain variable fragment
SDS-PAGE	sodium dodecyl sulphate polyacrylamide gel electrophoresis
SE-HPLC	size exclusion-high performance liquid chromatography
SM _{Ctrl}	optimal stored vaccine components (without lyophilization or stabilization)
STING	stimulator of interferon genes
TCID ₅₀	median tissue culture infection dose
TEM	transmission electron microscopy
T _H cells	T helper cells
TherVacB	heterologous protein prime/MVA vector boost vaccine
TherVacB _{Ctrl}	TherVacB control (without lyophilization, stabilization and stressing)
TNF- α	tumor necrosis factor alpha
WB	Western blot
WHO	World Health Organization
WT	wild-type

1 Introduction

1.1 The hepatitis B virus

In 1966, an Australia-antigen-positive hepatitis was described the first time during studies on Australian aborigines [1]. Four years later, the hepatitis B virus (HBV) was characterized for the first time [2]. HBV infection causes hepatitis B, an inflammatory liver disease. Hepatitis B is one of the major health problems worldwide. Despite the availability of a prophylactic vaccine, around 887 000 people die every year from consequences of HBV-associated diseases like liver cirrhosis or hepatocellular carcinoma [3].

1.1.1 Classification of HBV

The human HBV belongs to the family of *Hepadnaviridae* and the genus of *Orthohepadnavirus*. The members of this family comprise small, envelope DNA viruses which show a narrow host range and share a liver-specific tropism [4]. As HBV replicates via an RNA intermediate, it belongs to the group of pararetroviruses [5].

Based on genome comparisons, nine different genotypes (A-I) of HBV have been identified [6], whereby genotype C is the most common one with 26 % of global chronic HBV infections, followed by genotype D (22 %), E (18 %), A (17 %), B (14 %) and F-I together with less than 2 % [7].

While HBV is spread all around the world, genotype B and C occur almost exclusively in Asia, whereas genotype E is most prevalent in Sub-Saharan Africa (Figure 1). Genotype D shows a broad, global distribution and exists in many parts of the world like Asia, Africa and Europe. Genotype A is mainly found in Sub-Saharan Africa and to a smaller extent in Asia. The other genotypes F-I appear in Latin America and East Asia [7]. Another potential genotype “J” was found in a single Japanese patient, but as further reports of human infections are lacking, it has not been accepted as a relevant genotype of HBV [8, 9].

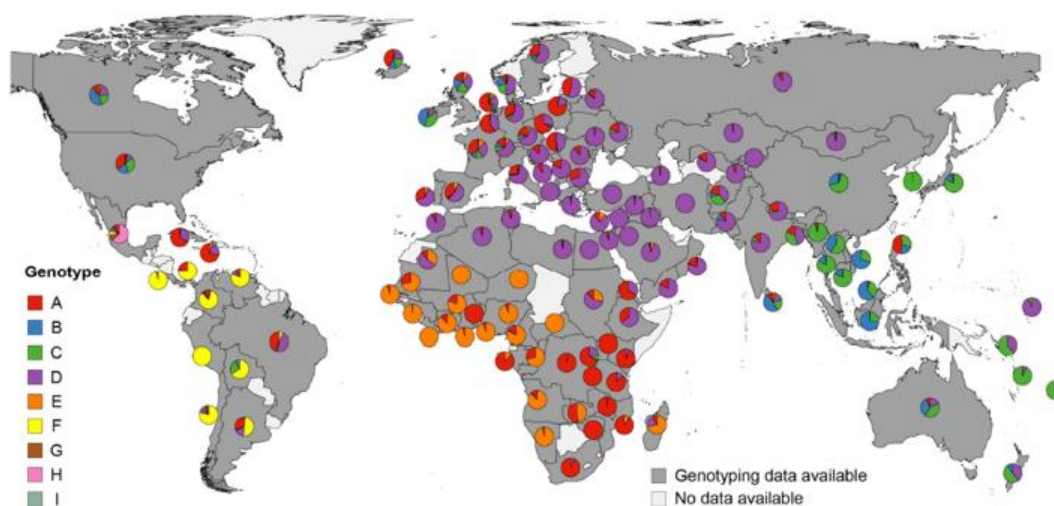


Figure 1. Global distribution of different HBV genotypes [7].

The genotypes differ from each other by more than 7.5 % of their nucleotide sequence [6]. Based on the variations of the small surface (S) protein epitopes, they can be further subdivided into nine subgenotypes with a nucleotide divergence greater than 4 %. Hereby, they can be summarized in four major serotypes: adw, adr, ayw and ayr [6].

1.1.2 Structure of HBV particles

The infectious virion of HBV, also called Dane particle, has a size of approximately 42 nm in diameter [10]. It consists of an envelope containing the three surface proteins of HBV S, middle (M) and large (L) embedded in a lipid layer and the icosahedral capsid. Inside of the capsid, the partially double-stranded, relaxed-circular DNA genome of HBV (rcDNA) and the viral polymerase are located.

Non-infectious subviral particles are secreted from infected cells and can be detected as HBV surface antigen (HBsAg) in patient blood [11]. They contain only the HBV surface proteins and therefore lacking capsid and rcDNA. HBsAg is the most important diagnostic marker for HBV infection. As shown in Figure 2, subviral particles can appear either as filamentous structures of varying sizes or as spherical structures with a size of 22 nm [12]. The spherical subviral particles are mostly composed of approximately one hundred S protein monomers and host derived lipids which are stabilized by extensive intermolecular disulfide cross-linking [13]. In addition to Dane particles and subviral particles, enveloped capsids without a rcDNA genome as well as putatively complete viral particles were observed in patient's sera [14-18]. The latter are very similar to Dane particles as the only difference is that their capsid encloses RNA instead of DNA. Typically, the serum of infected patients contains more subviral particles ($10^{14}/\text{mL}$) and empty virions ($10^{11}/\text{mL}$) than actual infectious HBV virions ($10^9/\text{mL}$) [5, 11, 17, 18]. RNA virions are detected at the lowest rate, with the concentration of $10^6/\text{mL}$ serum [14-16]. However, the quantities of these different particles can widely vary throughout the infection stages and between individual patients [5].

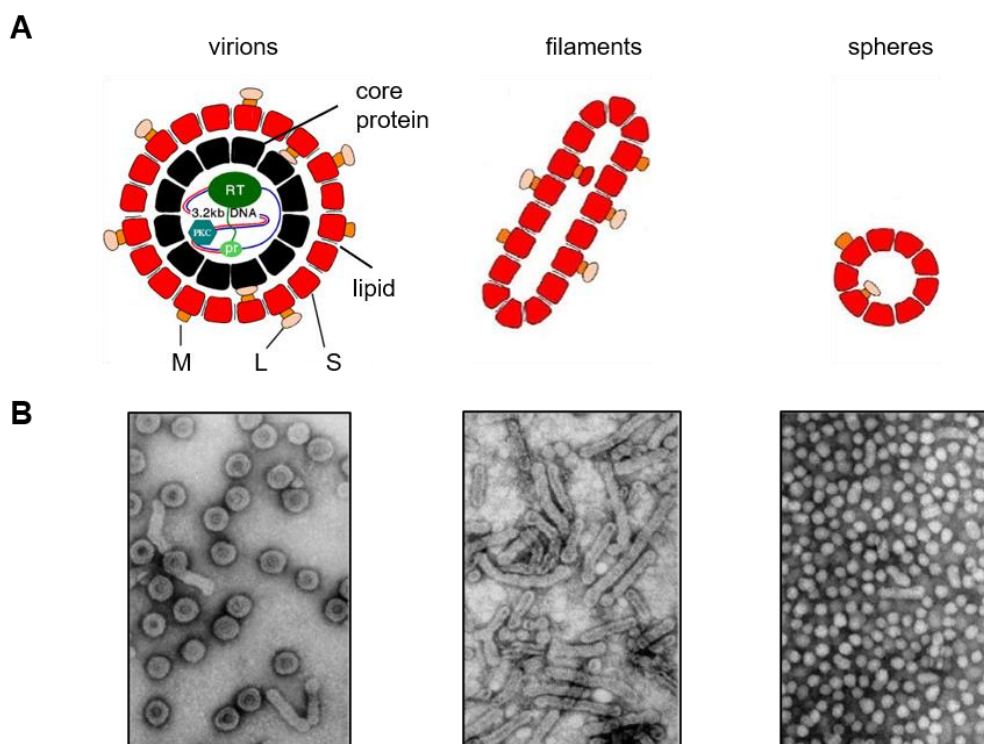


Figure 2. Virion and subviral particle structures of HBV.

(A) The envelope of the virion consists of small (S), middle (M) and large (L) surface protein, embedded in a lipid layer. It encloses the capsid, which consists of HBV core proteins and the relaxed-circular DNA (rcDNA) genome of HBV. The subviral particles of HBV appear as filaments or spheres which consist of HBV envelope proteins lacking the capsid. (B) Negative stained transmission electron microscopy pictures of Dane particles, filaments and spheres of HBV [12].

The HBV capsid is formed in the cytoplasm of infected cells through spontaneous self-assembly of 180 or 240 HBV core proteins depending on the triangulation number $T=3$ or $T=4$ of the capsid, respectively. To this purpose, the core monomers, which folding is stabilized by a hydrophobic core, combine to form dimers. The formation of a dimer with four helix bundles as the central component, results from the combination of two amphipathic α -helical hairpins. After exceeding a critical concentration of core dimers of approximately $0.8 \mu\text{M}$, the formation of trimers is initiated. The icosahedral structure is finally formed by the addition of further dimers [19-22]. As described, the assembly of the capsid proceeds spontaneously, however, it is supported by the presence of RNA, since the arginine-rich clusters located at the C-terminus of core protein interact with the RNA when the C-terminus is located on the inside of the capsid [21, 22]. Therefore, core proteins have the function of capsid assembly and additionally contain a nucleic acid binding domain that is crucial for packaging the pregenomic RNA (pgRNA) together with the viral polymerase.

The capsid encloses the partially double-stranded rcDNA genome of HBV which is about 3.5 kb long. The highly organized HBV genome encodes four partially overlapping open reading frames (ORFs), encoding seven structural and non-structural viral proteins, whereby each nucleotide has coding function: pre-surface-surface (preS-S), pre-core-core (preC-C), P and X (Figure 3).

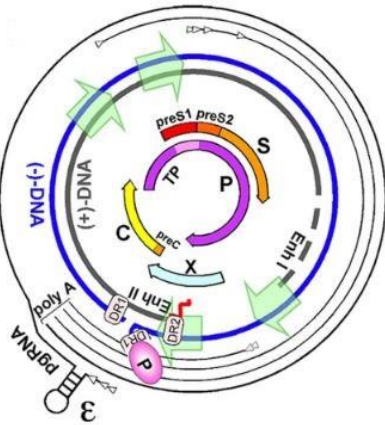


Figure 3. Genome organization of HBV.

The outer thin black lines display the viral transcripts with transcription starts shown in small white arrowheads. The encapsidation signal on pregenomic RNA (pgRNA) is defined by ϵ . Inner thicker circles (blue and grey) depict the full-length minus (-) strand and the incomplete plus (+) DNA strand. The innermost arrows represent the translated HBV proteins: envelope proteins (preS1, preS2, S), polymerase (P) protein, X protein, core (C) and pre-core protein (preC). Green arrows mark transcriptional enhancers Enh I/Enh II, direct repeats DR1/DR2 and the terminal protein domain of P protein TP [23].

The preS-S ORF encodes the three hepatitis B surface proteins forming the envelope of the HBV particle. These proteins share the same C-terminal domain but vary in the N-terminal domain due to different start codons for protein translation. The S protein consists of the C-terminal S-domain, the M protein in addition contains the preS2-domain and the L protein includes both, the preS1- and preS2-domains [24].

The viral polymerase encoded by P ORF functions as reverse transcriptase, RNaseH and as a terminal protein which serves as primer during synthesis of the rcDNA genome [24].

The preC-C ORF encodes for the HBV core and e protein, which encloses the core sequence with an additional N-terminal peptide (preC). HBV e protein is proteolytically processed and secreted as HBV e antigen (HBeAg).

HBeAg mediates humoral and cell-mediated immune evasion as the presence of HBeAg seems to elicit HBe/HBcAg-specific T-cell tolerance by the prevention of anti-HBc seroconversion [25-27]. As HBeAg is secreted from infected hepatocytes, it is used as a diagnostic marker of HBV infection. The loss of HBeAg is correlated with the clearance of acute infection [12, 28].

The smallest ORF, the X ORF, encodes the non-structural HBV X protein (HBx) which is essential for initiation and maintenance of HBV replication after infection indicating the oncogenic potential of HBV [29, 30]. In addition, HBx plays an important role in viral life cycle as it acts as a transcriptional activator, stimulates cytoplasmic signal transduction pathways and may influence the epigenetic mechanism of viral transcription [30, 31].

One crucial step within the HBV replication cycle is the formation of covalently closed circular DNA (cccDNA), the persistence form of HBV (Figure 4). HBV infects hepatocytes through unspecific and reversible binding to heparan sulfate proteoglycans [32], followed by specific binding to its functional receptor sodium taurocholate cotransporting polypeptide (NTCP) [33]. The cell entry of HBV occurs via clathrin-dependent endocytosis [34]. After uncoating and release of the capsid into the host cell cytoplasm, the capsids are translocated to the nuclear

membrane where the rcDNA genomes are released into the nucleus [35]. Inside, the rcDNA is converted to cccDNA by cellular enzymes and serves as a transcription template for all viral RNAs from which viral proteins are translated. The pgRNA is encapsidated together with HBV polymerase followed by reverse transcription to rcDNA [23, 24]. Mature, rcDNA-containing capsids are either recycled and transported back to the nucleus where rcDNA is again released into the nucleus or enveloped at the endoplasmic reticulum (ER) depending on the concentration of available envelope proteins [23, 24]. Enveloped virions and subviral filaments are secreted via multivesicular bodies whereas subviral spheres leave the cells via the ER and Golgi complex [36-38].

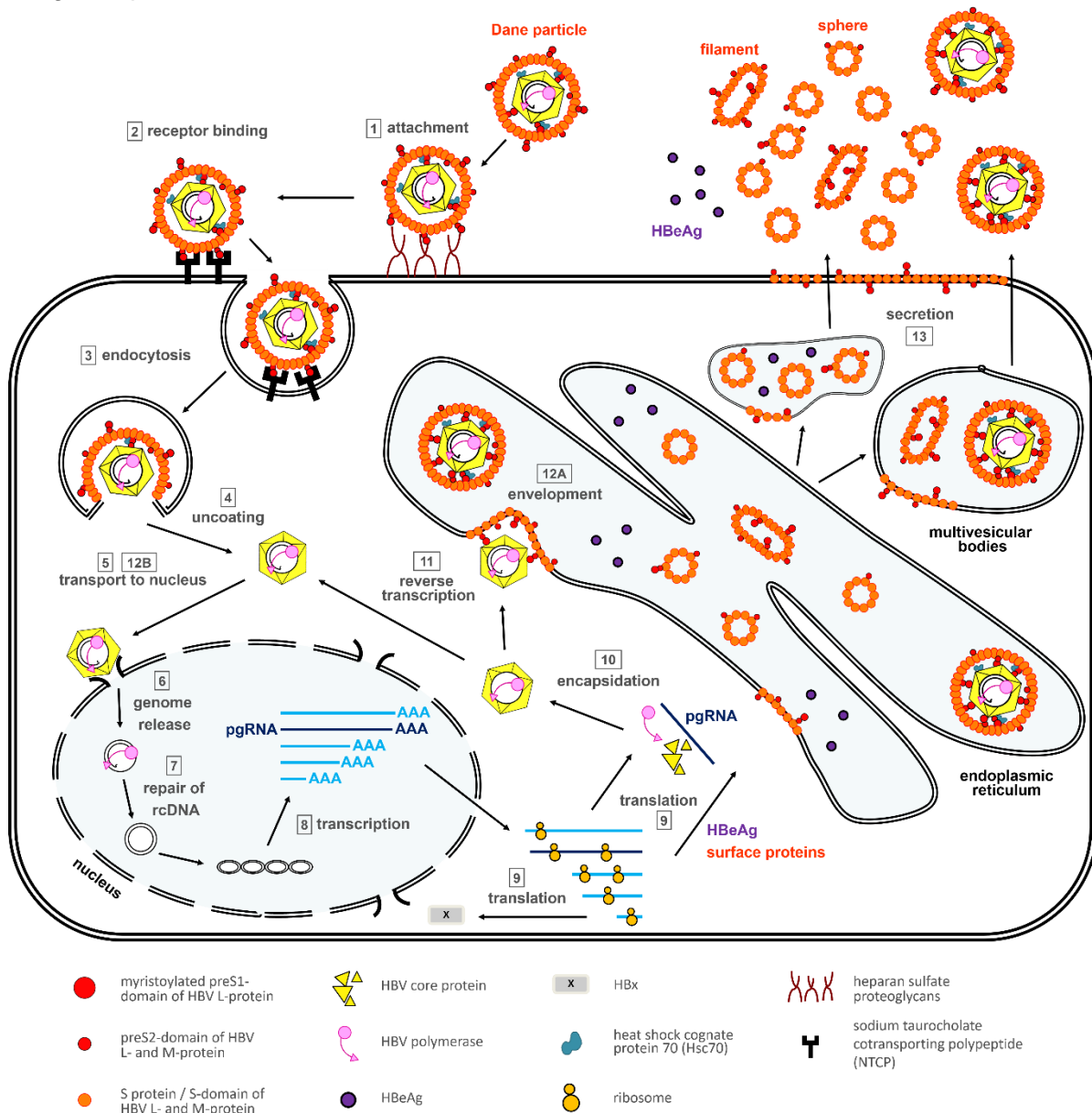


Figure 4. Schematic illustration of HBV life cycle.

(1) Unspecific and reversible attachment of HBV to heparan sulfate proteoglycans. (2) Specific binding to sodium taurocholate cotransporting polypeptide (NTCP). (3) Clathrin-dependent endocytosis of HBV. (4) Uncoating, (5) transport and (6) genome release into the nucleus. (7) Conversion of relaxed circular DNA (rcDNA) to covalently closed circular DNA (cccDNA). (8) Transcription of viral RNAs. (9) Translation of viral proteins. (10) Encapsidation and (11) reverse transcription of pregenomic RNA (pgRNA) to rcDNA. (12A) Envelopment of the capsid or (12B) recycling and transport to the nucleus. (13) Secretion of virions and subviral particles from the cell [39].

1.1.3 Pathogenesis of HBV infection

According to the World Health Organization (WHO), around 257 million people are chronically infected with HBV [3]. As shown in Figure 5, chronic HBV carriers are distributed all over the world. Nevertheless, very high frequencies of global HBV infections are reported in Eastern and Southeast Asia with 36.6 % and Sub-Saharan Africa with 32.3 % [7].

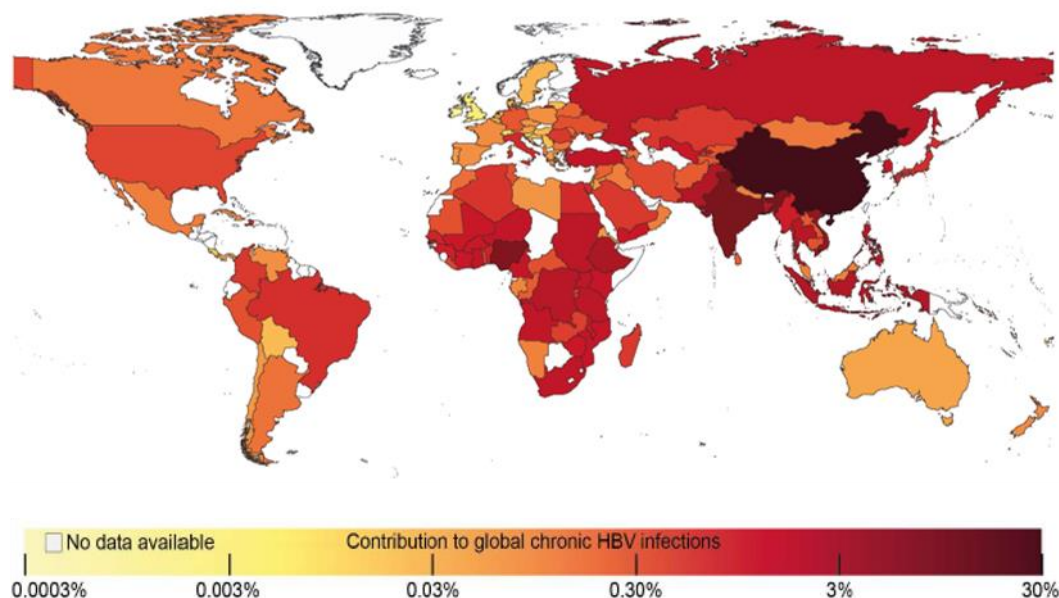


Figure 5. Distribution of global chronic HBV infections worldwide (6).

HBV transmission can occur parenteral through contact with infectious blood or blood products, unsterile needles or unprotected sex, as well as perinatal from an infected mother to her newborn child during birth [4].

The infection of HBV can be either acute and self-limiting or become chronic. Approximately 95 % of the adult patients can clear the infection and the disease often proceeds asymptotically. Nevertheless, 0.5-1 % of acutely infected patients die from fulminant hepatitis and liver failure [40, 41]. If the HBV infection occurs in the first six months of life, up to 90 % of the infected individuals develop chronic hepatitis B. Young children who get infected until the age of 3 years, as well as immunosuppressed individuals suffer from an increased risk (30-90 %) to develop a chronic course of the disease [40-42]. Most of the chronically infected patients die from consequences of HBV infection, like liver cirrhosis or hepatocellular carcinoma. As HBV is a non-cytopathic virus, HBV-related liver pathogenesis occurs mostly due to consequences of host immune response triggering inflammation and subsequent liver damage [43].

HBsAg, the first serological marker to diagnose primary HBV infection, appears in the blood of patients after an incubation period of 4-10 weeks. The infection is well established if HBsAg and high viral titers can be detected in patient's sera. A short time after HBsAg is detected, immunoglobulin M (IgM) antibodies against the HBV core protein (anti-HBc) become measurable in the sera of the patients [44]. They disappear around six months after infection, replaced by immunoglobulin G (IgG) antibodies against HBcAg which persist lifelong [44-46]. Circulating HBeAg becomes evident if 75-100 % of hepatocytes are infected. After the infection

is well established, an increase of alanine aminotransferase (ALT) levels can be observed in patient's blood indicating liver inflammation raise. First symptoms of the resolution of an HBV infection and the reduction of viral replication can be identified by the seroconversion of HBeAg to anti-HBe antibodies [44]. The recovery phase of the disease is also characterized by ALT normalization. After clearance of infection, HBsAg and HBeAg disappear, whereas neutralising antibodies against HBsAg (anti-HBs) become measurable which defines a self-limiting infection [28]. These antibodies mediate protective immunity against HBV reinfection.

In contrast to the acute infection, no anti-HBs antibodies and only in some chronic infected patients anti-HBe can be detected [28, 47]. Presence of HBsAg in blood for more than six months defines the chronic course of HBV infection [48]. In addition, circulating viral DNA can be measured for years. ALT and HBeAg levels increase at the early phase of the disease, normalize later and may become detectable during the flare-ups [28, 49].

The adaptive immune system plays an important role in the control of HBV infection. Hereby, the main cell types are lymphocytes. B lymphocytes, also called B cells, are responsible for the humoral immune response targeting extracellular antigens, while T lymphocytes, or T cells, cause cell-mediated immunity against intracellular antigens. The main populations of T cells are CD8⁺ T cells and CD4⁺ T cells. CD8⁺ T cells migrate through the body to find and eliminate cells that express foreign antigens. CD4⁺ T cells, also called T helper (T_H) cells, usually have a supportive function as they initiate and enhance the function of CD8⁺ T cells, B cells and the innate immune system by the secretion of cytokines [50].

The HBV-specific B- and T-cell responses determine the outcome of HBV infection. Acute self-limiting HBV-infection is characterized by a strong antibody and effector T-cell response [51, 52]. HBV-specific CD8⁺ T cells are enriched in the liver and are able to clear HBV-infected hepatocytes by secretion of T_H1 antiviral cytokines like interferon gamma (IFN- γ) and tumor necrosis factor alpha (TNF- α) as well as direct cytotoxic mechanisms as ligand-ligand (e.g. FasL/Fas) or perforin/granzyme-induced cell death [53-55]. Moreover, CD8⁺ T cells can directly lyse infected hepatocytes what induces liver damage [56]. For the prevention of HBV spread to non-infected hepatocytes, neutralizing anti-HBs antibodies are essential [52]. HBV persistence, however, results from an insufficient immune control of HBV infection with scarce, dysfunctional T cells and no neutralizing antibodies [51, 52, 57]. It was shown that long-term high viremia negatively influence the virus-specific T-cell response, thereby only a very limited virus-specific CD8⁺ T-cell response occurs in chronically infected patients [58]. Furthermore, T cells can become tolerant and prone to apoptosis triggered by the prolonged exposure to viral antigens during chronic infection [59].

1.1.4 Prophylaxis and available treatment options for chronic hepatitis B

Since 1982, highly effective and safe prophylactic vaccines against HBV are available. First, they consisted of purified HBsAg particles harvested from the plasma of chronic hepatitis B carriers. As the human source became a limiting factor for large-scale manufacturing and the concerns associated with human blood products increased, recombinant HBsAg, which was

produced in baker's yeast *Saccharomyces cerevisiae*, was used for the second generation of this vaccine form [60, 61]. Prophylactic vaccines lead to protection in more than 95 % of vaccinated individuals by the efficient induction of high-titer neutralizing antibodies against HBV surface proteins [62]. For a successful immunization three doses of hepatitis B vaccine have to be applied. Since 1992, the WHO recommended the hepatitis B vaccination in national immunization programmes worldwide.

In addition to the active vaccination, a passive form is available. It is used for immunocompromised patients as post-exposure prophylaxis of non-vaccinated individuals, to protect infants from vertical transmission from their infected mother or if a person had contact with HBV infected material. Hereby, it is important that the immunization is applied directly after exposition. This vaccine form consists of recombinant HBsAg and hepatitis B immunoglobulins which are derived from plasma of vaccinated patients with high anti-HBs titers [41, 63].

For the treatment of chronic hepatitis B patients, two main options are currently available: (pegylated) interferon alpha (IFN- α) and nucleos(t)ide analogues (NUCs). Treatment with IFN- α modulates the host immune system to help fighting against HBV. However, this therapy is very inefficient as it leads to HBsAg seroconversion in less than 10 % of patients [64]. Furthermore, the treatment induces many side effects like hepatitis flares, fever, thrombocytopenia, depression and myalgias, restricting the dose and duration of the therapy [28].

The group of NUCs consists of lamivudine, adefovir, entecavir, telbivudine, tenofovir disoproxil fumarate and tenofovir alafenamide [65]. These drugs suppress HBV replication by inhibition of the viral reverse transcriptase and are very effective as long as they are taken [66]. However, serological HBsAg loss can be hardly achieved during treatment and only in around 50 % of the HBeAg-positive patients HBeAg seroconversion can be observed [67].

Apart from general disadvantages, such as serious side effects and expensive long-term treatment, both therapies are not satisfactory since they can only control the virus but rarely result in HBV cure [68, 69]. These treatment options cannot directly target or eliminate the cccDNA. The persistence of cccDNA in the nucleus of infected hepatocytes causes viral reactivation in case of discontinuation of the medication. Therefore, most patients require long-term administration of the treatment [70].

1.2 Therapeutic vaccination as a potential treatment option of chronic hepatitis B

As none of the existing therapies leads to a fully satisfactory outcome, new treatment options for patients suffering from chronic HBV infection are urgently needed. Therapeutic vaccination is a promising approach as it aims to reactivate the patients defective immune response and therefore, overcome the functional defective HBV-specific T-cell response and the virus-specific immune tolerance of the patient [71]. This should enable the immune system to efficiently target the infected cells to control or even eliminate HBV. For this purpose, multi-specific and polyfunctional effector T-cell responses are very important.

Over the last years, various therapeutic vaccines were tested in clinical trials [5, 72, 73]. Applying the prophylactic vaccine consisting of recombinant HBsAg alone or in combination

with lamivudine failed [74, 75]. These strategies efficiently induced antibodies but insufficient HBV-specific CD8⁺ T-cell responses, required to control and eliminate pre-existing HBV infection. Another approach using recombinant HBsAg and anti-HBs antibody (HBsAg-HBIG) complexes with alum as adjuvant, demonstrated promising results among healthy adults and chronic hepatitis B patients in phase I, IIa and IIb clinical trials [76]. However, results of a phase III study were disappointing as the effects on HBV viral load and liver functions were similar to the control group receiving only alum [77].

In addition, new formulations with heat-inactivated, recombinant yeast expressing HBsAg, HBcAg and HBx antigens (GS-4774) were tested in phase I and II clinical trials [78, 79]. The study in healthy volunteers demonstrated that GS-4774 was safe and could elicit HBV-specific T-cell response [78]. The results in chronic hepatitis B patients confirmed the good safety profile of the vaccine, however no clinical benefits could be observed in comparison with patient receiving approved HBV antivirals [79]. The combination of GS-4774 with tenofovir did not show an improvement of the treatment as the vaccine did not reduce HBsAg levels in chronic hepatitis B carriers [80].

Among various approaches, HeberNasvac[®] represents a promising candidate for the treatment of chronic hepatitis B. It is based on a combination of HBcAg and HBsAg and has been granted marketing authorization in Cuba. The phase I clinical trial in healthy adults showed that the vaccine was safe, well-tolerated and immunogenic [81]. Further studies in treatment-naïve chronic hepatitis B patients, confirmed the safety of HeberNasvac[®] and the enhancement of viral control by the vaccine [82-84]. The comparison of HeberNasvac[®] and pegylated IFN during phase III clinical trial demonstrated a superior reduction of the viral load in patients treated with HBsAg and HBcAg combination [84]. However, experiments in naïve mice showed strong cellular immune responses mainly due to CD4⁺ T cells, whereas the essential for viral clearance CD8⁺ T-cell response was low [85]. In a current phase IIb/III trial efficacy of HeberNasvac[®] is evaluated as an adjunct therapy to NUCs for the control of HBV replication after finishing the treatment with antivirals (NCT02249988).

DNA-based vaccines encoding HBV envelope proteins that are meant to induce HBV-specific T cells and reduce viremia turned out to be ineffective in phase I or I/II trials [86-88]. These therapies showed promising results in preclinical models but were not immunogenic enough to break immune tolerance in chronic HBV carriers. The combination with a poxvirus vector encoding for the HBV envelope proteins as a boost indicated encouraging results in chimpanzees but did not lead to the induction of sufficient multi-specific T-cell response in chronic hepatitis B patients [89, 90]. A new candidate called INO-1800 which is a mixture of recombinant DNA plasmids encoding HBsAg and HBcAg is currently evaluated in phase I clinical trial (NCT02431312). Preclinical experiments showed that the immunization with this vaccine induced potent HBV-specific B- and T-cell responses which led to the elimination of targeted hepatocytes in mice [91].

Currently, two peptide-based approaches are tested in clinical trials: HepTcell (FP-02.2) is formed by nine synthetic peptides derived from the most conserved domains of HBV which includes CD4⁺ and CD8⁺ T-cell epitopes targeting all HBV genotypes (phase I; NCT02496897).

The other candidate ϵ PA-44 consists of immunodominant epitopes derived from PreS2 18-24 region, core-18-27 and tetanus toxoid and is tested in a phase II trial together with entecavir (NCT01326546).

Therapeutic vaccines based on viral vectors like adenovirus or modified vaccinia virus Ankara (MVA) were also evaluated in clinical trials. A DNA and MVA vaccine which was based on HBV M protein was well tolerated in humans, however, did not lead to the control of HBV infection [90]. Another candidate is based on the non-replicative adenovirus serotype 5 and encodes a fusion protein composed of a truncated HBcAg, a modified HBV polymerase and two HBV envelope domains (TG1050). Preclinical results showed the induction of a robust, long-lasting HBV-specific T-cell response and the seroconversion to anti-HBs in HBV-persistent mice [92]. A phase Ib trial showed a good safety profile of TG1050 and the induction of HBV-specific cellular immune response following vaccination in chronic hepatitis B patients under antiviral treatment [93]. Even though patients reached undetectable or unquantifiable hepatitis B core-related antigen levels by the end of the study, only a minor decreased of HBsAg was observed.

1.2.1 Heterologous protein prime/MVA vector boost vaccination strategy

Recently, a heterologous protein prime/MVA vector boost vaccination strategy [94], termed TherVacB, was developed by the Institute of Virology (HMGU/TUM; Figure 6). Preclinical experiments in mouse models indicated that it could be one of the most promising therapeutic vaccines as it efficiently induces HBV-specific immune responses which successfully eliminate persistence HBV infection [71, 95].

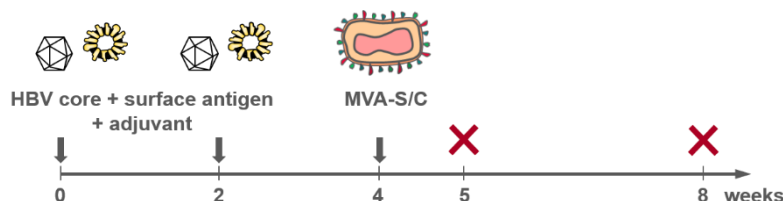


Figure 6. Heterologous protein prime/MVA boost vaccination strategy.

On week 0 and 2 priming with adjuvanted HBsAg and HBcAg is performed, followed by the boost with MVA-S/C on week 4. Depending on the experiment the mice were sacrificed on week 5 (HBV-naïve mice) or week 8 (AAV-HBV infected mice) after start of immunization. Modified from [73].

Priming with particulate HBsAg and HBcAg on week 0 and 2 leads to the induction of HBV-specific B- and T-cell responses. The antigens are formulated with an appropriate adjuvant. During this study, the stimulator of interferon genes (STING) activator bis-(3',5')-cyclic dimeric adenosine monophosphate (c-di-AMP) was used. C-di-AMP is a second messenger molecule in bacteria and archaea and constitutes a very promising adjuvant candidate inducing a simultaneous T_H1/T_H2 -based immune response by immunization via the mucosal route [96]. The following boost with MVA-C and/or MVA-S, expressing core or S protein, on week 4 amplifies HBV-specific effector $CD8^+$ T-cell responses. The induced antibodies as well as the multi-functional and multi-specific T-cell responses are necessary to control HBV spread and the elimination of the virus-infected hepatocytes,

respectively [71]. Previously, it was shown that the described therapeutic vaccine is able to break HBV immune tolerance in HBV transgenic and adeno-associated virus (AAV)-HBV mouse models [94, 95].

In this study, the AAV-HBV mouse model was used as it is suitable to examine novel immunotherapeutic approaches. AAV-mediated HBV genome transfer into the mouse liver, enables replication of the HBV genome over months and development of HBV-specific immune tolerance. Moreover, the AAV-HBV genome remains episomal upon AAV-HBV transduction which allows studying of the elimination of infected hepatocytes [97]. In addition, the formation of HBV cccDNA was observed in mice after AAV-HBV transduction in contrast to other mouse models, like HBV transgenic mice [24, 98].

1.2.2 HBsAg and HBcAg as vaccine components

Recombinant HBsAg is produced in yeast and since 1984 applied in large-scale vaccination campaigns as prophylactic vaccine against HBV [61]. The HBsAg consists of 226 amino acids (AA), whereby the cysteine rich 99-169 AA region is defined as the immunodominant loop. The AA 124-147 are named as the “a” determinant which is an important neutralizing epitope and the majority of HBsAg-specific neutralizing antibodies bind here [99, 100]. In addition, this region is essential for full HBsAg antigenicity [101]. The HBsAg has a molecular weight of 24 kDa in unglycosylated form. Yeast-produced HBsAg resembles spherical HBV subviral particles with a size of around 22 nm [102].

The HBcAg, is routinely produced in *Escherichia coli* (*E. coli*) which was first accomplished in 1979 [103]. Three years later, Cohen and Richmond described that bacterial HBcAg has the same antigenic properties and morphology as the HBV core protein prepared from HBV infected liver tissue [104]. HBcAg appears as particles with a size of approximately 32-36 nm [105]. The characteristic spikes on the surfaces of these particles indicate the four-helix bundles consisting of two anti-parallel helices donated by each monomer. The tips of the α -helical hairpins represents the major immunodominant epitope of the antigen [19, 20]. The HBcAg with a molecular weight of 21.5 kDa, is highly conserved among the different genotypes and is 183-185 AA long, depending on the corresponding genotype [106]. The antigen consists of an N-terminal assembly domain (AA 1-140) linked to a protamine-like arginine-rich C-terminus required for non-sequence specific packaging of RNA [105, 107-109]. The linker domain (AA 141-149) performs morphogenic functions and manages encapsidation of nucleic acids [108, 109].

1.2.3 MVA as vaccine vector

MVA belongs to the family of *poxviridae* and the genus of *orthopoxvirus*. The virus particle has a size of roughly 360 x 270 x 250 nm and a brick-like morphology [110, 111]. As shown in Figure 7, a dumbbell-shaped core with two lateral bodies is located in the inside of the particle.

The main part of the viral core is the double stranded DNA genome of MVA with a size of 178 kb. Each MVA particle has one or two lipid shells depending on its maturation state [4, 112].

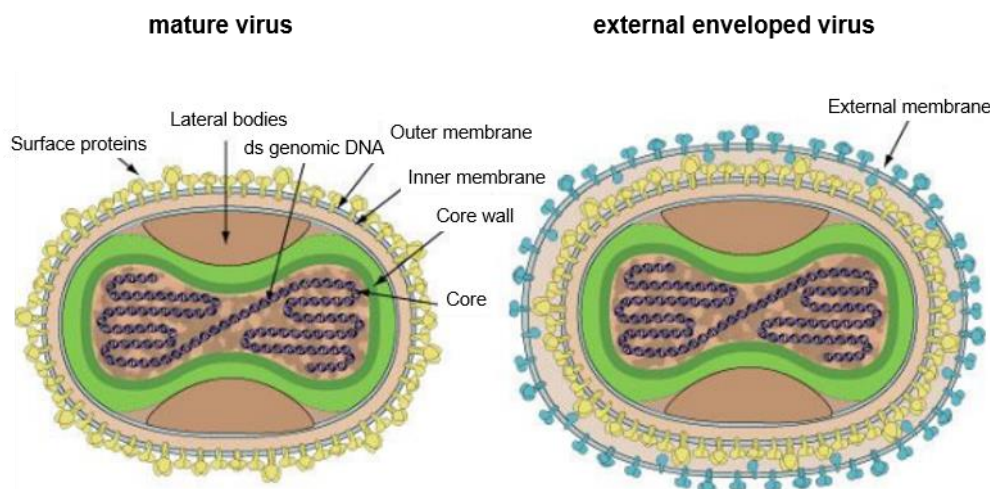


Figure 7. Schematic structure of MVA particle.

The virus consists of one or two lipid shells enclosing a dumbbell-shaped core with two lateral bodies. Inside the core, the double stranded (ds) genomic DNA is located. Modified from [113].

The name Ankara refers to the vaccinia institute Ankara in Turkey, where the original strain of MVA, the Chorioallantois Vaccinia virus Ankara (CVA), was held over years through donkey-calf-donkey passages and was used as basis for human smallpox vaccine. In 1975, MVA was transferred to Germany and developed over passaging of CVA on primary chicken embryo fibroblast (CEF) cells. After 516 passages, the newly developed virus was called MVA and after additional 54 passages, MVA was declared as uniform and genetically stable [114]. During that time, MVA developed a highly attenuated phenotype. The passaging led to a loss of around 15 % (~30 kb) of the original viral genome causing six major deletions, mainly located at both terminal part of the viral genome (Del I-Del VI) [115]. MVA lost genes which code e.g. for proteins for the regulation of the host genome, virulence factors as well as structural or immunomodulatory proteins [115-117].

MVA is an ideal candidate as a human vaccine vector as foreign genetic information can be inserted into the genome of infectious MVA. After the infection of the target subject with the viral vector, this insertion leads to the expression of the foreign genes in the host and the induction of an immune response against the foreign antigens [4]. In addition, MVA can infect mammalian cells, but new infectious particles cannot be produced as the partial genome loss caused a blockade during the morphogenesis in non-permissive cells. Nonetheless, viral gene expression, DNA replication and protein synthesis can be performed despite the deletions. These processes are necessary for the humoral and cellular immune responses which are in turn important for the use as a vaccine vector. Another important point is that the replication of MVA only takes place in the cytosol of the host cell making the integration of the viral genome into the host genome impossible.

The unique characteristics of MVA as safety, efficient protein synthesis and gene expression, the ability to induce antigen specific immune response and the possibility to insert foreign genes in its genome make the virus to an excellent candidate for preclinical and clinical

research and vaccine development [118-122]. The application of MVA is already described in several clinical studies where the MVA was used for the prophylaxis and treatment of infectious diseases such as human immunodeficiency virus (HIV) infections, tuberculosis, malaria or influenza [123-127]. Moreover, MVA was utilized in studies concerning therapeutic vaccination against lung, prostate and cervical cancers as well as melanoma [128-131].

1.3 Solving the cold chain problem

The lack of a continuous cold chain is often a major challenge in large-scale vaccination campaigns. Especially in low- and middle-income countries or hard-to-reach areas continuous cooling can often not be provided due to low infrastructure, high costs and logistical problems [132-135].

1.3.1 WHO recommendations

The WHO recommends for nearly all vaccines a transport and storage temperature of 2-8 °C as many vaccines lose their potency at higher temperatures due to the thermal instability of their components [133, 136]. Addressing this problem, the WHO has presented two different guidelines: the “controlled temperature chain” (CTC) and the “extended controlled temperature condition” (ECTC). Both describe requirements for vaccines in countries with high outdoor temperatures [134, 137]. According to the CTC guideline every vaccine should be suitable for a single excursion at 40 °C for a minimum of 3 days without losing vaccine efficacy, whereas ECTC demands the testing and labelling of vaccines for a transport and storage in temperatures over 2-8 °C. Compliance with the WHO guidelines facilitates vaccine application worldwide by enabling a higher flexibility during vaccination campaigns, simplifying vaccine delivery, reducing the costs, improving vaccine effectiveness and preventing health consequences caused by administering the inactive vaccines [133, 134, 138, 139]. MenAfriVac™, a meningitis A vaccine, was the first vaccine which fulfilled the CTC criteria. In 2012, MenAfriVac™ was licensed for possible use after exposure to temperatures up to 40 °C for a maximum of 4 days [140]. Lydon et al described a mathematic model which estimated major economic benefits which could be achieved by thermostable MenAfriVac™ during mass vaccination campaigns as compared to the traditional cold chain system [141]. These findings were confirmed by the Benin study which reported the first field use of MenAfriVac™. Clear benefits of using the vaccine outside the cold chain could be seen: more people could be vaccinated, a high flexibility was observed and the logistic burden could be reduced. There was no need for a return to health center every night to get cold-stored vaccines and the difficulties of hand-carrying large ice boxes over rough paths or during river crossings to reach the vaccinees could be avoided [142]. As a result, the health benefits of the introduction of MenAfriVac™ in nine African countries were reported, demonstrating a considerable reduction in disease burden and a reduced epidemic risk [143].

1.3.2 Various drying methods for pharmaceutical products

The need for heat-stable vaccines which can be transported and stored outside the cold chain was recognized not only by the WHO but also by other scientists who investigated different approaches to develop thermostable products. At this timepoint various strategies exist to increase stability of vaccines: engineering of vaccines, e.g. creation of a mutant antigen for a recombinant meningococcal vaccine [144, 145] or modification of a malaria protein vaccine by introduction of 18 mutations [146], addition of stabilizing adjuvants or sugars and drying of the vaccine components.

Vaccine stability, especially thermal stability, can be strongly increased through drying of the components [147-149]. The lyophilization process circumvents the possibility of physical and chemical reactions as well as high molecular mobility which are common in liquid formulation. Therefore, liquid formulations have to be transported and stored under refrigerated conditions and have a short shelf life [147, 150].

At the beginning of the lyophilization process the pharmaceutical components are frozen followed by two drying phases under vacuum. The goal of the primary drying is to remove frozen water by directly changing it from solid form to gas phase through sublimation under vacuum. During the secondary drying the remaining non-frozen water is removed by evaporation. Afterwards, a highly porous cake structure is formed which can be easily reconstituted in water before application [151]. The cake consists of fluffy flocs and should be only localized at the bottom of the vial showing a straight surface. The other parts of the vial should be clear indicating no bubbles, rings, "meltback", dust, water droplets etc. In addition, the size and shape of the cake should be similar to the original liquid sample which was filled in the vial. Moreover, a uniform color and texture of the lyophilized cake should be detectable [152].

It is very important that the reconstituted components are kept cold and applied as soon as possible as many vaccines lose their potency within hours to days after reconstitution. As an example, the WHO requires that reconstituted vaccines like measles, mumps, rubella or yellow fever vaccine should be used within the six hours after reconstitution [136].

Despite many advantages of the lyophilization, this process can also result in degradation or destabilization of the product as a consequence of the different freezing and subsequent drying steps [147]. Therefore, stabilizing excipients like sugars, polymers or amino acids are often added to the formulation to protect the components by replacing water as hydrogen bond forming partner or by forming a glassy matrix in which the pharmaceutical component is embedded [151, 153, 154]. This is defined as cryoprotection in case of sheltering against freezing or lyoprotection which protects against dehydration during the drying [155].

Lyophilization is the most common, well-known technique in the industry to transform a liquid product into a solid form. In addition to this method, spray- or foam-drying are also used to produce solid products. During spray-drying the liquid starting material is converted into a dried powder in one single step. In general, the solution is transformed into fine droplets through atomization, quickly dried in a large chamber by warm gas and collected by cyclone separation or baghouse filtration. As shown in Figure 8A the spray-dried final product consists of a powder with a fine particulate structure, whereas the lyophilized end product is composed of fluffy flocs.

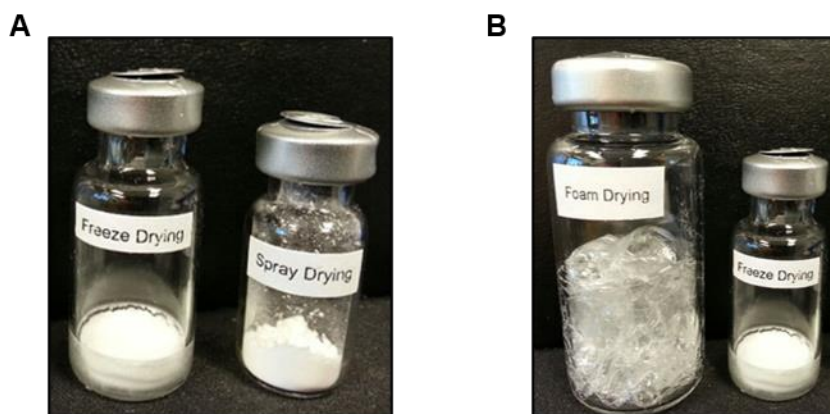


Figure 8. Appearance comparison of lyophilized (freeze-dried), spray-dried and foam-dried live attenuated influenza samples.

(A) Freeze-dried and spray-dried samples. (B) Foam-dried and freeze-dried samples. Modified from [156].

The big advantages of spray-drying are that it is simpler, cheaper and faster than lyophilization. Furthermore, this method offers high volume product throughput, is more scalable at lower costs and the powder form facilitates its conversion into capsules and tablets. Nevertheless, spray-drying also comes with considerable drawbacks. Due to fast drying, the product is exposed to extremely high temperatures and atomization pressure which can negatively affect product stability. Furthermore, shear stress and high surface tension have to be considered if this method is applied [157, 158].

In contrast to the extremely low and high temperatures, which are applied during lyophilization and spray-drying respectively, foam-drying happens at near ambient temperatures which reduces the stress on the material [159, 160]. By controlling the temperature very carefully, freezing is also avoided during foam-drying which may reduce the possibility of aggregation [161]. To generate stable foam structures, the solution is dehydrated by boiling or foaming in one single step under reduced vapor pressure followed by rapid evaporation [158]. For this process excellent vacuum control is indispensable [161, 162]. As shown in Figure 8B foam-dried products appear as translucent, foamy structures with large volumes which look distinctively different than the lyophilized cake structure.

Foam-drying has also several disadvantages like surface tension stress which is associated with cavitation and the need for optimizing vacuum levels to achieve effective foaming. In addition, the remaining water content after foam-drying is higher than after lyophilization which would require a secondary drying step. This in turn negatively influence the energy and time which is saved during foam-drying in contrast to lyophilization. Special attention must be paid to the sterility of the product as boil over can occur during the process. As visible in Figure 8B, the appearance of foam-dried product is more heterogeneous than the lyophilized cake structure which could make the industrial quality control and product characterization more difficult [158]. This method still needs to be further optimized to establish a robust technique which can be implemented in industrial processes.

1.3.3 Stabilizing excipients

To avoid the disadvantages of the described drying methods, stabilizing substances are often added to the product for protection. As an example, protein denaturation caused by dehydration during spray-drying can be prevented by the addition of excipients like sugars, polyols or amino acids. These molecules are able to replace hydrogen bonds during drying which were previously provided by water molecules. In addition, buffering against pH changes, preferential hydration (e.g. nonreducing sugars such as sucrose or trehalose), providing steric hindrance of protein-protein interactions (e.g. polymers and protein stabilizers such as serum albumin) and decreasing adsorption and aggregation (e.g., nonionic surfactants such as polysorbate) are possible options to increase heat-stability of biological components [163].

Approximately one third of therapeutic proteins used in the pharmaceutical industry are formulated with sugars [164]. Sucrose (20 %) and sorbitol (14 %) are the most common ones in licensed vaccines. As trehalose is the most frequently used sugar in experimental vaccines (32 %) and is described as stabilizer and cryoprotectant, it could be a promising candidate for the future [165, 166]. In additional 25-30 % of licensed and experimental vaccines amino acids are used as additive to increase protein solubility and stability [164].

When choosing the stabilizing substances, it is recommended to use components which are already used in commercial vaccines or “generally recognized as safe” (GRAS) excipients. This designation of the Food and Drug Administration (FDA) describes chemical and substances added to food which have been proven by experts as safe. Therefore, time can be saved during the certification and qualification of the vaccine by national and international regulatory authorities. In current live attenuated vaccine formulations, GRAS protein excipients such as human serum albumin and/or gelatin with one or more amino acids and one or more sugar components are used as stabilizers [164]. Some examples of GRAS excipients are listed in the following Table 1.

Excipient class	Examples
Amino acids	arginine, aspartate, glycine, glutamate, histidine, lysine, proline
Antioxidants	ascorbic acid, EDTA, malic acid
Proteins	human albumin, gelatin
Sugars/polyols	dextrose, glycerol, lactose, mannitol, myoinositol, sorbitol, sucrose, trehalose
Surfactants	pluronic, tween, polysorbate

Table 1. Various GRAS excipients used for stabilization in licensed viral vaccines [164].

In the following paragraph, the examples of recently reported thermostable vaccines are described. Air-dried live attenuated herpes simplex virus (HSV)-2 vaccine and inactivated influenza vaccine were able to maintain efficacy despite heat-exposure for 2 months at 40 °C or 3 months at 40 °C due to the addition of the FDA-approved material trehalose and pullulan [167]. Lovalenti et al heat-stabilized lyophilized, spray-dried or foam-dried live attenuated influenza vaccine with different excipient like sugars, amino acids, antioxidants and proteins. They demonstrated that the selection of suitable stabilization substances strongly depends on

the process of drying [156]. Ohtake et al formulated a live attenuated spray-dried measles vaccine with sugar and proteins which was stable for 8 weeks at 37 °C [157]. In addition, this group used trehalose, methionine and gelatin as stabilizers for a foam-dried *Salmonella Typhi* bacterial vaccine reaching a heat-stability of 12 weeks at 37 °C [162]. Naik et al presented a lyophilized live attenuated rotavirus vaccine containing sucrose and glycine which is licensed in India and can be stored below 25 °C for 36 months, for 18 months at 37 °C or 40 °C and for a short timeframe at 55 °C [168].

Heat-stability can also be increased by using stabilizing adjuvants. Chen et al achieved a storage duration of 24 months at 37 °C for a spray-dried recombinant hepatitis B vaccine containing an aluminium salt adjuvant [169]. Pelliccia et al demonstrated that the addition of polyethylene glycol (PEG), gold nanoparticles and sucrose can maintain the immunogenicity of adenoviral vaccine formulation for 10 days at 37 °C [170]. In addition, Hassett et al showed that aluminum hydroxide alone or together with glycopyranoside lipid A can maintain immunogenicity of lyophilized recombinant ricin A toxin and anthrax vaccine despite heat-exposure for 4 or 16 weeks at 40 °C [171, 172]. Similar to this approach, a lyophilized Ebola vaccine was adjuvanted with microparticulated aluminum hydroxide reaching a storage stability for 3 months at 40 °C, which was proven in BALB/c mice [173].

A very interesting albeit costly method is described for an inactivated influenza vaccine as it is encapsulated in microneedle patches using different stabilizing adjuvant formulations [174-176]. In addition, Alcock et al described the stabilization of adenovirus and MVA by drying onto polypropylene or glass fiber membranes using sucrose and trehalose [177]. Nevertheless, these methods are not commonly used as they require special equipment for drying.

In this study, stabilizing amino acid-based formulations (SAAF) from LEUKOCARE were used as stabilizing excipients. Previously, SAAFs were applied in different projects to heat-stabilize biological components like antibodies, viral vectors or several vaccines. As recently demonstrated, specifically tailored SAAF have a high potential to avoid stress-mediated degradation of such complex molecules [178-180].

SAAFs are water soluble formulations which are composed of different natural small molecules like amino acids, saponins and sugars. All SAAFs are used in pharmaceutical quality, were tested non-toxic and are already approved and accepted by regulators as excipients in various pharmaceuticals [178].

For the selection of the most suitable SAAF, the type of target molecule and the consistency of the component (liquid or lyophilized) is important. In addition, it has to be defined in advance if the final product should be heat and/or freeze stable. According to the knowledge about the mode of action of SAAF and lyophilization, it is assumed that during freeze-drying the excipients of the SAAF sequentially replace water by substituting the stabilizing hydrogen bonds between the protein and the water molecules in the hydrate shell. In addition, SAAF replace water by forming other non-covalent interactions with the target protein. As shown in Figure 9, freeze-dried SAAF form a glassy state and an amorphous shell to protect the three-dimensional structure of the stabilized component. Additionally, containing radical scavenging excipients and antioxidants, SAAF protect the target molecule against oxygen

radical formation during increased temperature or irradiation and provide anti-oxidative effects. Before application, lyophilized SAAF-formulated products can be easily reconstituted in water [181, 182].

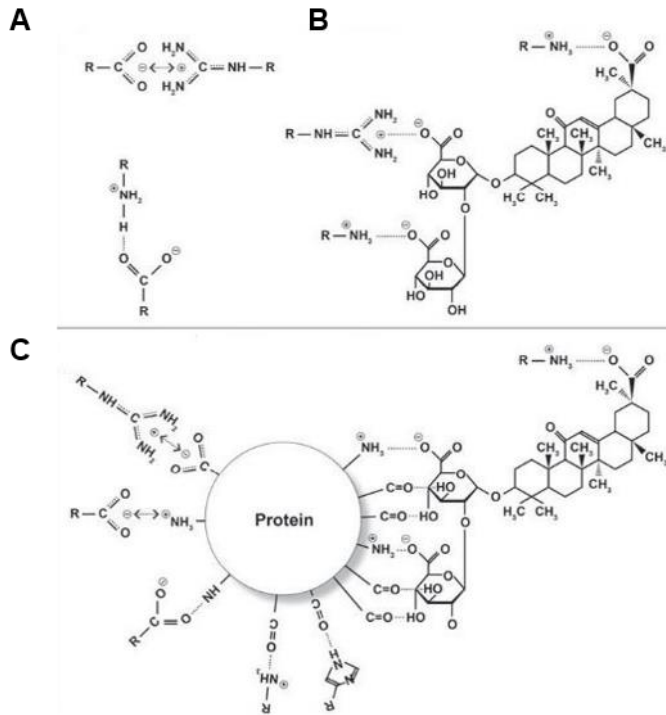


Figure 9. Assumed mode of action of SAAF.

(A) Interactions between the various functional groups of amino acids. (B) Interaction between basic functional groups of amino acids with other excipients within the SAAF. As example glycyrrhizic acid is shown. (C) Sequential replacement of the stabilizing hydrogen bonds between protein and water molecules by SAAF [182].

1.4 Aim of the study

Therapeutic vaccination represents a novel promising treatment strategy as it aims to efficiently induce HBV-specific B- and T-cell responses which support the host immune system to eliminate the persistent HBV infection. A major challenge in global vaccine application is that the vaccine components require appropriate cooling during transport and storage to maintain efficacy. As many hepatitis B patients are living in countries with high outdoor temperatures, where often no cold chain can be maintained to secure that the vaccine remains intact, the thermostability of the vaccine should be a major concern.

The goal of this study was to develop of a lyophilized, thermostable, therapeutic vaccine to combat chronic hepatitis B using SAAFs from LEUKOCARE. The recently described, heterologous protein prime/MVA vector boost vaccination strategy, named TherVacB, served as the basis for this approach.

The aim of the first part of this thesis was the selection of the most suitable recombinant HBcAg and HBsAg representing the two components of the prime immunization. To this purpose, the integrity and purity of antigens from various providers should be compared. In parallel, we aimed to create and characterize a new bicistronic MVA, expressing core and S protein

(MVA-S/C) which would facilitate the booster immunization of TherVacB. For a precise and specific *in vitro* characterization of the vaccine components, different assays to test purity, antigen integrity and MVA-S/C infectivity should be established or improved.

In the second part, heat-stability of all three TherVacB components should be evaluated. To improve TherVacB thermal stability, the effect of lyophilization on antigen integrity and MVA-S/C infectivity in the presence of SAAF was evaluated. To address the question which SAAF is the most suitable one for the TherVacB approach, the potency of vaccine components stabilized with various SAAFs was compared *in vitro* after lyophilization and/or heat-stressing. Finally, to verify the selection process and to confirm the immunogenicity of optimally stabilized vaccine components *in vivo*, an experiment in HBV-naïve mice was performed.

The aim of the third part was to evaluate the success of SAAF-stabilization *in vitro* by comprehensive analysis of a SAAF-stabilized vaccine by comparison to a non-stabilized one. The first goal was to fulfill the WHO CTC criteria, therefore the maintenance of antigen integrity as well as MVA-S/C infectivity upon storage at 40 °C for 3 days should be examined. To further improve the thermostability of TherVacB, even more extreme stressing conditions like 25 °C and 40 °C for an exposure time up to 3 months should be applied to SAAF-stabilized vaccine components. Finally, the effect of SAAF-stabilization on TherVacB was evaluated after 1 year of storage at 25 °C.

The fourth part of this thesis aimed at analysing the immunogenicity of SAAF-stabilized TherVacB *in vivo*. First, the success of SAAF-stabilization should be tested in HBV-naïve mice after prolonged storage of the stabilized vaccine components at 25 °C and 40 °C similar to the conditions in the *in vitro* experiments. Afterwards, two stressing conditions were chosen to investigate the capability of SAAF-stabilized TherVacB to break HBV-specific immune tolerance in mice persistently infected with adeno-associated virus vector carrying an HBV genome (AAV-HBV).

2 Results

Throughout this part of the thesis, the development of a thermostable, therapeutic hepatitis B vaccine is reported. The following chapters describe (I) the choice or generation and characterization of the three TherVacB components, (II) the selection of suitable stabilization substance, (III) subsequent challenging of the stabilized vaccine components against evaluated temperatures over short and long-term storage periods *in vitro* and (IV) the proof of concept within *in vivo* experiments. Parts of these results will be published in Sacherl and Kosinska et al [183].

2.1 Characterization of vaccine components

2.1.1 Generation of MVA-S/C

Previous data showed that simultaneous application of the two vectors MVA-C and MVA-S led to an induction of broader and stronger HBV-specific immune responses than an immunization with only one of the two MVAs [94]. To improve the TherVacB approach, a bicistronic MVA vector expressing both HBV core and S protein, MVA-S/C, was constructed and generated within this study (Figure 10A). Therefore, only one component is required for the TherVacB boost, which would make the future clinical approval easier as only one vector would have to be verified by the regulatory authorities. In addition, as the maximal amount of virus, which is allowed for administration in humans, is limited by the regulatory authorities, MVA-S/C permits the duplication of infected cells expressing core and S proteins without changing the absolute number of MVA particles. Generation of the MVA-S/C was done in cooperation with Martin Kächele.

The MVA-S/C construct contains the coding sequences of HBV S protein (HBs; genotype A, serotype adw) and HBV core protein (HBc; genotype D, serotype ayw) linked by a porcine teschovirus-1 2A (P2A) gene sequence [184]. In cells infected with MVA-S/C, one single mRNA is transcribed and translated into similar amounts of HBV core and S protein (Figure 10B, C). During translation, the P2A-mediated self-cleavage of the polypeptide by a ribosome skipping effect, generates two separate proteins: HBV S and core which fold independently from each other [185, 186]. S proteins can spontaneously form spherical particles in the ER, which can be secreted from the cells (Figure 10B), whereas core monomers can automatically assemble into capsids in the cytoplasm of infected cells (Figure 10C). In rare cases, it might happen that the self-cleavage of the P2A peptide is not efficient, resulting in the generation of fusion proteins representing the uncut form of the polypeptide (Figure 10D) [185]. If these fusion proteins cannot be successfully folded, they are most likely degraded via the proteasome. In case of successful folding, it is possible that the fusion proteins get integrated into spherical particles or may be located as transmembrane protein on the cell surface.

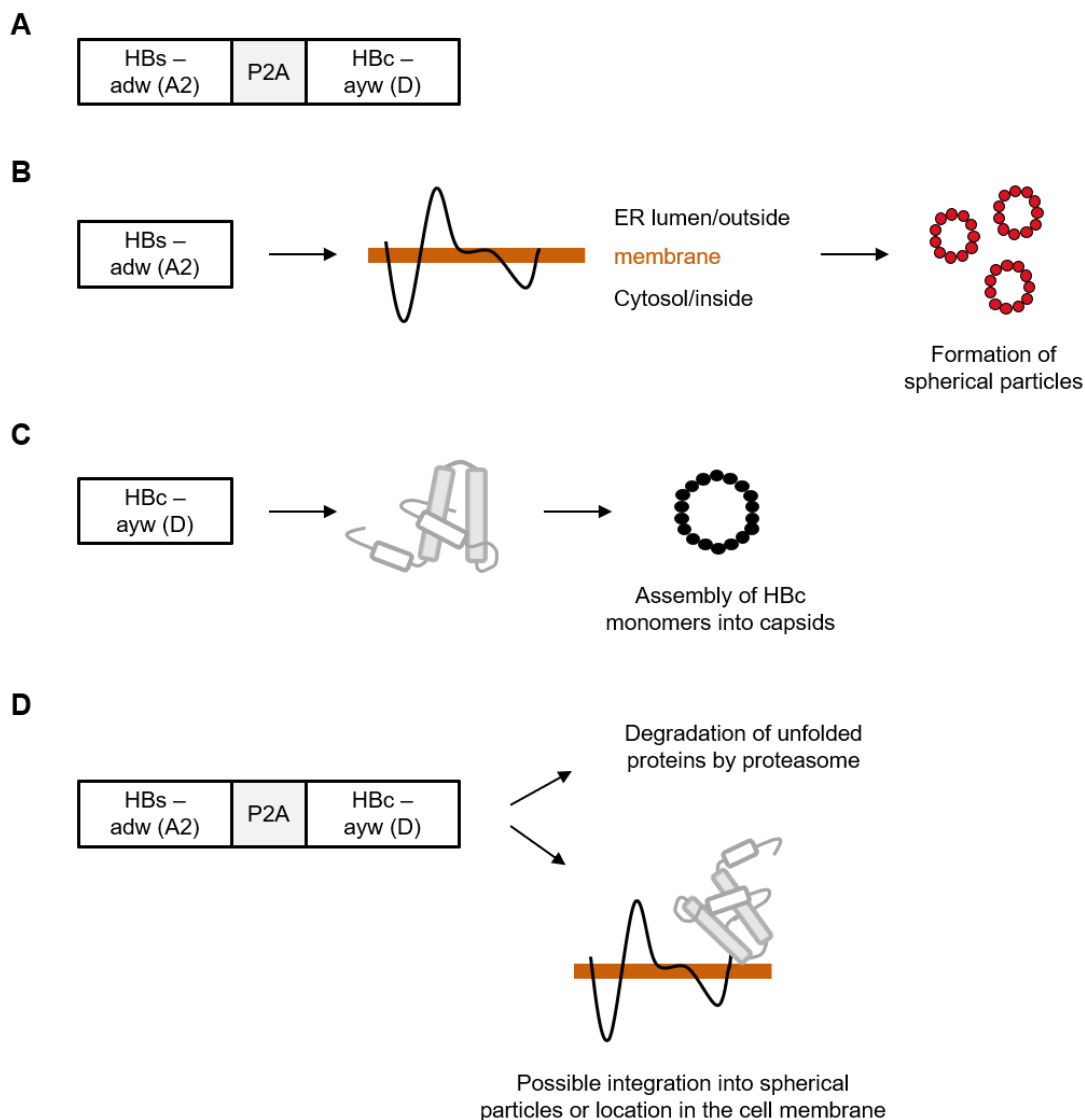


Figure 10. MVA-S/C construct and possible protein products.

(A) Scheme of MVA-S/C construct expressing HBV S protein (HBs; genotype A, serotype adw) and core protein (HBc; genotype D, serotype ayw) linked by a P2A sequence. Infection with MVA-S/C leads to the expression of three different proteins. (B) The S protein is a viral transmembrane protein capable of forming spherical particles, which can be secreted from the infected cells. (C) The core proteins spontaneously assemble into capsids in the cytoplasm of infected cells. (D) Fusion proteins of HBV core and S protein may be generated after unsuccessful self-cleavage of the P2A peptide. Unfolded proteins are most likely degraded by the proteasome, whereas folded proteins may be integrated into spherical particles or located in the cell membrane.

MVA-S/C was generated by homologous recombination (Figure 11). For this process, the transfer vector pIIIH5red K1L containing the strong early/late promoter PmH5, an mCherry expression cassette enclosed by two identical repetitive sequences (del), as well as two flank sequences, was used. Flank 1 and flank 2 are located up- and downstream of the insert and refer to MVA DNA sequences adjacent to deletion (Del) site III, therefore, targeting Del site III for insertion of recombinant genes (Figure 11A). The S/C expression cassette was synthesised by Addgene and cloned into the transfer vector. Next, the vector plasmid was transfected into CEFs which were simultaneously infected with MVA wild-type (MVA-WT). Following this, homologous recombination between the flanking sequences led to the insertion of the whole S/C cassette into the Del site III of the MVA-WT genome (Figure 11B). The resulting

recombinant virus should express all proteins encoded by the S/C insert including mCherry, resulting in a red fluorescence of the cells infected with this virus. To isolate the recombinant virus through plaque passages, the easily visible fluorescence signal was used to distinguish the infected cells from non-fluorescent cells infected only by MVA-WT. After obtaining a sample which only consists of recombinant virus without MVA-WT, mCherry-free recombinant MVA-S/C was obtained during plaque passages by intragenomic homologous recombination between the two identical del sites, which are located up- and downstream of the mCherry gene (Figure 11C).

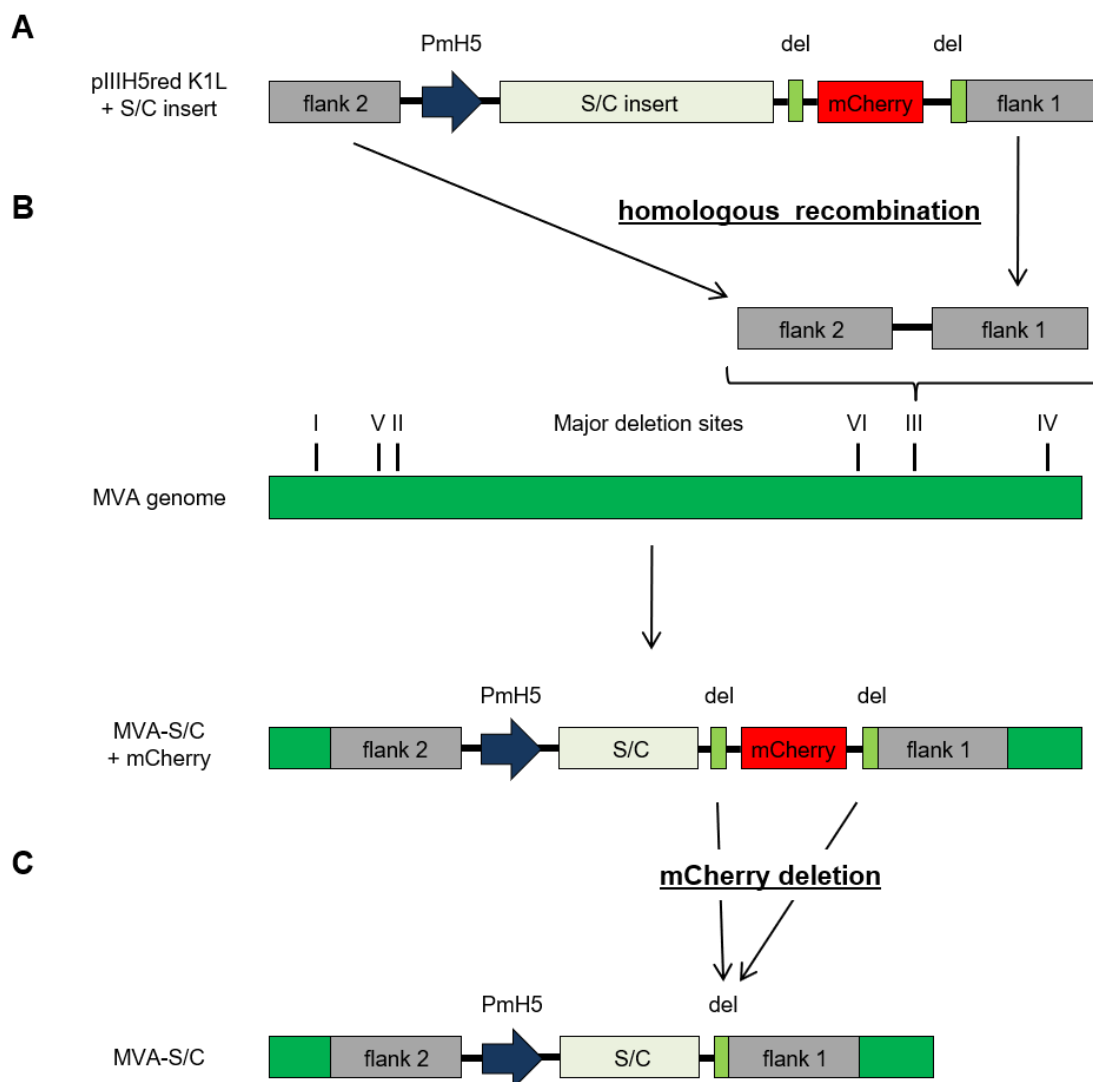


Figure 11. Generation of MVA-S/C.

(A) Vector plasmid pIIIH5red K1L consisting of two flank regions (flank 1 and flank 2), which are located up- and downstream of the S/C insert, strong early/late promoter PmH5 and an mCherry expression cassette enclosed by two identical del regions. (B) Insertion of the whole S/C cassette into deletion (Del) site III of the MVA-WT genome by homologous recombination between the flanking regions of the plasmid. Afterwards fluorescent recombinant virus was isolated by plaque passages. (C) mCherry deletion by intragenomic homologous recombination. Modified from [187].

To investigate whether the complete S/C sequence was correctly inserted into Del III region of the MVA genome, PCR and Sanger sequencing were performed. The PCR product sizes of the MVA-S/C insert and empty MVA Del I-VI sites are listed in Table 2.

Primer	Size (bp)
Del I	291
Del II	354
Del III	447
Del IV	502
Del V	603
Del VI	702
S/C insert	1852

Table 2. PCR product sizes of MVA Del I-IV region and MVA-S/C insert.

The expected PCR-product of MVA-S/C insert with a size of 1852 base pair (bp) was detected by PCR and subsequent agarose gel electrophoresis in the Del III site of the MVA-WT genome (Figure 12A). In contrast, MVA-WT showed a smaller band of around 447 bp reflecting the empty Del III region. After three years, a control PCR was performed and displayed a similar result, which demonstrates that despite many viral passages the intact S/C insert is still located in the right location of the MVA genome (Figure 12B). PCRs with primers specific for the five remaining Del sites (I, II, IV-VI) indicated specific integration of the S/C insert into Del III while the other Del regions remained empty and showed similar PCR products for the recombinant MVA-S/C and MVA-WT (Figure 12C). In addition, the correct integration of the whole S/C cassette into the MVA-S/C genome was confirmed by Sanger sequencing.

To check for the proper S and core protein expression, chicken fibroblast cell lines (DF-1) were infected with MVA-S/C or MVA-WT as a negative control at an MOI of 0.1 and incubated at 37 °C, 5 % CO₂ for 48 h. HBcAg-specific Western Blot (WB) analysis of the cell lysates displayed two main bands referring to core monomers (21.5 kDa) and core dimers (42 kDa; Figure 12D). HBsAg-specific WB analysis showed the naive and glycosylated forms of S monomers with the expected sizes of around 24 and 27 kDa (Figure 12D). A further signal observed at 45 kDa refers to S dimers. No specific signals were observed in DF-1 cells infected with MVA-WT. To determine the secretion of HBeAg and HBsAg, the supernatants of MVA-S/C- or MVA-WT-infected DF-1 cells were collected after 0, 2, 4, 8, 12, 24 and 48 h post infection and analyzed by Enzyme linked immunosorbent assay (ELISA). Increasing amounts of HBeAg and HBsAg were detected over time, indicating the expression of HBV S and core protein (Figure 12E). In contrast, no HBsAg or HBeAg was measured in the supernatant of cells infected with MVA-WT.

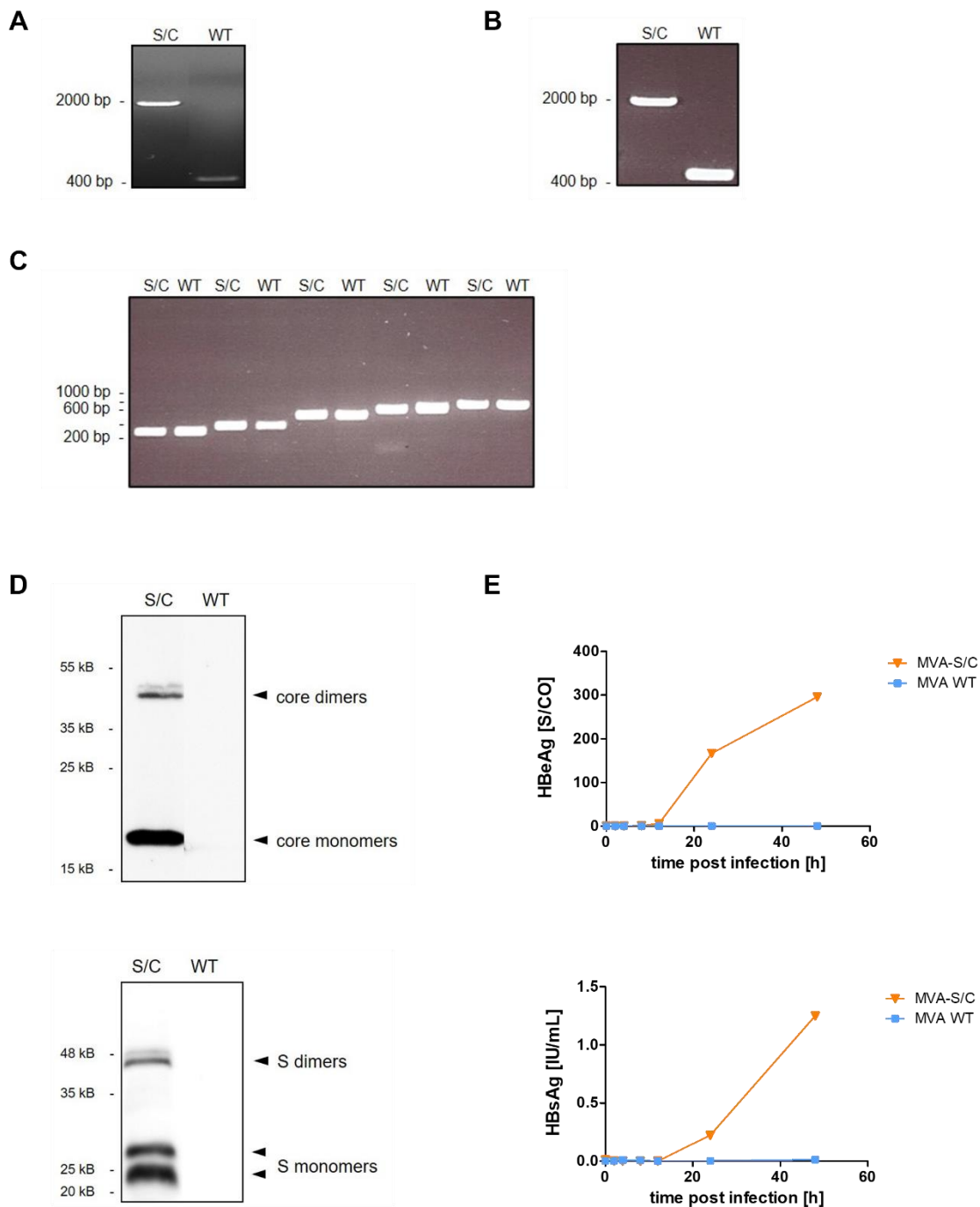


Figure 12. Verification of the S/C insert.

After MVA-S/C production in DF-1 cells, viral DNA was isolated and analyzed by PCR and subsequent agarose gel electrophoresis. PCR products using primers specific for Del III region of the MVA-S/C and the MVA-WT directly after the generation of the recombinant virus (A) and after many viral passages (B). (C) PCR products of MVA-S/C and MVA-WT after amplification using primers specific for Del I, II, IV-VI regions of MVA genome. DF-1 cells were infected with MVA-S/C at an MOI of 0.1 and incubated at 37 °C, 5 % CO₂. As a negative control MVA-WT was used. (D) Cells were lysed after 48 h and HBcAg- and HBsAg-specific WB analysis was performed. (E) The secretion of HBeAg and HBsAg in the supernatant of MVA-S/C-infected cells was measured after 0, 2, 4, 8, 12, 24 and 48 h post infection by ELISA.

Taken together, these data demonstrate the successful generation of MVA-S/C expressing HBV core and S protein.

2.1.2 Characterization of MVA-S/C

Following the generation of MVA-S/C, the vector was thoroughly characterized. Efficient MVA production is restricted to a few permissive cell lines such as baby hamster kidney (BHK-21), CEFs or DF-1 cells. During this study, the MVA-S/C was produced in DF-1 cells as they are easy to maintain and were described as an excellent producer cell line for MVA [188-190].

To determine the optimal harvesting time during the virus production, MVA-S/C growth kinetics were analyzed over time. To this purpose, the viral titers were determined 0, 4, 8, 12, 24, 48 and 75 h post infection by plaque assay.

As shown in Figure 13A, a continuous MVA-S/C growth was detected starting at 4 h post infection, until the saturation was achieved at 48 h post infection. As the viral titer decreased afterwards, 48 h was assumed as the optimal harvesting time point to achieve the highest output. During this study, viral titers of around 5×10^9 TCID₅₀/mL were reached after purification.

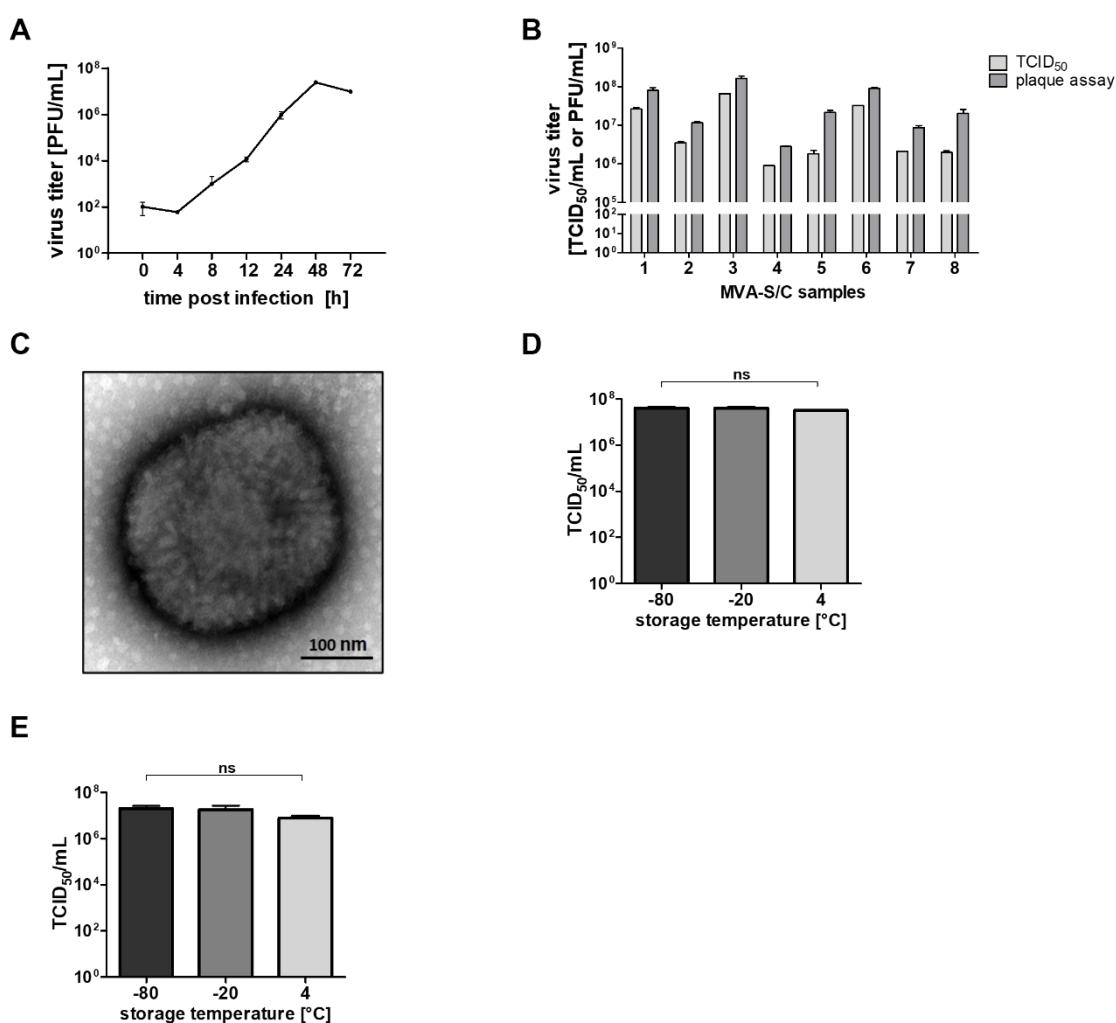


Figure 13. Characterization of MVA-S/C.

(A) DF-1 cells were infected with MVA-S/C at an MOI of 0.1 and harvested after 0, 4, 8, 12, 24, 48 and 72 h post infection. Viral titers were analyzed by plaque assay. (B) Comparison of MVA-S/C titers determined by TCID₅₀ or plaque assay. (C) Morphological analysis of negative stained MVA-S/C by TEM at a magnification of 40000x. Scale indicates 100 nm. MVA-S/C titers in viral samples stored at -80, -20 and 4 °C after 3 days (D) and 3 months (E) determined by TCID₅₀. Statistical analysis was performed using unpaired t-test. Asterisks mark statistically significant differences: ns - not significant.

Several methods were described to determine the infectious MVA titer. These assays are based on the MVA-induced cytopathic effect (CPE), immunofluorescence staining or the use of reporter genes (e.g. GFP). In this study, TCID₅₀ and plaque assays were performed. Viral titers determined by TCID₅₀ were defined by counting positive wells based on the virus-induced CPE in infected cells. During plaque assay, an antibody against MVA proteins followed by visualization via a chromogenic substrate is used to stain viral plaques. To determine the comparability of TCID₅₀ and plaque assay, different viral samples were titrated with the respective methods and compared afterwards.

As shown in Figure 13B, a 0.5-1 log difference in MVA-S/C titers was detected between the two methods confirming the reported value of 0.7 log [191]. The observed viral titers defined by plaque assay were higher. The visualization of the plaques by antibody staining proved to be more sensitive and easier to recognize compared to identifying infected cells under the light microscope. Even if the plaque assay is faster to perform, this technique is more expensive than the TCID₅₀ as an additional antibody and chromogenic substrate are needed. As both methods are reliable and demonstrated similar results in repetitive experiments, in further studies the MVA-S/C titers were determined only by TCID₅₀.

To characterize MVA-S/C morphology transmission electron microscopy (TEM) was performed. The TEM analyses presented in this work were done in cooperation with Dr. Sandra Eßbauer. As visualized in Figure 13C, the typical brick-like morphology of orthopoxvirus and a size around 250-300 nm was observed for MVA-S/C.

To determine the best storage conditions for MVA-S/C, the virus was exposed to -80 °C, -20 °C and 4 °C for 3 days or 3 months. The subsequent TCID₅₀ analysis displayed comparable numbers of infectious MVA-S/C particles for all examined conditions (Figure 13D, E). However, the highest MVA-S/C titer was detected after storage at -80 °C. Therefore, MVA-S/C was stored at -80 °C in future experiments.

2.1.3 Comparison of antigens from different manufacturers

HBcAg and HBsAg, produced from different companies, may differ in genotype, concentration and quality aspects. To address the question which antigen manufacturer was suitable for the supply of TherVacB antigens, the various HBcAg and HBsAg were comprehensively studied. Therefore, different analytical methods applied for both antigens were established or improved (Table 3). Native agarose gel electrophoresis (NAGE) was routinely used for HBcAg analysis, but could not be performed for HBsAg, as it does not carry a sufficient negative charge to run under the applied conditions.

Method	HBcAg	HBsAg
ELISA	✓	✓
WB	✓	✓
DLS	✓	✓
TEM	✓	✓
NAGE	✓	✗

Table 3. Different analytical methods for characterization of HBcAg and HBsAg.

As listed in Table 4, four different HBcAg providers were available for selection: Riga, CIGB, HMGU and HeberNasvac[®]. The latter was included out of interest as it consists of HBcAg as well as HBsAg and is a commercially available product. However, the provided concentration is too low for the TherVacB approach.

Provider	Genotype	Length	Molecular weight [kDa]
Riga	D	Full-length (AA 1-183)	21.1
CIGB	A	Full-length (AA 1-185)	21.3
HMGU	A	Truncated (AA 1-149)	16.8
HeberNasvac [®] (Heb)	A	Full-length (AA 1-185)	21.3

Table 4. Characteristics of investigated HBcAg from various providers.

All the HBcAg from different sources were detected by ELISA at similar concentrations (Figure 14A). ELISA findings were supported by comparable dynamic light scattering (DLS) curves detected for all candidates with the exception of HeberNasvac[®], which showed a broader curve as it contains both antigens (Figure 14B). DLS analysis also confirmed high purity of the samples, as only one narrow peak was detected for each of the tested HBcAg. In addition to ELISA and DLS measurements, NAGE was used as an independent test to analyze native HBcAg capsids (Figure 14C). During NAGE, the native HBcAg particles migrate as distinct sharp-edged bands through the gel [192]. The nucleic acids inside the particles were stained by Roti[®]GelStain followed by protein content staining with Coomassie brilliant blue. The various HBcAg samples efficiently assembled into capsids as sharp-edged bands were observed. The obtained bands for Riga and CIGB samples run at a comparable height. The HBcAg sample from HMGU represents the truncated form of HBcAg lacking the C-terminal nucleic acid-binding domain which is present in full-length HBcAg. Therefore, a slightly higher band was observed for the HMGU sample, due to its slightly reduced negative charge, in comparison to Riga and CIGB. In addition, a hardly visible band was determined for the HMGU sample by Roti[®]GelStaining, demonstrating the reduced content of nucleic acids in this HBcAg. The band of HeberNasvac[®] was observed at the same size as Riga and CIGB, but showed a reduced intensity, due to its low concentration. HeberNasvac[®] would require a sample volume exceeding the possible loading volume of one gel pocket to achieve a similarly strong signal as Riga and CIGB.

HBcAg-specific WB analysis showed bands on a similar size for Riga, CIGB and HeberNasvac[®] samples (Figure 14D). In contrast, lower bands and a higher concentration of HBcAg dimers were observed for the truncated HMGU sample when compared to other

samples. The signal of the Riga sample was weaker compared to the other antigens, possibly because the detection antibody binds less well to genotype D than to genotype A. Finally, the HBcAg samples were negatively stained and analyzed by TEM. As shown in Figure 14E, particles with the expected size of 27-34 nm were observed in all HBcAg samples. All TEM samples showed high purity confirming DLS data.

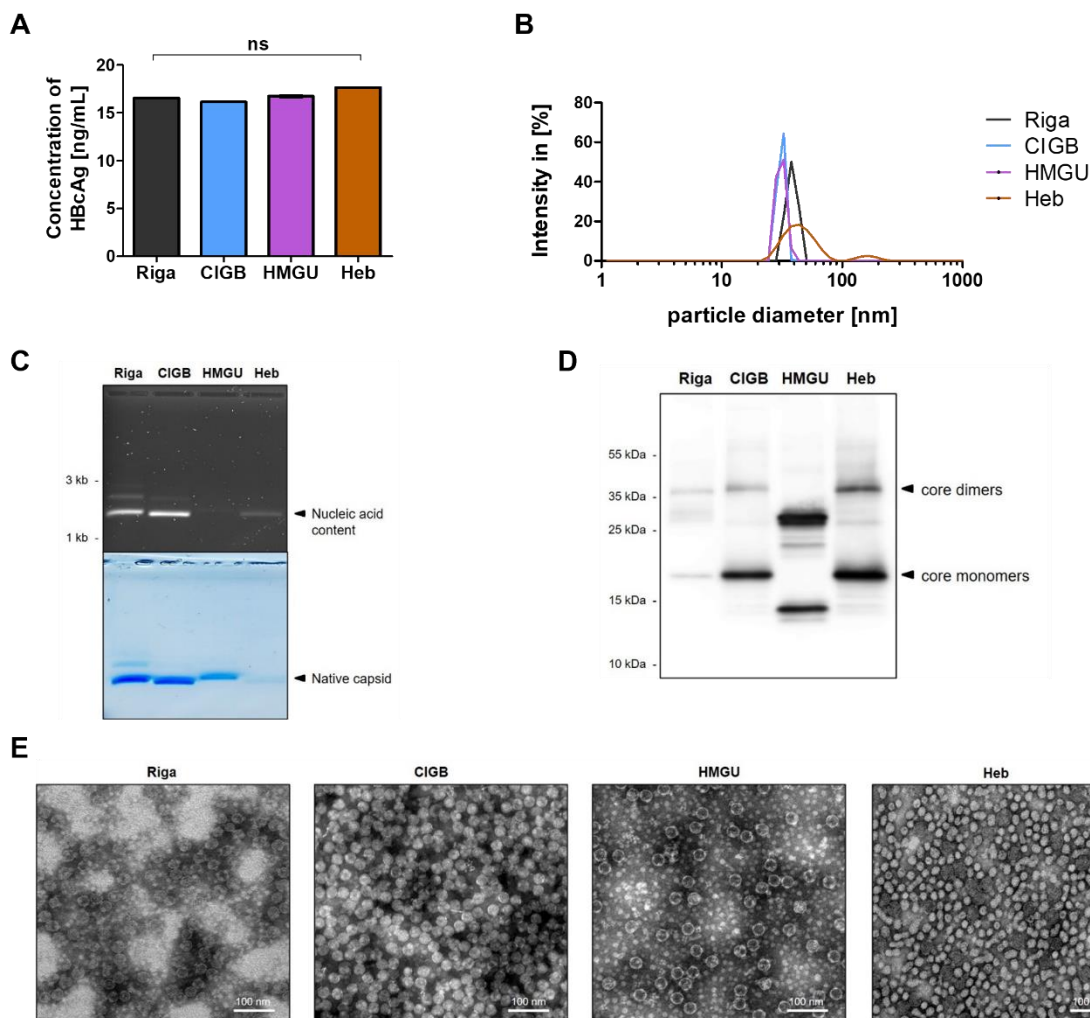


Figure 14. Comparison of HBcAg from different providers.

HBcAg samples from various manufacturers were analyzed by HBcAg-specific ELISA (A), DLS (B), NAGE (C), HBcAg-specific WB (D) and negative stain TEM analysis at a magnification of 40000x (E). Scales indicate 100 nm. Statistical analysis was performed using unpaired t-test. Asterisks mark statistically significant differences: ns - not significant.

The comparison of HBsAg from different manufacturers included four candidates: Biovac, CIGB, Dynavax and HeberNasvac[®], the mixture of both antigens (Table 5).

Provider	Genotype	Length	Molecular weight [unglycosylated; kDa]
Biovac	A	Full-length (AA 1-226)	25.3
CIGB	A	Full-length (AA 1-226)	25.3
Dynavax	A	Full-length (AA 1-226)	25.3
HeberNasvac [®] (Heb)	A	Full-length (AA 1-226)	25.3

Table 5. Characteristics of investigated HBsAg from various manufacturers.

All HBsAg samples from different suppliers were detected by ELISA at similar concentrations (Figure 15A). In addition, high purity of all HBsAg samples was observed by DLS (Figure 15B). Moreover, DLS analysis showed comparable particle diameters for HBsAg from Biovac, Dynavax and HeberNasvac®. In contrast, larger particle diameters were detected for HBsAg from CIGB. HBsAg-specific WB analysis showed bands at the same height for all candidates, except the Dynavax sample which ran slightly higher (Figure 15C). TEM analysis of all HBsAg samples displayed highly pure particles with a size of around 22 nm (Figure 15D). The comparatively larger size of CIGB HBsAg, which was detected by DLS, was not visible by TEM. A possible explanation could be that DLS analysis measures the overall hydrodynamic particle, which cannot be detected by TEM.

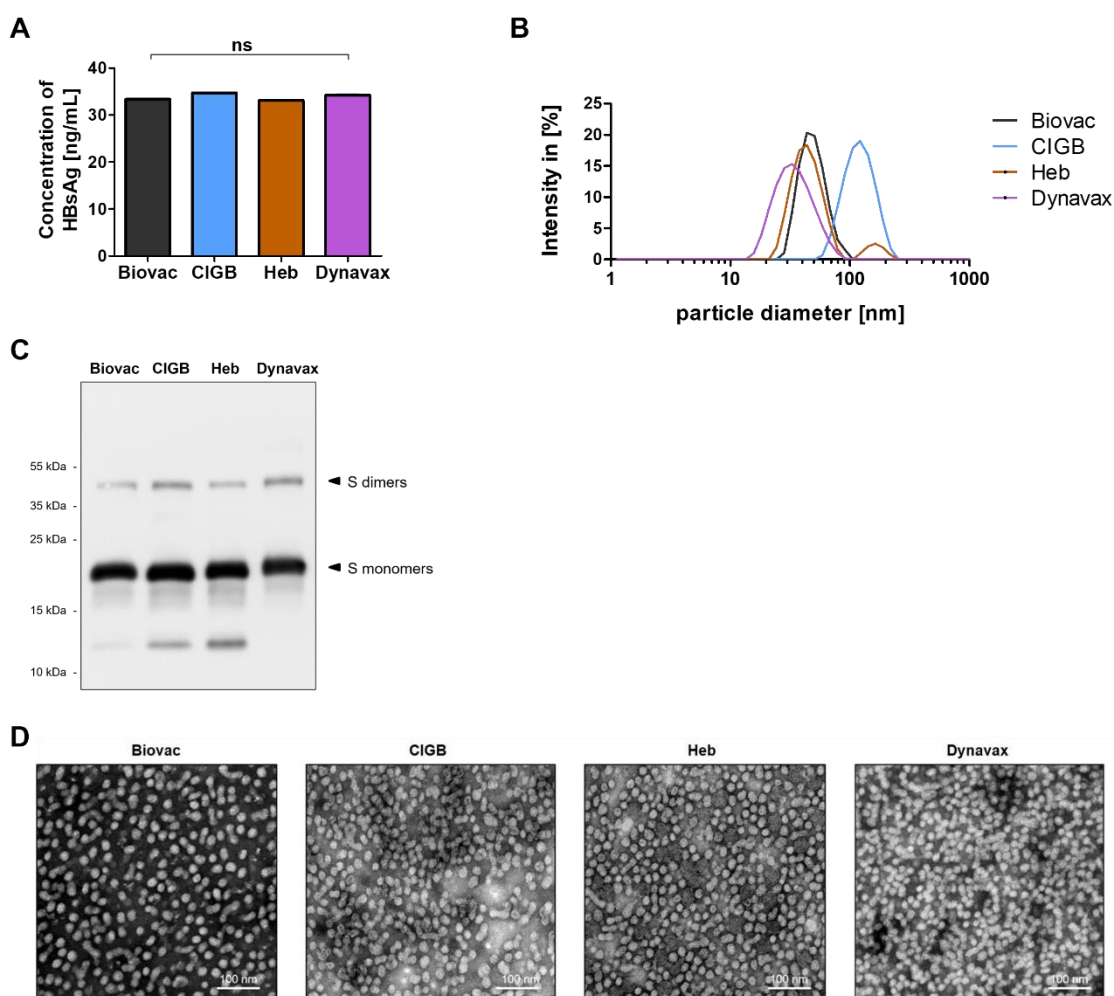


Figure 15. Comparison of HBsAg from different providers.

Various HBsAg samples were analyzed by HBsAg-specific ELISA (A), DLS (B), HBsAg-specific WB (C) and negative stain TEM analysis at a magnification of 40000x (D). Scales show 100 nm. Statistical analysis was performed using unpaired t-test. Asterisks mark statistically significant differences: ns - not significant.

Taken together, these data demonstrate a good integrity of HBcAg and HBsAg from different antigen manufacturers. The antigens of choice for the subsequent steps of this project were HBcAg from Riga and HBsAg from Biovac as they have suitable concentrations for *in vitro* and *in vivo* testing and were easily accessible in higher amounts. In addition, these antigens were already produced under good manufacturing practise (GMP) conditions providing an important benefit for the upscaling of the manufacturing process and the future use in the clinic.

2.1.4 Optimal storage conditions for HBV antigens

In order to examine the best storage conditions for HBcAg and HBsAg, the antigens were exposed to -80 °C, -20 °C and 4 °C for 3 days or 3 months. The strongest ELISA signal was detected for antigens which were stored at 4 °C (Figure 16A, B). A significantly reduced stability was observed for both antigens stored at lower temperatures, whereby slightly higher ELISA signals were detected after storing at -20 °C, compared to -80 °C. Interestingly, the comparison of both antigens showed more antigen loss for HBcAg after freezing than for HBsAg. The reduction of antigen was independent of storage time as similar values were detected after 3 days and 3 months for both antigens. The NAGE and WB analysis showed no noticeable differences between the examined storing conditions, therefore, the results of 3 months storage period, which are depicted in Figure 16C, D are representative for both time points. For further storage of the antigens, a temperature of 4 °C was chosen, as ELISA data demonstrated the maintenance of antigen integrity under this condition. These results were confirmed by the antigen providers.

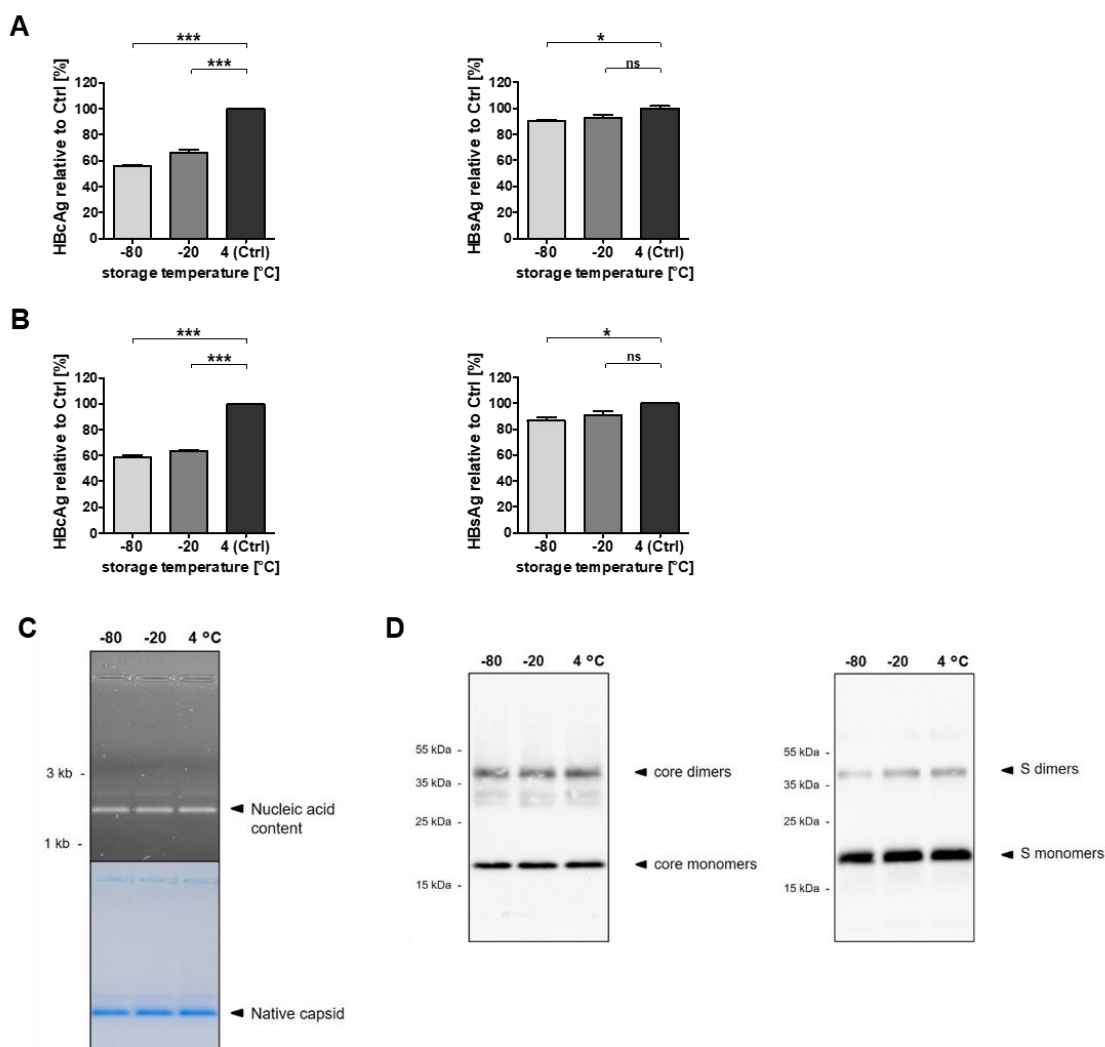


Figure 16. HBcAg and HBsAg demonstrated highest stability after storage at 4 °C.

Following HBcAg and HBsAg storage at -80 °C, -20 °C and 4 °C, HBcAg- and HBsAg specific ELISA was performed after 3 days (A) and 3 months (B) of temperature exposure. NAGE of HBcAg (C) and HBcAg- and HBsAg specific WB analysis (D) after 3 months storage period. Statistical analysis was performed using unpaired t-test. Asterisks mark statistically significant differences: * $p \leq 0.05$; *** $p \leq 0.001$; ns - not significant.

2.2 Loss of antigen integrity and MVA-S/C infectivity after a storage at higher temperatures over time

Since many vaccines lose their potency during storage outside the cold chain [133, 136], thermal stability of TherVacB components was evaluated. Therefore, non-stabilized single HBcAg, HBsAg and MVA-S/C kept in solution were exposed to a temperature gradient ranging from 25 °C up to 40 °C for 1, 3, 7, 14, 21 or 28 days. The temperature of 40 °C was chosen according to the WHO CTC guideline [134], whereas the temperature of 25 °C represents the upper limit of room temperature (RT). As positive controls the corresponding vaccine components stored under optimal conditions (antigens: 4 °C, MVA-S/C: -80 °C), were used (SM_{ctrl}).

After storage at 25 °C for 28 days, significantly decreased ELISA signals were detected for both antigens as compared to SM_{ctrl} (Figure 17A, B). The reduced stability was more pronounced for HBsAg (80 %) than for HBcAg (25 %). Already after 1 day of heat-exposure at 40 °C without stabilization, HBsAg showed a reduction of approximately 35 % of ELISA signal, whereas for HBcAg this decrease was lower (25 %). After exposing to WHO CTC criteria (40 °C for 3 days), a complete loss of HBsAg and a decrease of approximately 60 % of HBcAg integrity was observed. For HBcAg this trend continued over time leading to almost complete loss of the ELISA signal after 28 days at 40 °C (Figure 17B). A temperature reduction of 2 °C or 4 °C showed no positive effect on antigen integrity as a storage at 36 °C and 38 °C resulted in similar findings as for 40 °C (Figure 17A, B). The results of HBcAg-specific ELISA were additionally confirmed by NAGE.

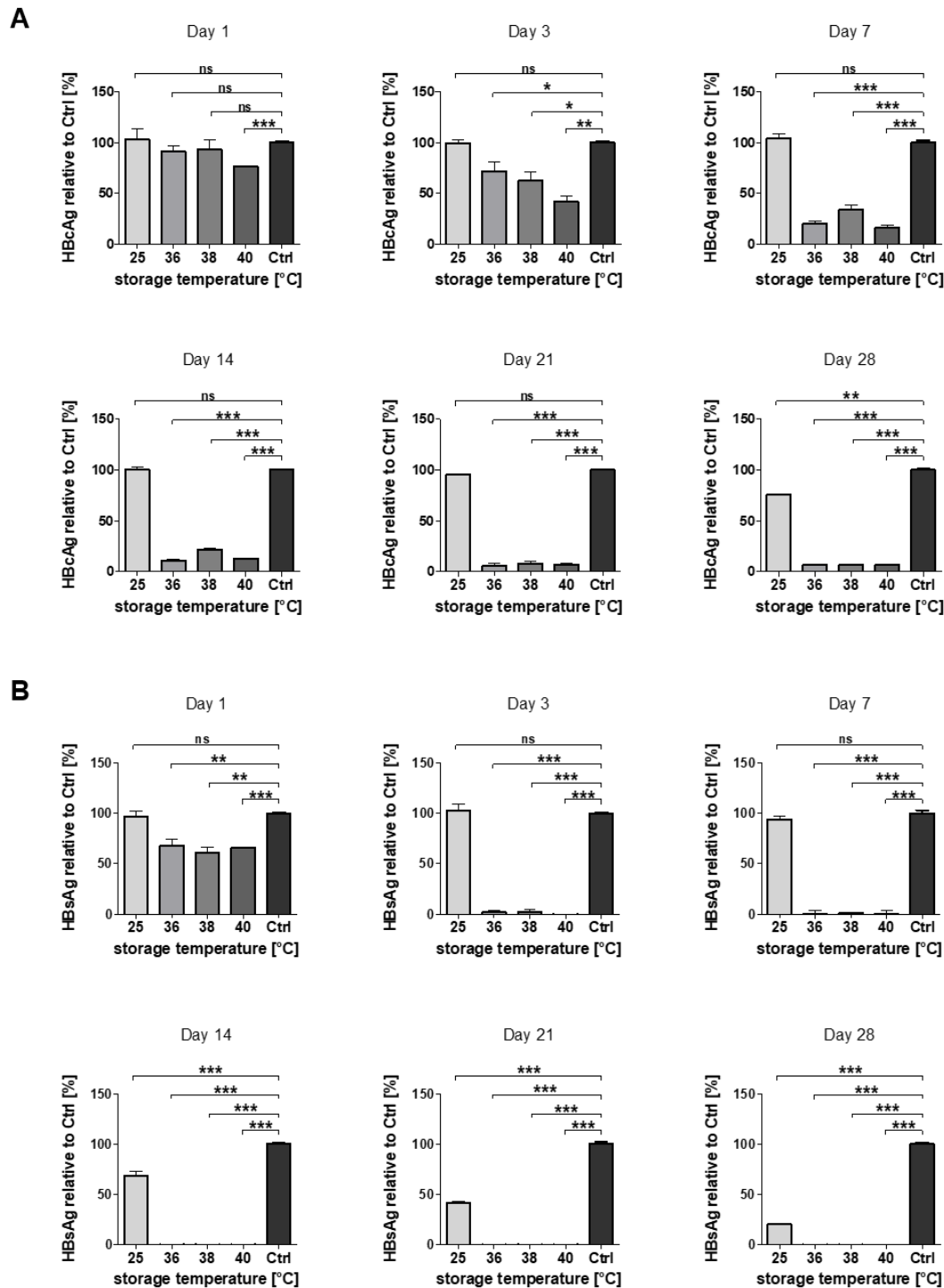


Figure 17. Heat-exposure led to antigen instability.

HBcAg and HBsAg samples were stored at 25 °C, 36 °C, 38 °C and 40 °C for 1, 3, 7, 14, 21 and 28 days. As control antigens, stored under optimal conditions (Ctrl), were used. Antigen integrity was analyzed by HBsAg- (A) and HBcAg-specific (B) ELISA. Statistical analysis was performed using unpaired t-test. Asterisks mark statistically significant differences: * $p \leq 0.05$; ** $p \leq 0.01$; *** $p \leq 0.001$; ns - not significant.

By analysing the MVA-S/C, a lower viral titer was determined after a storage at 25 °C for 28 days compared to SM_{Ctrl}, which was optimally stored at -80 °C (Figure 18). Interestingly, the MVA-S/C vector used in this study, proved to be quite stable at RT for the examined timeframe. In contrast, after exposing MVA-S/C to WHO CTC storage conditions (40 °C,

3 days), already a tenfold reduction of viral titer was detected, whereas only after 1 day of temperature stressing no decrease was observed compared to the SM_{Ctrl}. After heat-exposure for 14 days at 40 °C a complete loss of MVA-S/C infectivity was detected. The slight reduction in titer of the SM_{Ctrl} observed at day 28 compared to day 0, was most likely due to thawing and freezing steps this sample underwent.

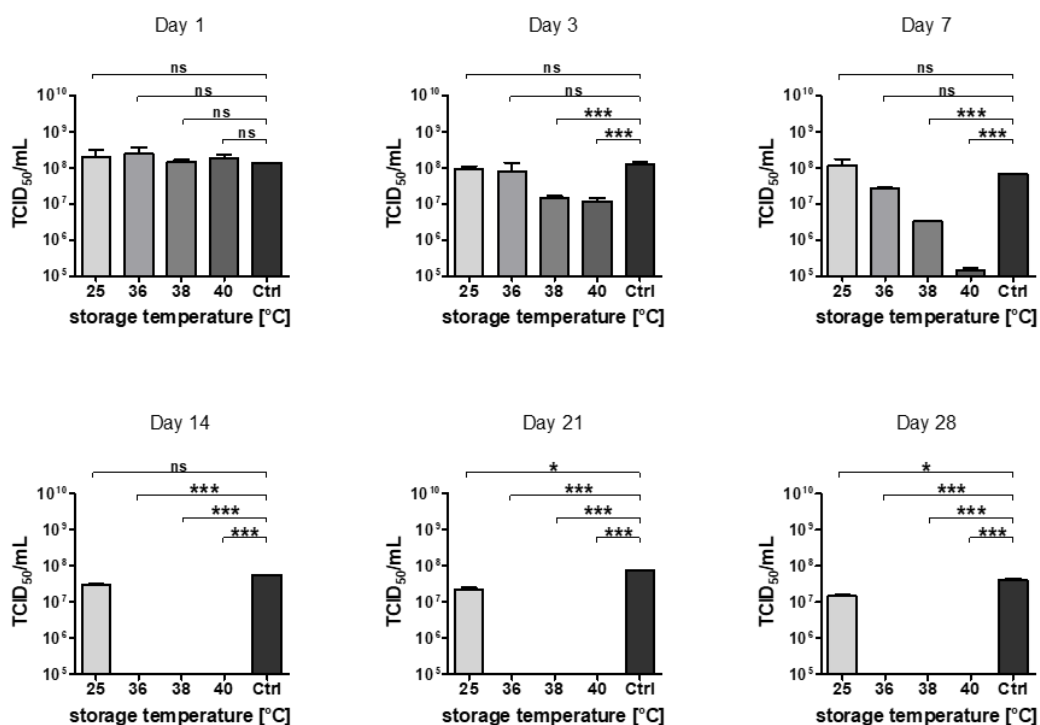


Figure 18. Heat-exposure resulted in reduction of MVA-S/C infectivity.

MVA-S/C samples were heat-exposed at 25 °C, 36 °C, 38 °C and 40 °C for 1, 3, 7, 14, 21 or 28 days. As control MVA-S/C, stored under optimal conditions (Ctrl), was used. MVA-S/C titers were determined by TCID₅₀. Statistical analysis was performed using unpaired t-test. Asterisks mark statistically significant differences: * $p \leq 0.05$; *** $p \leq 0.001$; ns - not significant.

In summary, these data indicate that stabilization of the vaccine components is essential to prevent loss of vaccine potency when the vaccine cannot be continuously cooled.

2.3 Impact of lyophilization on vaccine components *in vitro*

To facilitate TherVacB application worldwide, without the need to provide a cold chain, the chosen stabilization approach for the vaccine components was lyophilization in the presence of stabilizing amino acid-based formulations (SAAFs) selected from the LEUKOCARE database. As previously described, thermal stability could be considerably increased by freeze-drying of the vaccine components [147-149]. However, the addition of stabilizing reagents, called cryo- and lyoprotectants, is often needed to prevent damaging of the biological compounds, as the lyophilization process is associated with a high degree of stress for the biomolecules during freezing and drying steps [151, 153-155]. Therefore, in the next step the effect of lyophilization on TherVacB components was comprehensively analyzed. The exemplary results obtained for SAAF 1.1 (F1.1), which was finally selected as the most suitable

formulation for TherVacB components, are presented in the following. In addition, these data represent the results of day 0 of the short and long-term *in vitro* studies described in this thesis (chapter 2.5).

2.3.1 MVA-S/C

First, the impact of lyophilization on MVA-S/C was studied. To this end, vector samples were formulated with SAAF 1.1 (F1.1) or PBS and directly analyzed after lyophilization and reconstitution (referred as day 0). As a positive control, non-lyophilized, optimally stored MVA-S/C (SM_{Ctrl}) was used.

The addition of SAAF seemed to protect the MVA-S/C sample during freeze-drying as a good quality of the pharmaceutical cake structure, consisting of flaky flocks, was observed. In contrast, lyophilization without prior stabilization resulted in a thin, non-fluffy product with a much smaller size and a different shape than the SM_{Ctrl} (Figure 19A). Interestingly, similar MVA-S/C titers were observed in all three samples independent of lyophilization or stabilization status (Figure 19B).

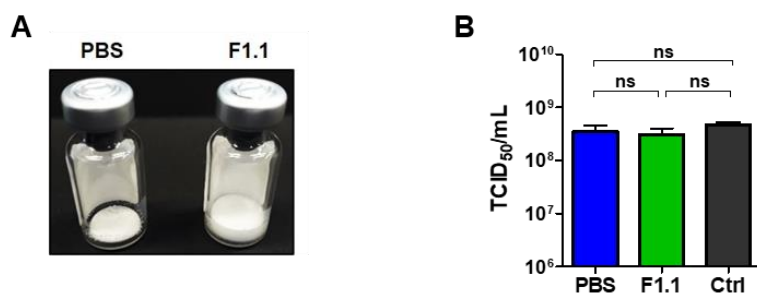


Figure 19. Lyophilization did not cause MVA-S/C infectivity reduction.

Stabilized (F1.1) or non-stabilized (PBS) MVA-S/C were directly analyzed after lyophilization. As control non-lyophilized, optimal stored MVA-S/C (Ctrl) was used. (A) Pharmaceutical cake structures. (B) MVA-S/C titers were determined by TCID₅₀. Statistical analysis was performed using unpaired t-test. Asterisks mark statistically significant differences: ns - not significant.

These data indicate that lyophilization does not negatively influence MVA-S/C infectivity.

2.3.2 Antigens

In contrast to the relatively stable MVA-S/C, this study showed that HBcAg integrity mainly decreased after freezing, whereas HBsAg was very unstable at high temperatures (Figure 16, Figure 17). Consequently, the question arose, whether the lyophilization process has a negative effect on HBV antigens, as freezing (-50 °C), primary- and secondary drying (-35 °C, 20 °C) steps occur during this procedure. Therefore, SAAF-stabilized (F1.1) and non-stabilized antigens (PBS) were comparatively analyzed directly after lyophilization and reconstitution either as single components or in combination. As positive controls single antigens without lyophilization (SM_{Ctrl}) were used.

After lyophilization, pharmaceutical cake structures as expected were observed for the SAAF-stabilized samples. The cake was localized on the bottom of the vial and displayed intact surfaces, fluffy, floc-like cake textures and similar volumes as the SM_{Ctrl} in solution (Figure 20A). In contrast, non-stabilized samples showed collapsed cakes with uneven surfaces and different shapes than SM_{Ctrl}.

ELISA data demonstrated that the lyophilization process led to a complete loss of HBcAg integrity in the non-stabilized sample (Figure 20B). Even with SAAF-mediated stabilization, a reduced ELISA signal of HBcAg was measured compared to SM_{Ctrl}. The loss of single component stability was also detected for HBsAg, although it was not as pronounced as for HBcAg. Interestingly, the data clearly showed that the combination of both antigens resulted in increased stability of HBcAg and HBsAg. The addition of SAAF to the combined antigens completely abolished the negative effects of lyophilization.

HBcAg-specific ELISA results were supported by NAGE, which showed similar signals for the SAAF-stabilized antigen combination and the SM_{Ctrl} (Figure 20C), while SAAF-stabilized single HBcAg displayed a weaker signal. After lyophilization of single HBcAg in PBS, no signal was detected anymore, whereas the combined antigens were clearly detected, although the signal was weak. The slight smear observed in the samples of the antigen combinations results from the addition of HBsAg in these formulations.

The beneficial influence combining both antigens and SAAF-stabilization was further confirmed by DLS analysis, as similar curves were measured for stabilized, combined antigens and SM_{Ctrl} (Figure 20D). In contrast, larger diameter of particles was observed for the non-stabilized samples. Large particle diameters, indicating aggregates, were detected, especially for the non-stabilized single HBcAg and the correlation function of this measurement was almost not evaluable.

SE-HPLC analysis demonstrated increased stability of the single antigens formulated with SAAF, whereby a slightly lower peak was detected for the stabilized HBcAg compared to the stabilized HBsAg or the SM_{Ctrl} (Figure 20E). No peak was measured if HBcAg only was lyophilized in PBS, whereas the single HBsAg showed a considerable reduction in signal compared to the SAAF-stabilized HBsAg or SM_{Ctrl}. The SAAF-stabilized combination of the antigens displayed a similar peak as the SM_{Ctrl}, confirming the beneficial impact of SAAF on the antigen combination. The non-stabilized, combined antigens showed a reduced peak intensity of the main peak compared to SM_{Ctrl} and a shoulder eluting before the main peak suggesting the formation of aggregates.

HBcAg- and HBsAg-specific WB analysis confirmed the positive effects of both, antigen combination and stabilization with SAAF during freeze-drying (Figure 20F). Similar antigen-specific bands of expected size were detected for all SAAF-stabilized samples. In contrast, lyophilization of single HBcAg in PBS led to a very weak WB signal compared to SM_{Ctrl}. However, non-stabilized, combined antigens showed similar bands as the SM_{Ctrl}. The HBsAg-specific WB analysis demonstrated comparable bands of the expected size for all samples indicating that lyophilization did not lead to the degradation of HBsAg.

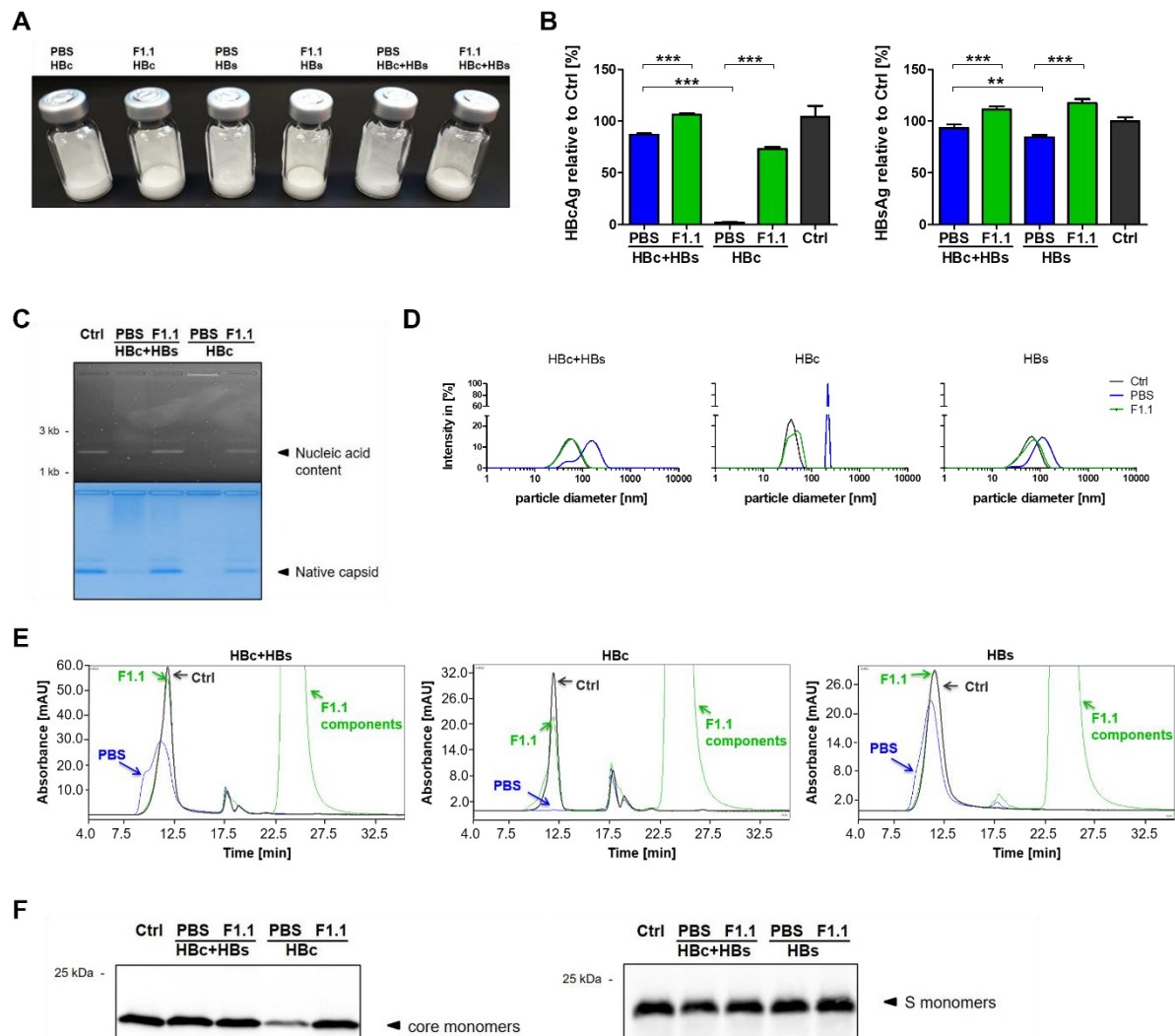


Figure 20. Negative impact of lyophilization on antigen integrity.

Stabilized (F1.1) and non-stabilized (PBS) HBcAg and HBsAg in combination or as single components, were comprehensively studied directly after lyophilization. As control non-lyophilized, optimal stored antigens (Ctrl) were used. (A) Pharmaceutical cake structures. (B) HBcAg- and HBsAg-specific ELISA. (C) NAGE of HBcAg. DLS (D), SE-HPLC (E) and HBcAg- and HBsAg-specific WB (F) analysis. Statistical analysis was performed using unpaired t-test. Asterisks mark statistically significant differences: ** $p \leq 0.01$; *** $p \leq 0.001$.

Taken together, these data demonstrate that the negative effect of lyophilization, in particular for the HBcAg, was prevented by combining both HBV antigens with SAAF in one formulation.

2.3.3 Impact of storage time after reconstitution on TherVacB vaccine

Many lyophilized vaccines should be administered as soon as possible or at the latest six hours after reconstitution, as they lose their potency very fast [133, 136]. Therefore, throughout this study the samples for *in vitro* analysis or *in vivo* application were used within two hours after reconstitution and stored at 4 °C until use. To examine the impact of storage duration after reconstitution on the stability of TherVacB components, first SAAF-stabilized (F.1.1) and non-stabilized (PBS) HBV antigens were analyzed by ELISA directly on the day of reconstitution or one day after reconstitution (a.R). Storage of the samples between

reconstitution and analysis was always at 4 °C (Figure 21A). As positive control SM_{Ctrl} without lyophilization was used.

Lower ELISA signals were measured for HBcAg and HBsAg 1 day a.R. as compared to directly analyzed antigens confirming that the reconstituted samples lost integrity over time, independently of stabilization (Figure 21B). Nevertheless, significantly higher signals were measured for the SAAF-stabilized samples than for the non-stabilized samples.

All HBcAg and HBsAg-specific ELISA of lyophilized samples throughout this thesis were performed three times independently to confirm the results. Each repetition resulted in similar findings, as it is representatively shown in Figure 21B for the two experiments. However, the presentation of an average result obtained from the three independent experiments on one graph was not possible as different values were measured due to the decrease in antigen integrity a.R. That is why throughout this thesis one representative ELISA containing technical triplicates is shown for every experiment.

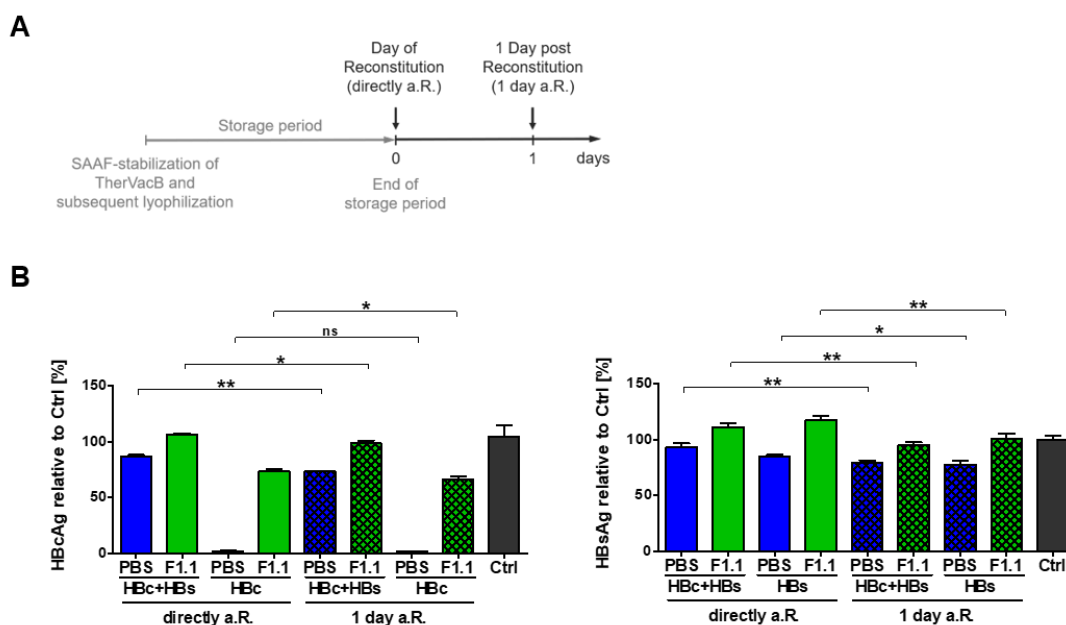


Figure 21. Antigen integrity of reconstituted samples decreased after 1 day of storage.

Stabilized (F1.1) and non-stabilized (PBS) HBcAg and HBsAg in combination or as single components, were lyophilized, stored and reconstituted. The HBcAg- and HBsAg-specific ELISA was performed directly after reconstitution (a.R.) or 1 day a.R. upon overnight storage at 4 °C. As control non-lyophilized antigens (Ctrl) were used. (A) Experimental set-up. (B) HBcAg- and HBsAg-specific ELISA. Statistical analysis was performed using unpaired t-test. Asterisks mark statistically significant differences: * $p \leq 0.05$; ** $p \leq 0.01$; ns - not significant.

To investigate the impact of storage time after reconstitution on MVA-S/C infectivity, viral titers in reconstituted samples were determined directly a.R. and 3 months later upon storage at 4 °C. Such a long storage period was chosen, as in previous experiments (chapter 2.1.2, 2.3.1) no influence of lyophilization process on MVA-S/C infectivity and a high stability at 4 °C was observed. Therefore, no reduction in viral titers was expected 1 day a.R. upon overnight storage at 4 °C.

As shown in Figure 22, no differences in MVA-S/C titers were determined between the samples analyzed on the day of reconstitution and 3 months a.R.

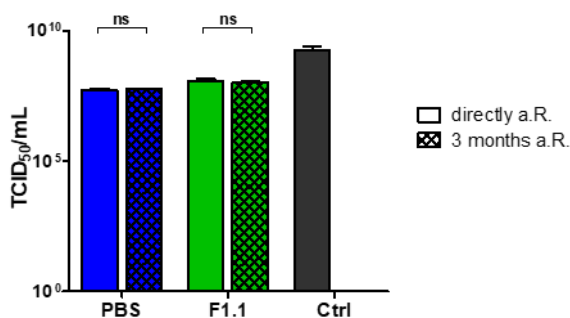


Figure 22. No influence on MVA-S/C infectivity after storage of reconstituted samples for 3 months.

Stabilized (F1.1) and non-stabilized (PBS) MVA-S/C were analyzed and reconstituted. As control non-lyophilized MVA-S/C (Ctrl) was used. TCID₅₀ based determination of viral titers was performed directly a.R. and after 3 months a.R. upon storage at 4 °C. Statistical analysis was performed using unpaired t-test. Asterisks mark statistically significant differences: ns - not significant.

The data demonstrate that reconstituted HBcAg and HBsAg samples lost integrity over time. To secure the antigen potency, lyophilized HBcAg and HBsAg have to be applied as soon as possible after reconstitution. In contrast, the storage time of reconstituted MVA-S/C sample showed no impact on MVA-S/C titer confirming the high stability of the vector.

2.4 Selection of most suitable stabilization formulation

2.4.1 Initial selection of SAAF variants for stabilization of HBcAg

For the development of a thermostable vaccine, the addition of stabilizing excipients to the formulation is necessary to protect the biological compounds from damages caused by lyophilization or thermal stressing [151, 153-155]. To achieve high stability of TherVacB vaccine, the SAAFs from LEUKOCARE database were employed. The LEUKOCARE library combines detailed information from literature and previous projects, molecular structures of target molecules, important chemical and physical molecular degradation pathways of biological molecules in defined stress situations as well as the effectiveness of individual excipients for protecting against these circumstances and the respective degradation pathways [180]. Therefore, it allowed a fast preselection of potentially suitable formulations for the TherVacB components.

For initial testing, 32 different SAAFs were selected from the LEUKOCARE database as potential candidates to stabilize HBcAg. As shown in Figure 23A, the main excipient mixture chosen for this project is SAAF I. SAAF II-VIII are modified compositions derive from the main excipient mixture. Every group of excipient mixtures (SAAF I-VIII) was further modified leading to four subgroups (A-D). They consist of one, two or three additional components, which are the same for each subgroup. These are trehalose (a disaccharide of two α -1, 1-glycosidic linked glucose molecules), with or without glycyrrhizinic acid (a saponin and triterpenoid from the roots of the liquorice plant) and with or without chitosan (a naturally occurring polysaccharide derived from chitin). This project was performed in cooperation with Dr. Katrin Singethan and Dr. Clemens Jäger.

In order to test the stabilization effect of various excipients, lyophilized and SAAF-stabilized HBcAg samples were stored at 45 °C for 28 days and afterwards thoroughly analyzed. The temperature of 45 °C was chosen to cause maximal thermal stress for the antigen and slightly differs from the temperature which was predominantly used in this study (40 °C). As negative control lyophilized, non-stabilized antigen (PBS) and as positive control SM_{Ctrl} without lyophilization, stabilization or temperature stressing were used. In this thesis, only the group I (SAAF I A-D) is presented, as an example of the comprehensive analysis of the 32 different SAAFs.

The stabilization of HBcAg with subgroups A and B of SAAF group I led to efficient assembly of capsids, as similar signals were detected by NAGE at days 0 and 28 for stabilized samples and SM_{Ctrl} (Figure 23B). In contrast, non-stabilized samples showed loss of antigen integrity already after lyophilization as no NAGE signal was detected. All HBcAg samples additionally stabilized with chitosan (SAAF I C and D) stuck in the pocket of the agarose gel indicating formation of large aggregates. DLS analysis confirmed the efficient stabilization of HBcAg with SAAF I A and B (Figure 23C). In addition, the presence of large aggregates in samples stabilized with SAAF I C and D directly after lyophilization at day 0 and 28 days later was confirmed by DLS analysis. The correlation function of measurements of HBcAg formulated with SAAF I D was even not evaluable.

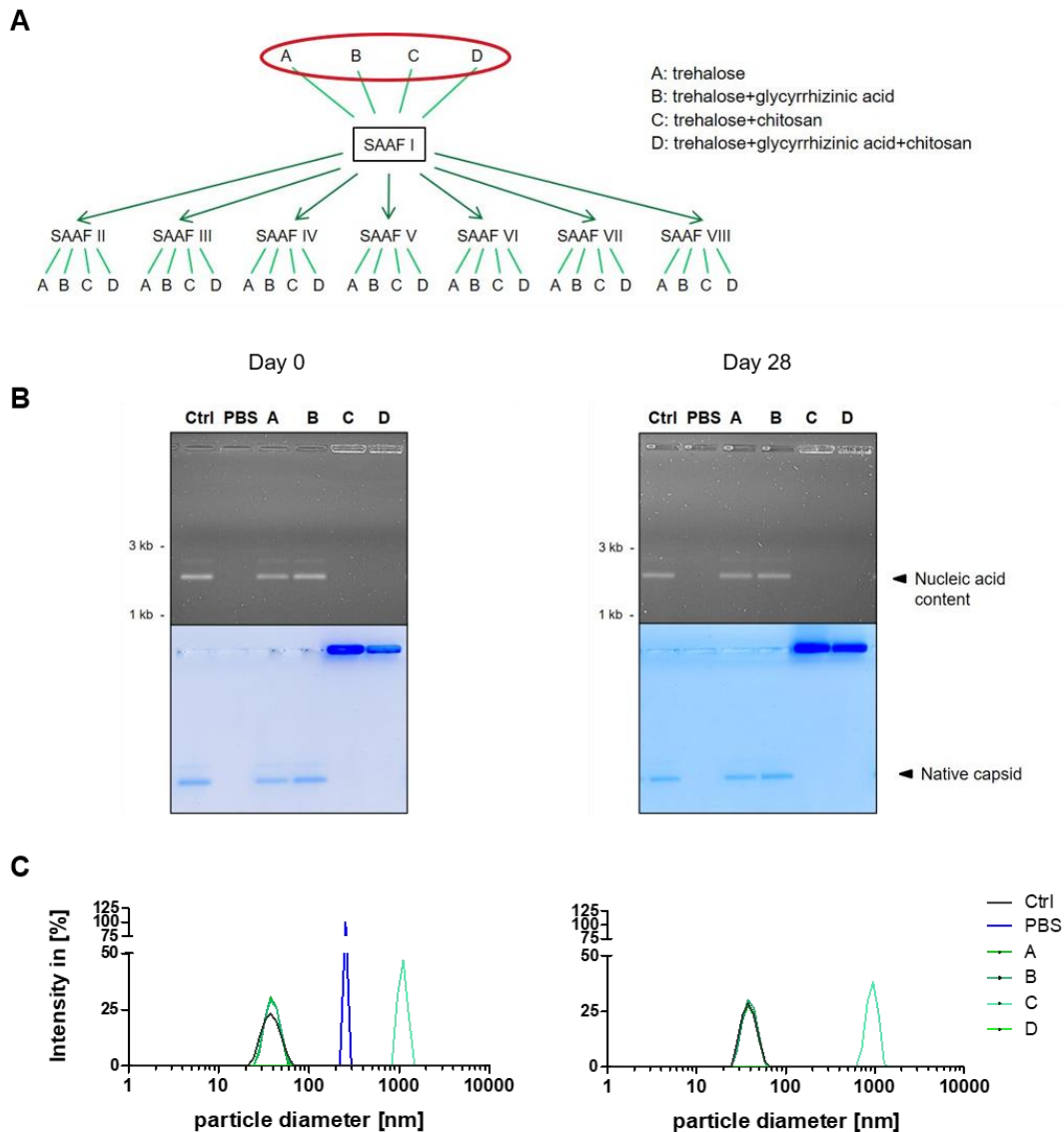


Figure 23. SAAF I A and B stabilized HBcAg during lyophilization and storage at 45 °C for 28 days.

(A) Overview and origins of 32 preselected SAAFs tested throughout this study. SAAF I represents the main excipients mixture and SAAF II-VIII are modified compositions derive from this mixture. Every group (SAAF I-VIII) was further modified leading to four subgroups A-D, which additionally contained trehalose, with or without glycyrrhizinic and with or without chitosan. Exemplary analysis of HBcAg stabilized with exceptions of group I (SAAF I A-D), marked by red ellipse, are shown. SAAF I A-D-stabilized and non-stabilized (PBS) HBcAg samples were lyophilized and analyzed directly (day 0) or after a storage at 45 °C for 28 days. As control HBcAg without lyophilization, stabilization and storage (Ctrl) was used. (B) NAGE and (C) DLS analysis.

These data demonstrate that SAAF I A and B efficiently stabilized HBcAg, in contrast to SAAFs containing chitosan (SAAF I C, D). In additionally performed comprehensive analysis, SAAF I A was proven to be the most suitable SAAF for HBcAg (unpublished data; [193]).

2.4.2 Selection of most suitable SAAF for stabilization of HBsAg

The results of this study clearly showed that effective heat-stabilization of HBsAg, the second component of priming TherVacB immunization, is crucial (Figure 17). Therefore, the next part

of the study aimed to choose the most optimal SAAF, which would allow for effective HBsAg stabilization. As shown in Figure 24A, HBsAg was formulated with nine different SAAFs variants (F1-F9), which represent modifications of SAAF I A, previously determined as the most suitable candidate for HBcAg (chapter 2.5.1). SAAF I A is referred to as A from here on.

To determine the stabilizing efficacy of the selected SAAFs (F1-F9 and A), lyophilized and SAAF-stabilized HBsAg was exposed to 40 °C/75 % relative humidity (RH) for 0, 3, 14 or 28 days. The temperature of 40 °C was chosen as it is required within the WHO CTC guideline, whereas an exposure time longer than the recommended 3 days was applied to challenge the SAAFs against a more severe stress situation. In contrast to the presented HBcAg results, these experiments were conducted according to International Council for Harmonisation of Technical Requirements for Pharmaceuticals for Human Use (ICH)-conditions, defining that stressing in certain temperatures should be combined with specific RH values for the stability testing of medicinal products [194]. The aim of ICH is the harmonisation of the evaluation criteria of human medicinal products as a basis for drug approval in Europe, the USA and Japan [195]. Since the foundation of this organization, several uniform, recommending guidelines (ICH-guidelines) for the evaluation of quality, efficacy and safety of medicinal products as well as preclinical and clinical requirements were published and implemented in the participating countries. One of the ICH-guidelines specifies that a temperature of 40 °C should be applied together with 75 % RH. These parameters (40 °C/75 % RH) also describe the conditions, which are used for accelerated aging studies during pharmaceutical development.

In the experiments lyophilized, non-stabilized vaccine components were included as negative controls (PBS). As positive controls, the vaccine components without lyophilization, stabilization or temperature stressing (SM_{Ctrl}) were used. During this experimental setup other glass vials were utilized as the volume of the samples tested here was lower. In addition, the samples were dialysed into the corresponding SAAF instead of diluting HBsAg in SAAF.

The HBsAg-specific ELISA and DLS analysis of SAAF-stabilized samples showed that all of the tested SAAFs (F1-F9, A) stabilized HBsAg over time with comparably high efficacies, which nearly reached the signal of SM_{Ctrl} (Figure 24B, C). The ELISA signals and particle diameters, determined by DLS, vary only slightly within one sample at examined time points. In contrast, lyophilization of non-stabilized HBsAg resulted in approximately 50 % integrity loss in terms of ELISA activity, compared to SM_{Ctrl} (Figure 24B). After storage at 40 °C, hardly detectable ELISA signal was observed for the non-stabilized sample already from day 3 onwards. In addition, DLS measurements displayed large particle diameters after lyophilization in PBS (day 0) and a non-evaluable measurement at day 3, 14 and 28 (Figure 24C).

The analysis of the different cake structures and SE-HPLC measurements over time partially showed large deviations of the stabilization effect of various SAAFs. To simplify the data presentation, the exemplary comparison of SAAF 1, SAAF 8 (further referred as F1 and F8) and PBS without storage (day 0) and after 28 days heat-exposure is shown in Figure 24D, E. The comparison of various cake structures after lyophilization demonstrated a good quality of cake structure for the F1-stabilized sample, in contrast to the worse cake appearance of the F8-stabilized HBsAg (Figure 24D). After 28 days of storage, cake quality was reduced for all

formulations, however a better cake structure was still observed for the F1-stabilized sample than for F8 (Figure 24E). Interestingly, after 14 days the F1-stabilized sample still showed a good quality of cake structure, whereas for the F8-stabilized HBsAg the cake appearance was continued to worsen. In case of the non-stabilized sample (PBS), already after lyophilization a collapsed cake was observed (Figure 24D).

SE-HPLC analysis demonstrated that all investigated SAAFs stabilized HBsAg despite extensive temperature stressing (Figure 24D, E). However, the F8-stabilized sample showed a different curve pattern compared to F1-stabilized HBsAg, suggesting the formation of aggregates in the sample formulated with F8. This observation was even more evident after 28 days (Figure 24E). In addition, the curve indicated a degradation shoulder after the peak in the F8-stabilized sample after a 28 days storage period. However, by comparing the results of SAAF-stabilized samples to non-stabilized ones, the beneficial stabilization effect of all SAAFs on HBsAg was clearly seen. Lyophilization in PBS resulted in a strongly decreased peak, which refers to aggregates, and after 28-days heat-exposure no peak was detected anymore.

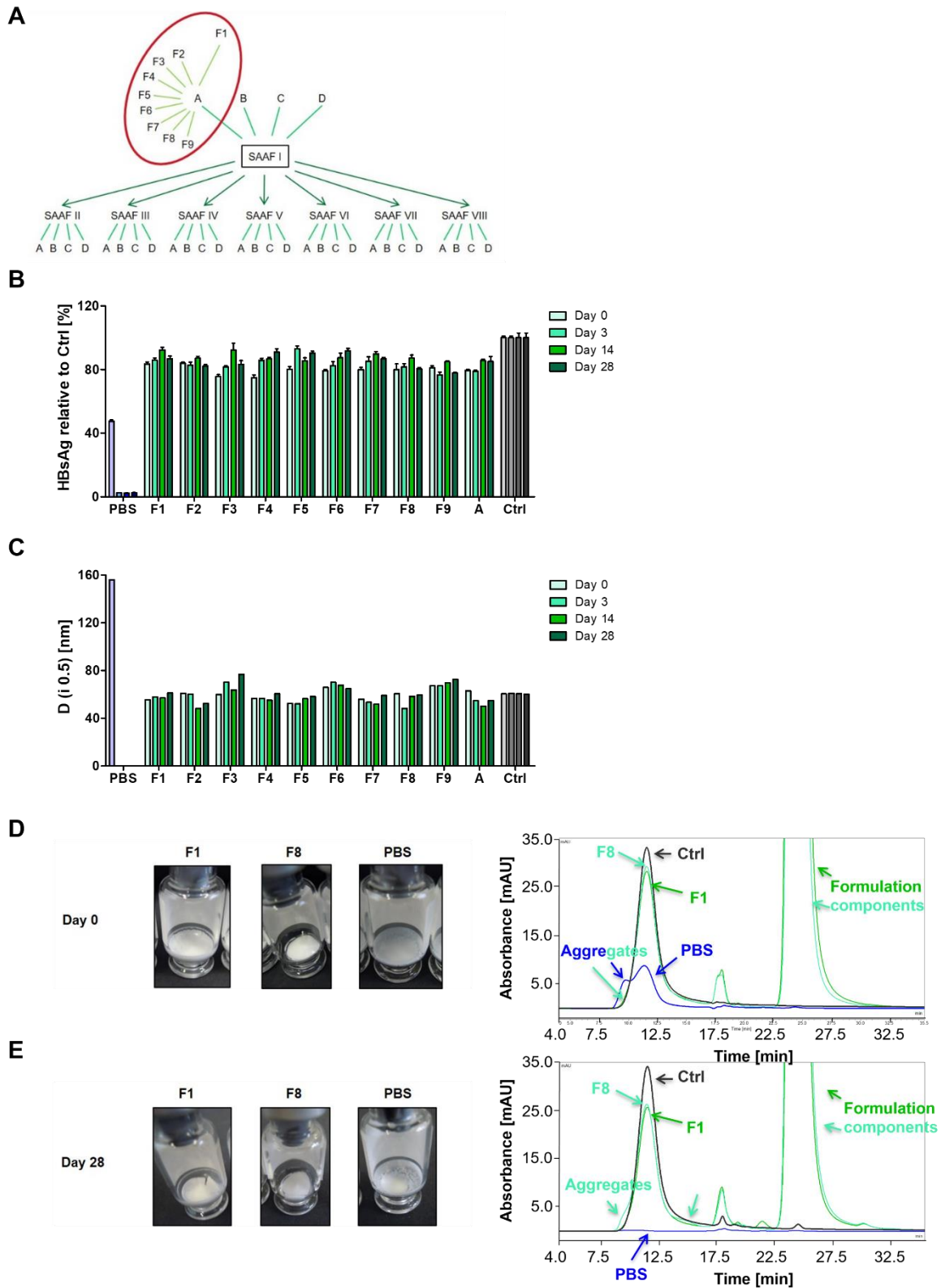


Figure 24. Selected SAAFs efficiently stabilized HBsAg.

(A) Overview and origins of ten preselected SAAFs tested in this study, marked by red ellipse. SAAF F1-F9 were created based on SAAF I A (referred as A). SAAF F1-F9, A-stabilized and non-stabilized (PBS) HBsAg samples were stored at 40 °C/75 % RH for 0, 3, 14 or 28 days and comprehensively analyzed over time. As control HBsAg without lyophilization, stabilization and storage (Ctrl) was used. HBsAg-specific ELISA (B) and DLS analysis (C). The D (i 0.5) value describes the mean size, where 50 % of all particles is smaller than the measured one. Pharmaceutical cake structures (D) and SE-HPLC chromatograms (E) of F1, F8 and PBS without (day 0) and after 28 days heat-exposure.

In summary, all investigated SAAFs demonstrate beneficial effects on HBsAg stability, albeit with different efficacies. To select the most suitable SAAF for HBsAg, all results were precisely compared to define the SAAF with the most similar values as the SM_{Ctrl} and the most consistent results over time in all applied methods. In addition, the selection process was supported by experiences from several related LEUKOCARE projects. Finally, SAAF 1 (F1) was chosen for further analysis.

2.4.3 Selection of most suitable SAAF stabilizing the combination of HBcAg and HBsAg

The combination of the vaccine components HBsAg and HBcAg with a single SAAF in one formulation could significantly facilitate the TherVacB application, as only one injection per prime immunization would be necessary. In a previous chapter (2.4.2), it was shown that combined HBcAg and HBsAg demonstrated a better stability than the single components after lyophilization. As very similar SAAFs were selected for single HBcAg and HBsAg, it was expected that these formulations can also stabilize the antigens in combination. To improve the stabilizing efficiency of the HBcAg and HBsAg combination with SAAF even more, further ten SAAFs (F1.2-F1.11) were chosen (Figure 25A). These formulations are modifications of SAAF 1 (F1 further referred as F1.1), which was selected as the most suitable SAAF for HBsAg. SAAF I A was not further included, as it was previously shown that SAAF I A did not stabilize HBsAg as well as HBcAg (Figure 24). Since HBcAg demonstrated a higher stability than HBsAg during temperature exposure (Figure 17) and SAAF 1 contained a very similar excipients composition as SAAF I A, it was assumed that this formulation can also stabilize HBcAg very well.

Previously, the SAAF-stabilization during storage at higher temperatures was proven for the single antigens (chapter 2.4.1, 2.4.2). Therefore, the chosen SAAFs (F1.1-F1.11) were tested within these experiments regarding the lyo- and cryoprotection of the antigen combination during lyophilization without storage (day 0). As positive controls vaccine components without lyophilization or stabilization (SM_{Ctrl}) were used.

The detailed analysis of SAAF-stabilized and non-stabilized samples demonstrated that all eleven selected SAAFs stabilized the combined antigens during lyophilization. Pharmaceutical cake structures as expected were observed for all SAAF-stabilized samples (Figure 25B). The cakes were located completely at the bottom of the vial and consisted of fluffy flocs of uniform color, texture and straight surfaces, comparable to the control sample SM_{Ctrl} . By contrast, the non-stabilized sample showed a collapsed cake.

The results of ELISA, NAGE, DLS and WB analysis clearly demonstrated that the addition of all tested SAAFs maintained integrity of HBcAg and HBsAg combination during lyophilization. Interestingly, all tested SAAF candidates showed comparably outstanding stabilizing efficacy by reaching signals and curves similar to SM_{Ctrl} (Figure 25C-F). In contrast, lyophilization in PBS resulted in a loss of antigen integrity since a reduced signal was observed in ELISA and no signal was determined by NAGE (Figure 25C, D). In addition, unusually large particles were

detected by DLS (Figure 25E). Only by HBcAg- and HBsAg-specific WB analysis, similar signals were detected for SAAF-stabilized and non-stabilized samples, confirming the previous data that lyophilization followed by temperature exposure did not result in degradation of HBsAg when combined with HBcAg (Figure 25F). The effect of lyophilization on antigens was described in detail in chapter 2.3.2.

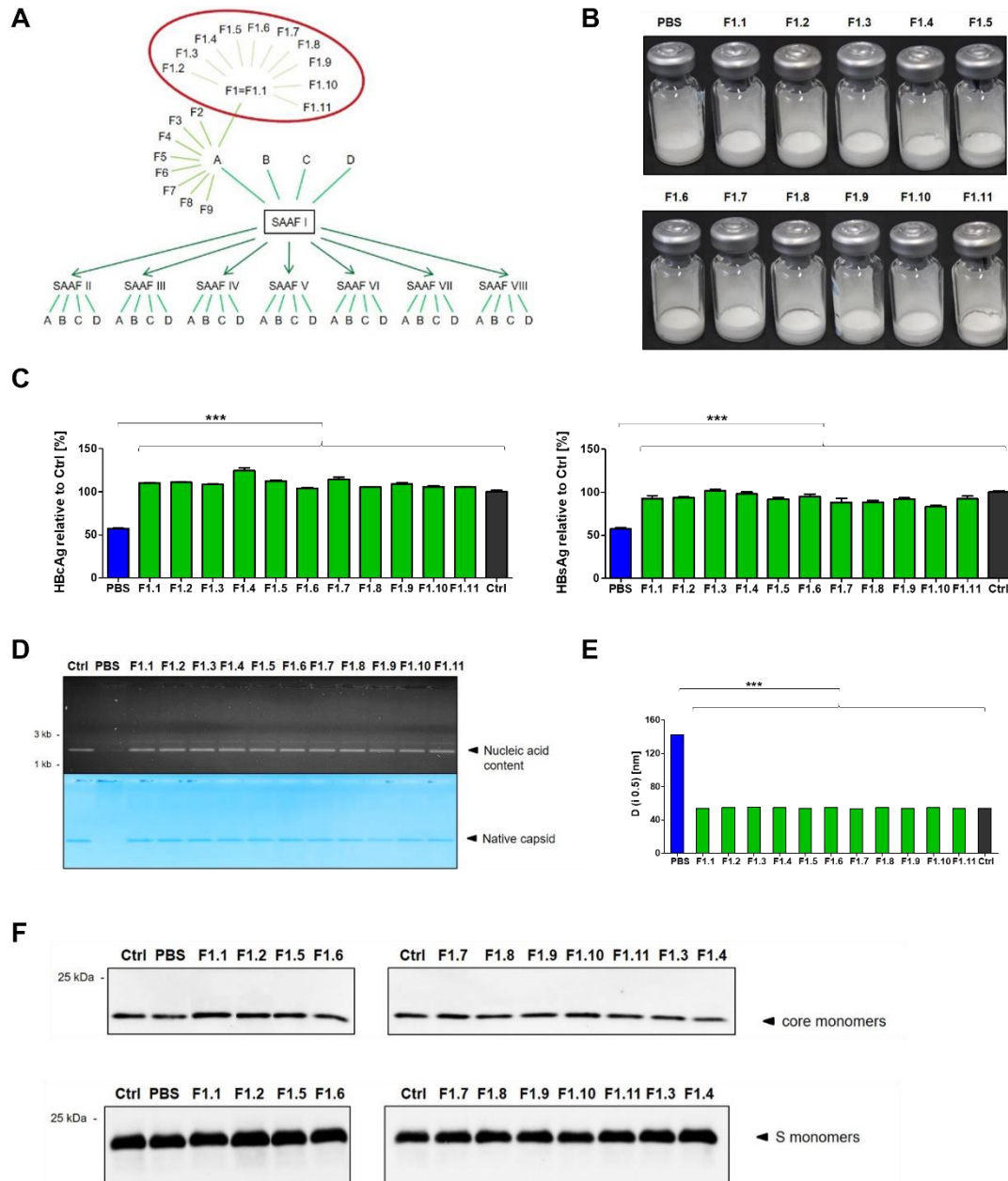


Figure 25. All selected SAAFs stabilized antigen combinations during lyophilization.

(A) Overview and origins of eleven preselected SAAFs tested in this study, marked by red ellipse. SAAF F1 is referred as F1.1. SAAF F1.2-F1.11 were created based on SAAF F1. SAAF F1.1-F1.11-stabilized and non-stabilized (PBS) antigen combinations were comprehensively studied after lyophilization (day 0). As control antigens without lyophilization, stabilization and storage (Ctrl) were used. (B) Pharmaceutical cake structures. (C) HBcAg- and HBsAg-specific ELISA. (D) NAGE of HBcAg. (E) DLS analysis. The D (i 0.5) value describes the mean size, where 50 % of all particles is smaller than the measured one. (F) HBcAg- and HBsAg-specific WB analysis. *** $p \leq 0.001$.

Taken together, these data demonstrate that all selected SAAFs efficiently stabilized HBV antigen combinations. However, minor differences detected by ELISA and experiences from other LEUKOCARE projects resulted in the selection of SAAFs 1.1-1.4 for further experiments.

2.4.4 Final selection of most suitable SAAF for TherVacB vaccine in HBV-naïve mice

After selection of the most suitable four SAAFs (F1.1-1.4) *in vitro*, an *in vivo* experiment in HBV-naïve mice (C57BL/6) was performed to identify the best candidate for the TherVacB approach. This experiment was performed in cooperation with Dr. Anna Kosinska. The specific excipients of the SAAFs F1.1-F1.4 are listed in Table 6.

SAAF	Excipients
F1.1	Alanine, Arginine, Glutamic acid, Lysine, Histidine, Tryptophan, Citric acid, Trehalose, pH 7
F1.2	Alanine, Arginine, Glutamic acid, Histidine, Tryptophan, Methionine, Glutamine, Citric acid, Trehalose, Sorbitol, Mannitol, Polysorbate 80, pH 7
F1.3	Alanine, Arginine, Glutamic acid, Lysine, Histidine, Glycine, Sucrose, Mannitol, pH 7
F1.4	Alanine, Arginine, Glutamic acid, Histidine, Tryptophan, Methionine, Glutamine, Proline, Citric acid, Trehalose, Polysorbate 80, pH 7

Table 6. Excipients of the SAAFs F1.1-F1.4.

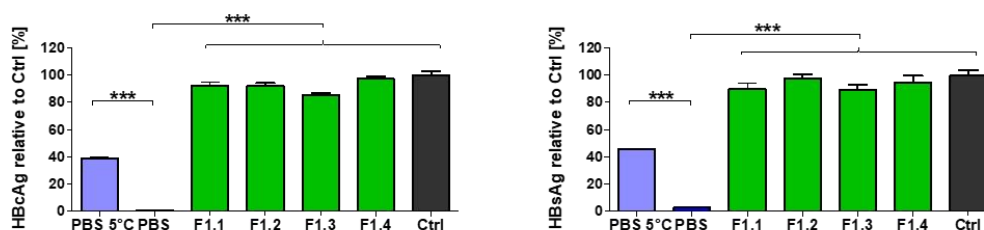
The SAAF-stabilized (F1.1-F1.4) and non-stabilized (PBS) vaccine components were heat-exposed at the WHO CTC required temperature of 40 °C/75 % RH for 1 month. As a positive control the vaccine without stabilization or temperature exposure (TherVacB_{Ctrl}) was used. As an additional control, lyophilized and non-stabilized vaccine, which was stored at 5 °C for 1 month, was included in this experimental setup.

An additional control experiment to analyze antigen integrity and MVA-S/C infectivity, used for immunizations, was performed in parallel *in vitro*. ELISA of the SAAF-stabilized, lyophilized and heat-exposed HBsAg and HBcAg showed that all four tested SAAFs reached signals comparable to the TherVacB_{Ctrl} (Figure 26A). In contrast, without stabilization antigens lost their integrities. Lyophilization of the non-stabilized antigens followed by storage at 5 °C resulted in a strong decrease (~50-60 %) of HBcAg and HBsAg integrity. The HBcAg-specific ELISA results were supported by NAGE as an intact native HBcAg was detected for the SAAF-stabilized and the TherVacB_{Ctrl} samples, unlike the non-stabilized ones (Figure 26B). Figure 26 shows the representative HBcAg and HBsAg data obtained for one of the two prime immunizations.

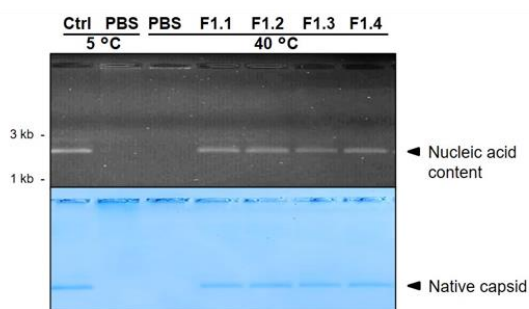
In parallel to the selection of the most suitable SAAF for HBcAg (chapter 2.4.1), various SAAFs were tested regarding the stabilizing efficacy of MVA-C. It was shown that MVA-C stabilized with SAAF I A maintained high viral titers despite a storage at 45 °C for 28 days (unpublished data; [193]), which led to the assumption that formulation of MVA-S/C with SAAFs 1.1-1.4

would also result in increased viral stability. Indeed, MVA-S/C analysis demonstrated that all four selected SAAFs (F1.1-F1.4) were able to prevent major loss of infectious viral particles despite 40 °C-storage (Figure 26C). In contrast, without stabilization heat-exposed MVA-S/C showed significantly lower titers. Overall, MVA-S/C demonstrated a high stability against heat-stressing, as highly infectious virus was still detected after storage at 40 °C for 28 days. In addition, the lyophilization in PBS and the following storage at 5 °C did not cause a significant reduction in the MVA-S/C titer and demonstrated a similar result to TherVacB_{Ctrl}. These data indicated that MVA-S/C remained stable during lyophilization (reported in detail in chapter 2.3.1) and further storage.

A



B



C

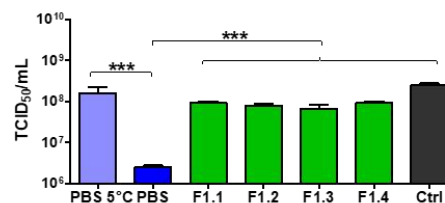


Figure 26. SAAFs 1-4 stabilized vaccine components during storage at 40 °C for 1 month.

TherVacB was formulated with four selected SAAFs (F1.1-F1.4). After storing at 40 °C/75 % RH for 28 days, HBsAg/HBcAg-integrity and MVA-S/C titers were analyzed *in vitro*. As control TherVacB_{Ctrl} components (Ctrl) were used. (A) HBsAg- and HBcAg-specific ELISA. (B) NAGE of HBcAg. (C) TCID₅₀ of MVA-S/C. Statistical analysis was performed using unpaired t-test. Asterisks mark statistically significant differences: *** $p \leq 0.001$. Modified from [183].

For the *in vivo* part of this experiment, HBV-naïve mice (C57BL/6) were immunized with the SAAF-stabilized or non-stabilized heat-exposed vaccine components using a heterologous protein-prime/MVA vector boost vaccination strategy [94] (Figure 27A). On week 2 and 4 priming with c-di-AMP adjuvanted HBsAg and HBcAg was performed, followed by the booster immunization with MVA-S/C on week 4. Throughout all presented mouse experiments, the TherVacB vaccine was administered intramuscularly (i.m.), which has been demonstrated to be superior to subcutaneous (s.c.) or intraperitoneal (i.p.) delivery (Su, Kosinska, personal communication). One week after the boost, mice were sacrificed and HBV-specific antibody titers in serum as well as T-cell responses in the spleens of the mice were analyzed. Non-vaccinated HBV-naïve mice were used as negative controls.

All mice receiving vaccination displayed significantly higher anti-HBs and anti-HBc titers as compared to negative values obtained in non-vaccinated controls (Figure 27B). Despite the heat-exposure, high HBV-specific antibody levels were detected in all SAAF-stabilized groups, which were comparable in titer to the TherVacB_{Ctrl} group. The TherVacB induced anti-HBs

antibody response was independent of the stabilization status of the vaccine components as no difference was observed between all vaccinated groups. In contrast, anti-HBc antibody titers were higher in all SAAF-stabilized groups compared to the non-stabilized and heat-exposed ones. Nevertheless, a significant difference was still detected for the non-stabilized group compared to non-vaccinated mice. Lyophilization without stabilization followed by storage at 5 °C indicated no negative effect on HBV-specific antibody responses, as equal titers were observed in mice immunized with TherVacB_{Ctrl}.

Intracellular cytokine staining (ICS) of splenocytes isolated from immunized mice, showed that all SAAF-stabilized vaccines induced strong core- and S-specific CD8⁺ T-cell responses, comparable to vaccination with TherVacB_{Ctrl} (Figure 27C). In contrast, in the mice receiving TherVacB vaccine after heat-stressing, but without stabilization no HBV-specific CD8⁺ T cells were detected, as in non-vaccinated mice. In the groups immunized with lyophilized, non-stabilized and at 5 °C stored vaccine the observed core- and S-specific CD8⁺ T-cell responses were lower than in the TherVacB_{Ctrl} group, but still higher compared to non-vaccinated mice.

In all vaccinated groups a positive core-specific CD4⁺ T-cell response was detected, as compared to non-vaccinated mice (Figure 27D). The induction of core-specific CD4⁺ T cells was independent of stabilization, as no significant differences were observed between SAAF-stabilized, non-stabilized and TherVacB_{Ctrl} vaccines. In addition, most of the animals showed a negative S-specific CD4⁺ T-cell response.

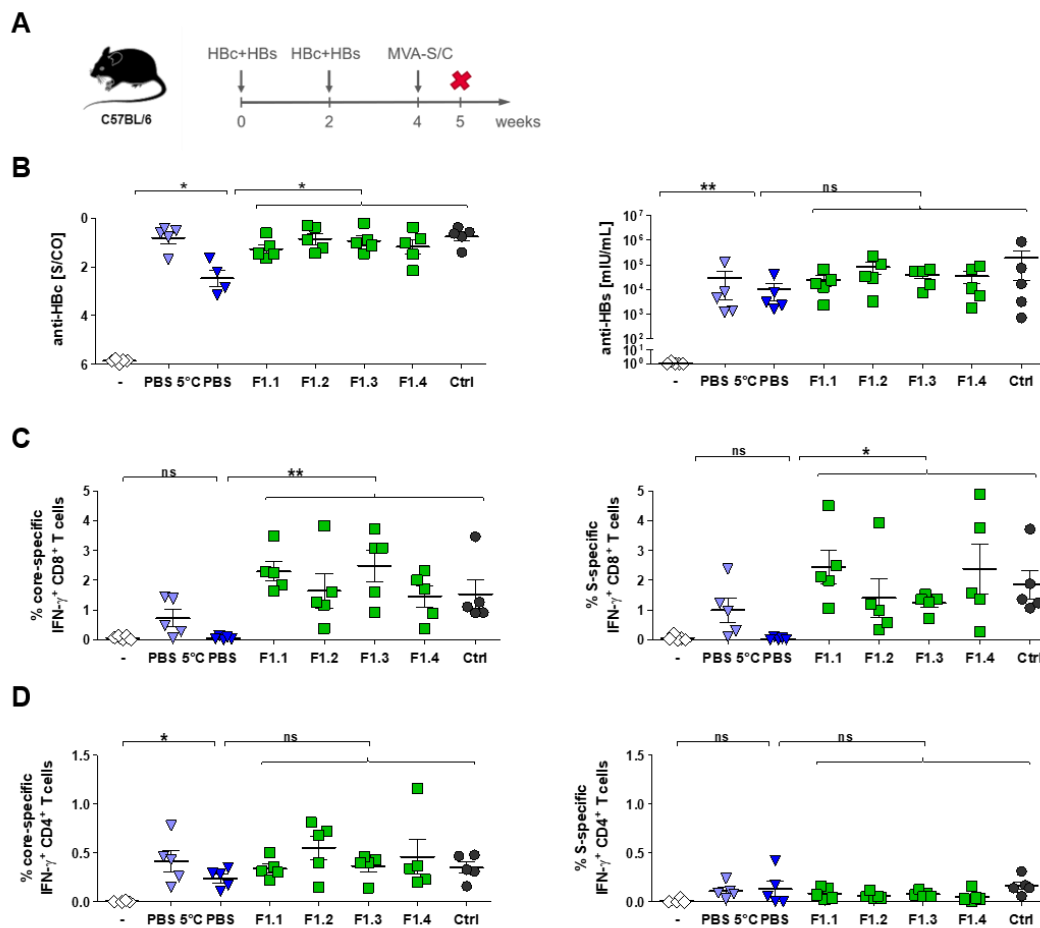


Figure 27. Stabilization with SAAFs induced HBV-specific immune response in HBV-naïve mice despite heat-exposure.

HBV-naïve mice (C57BL/6) were immunized with F1.1-1.4-stabilized or non-stabilized heat-stressed vaccine components according to the TherVacB regimen (A). Mice immunized with non-stabilized and non-stressed vaccine (PBS 5 °C) or TherVacB_{Ctrl} (Ctrl) or non-vaccinated mice (-) served as controls. One week after boost, HBV-specific antibody titers and T cells in the spleen were analyzed. (B) Serum anti-HBc and anti-HBs titers. Core- and S-specific IFN- γ ⁺ CD8⁺ (C) and CD4⁺ (D) T-cell responses determined by intracellular cytokine staining (ICS) following *ex vivo* stimulation with HBV-specific peptides (C_{pool}, S_{pool}). Five mice per group were analyzed. Statistical analysis was performed using Mann-Whitney test. Asterisks mark statistically significant differences: * $p \leq 0.05$; ** $p \leq 0.01$; ns - not significant. Modified from [183].

In summary, these data demonstrate a successful heat-stabilization of all three TherVacB components with the selected SAAFs *in vitro* and *in vivo*. As compared to SAAF 1.2-1.4, SAAF 1.1-stabilized vaccine elicited a superior HBV-specific CD8⁺ T-cell response, which was equally strong for both antigens and the most comparable in magnitude within the group. Therefore, SAAF 1.1 was selected as the most promising stabilization formulation for all TherVacB components and will be further referred as SAAF throughout this study. As one suitable SAAF was selected for both antigens and combination of HBcAg and HBsAg demonstrated an improved stability after lyophilization, the results of antigen combination are always presented in following chapters, except if it is stated otherwise (chapter 2.5.4 and 2.6.3).

2.5 Detailed analysis of vaccine components during storage at 25 °C or 40 °C *in vitro*

2.5.1 Successful achievement of WHO CTC guideline

Following the selection of the most suitable SAAF to stabilize the combination of HBcAg and HBsAg as well as MVA-S/C, the TherVacB vaccine formulations were comprehensively studied during storage at higher temperatures over time. In the first set of experiments, vaccine components were thermal stressed at 40 °C/75 % RH for 3 days, to examine whether the chosen SAAF stabilization fulfills the WHO CTC criteria. As a control for temperature stressing, vaccine components were stored at 5 °C after lyophilization. As positive controls single vaccine components without lyophilization, stabilization and temperature exposure (SM_{Ctrl}) were used.

Despite storage at accelerated aging conditions, intact pharmaceutical cake structures containing fluffy flocs with similar shapes as the SM_{Ctrl} sample in solution were observed for the SAAF-stabilized components (Figure 28A). In contrast, the non-stabilized samples displayed unsatisfactory, caved cake structures. By ELISA, NAGE, SE-HPLC, DLS and WB, it was verified that antigen integrity was maintained after 3 days storage at 40 °C by stabilizing the antigens with SAAF (Figure 28B-F). In contrast, strongly reduced or no signals were detected by ELISA and NAGE for the non-stabilized samples (Figure 28B, C). The SE-HPLC curve profile of the non-stabilized sample showed a reduced peak intensity of the main peak and an additional peak eluting before the main peak suggesting the formation of aggregates (Figure 28D). Moreover, DLS analysis displayed curves shifted towards higher particle diameter for non-stabilized samples, indicating large, most likely aggregated particles (Figure 28E). However, WB analysis showed specific signals for both antigens in non-stabilized samples (Figure 28F). This demonstrates that lyophilization and storage at 40 °C does not result in degradation of the antigens.

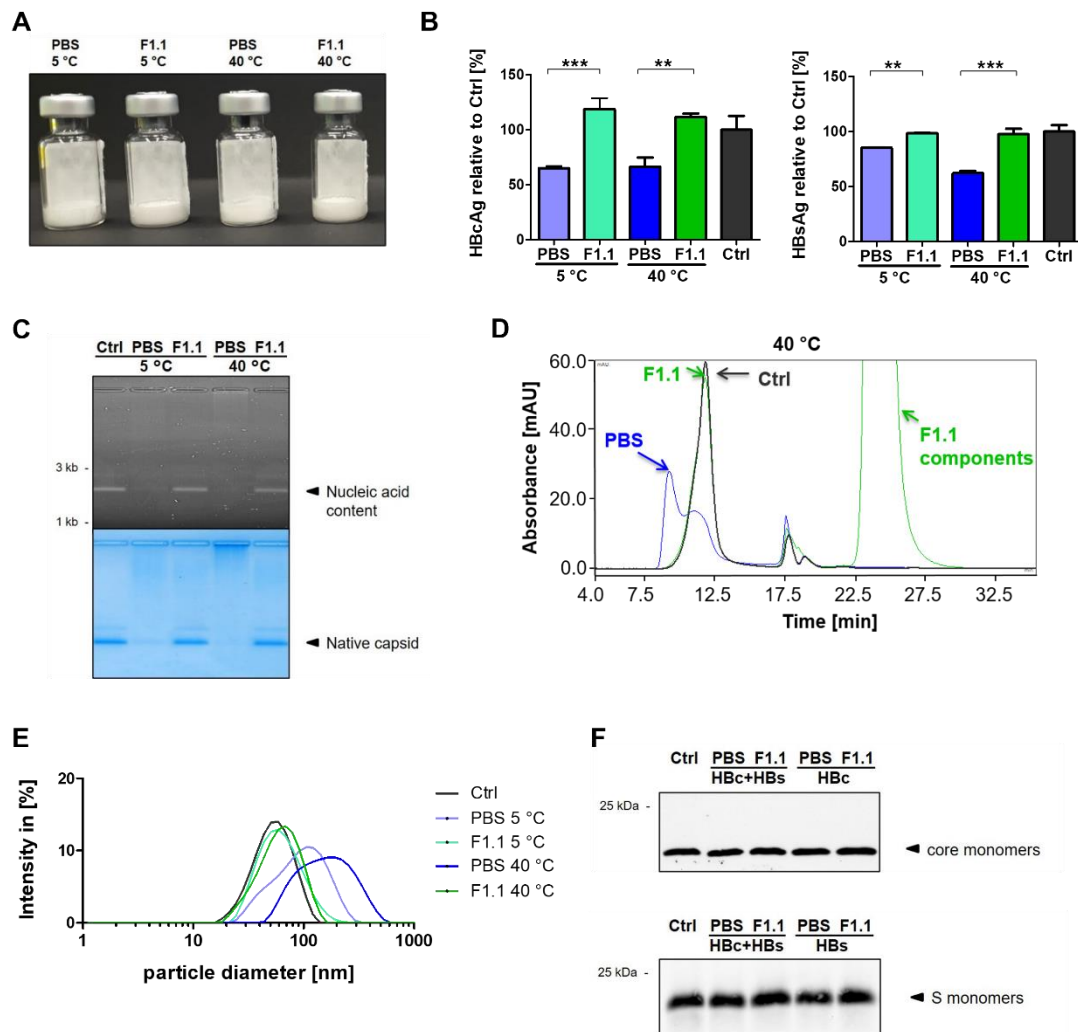


Figure 28. SAAF-stabilized antigens remained stable after 40 °C-exposure for 3 days.

SAAF-stabilized (F1.1) and non-stabilized (PBS) antigens were comprehensively analyzed after a storage at 5 °C or 40 °C/75 % RH for 3 days according to the WHO CTC criteria. As control SM_{Ctrl} without stabilization and storage (Ctrl) was used. (A) Pharmaceutical cake structures. (B) HBCAg- and HBsAg-specific ELISA. (C) NAGE of HBcAg. (D) DLS and (E) SE-HPLC analysis. (F) HBCAg- and HBsAg-specific WB analysis. Statistical analysis was performed using unpaired t-test. Asterisks mark statistically significant differences: ** $p \leq 0.01$; *** $p \leq 0.001$. Modified from [183].

SAAF-stabilization of MVA-S/C resulted in pharmaceutical cake structures as expected despite storage at accelerated aging conditions (Figure 29A). In contrast, the non-stabilized samples displayed collapsed thin, not fluffy cake structures with uneven shapes. $TCID_{50}$ analysis supported previous findings and demonstrated that the MVA-S/C vector is quite stable without additional stabilizers, as high titers were observed for all tested samples (Figure 29B). However, the results clearly show that SAAF-stabilization noticeably improved MVA-S/C heat resistance despite temperature stressing. Interestingly, the lyophilization process in PBS led to a negative influence on the cake structures, however not on MVA-S/C titers. Equally high titers were measured for the lyophilized and cold-stored MVA-S/C as for SM_{Ctrl} . In chapter 2.3, the effect of lyophilization on vaccine components was described in detail.

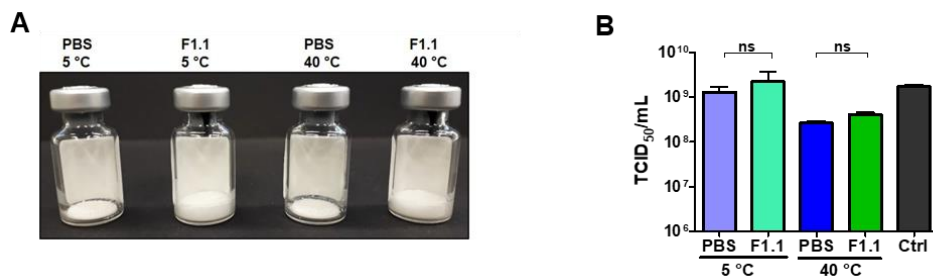


Figure 29. SAAF-stabilized MVA-S/C remained stable after 40 °C-exposure for 3 days.

SAAF-stabilized (F1.1) and non-stabilized (PBS) MVA-S/C were analyzed after exposure to 5 °C or 40 °C/75 % RH for 3 days. As control SM_{Ctrl} without stabilization and storage (Ctrl) was used. (A) Pharmaceutical cake structures. (B) MVA-S/C titers determined by TCID₅₀. Statistical analysis was performed using unpaired t-test. Asterisks mark statistically significant differences: ns - not significant. Modified from [183].

Taken together, these results demonstrate that the addition of SAAF to TherVacB components results in a thermostable vaccine which fulfills the WHO CTC guideline.

2.5.2 Maintenance of antigen integrity and MVA-S/C infectivity after formulation with SAAF during storage at 25 °C and 40 °C up to 3 months

Extended stability at higher temperatures could remarkably simplify TherVacB application worldwide, as a prolonged transport from the manufacturer to the patient and a longer storage time would be possible. Therefore, after successful stabilization of TherVacB for 3 days at 40 °C, the question was addressed whether SAAF-formulated vaccine could remain intact over prolonged storage for 14 days, 1 month and even 3 months under accelerated aging conditions (40 °C/75 % RH). As positive control the SM_{Ctrl} without stabilization and temperature exposure was used.

Intact and functional HBcAg and HBsAg (Figure 30A-D) as well as high infectious MVA-S/C titer (Figure 30E, F) was detected by all applied methods despite thermal stressing over 14 days. In contrast, non-stabilized antigens showed reduced antigen integrity and a decrease in viral titers after heat-exposure confirming the results previously described for 3 days of storage.

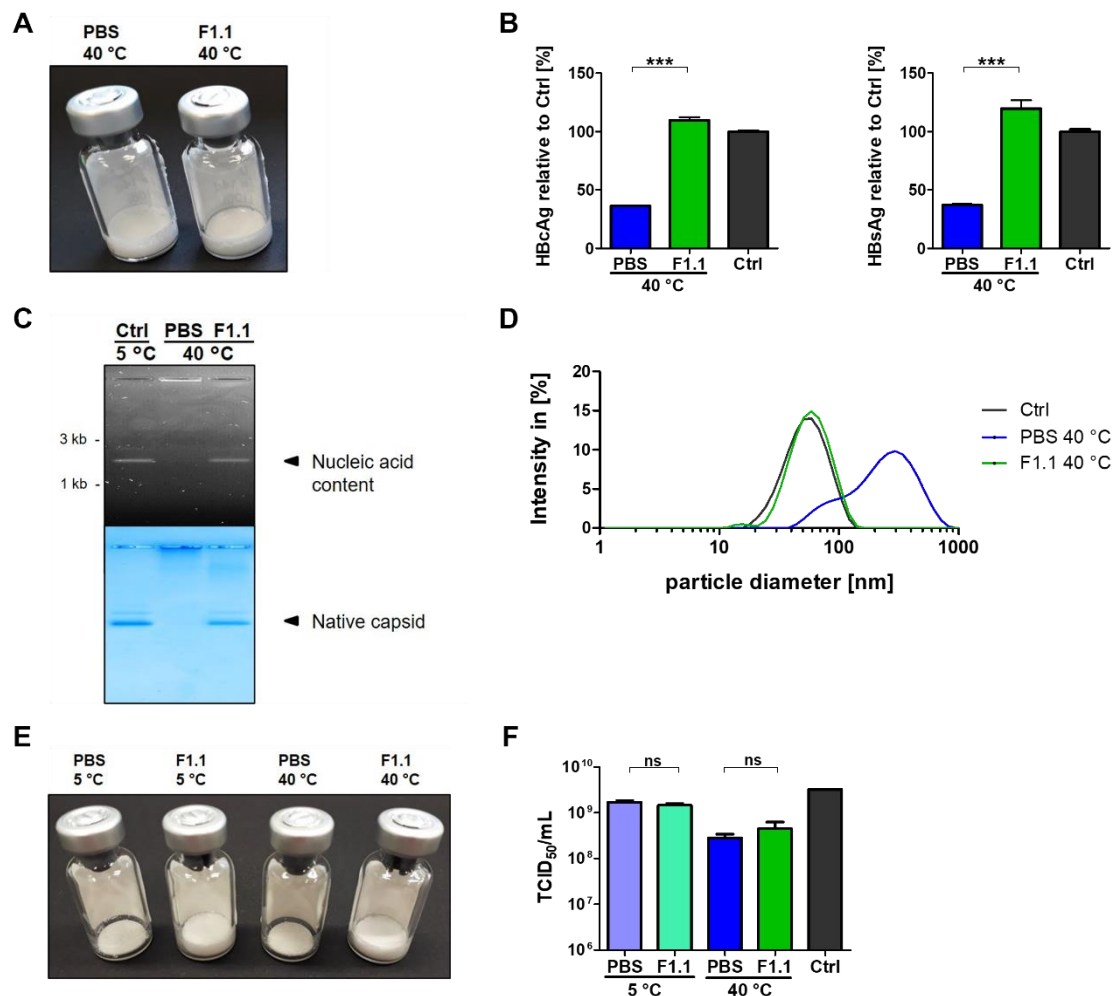


Figure 30. SAAF-stabilization led to intact antigens and high infectious MVA-S/C titer despite storage at 40 °C for 14 days.

SAAF-stabilized (F1.1) and non-stabilized (PBS) TherVacB components were stored at 40 °C/75 % RH for 14 days and afterwards comprehensively analyzed. As control SM_{Ctrl} without stabilization and storage (Ctrl) was used. (A) Pharmaceutical cake structures of antigens. (B) HBcAg- and HBsAg-specific ELISA. (C) NAGE of HBcAg. (D) DLS analysis. (E) Pharmaceutical cake structures of MVA-S/C. (F) MVA-S/C titers determined by TCID₅₀. Statistical analysis was performed using unpaired t-test. Asterisks mark statistically significant differences: *** $p \leq 0.001$; ns - not significant.

Following the stressing for 14 days, TherVacB components were further exposed to 5 °C, 25 °C/60 % RH or 40 °C/75 % RH for 1 or 3 months. A temperature of 25 °C for a prolonged TherVacB stressing was included in these experiments to further investigate the stability of SAAF-formulated TherVacB at RT or around that temperature.

After 1 month of storage at 25 °C or 40 °C, lyophilized antigens with SAAF-stabilization showed pharmaceutical cake structures as expected, contrary to non-stabilized antigens (Figure 31A). The HBcAg- and HBsAg-specific ELISA verified intact antigens after SAAF-stabilization, whereas without stabilization both antigens lost integrity after thermal stressing (Figure 31B). NAGE of HBcAg additionally confirmed these results showing similar bands for SAAF-stabilized and SM_{Ctrl} samples, in contrast to non-stabilized ones (Figure 31C). DLS and SE-HPLC analysis displayed comparable curves for the SAAF-stabilized, stressed antigens and the positive control, SM_{Ctrl} (Figure 31D, E). In contrast, larger particle diameters

were detected by DLS for the non-stabilized antigens, suggesting heat-mediated aggregation of HBcAg and HBsAg (Figure 31D). SE-HPLC analysis of non-stabilized antigens led to a similar result as a very small peak, which was shifted to the left indicating aggregates, was observed (Figure 31E). Moreover, after harsher exposure at 40 °C no SE-HPLC measurement were performed, as the non-stabilized sample showed a high sample turbidity referring to aggregates, which would probably cause blockage of the column. HBcAg- and HBsAg-specific WB analysis demonstrated no degradation of antigens after prolonged storage at higher temperatures (Figure 31F). All applied methods showed no significant differences in antigen integrity between the 25 °C- and 40 °C-exposed SAAF-stabilized samples, confirming that the success of stabilization was independent of the storage temperature.

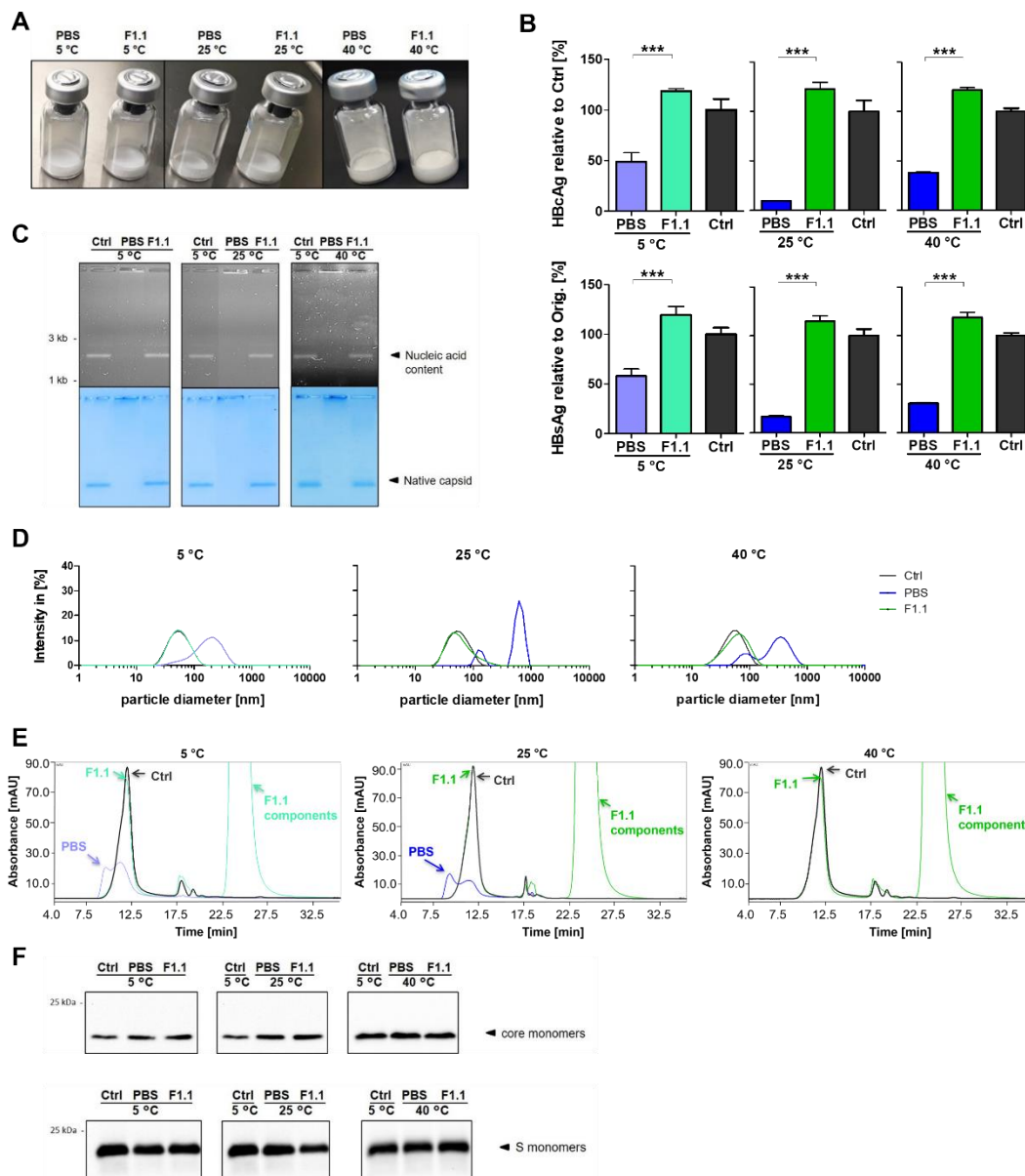


Figure 31. Formulation with SAAF led to stable antigens despite 1 month of heat-exposure.

Integrities of SAAF-stabilized (F1.1) and non-stabilized (PBS) antigens were analyzed after 1 month of storage at 5 °C, 25 °C/60 % RH or 40 °C/75 % RH. As control SM_{Ctrl} without stabilization and storage (Ctrl) was used. (A) Pharmaceutical cake structures of antigens. (B) HBcAg- and HBsAg-specific ELISA. NAGE (C), DLS (D) and SE-HPLC (E) analysis of antigens. (F) HBcAg- and HBsAg-specific WB. Statistical analysis was performed using unpaired t-test. Asterisks mark statistically significant differences: *** $p \leq 0.001$. Modified from [183].

Interestingly, the extension of temperature stressing to 3 months demonstrated similar results concerning HBcAg and HBsAg integrity as obtained for 14 days and 1 month of stressing. The stabilization with SAAF clearly protected the antigens from temperature-mediated damages, which was verified by ELISA, NAGE, DLS, SE-HPLC and WB (Figure 32). In contrast, lyophilization and subsequent storage of the antigens in PBS led to a considerable loss of structural and functional integrity. By comparing the different storage temperatures (25 °C and 40 °C), the results indicate that the structure of the antigens was excellently maintained by formulation with SAAF for both conditions, even after the 3-months storage period.

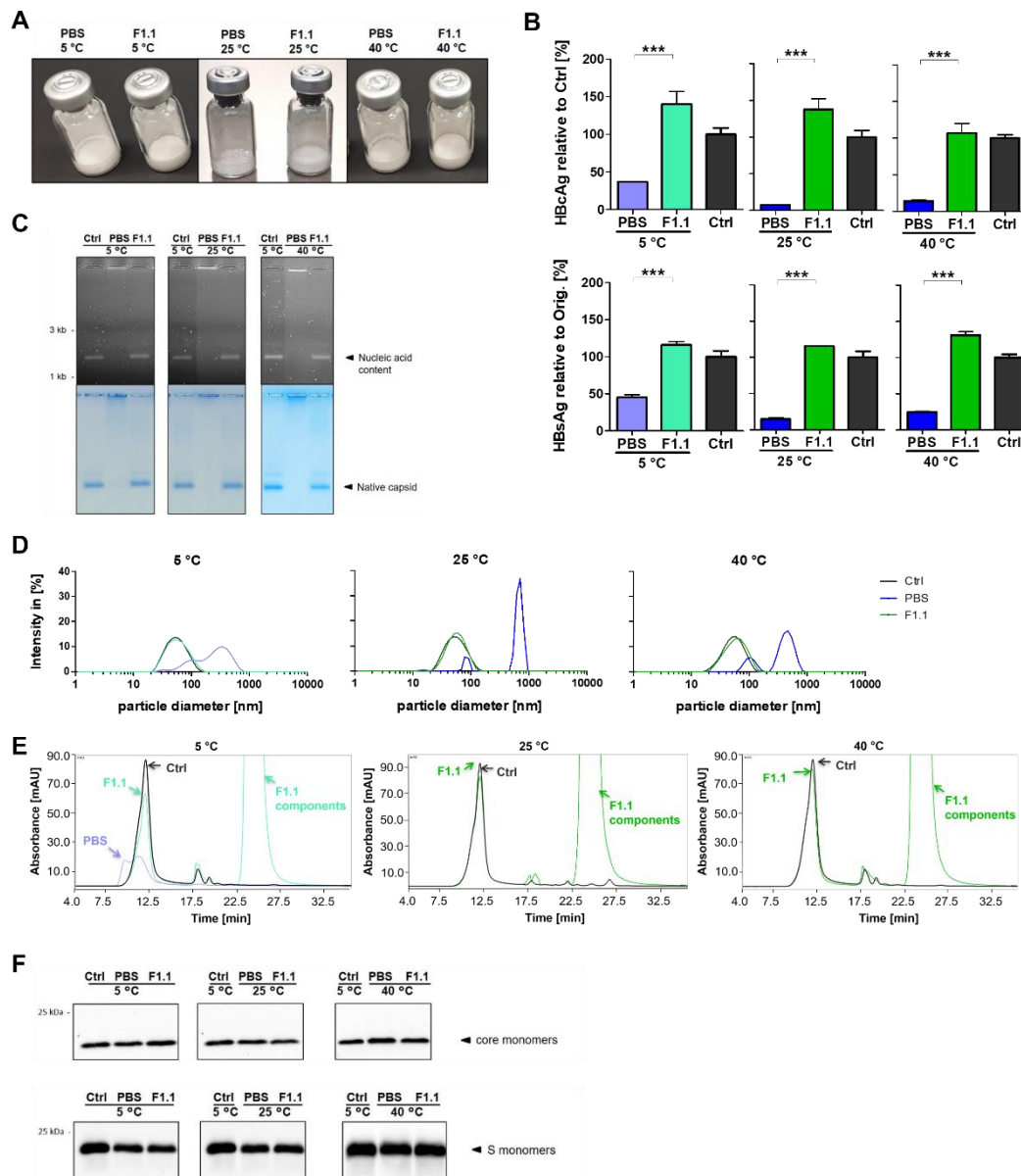


Figure 32. Stabilization with SAAF maintained antigen integrity despite 3 months of storage at 25 °C or 40 °C.

SAAF-stabilized (F1.1) and non-stabilized (PBS) antigens were exposed to 5 °C, 25 °C/60 % RH or 40 °C/75 % RH. Antigen integrity was comprehensively examined after 3 months of storage. As control SM_{Ctrl} without stabilization and storage (Ctrl) was used. (A) Pharmaceutical cake structures of antigens. (B) HBcAg- and HBsAg-specific ELISA. NAGE (C), DLS (D) and SE-HPLC (E) analysis of antigens. (F) HBcAg- and HBsAg-specific WB. Statistical analysis was performed using unpaired t-test. Asterisks mark statistically significant differences: *** $p \leq 0.001$. Modified from [183].

Following HBcAg and HBsAg analysis, the effect of SAAF-stabilization on MVA-S/C during 1 and 3 months of exposure at 5 °C, 25 °C/60 % RH or 40 °C/75 % RH was examined.

Formulation of MVA-S/C with SAAF resulted in pharmaceutical cake structure as expected despite the prolonged stressing, in contrast to the non-stabilized samples for both tested time points and temperatures (Figure 33A). Moreover, high MVA-S/C titers were determined by TCID₅₀ even without stabilization (Figure 33B). However, by formulation with SAAF, MVA-S/C infectivity after stressing was significantly improved, especially after 3 months of storage.

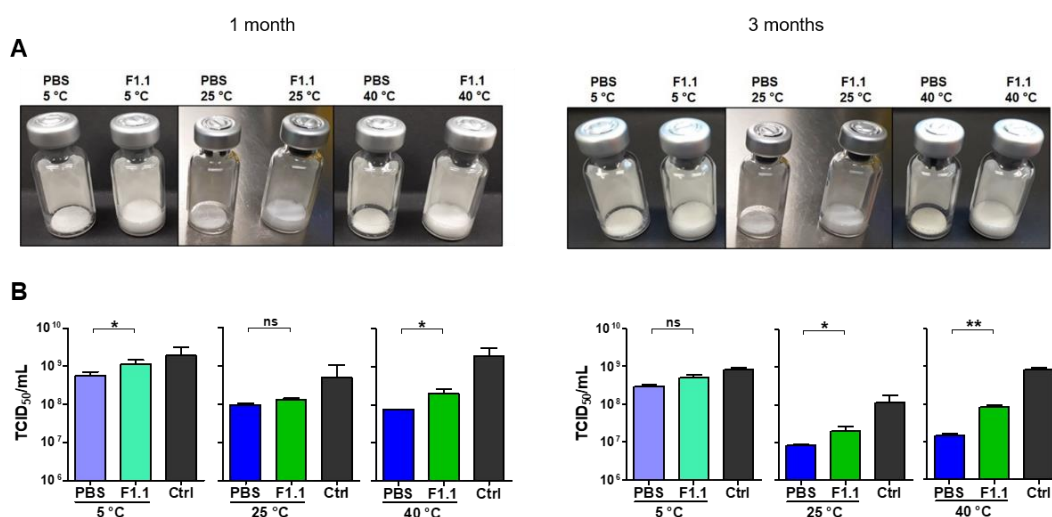


Figure 33. Formulation with SAAF improved MVA-S/C infectivity after 1 and 3 months of storage at 25 °C or 40 °C.

SAAF-stabilized (F1.1) and non-stabilized (PBS) MVA-S/C samples were analyzed after storage at 5 °C, 25 °C/60 % RH or 40 °C/75 % RH for 1 and 3 months. As control SM_{Ctrl} (Ctrl) was used. Pharmaceutical cake structures (A) and TCID₅₀ analysis (B) of MVA-S/C after temperature exposure. Statistical analysis was performed using unpaired t-test. Asterisks mark statistically significant differences: * $p \leq 0.05$; ** $p \leq 0.01$; ns - not significant. Modified from [183].

In addition, the impact of SAAF-stabilization on the morphology of vaccine components after heat-exposure was examined. The TEM analysis clearly demonstrated that HBcAg and HBsAg (Figure 34A) as well as the MVA-S/C (Figure 34B) preserved a similar morphology as the respective SM_{Ctrl} controls. Interestingly, the same antigen structures were seen for the non-stabilized antigens after heat-exposure as for the SM_{Ctrl}. However, besides the representative pictures shown in Figure 34A, a lot of black fields, caused by large aggregates, were additionally observed on the grid of non-stabilized antigen sample. TEM analysis of the MVA-S/C showed no noticeable differences in visual appearance of SAAF-stabilized, non-stabilized or SM_{Ctrl} samples despite storage at 40 °C. This finding reflected TCID₅₀-results showing highly infectious MVA-S/C in all samples, even after prolonged heat-exposure.

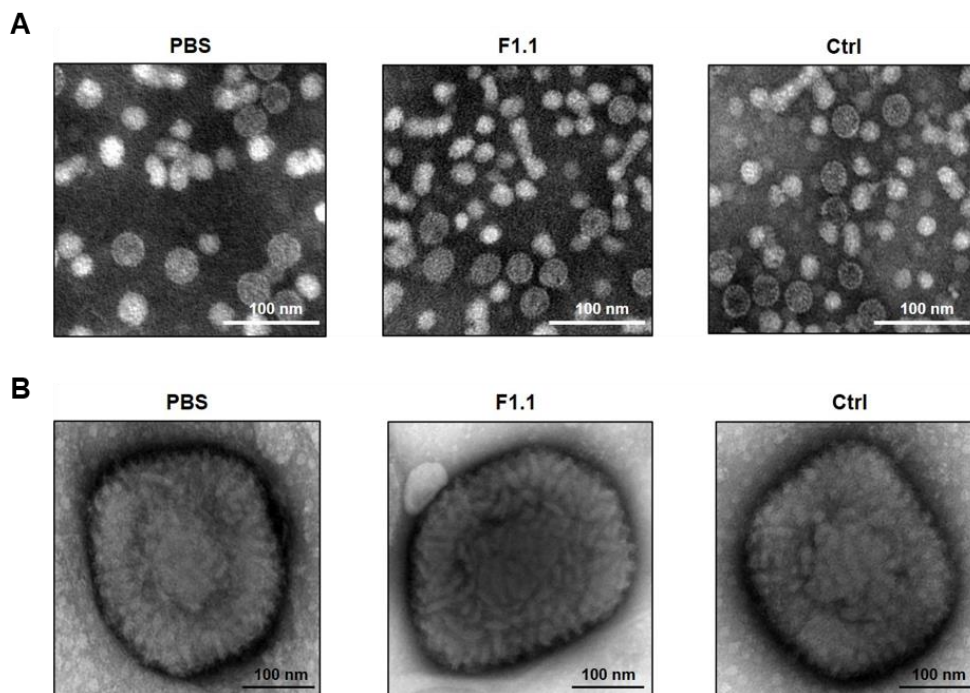


Figure 34. Heat-exposure did not cause structural differences of vaccine components.

Morphology studies of SAAF-stabilized (F1.1) and non-stabilized (PBS) TherVacB components were performed after 1 month of heat-exposure at 40 °C/75 % RH. As control SM_{Ctrl} without stabilization and storage (Ctrl) was used. TEM analysis of negative stained HBcAg and HBsAg (A) as well as MVA-S/C (B) at a magnification of 40000x. Scales show 100 nm. Modified from [183].

In summary, these results confirm a successful SAAF-stabilization of HBcAg and HBsAg despite a 25 °C or 40 °C heat-exposure for up to 3 months. In addition, SAAF-formulation significantly improved MVA-S/C infectivity after prolonged storage at high temperatures.

2.5.3 Preservation of antigen integrity and MVA-S/C infectivity after SAAF-stabilization during long-term storage at 25 °C for up to 12 months

European Medicines Agency (EMA), ICH and WHO require successful stability studies over a 12 months storage period at 25 °C/60 % RH for pharmaceutical products being applied in countries with climate zones 1 (temperate climate) and 2 (subtropical and Mediterranean climate) [194, 196]. These long-term testing conditions are applicable in Germany, Switzerland, Italy, United Kingdom, Japan, Sweden, United States of America [196]. The testing of TherVacB components under these mandatory conditions, would facilitate future application of this vaccine in humans. Moreover, an even more extended transport and storage time as the already achieved 3 months at RT, would further increase the flexibility during vaccination campaigns and reduce the cost by saving the required cooling equipment. Therefore, in further experiments the question was addressed whether the SAAF-stabilization prevent loss of TherVacB potency after lyophilization and subsequent long-term storage for 6, 9 and 12 months at 25 °C/60 % RH *in vitro*. As a control for temperature stressing, vaccine components were stored at 5 °C after lyophilization. As positive control the SM_{Ctrl} without stabilization and temperature exposure was used.

HBcAg- and HBsAg-specific ELISA data demonstrated that both SAAF-stabilized antigens remained intact after stressing for 6, 9 and 12 months at RT (Figure 35A, B). As expected, non-stabilized antigens lost their integrities over time. NAGE and DLS results confirmed the ELISA data, as similar bands or curve patterns were detected for the SAAF-stabilized samples after stressing and SM_{Ctrl} (Figure 35C, D). In contrast, without stabilization the aggregated samples stuck in the pockets of the agarose gel during NAGE and showed much larger particles when measured by DLS. After a 12 months storage period, only few particles with a slightly increased diameter were detected by DLS in the SAAF-stabilized samples, indicating the appearance of small aggregates, which were not yet observed after 9 months of stressing (Figure 35D). As demonstrated in the previous analyses, after 6- and 9 months of storage, no degradation of antigens was observed by WB analysis. Similar HBcAg- and HBsAg-specific bands were detected in SAAF-stabilized as well as non-stabilized samples (Figure 35E). Nevertheless, after 12 months stressing, a slight decrease in WB signal was detected in non-stabilized samples, whereas the SAAF-stabilized antigens remained intact and showed similar bands as the SM_{Ctrl}.

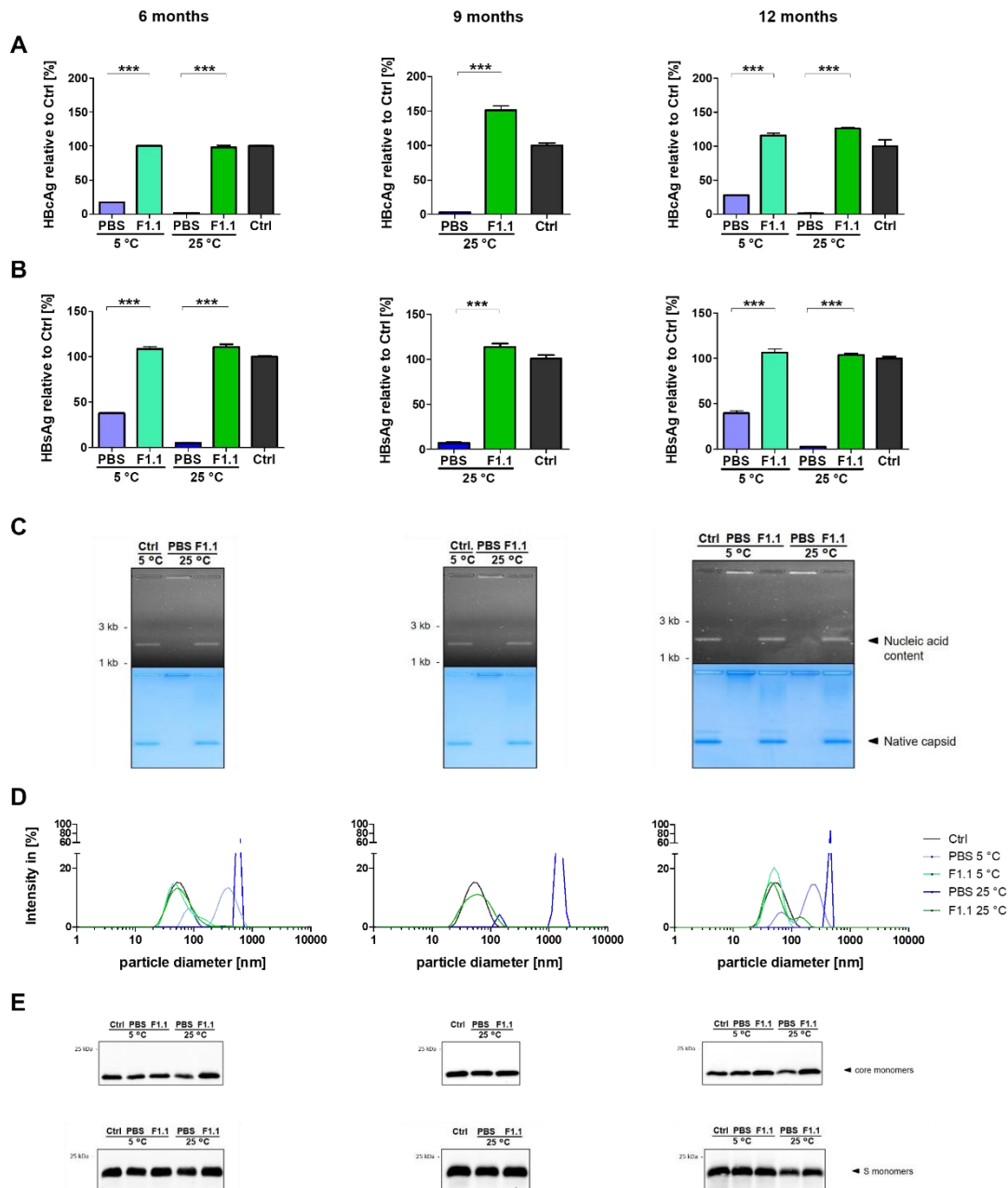


Figure 35. SAAF-stabilization of antigens retained their integrities after storage at RT up to 12 months.

Antigen integrity was comprehensively analyzed *in vitro* after storage of SAAF-stabilized (F1.1) and non-stabilized (PBS) antigens at 5 °C and 25 °C/60 % RH for 6, 9 and 12 months. As control SM_{ctrl} without stabilization and storage (Ctrl) was used. HBcAg- (A) and (B) HBsAg-specific ELISA. (C) NAGE of HBcAg. DLS (D) and HBcAg/HBsAg specific WB (E) analysis. Statistical analysis was performed using unpaired t-test. Asterisks mark statistically significant differences: *** $p \leq 0.001$. Modified from [183].

The SE-HPLC analysis performed after 9 and 12 months of storage, confirmed previous results, demonstrating that SAAF-stabilization of HBcAg and HBsAg led to long-term maintenance of their integrities (Figure 36). Nevertheless, a minor decrease in peak height was determined only after the 12 months exposure. For the antigen samples without stabilization, the measurements were not performed as the visible aggregates within the samples would certainly cause blockage of the column. However, the successful SE-HPLC analysis of these samples would probably not change the overall results, as previously shown, already after a storage period of 28 days at 25 °C only a minor peak was observed for the

non-stabilized antigens referring to soluble aggregates which form larger, visible aggregates after more extreme stressing conditions (Figure 31E).

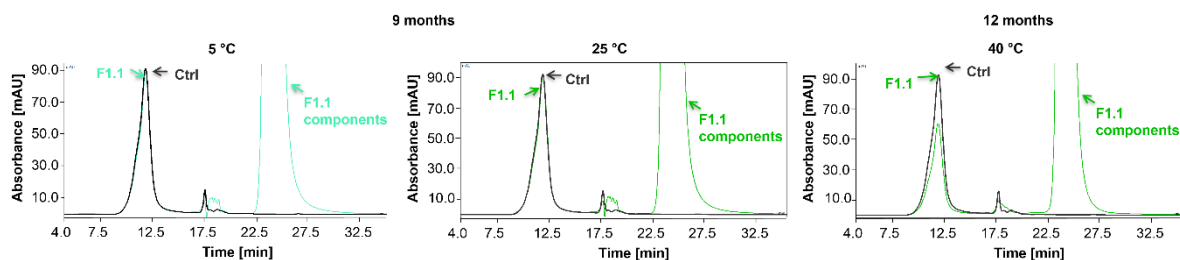


Figure 36. Formulation with SAAF led to stable antigens after 25 °C-exposure for up to 12 months.

SE-HPLC chromatograms of SAAF-stabilized (F1.1) samples were performed after exposure to 5 °C and 25 °C/60 % RH for 9 and 12 months. As control SM_{Ctrl} without stabilization and storage (Ctrl) was used. Modified from [183].

Next, long-term stability of MVA-S/C was studied over 12 months of exposure time at 25 °C. Surprisingly, even without stabilization and after storage for 1 year, infectious MVA-S/C particles were still detected, confirming the observation that the MVA-S/C is remarkable stable at RT (Figure 37). However, formulation with SAAF markedly improved the MVA-S/C infectivity, as significantly higher titers were determined in stabilized samples than in non-stabilized ones after RT-exposure at all examined time points.

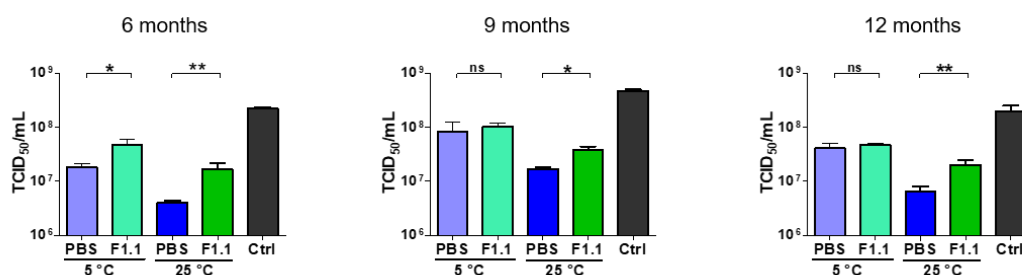


Figure 37. Formulation with SAAF improved MVA-S/C infectivity after a storage at RT for up to 12 months.

SAAF-stabilized (F1.1) and non-stabilized (PBS) MVA-S/C titers were determined by TCID₅₀ after a storage at 5 °C and 25 °C/60 % RH for 6, 9 and 12 months. As control SM_{Ctrl} without stabilization and storage (Ctrl) was used. Statistical analysis was performed using unpaired t-test. Asterisks mark statistically significant differences: * $p \leq 0.05$; ** $p \leq 0.01$; ns - not significant. Modified from [183].

In summary, these data demonstrate that the formulation of TherVacB components with SAAF remarkably allows storage even for 1 year of at RT without losing vaccine stability.

2.5.4 SAAF improves integrity of single antigens despite exposure to 25 °C or 40 °C

Analysis of the HBV antigen integrity directly after lyophilization (day 0) already indicated that formulation of their combination in SAAF was more efficient than the formulation of the single antigens (chapter 2.3). However, at the beginning of the storage experiments it was not known whether SAAF-stabilized, combined antigens could maintain their integrities after extensive stressing at higher temperatures. Therefore, all *in vitro* experiments, in which the SAAF 1.1 (F1.1) was comprehensively analyzed, were performed with the single HBcAg and HBsAg, in parallel to their combination. In the following figures, some representative examples of the

single antigen analyses after a storage at 40 °C for 3 days and 3 months (Figure 38) as well as at 25 °C for 6 and 12 months (Figure 39) are presented. For comparison, the samples with the antigen combination are also displayed. As positive control the SM_{Ctrl} without stabilization and storage was used.

Previously described results (chapter 2.3.2) demonstrated that lyophilization of the non-stabilized single antigen resulted in a complete loss of HBcAg integrity. The formulation with SAAF increased HBcAg stability, however the negative effect of freeze-drying was not completely prevented. The reduction of single antigen integrity was also observed for the HBsAg, although it was not as pronounced as for the HBcAg.

The results of single antigen stressing, presented in this chapter, reflected previously reported data directly after lyophilization (day 0). The ELISA, NAGE and DLS results of the single antigen experiments demonstrated that formulation with SAAF can significantly increase stability of single HBcAg or HBsAg after 3 days and 3 months storage duration at 40 °C (Figure 38A-D). However, a reduced HBcAg integrity, which further decreased after a longer storage time, was observed for the SAAF-stabilized single HBcAg compared to SAAF-stabilized, combined antigens or SM_{Ctrl} (Figure 38A, C, D). Interestingly, SAAF-stabilized single HBsAg displayed comparable ELISA signals as the antigen combination or SM_{Ctrl} (Figure 38B, D).

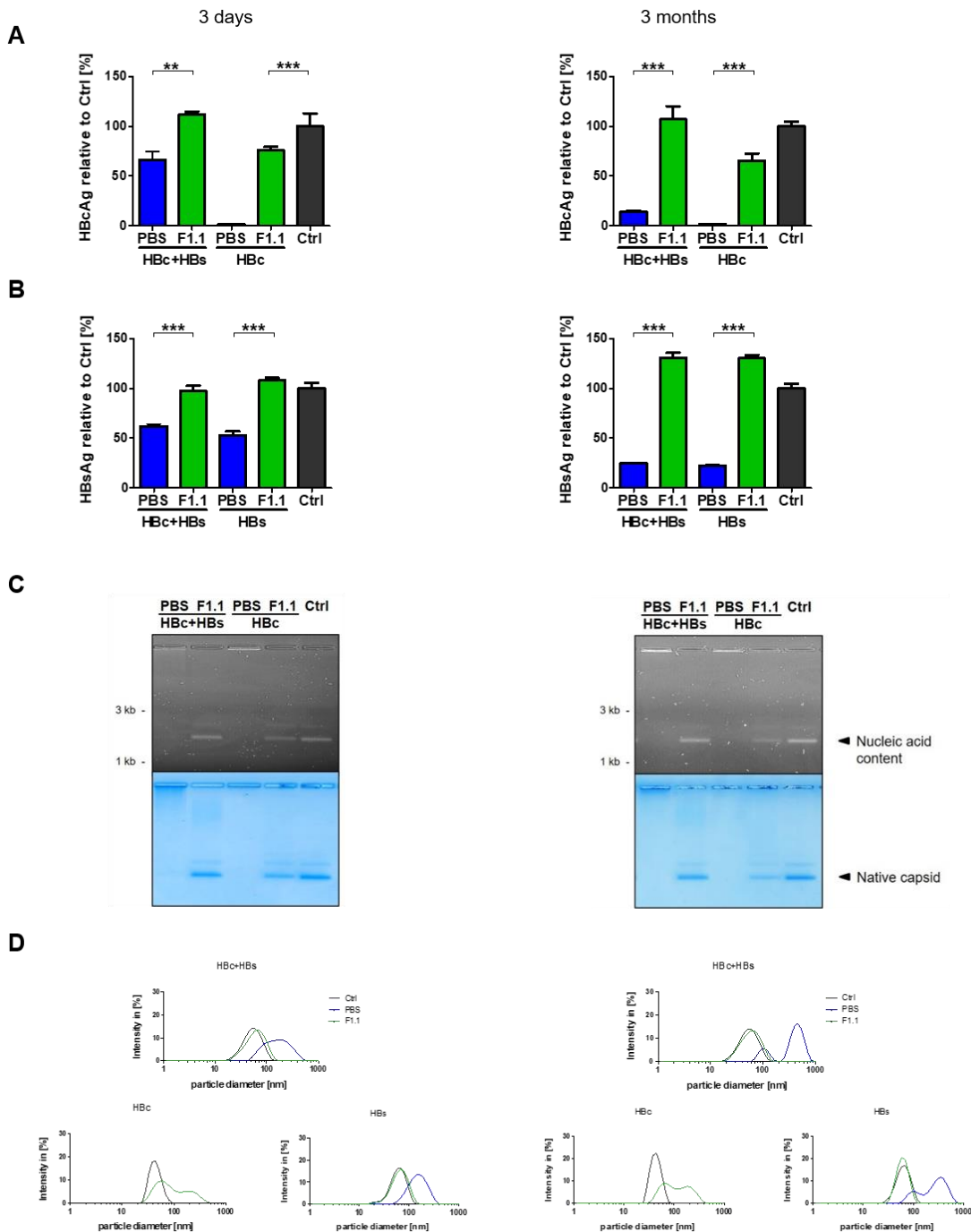


Figure 38. Formulation with SAAF led to stable antigens either in antigen combination or as single components after 40 °C-exposure for 3 days and 3 months.

SAAF-stabilized (F1.1) and non-stabilized (PBS) antigens in combination or as single components were stored at 40 °C/75 % RH for 3 days or 3 months. As control SM_{Ctrl} without stabilization and storage (Ctrl) was used. Antigen integrity was studied by HBcAg- (A) and HBsAg-specific (B) ELISA, (C) NAGE of HBcAg, (D) DLS analysis. Statistical analysis was performed using unpaired t-test. Asterisks mark statistically significant differences: ** $p \leq 0.01$; *** $p \leq 0.001$.

The results of the long-term experiments at RT demonstrated that the formulation with SAAF led to a strong increase of single HBcAg or HBsAg stability throughout all applied methods, compared to non-stabilized samples (Figure 39A-D). However, a complete prevention of the lyophilization- and temperature-derived damages was not achieved by the SAAF-stabilization

of the single antigens, predominately for the HBcAg. These findings reflected a similar picture as the results obtained for the short-term studies at 40 °C.

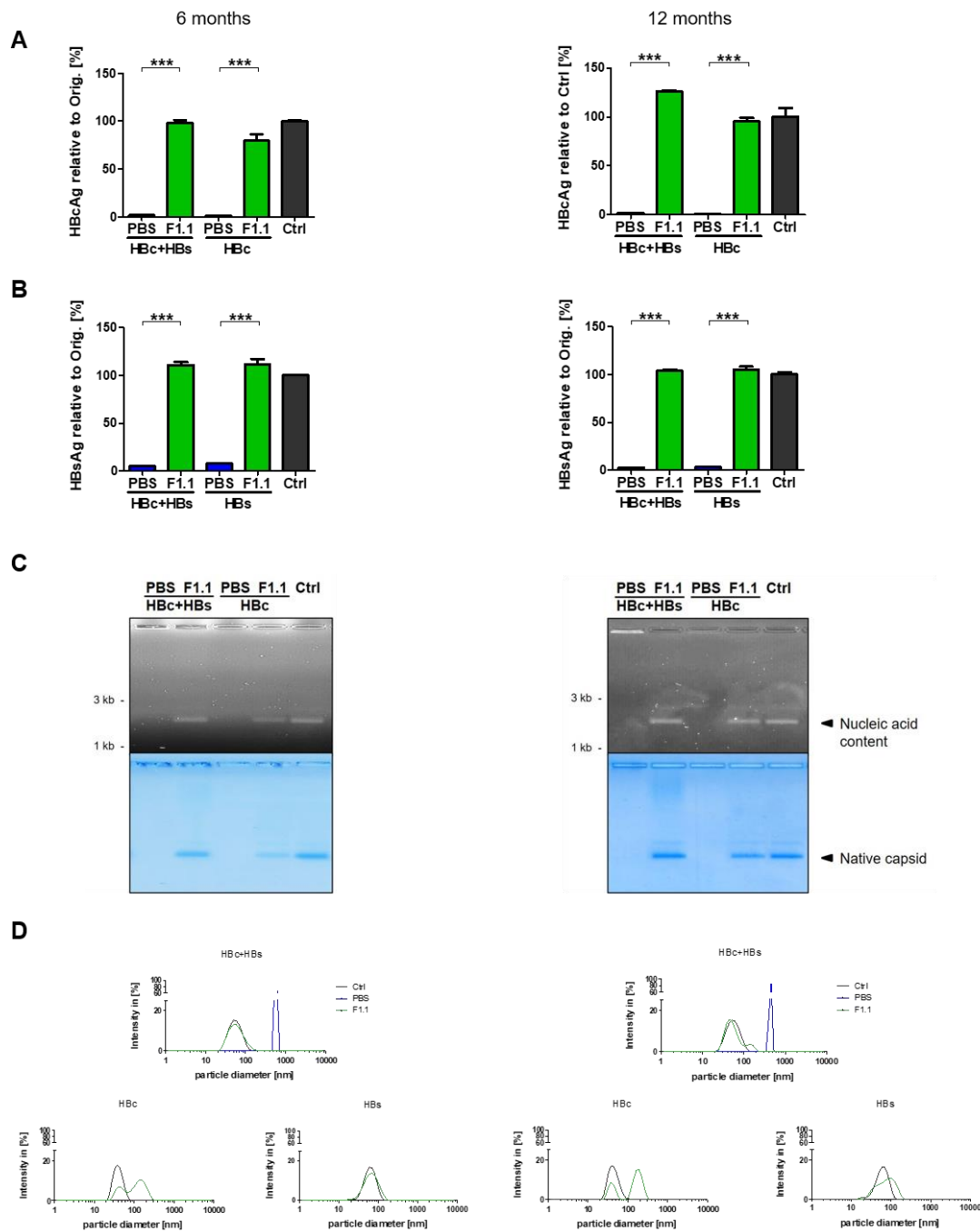


Figure 39. SAAF-stabilization remained antigen integrity after a storage at RT for 6 and 12 months.

SAAF-stabilized (F1.1) and non-stabilized (PBS) antigens in combination or as single components were analyzed after the RT-exposure for 6 and 12 months. As control SM_{Ctrl} without stabilization and storage (Ctrl) was used. (A) HBcAg-and (B) HBsAg-specific ELISA. (C) NAGE of HBcAg. (D) DLS analysis. Statistical analysis was performed using unpaired t-test. Asterisks mark statistically significant differences: *** $p \leq 0.001$.

Taken together, these data demonstrate that SAAF can effectively stabilize HBcAg and HBsAg either in combination or as single components during storage at higher temperatures. Nevertheless, a less pronounced stabilization effect observed for the single HBcAg, indicates that the antigen combination is more suitable for the thermostable TherVacB vaccine.

2.6 SAAF-stabilized vaccine induces immune response in different hepatitis B mouse models

Since outstanding results were obtained with SAAF-stabilized vaccine components during *in vitro* analysis, it was of a significant interest to verify the immunogenicity and thermostability of TherVacB vaccine *in vivo* after extensive heat-stressing. Therefore, the next set of experiments were performed in HBV-naïve mice and mice persistently infected with AAV carrying an HBV genome (AAV-HBV). AAV-HBV mimics persistent HBV infection in humans, as mice develop virus-specific immune tolerance resulting from the expression of HBV proteins in mouse hepatocytes over months. Furthermore, as the AAV-HBV genome remains episomal upon AAV-HBV infection, this model enables analysis of the elimination of infected hepatocytes [97]. Mouse experiments were performed in cooperation with Dr. Anna Kosinska.

2.6.1 Stabilized and heat-exposed vaccine induces an immune response in HBV-naïve mice after 1 and 3 months of storage period

In the first *in vivo* experiment, the thermostable TherVacB approach was tested in HBV-naïve mice (C57BL/6). As a successful SAAF-stabilization after thermal stressing up to 3 months was proven for the combined antigens and the MVA-S/C *in vitro* (chapter 2.5.2), for the following experiment the SAAF-stabilized and non-stabilized TherVacB components were stored for 1 and 3 months at 25 °C/60 % RH or 40 °C/75 % RH. As a positive control TherVacB vaccine without lyophilization, stabilization or heat-exposure (TherVacB_{Ctrl}) was used. In parallel to the immunization of the mice, *in vitro* control studies were performed to verify stability of antigens and MVA-S/C.

In vitro analysis confirmed the previous data (chapter 2.4.4, 2.5.2). SAAF-stabilization resulted in stable and intact HBcAg and HBsAg despite storage at higher temperatures for all examined conditions, in contrast to the non-stabilized samples (Figure 40A, B). Moreover, SAAF-stabilized antigens showed similar results as TherVacB_{Ctrl}. Figure 40 shows the representative HBcAg and HBsAg data obtained for one of the two prime immunizations.

Analysis of MVA-S/C titers by TCID₅₀ demonstrated that despite prolonged temperature stressing, highly infectious viral particles were detected in all samples (Figure 40C). However, SAAF-stabilized MVA-S/C demonstrated improved heat resistance, especially after 3 months of storage at 40 °C, confirming previously presented data (chapter 2.5.2).

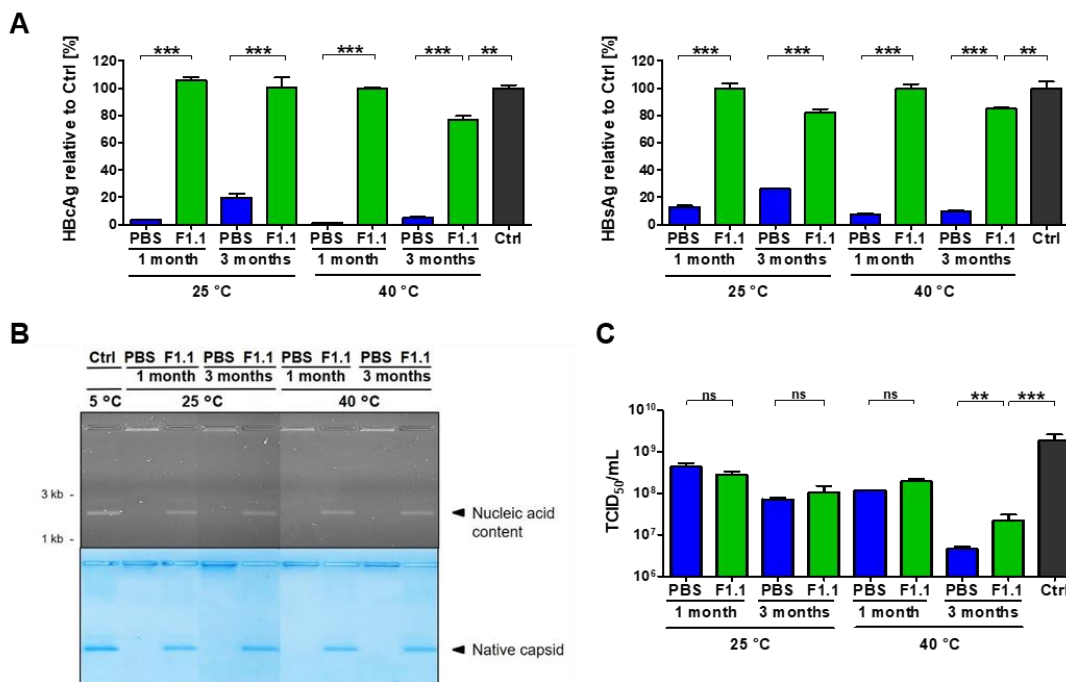


Figure 40. SAAF-stabilization maintained vaccine potency despite heat-exposure for 1 and 3 months.

Antigen integrity and MVA-S/C titers were analyzed *in vitro* after a storage of SAAF-stabilized (F1.1) and non-stabilized (PBS) TherVacB at 25 °C/60 % RH or 40 °C/75 % RH for 1 and 3 months. As control TherVacB_{Ctrl} components without stabilization or stressing (Ctrl) were used. (A) HBsAg- and HbcAg-specific ELISA. (B) NAGE of HbcAg. (C) MVA-S/C titers determined by TCID₅₀. Statistical analysis was performed using unpaired t-test. Asterisks mark statistically significant differences: ** $p \leq 0.01$; *** $p \leq 0.001$; ns - not significant. Modified from [183].

For testing immunogenicity *in vivo*, HBV-naïve mice were immunized with SAAF-stabilized or non-stabilized vaccine components according to the heterologous protein-prime/MVA vector boost regimen (Figure 41A). Mice were sacrificed one week after boost and HBV-specific antibody titers in serum, as well as HBV-specific T-cell responses in spleen were analyzed. Non-vaccinated HBV-naïve mice were used as negative controls.

High anti-HBc and anti-HBs titers were detected in all vaccinated groups in contrast to non-vaccinated mice, which did not induce any HBV-specific antibodies (Figure 41B, C). Similar anti-HBc antibody titers were determined for groups receiving the SAAF-stabilized and non-stabilized TherVacB after storage at 25 °C, as for TherVacB_{Ctrl} group (Figure 41B). After the exposure to 40 °C lower anti-HBc titers were measured in the mice immunized with the non-stabilized vaccine, whereas the SAAF-stabilized and the TherVacB_{Ctrl} groups showed comparable values. Interestingly, anti-HBs antibodies were elicited comparably strong after immunization with SAAF-stabilized- as well as non-stabilized TherVacB as similar antibody titers were detected for all vaccinated groups (Figure 41C).

ICS of splenocytes isolated from immunized mice, demonstrated that SAAF-stabilized vaccines induced strong core- and S-specific CD8⁺ T-cell responses, in contrast to non-vaccinated mice, independently from storage conditions (Figure 41D, E). The magnitude of core-specific CD8⁺ T-cell response was comparable between mice receiving SAAF-stabilized TherVacB components and TherVacB_{Ctrl} (Figure 41D). In contrast, a significantly weaker, or even absent core-specific CD8⁺ T-cell response was measured in the

groups immunized with non-stabilized vaccines. The results for core-specific CD8⁺ T-cell responses in SAAF-stabilized groups were comparable between different temperatures and duration of TherVacB stressing. In addition, equally strong S-specific CD8⁺ T-cell responses were measured in mice immunized with SAAF-stabilized and TherVacB_{Ctrl} components (Figure 41E). Only after the most extreme stressing conditions a slightly reduced S-specific CD8⁺ T-cell response was observed in the SAAF-stabilized group compared to TherVacB_{Ctrl}. By contrast, the results clearly showed that no S-specific CD8⁺ T-cell response was detected in the mice receiving non-stabilized TherVacB, already after exposure to the mildest stressing condition (25 °C/60 % RH for 1 month).

Analysis of CD4⁺ T cells demonstrated that comparable to non-vaccinated mice, a weak core-specific CD4⁺ T-cell response was detected in all vaccinated groups (Figure 41F). The magnitude of core-specific CD4⁺ T cells detected in groups receiving TherVacB vaccine was comparable to TherVacB_{Ctrl}, independently of using SAAF. Only in the mice immunized with TherVacB components stored at 25 °C for 3 months, a significantly higher core-specific CD4⁺ T-cell response was detected for the SAAF-stabilized group, in comparison to non-stabilized one. Higher frequencies of core-specific CD4⁺ T cells in mice receiving non-stabilized TherVacB components after a storage at 40 °C for 1 month was detected. This was an unexpected result as it was never be observed in any experiments and is most likely due to sample contamination. TherVacB vaccine induced only a very weak S-specific CD4⁺ T-cell response in few of the vaccinated mice, independently from stabilization and storage conditions (Figure 41G).

By comparing the *in vivo* results obtained for SAAF-stabilized vaccine components, which were stored for 1 and 3 months, no time-mediated differences were observed neither for the HBV-specific B- nor the T-cell responses after TherVacB immunization.

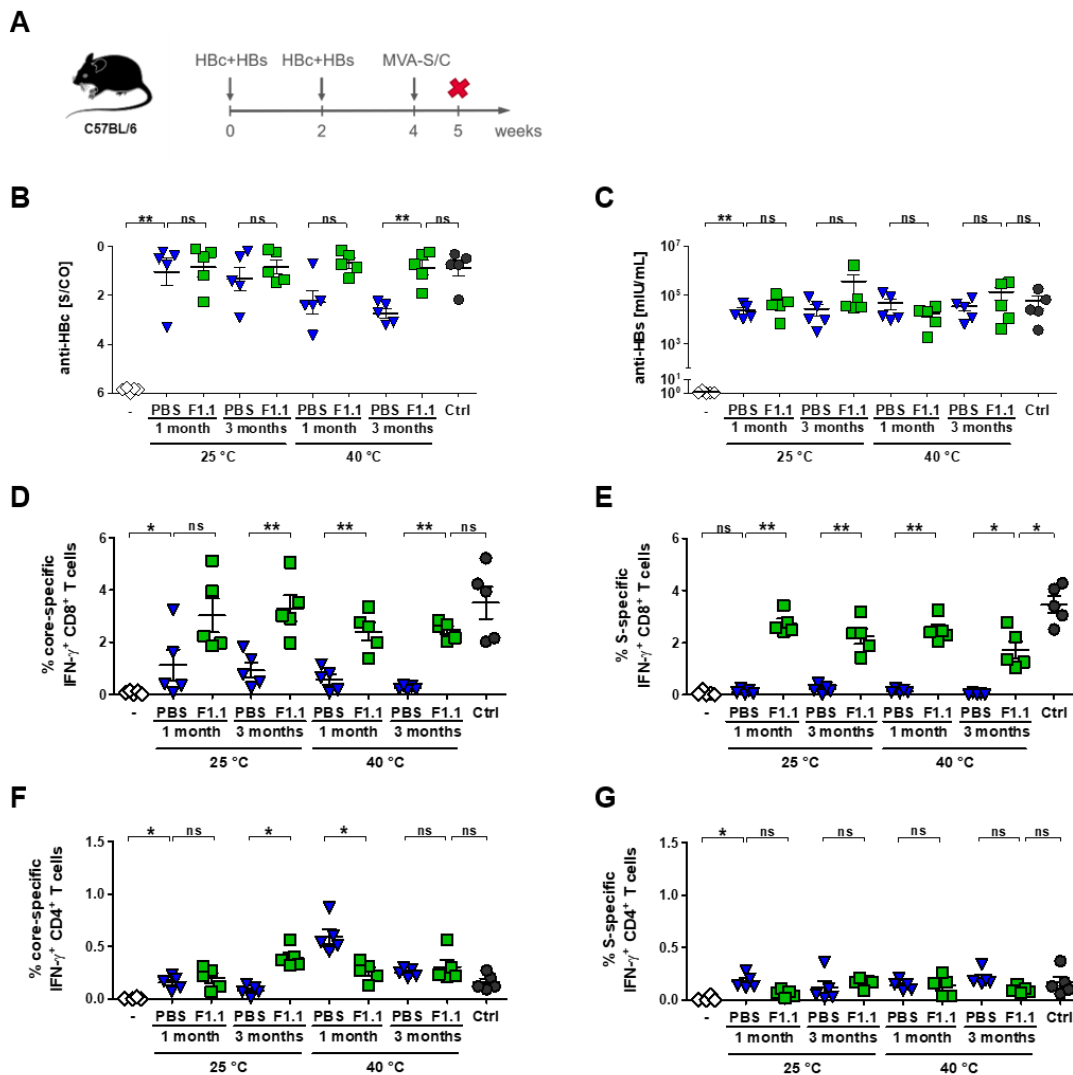


Figure 41. SAAF-stabilized vaccine induced strong HBV-specific immune response in HBV-naïve mice despite storage at 25 °C or 40 °C.

C57BL/6 mice were immunized according to the TherVacB regimen (A) with SAAF-stabilized (F1.1) and non-stabilized (PBS) after storage at 25 °C/60 % RH or 40 °C/75 % RH for 1 or 3 months. Mice immunized with TherVacB_{Ctrl} (Ctrl) or non-vaccinated mice (-) were used as controls. One week after boost, HBV-specific antibody titers in serum and T cells in spleen were measured. (B) anti-HBc and (C) anti-HBs levels. Core- (D) and S-specific (E) IFN- γ ⁺ CD8⁺ and core- (F) and S-specific (G) IFN- γ ⁺ CD4⁺ T-cell responses determined by ICS following *ex vivo* stimulation with HBV-specific peptides (C93, S208, C_{pool}, S_{pool}). Five mice per group were analyzed. Statistical analysis was performed using Mann-Whitney test. Asterisks mark statistically significant differences: * $p \leq 0.05$; ** $p \leq 0.01$; ns - not significant. Modified from [183].

Taken together, at every examined stressing condition, SAAF-stabilized TherVacB showed comparable results to TherVacB_{Ctrl}. In particular for the detected HBV-specific T-cell responses and the anti-HBc titers, SAAF-formulated TherVacB outperformed non-stabilized components. These results clearly demonstrate that SAAF-stabilized vaccine maintained remarkable immunogenicity even after 3 months of heat-exposure in HBV-naïve mice.

2.6.2 Stabilized and heat-exposed vaccine maintains efficacy in persistent HBV replication mouse model

After obtaining promising results in HBV-naïve mice, in the next step an AAV-HBV mouse model was used to address the question whether the SAAF-stabilization could ensure TherVacB efficacy in the setting of persistent HBV replication. A storage period for 1 month under accelerating aging conditions (40 °C/75 % RH) was chosen for challenging SAAF-stabilized and non-stabilized TherVacB. As a positive control TherVacB_{Ctrl} without stabilization or stressing was used.

Control *in vitro* analysis of the heat-exposed vaccine components confirmed previous results (chapter 2.4.4, 2.5.2, 2.6.1), showing that maintenance of antigen integrity and MVA-S/C infectivity was successfully achieved by formulation with SAAF (Figure 42A-C). Figure 42 shows the representative HBcAg and HBsAg data obtained for one of the two prime immunizations.

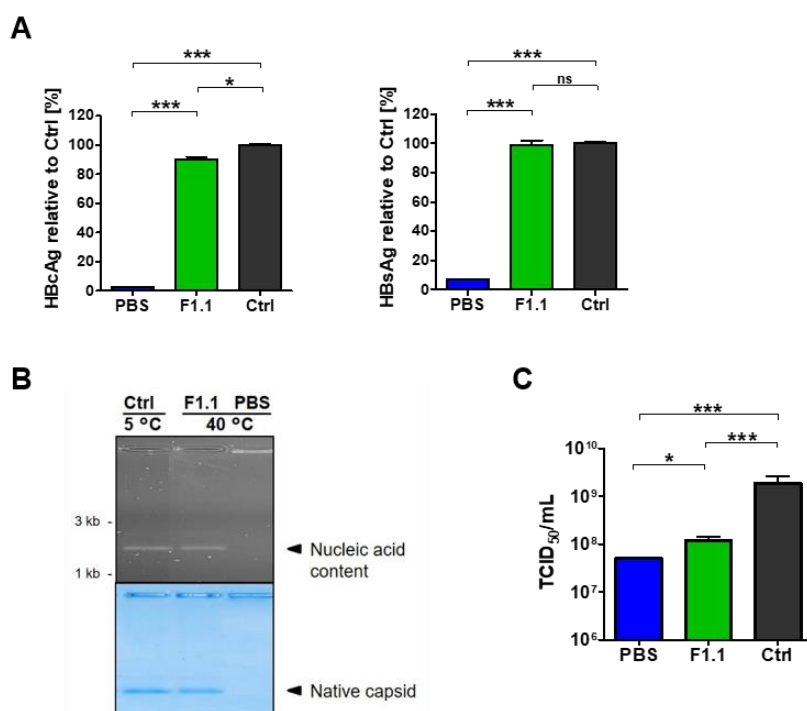


Figure 42. SAAF-stabilization maintained vaccine potency despite 40 °C-exposure for 1 month.

Vaccine stability was analyzed *in vitro* after storage of SAAF-stabilized (F1.1) and non-stabilized (PBS) TherVacB vaccine for 1 month under accelerated aging conditions at 40 °C/75 % RH. As control TherVacB_{Ctrl} components without stabilization or stressing (Ctrl) were used. (A) HBcAg- and HBsAg-specific ELISA. (B) MVA-S/C titers determined by TCID₅₀. Statistical analysis was performed using unpaired t-test. Asterisks mark statistically significant differences: * $p \leq 0.05$; *** $p \leq 0.001$; ns - not significant. Modified from [183].

To establish persistent HBV replication *in vivo*, C57BL/6 mice were i.v. injected with AAV-HBV. Four weeks later, mice were immunized with the SAAF-stabilized or non-stabilized heat-exposed vaccines using the heterologous protein prime/MVA vector boost vaccination regimen (Figure 44A). HBV-specific parameters in serum as well as HBV-specific T-cell responses in liver and spleen were analyzed at week 8, four weeks after the boost. Mice persistently infected with AAV-HBV, but not receiving any vaccine, served as an additional control group.

In contrast to non-vaccinated AAV-HBV infected mice, which did not possess any HBV-specific antibodies, high anti-HBc and anti-HBs titers in serum were detected in all vaccinated groups (Figure 44B). Mice immunized with SAAF-stabilized TherVacB components showed similar HBV-specific antibody titers as TherVacB_{Ctrl}. The group of mice receiving non-stabilized TherVacB vaccine displayed significantly lower anti-HBc titers as compared to SAAF-stabilized one. By contrast, the induction of anti-HBs antibodies was independent of stabilization of vaccine components. These observations were consistent with the results obtained in HBV-naïve mice (Figure 41B, C). Following induction of high anti-HBs levels, all vaccinated groups efficiently suppressed HBsAg in serum over time, unlike non-vaccinated mice, which did not show any anti-HBs (Figure 44C).

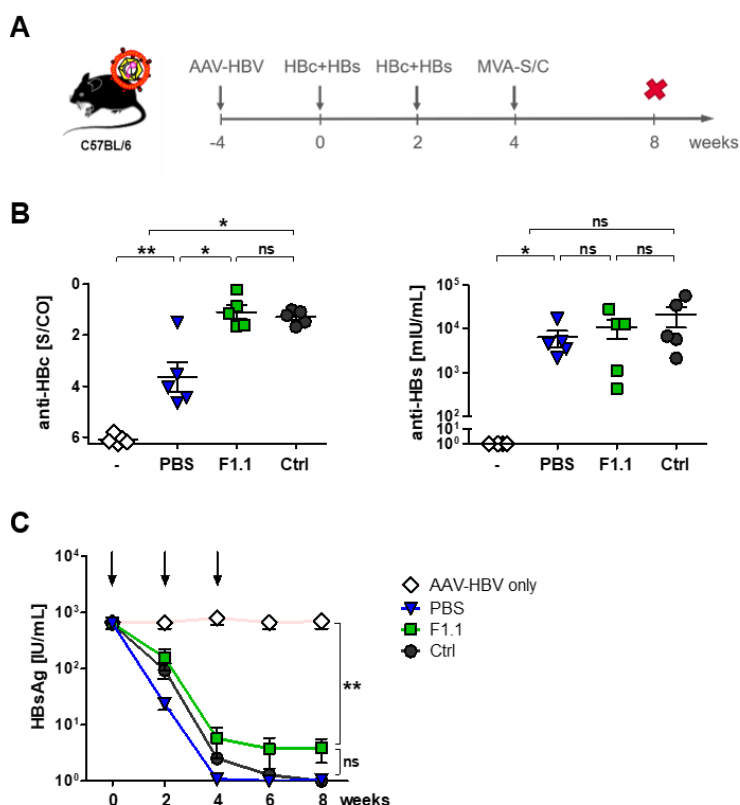


Figure 43. SAAF-stabilized TherVacB vaccine induced high HBV-specific antibody titers and reduced serum HBsAg levels despite 1 month of storage at 40 °C.

C57BL/6 mice were intravenously (i.v.) injected with AAV carrying an HBV genome (AAV-HBV). Four weeks later, AAV-HBV infected mice were immunized according to the TherVacB regimen (A) with SAAF-stabilized (F1.1) and non-stabilized (PBS) vaccine, which was stored for 1 month at 40 °C/75 % RH. Mice receiving TherVacB_{Ctrl} (Ctrl) or no vaccine (-) served as controls. (B) Serum anti-HBc and anti-HBs levels at week 8, four weeks after boost. (C) Time kinetics of serum HBsAg levels. Five mice per group were analyzed. Statistical analysis was performed using Mann-Whitney test. Asterisks mark statistically significant differences: * $p \leq 0.05$; ** $p \leq 0.01$; ns - not significant. Modified from [183].

ICS analysis of splenocytes and liver associated lymphocytes (LALs) isolated from immunized mice, showed that no positive core-specific CD4⁺ T cells were detected at the examined time point, neither in the livers nor in the spleens of mice receiving any TherVacB vaccine (Figure 44A, B). The S-specific CD4⁺ T-cell response detected in the spleen was mostly negative in all immunization groups and was comparable to the background values measured in non-vaccinated AAV-HBV infected mice (Figure 44B). However, a strong S-specific CD4⁺ T-cell response was detected in the livers of the mice immunized with SAAF-stabilized vaccine,

which was similar to TherVacB_{Ctrl}, whereas the non-stabilized group demonstrated only a very low S-specific CD4⁺ T-cell response (Figure 44A).

The immunization with SAAF-stabilized TherVacB led to induction of strong core- and S-specific CD8⁺ T-cell responses in the liver, in contrast to non-vaccinated mice, which showed no HBV-specific CD8⁺ T-cell response (Figure 44C). The magnitude of hepatic core- and S-specific CD8⁺ T-cell responses was similar in mice receiving SAAF-stabilized vaccine as in TherVacB_{Ctrl}. An equally strong S-specific CD8⁺ T-cell response in the spleen was detected in the SAAF-stabilized group and TherVacB_{Ctrl} (Figure 44D). In addition, a clearly positive, although weak core-specific CD8⁺ T-cell response was observed in the spleens of mice receiving SAAF-stabilized vaccine as compared to non-vaccinated mice. Without stabilization no significant HBV-specific CD8⁺ T-cell response neither in the liver nor in the spleen was detected, resembling the result obtained in non-vaccinated AAV-HBV infected mice.

Following the strong hepatic HBV-specific CD8⁺ T-cell response, sustained ALT increase was detected in mice, which received SAAF-stabilized vaccine and TherVacB_{Ctrl}, indicating increased CD8⁺ T cell-mediated liver damage (Figure 44E). Consequently, immunization with SAAF-stabilized vaccine resulted in a gradual decrease of serum HBeAg (Figure 44F). Both observations suggest T cell-mediated elimination of AAV-HBV-positive hepatocytes. The detected kinetics of HBeAg reduction in the SAAF-stabilized groups closely resembled the one detected for TherVacB_{Ctrl}. In contrast, neither an ALT increase nor an HBeAg reduction was detected in the mice immunized with non-stabilized vaccine, reflecting the levels measured for non-vaccinated controls.

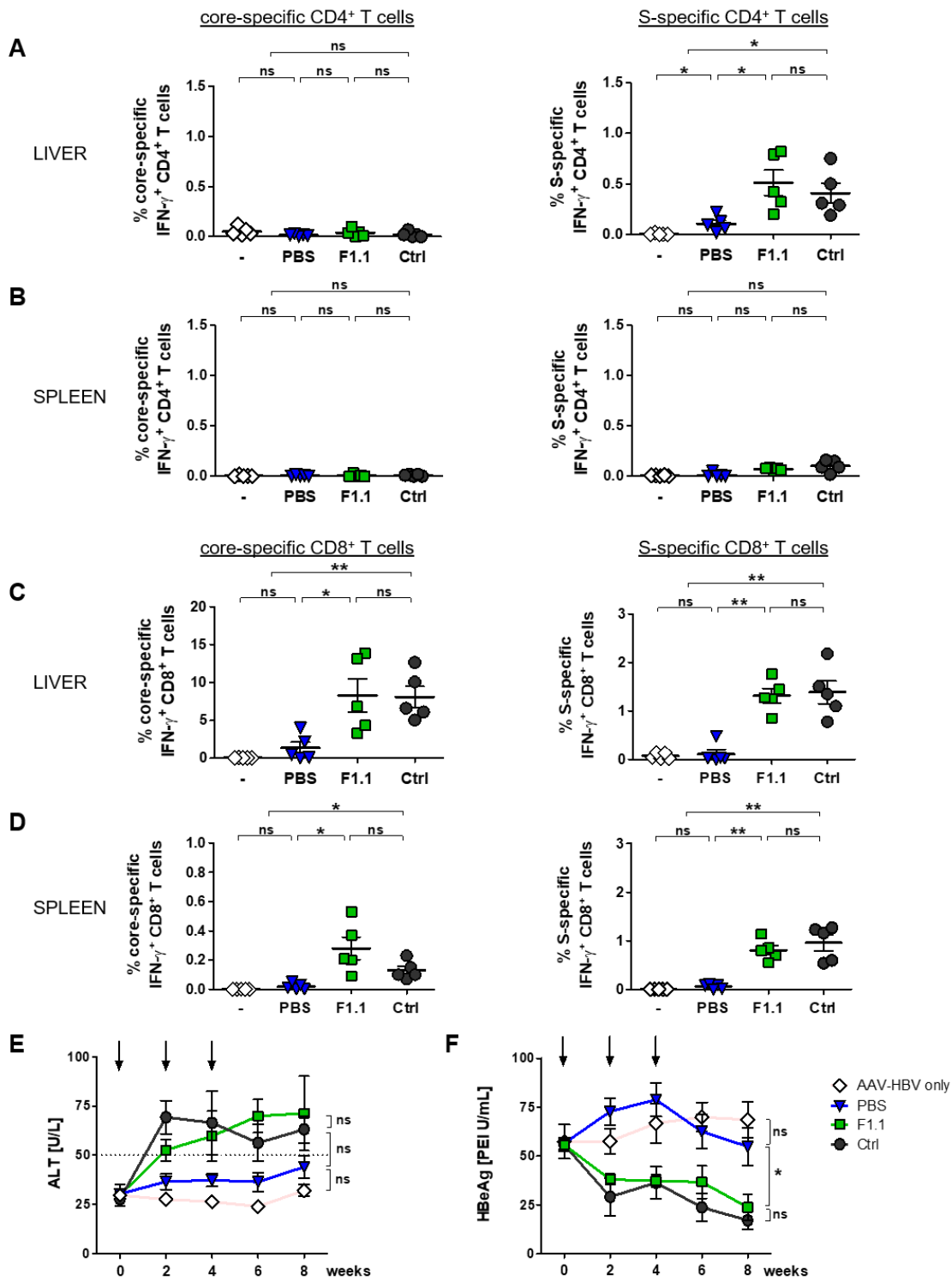


Figure 44. Formulation with SAAF led to the induction of a strong HBV-specific immune response in AAV-HBV infected mice despite 40 °C-exposure for 1 month.

C57BL/6 mice were transduced with AAV-HBV and four weeks later immunized according to the TherVacB regimen with SAAF-stabilized (F1.1) and non-stabilized (PBS) vaccine, which was stored for 1 month at 40 °C/75 % RH. Mice receiving TherVacB_{Ctrl} (Ctrl) or non-vaccinated mice (-) were used as controls. HBV-specific parameters and T cells were analyzed at week 8, four weeks after boost. Core- and S-specific IFN- γ ⁺ CD4⁺ T-cell responses in liver (A) and spleen (B) as well as core- and S-specific IFN- γ ⁺ CD8⁺ T-cell responses in liver (C) and spleen (D) determined by ICS following *ex vivo* stimulation with HBV-specific peptides (C93, S208, C_{pool}, S_{pool}). (E) Serum alanine aminotransferase (ALT) and (F) time kinetics of HBeAg levels. Five mice per group were analyzed. Statistical analysis was performed using Mann-Whitney test. Asterisks mark statistically significant differences: * p ≤0.05; ** p ≤0.01; ns - not significant. Modified from [183].

In summary, these results demonstrate that SAAF-stabilized vaccine induced high-titer HBV-specific antibodies and functional core- and S-specific CD8⁺ T-cell responses, even after prolonged storage at accelerating aging conditions. Moreover, this vaccine led to efficient suppression of HBsAg and HBeAg levels comparable to TherVacB_{Ctrl}.

2.6.3 One-year RT-exposed vaccine induces immune response in persistent HBV replication mouse model

In the last set of experiments, the efficacy of SAAF-stabilized TherVacB was analyzed after long-term storage according to EMA, ICH and WHO required conditions in AAV-HBV mouse model. To this purpose, TherVacB components were stored for 12 months at 25 °C/60 % RH, prior to onset of the *in vitro* and *in vivo* experiments. In contrast to mouse studies described above, the antigens were not combined for lyophilization and subsequent long-term storage in this experimental setup. The reason of this was that the 12 months storage period was initiated before the positive effect of antigen combination was known. As a positive control TherVacB_{Ctrl} without stabilization or stressing was used. In this experimental setup a further control group receiving SAAF-stabilized but non-stressed (5 °C) vaccine was included.

Control *in vitro* experiments confirmed previous data (chapter 2.6) demonstrating that in samples stabilized with SAAF distinctly intact HBcAg and HBsAg were detected, in contrast to non-stabilized samples (Figure 45A, B). Nevertheless, lower ELISA signals, were detected for the SAAF-stabilized HBcAg compared to TherVacB_{Ctrl}, whereas for the SAAF-stabilized HBsAg comparable signals were measured. These data were confirmed by previous findings showing the beneficial usage of combined antigens in comparison of single components (chapter 2.4.2). Figure 45 shows the representative ELISA (Figure 45A) and NAGE (Figure 45B) results obtained for one of the two prime immunizations.

The analysis of MVA-S/C demonstrated that formulation with SAAF strongly improved MVA-S/C infectivity compared to non-stabilized samples (Figure 45C). In addition, a slightly higher titer was determined for the SAAF-stabilized, non-stressed MVA-S/C sample in comparison with SAAF-stabilized MVA-S/C samples after long-term RT-storage.

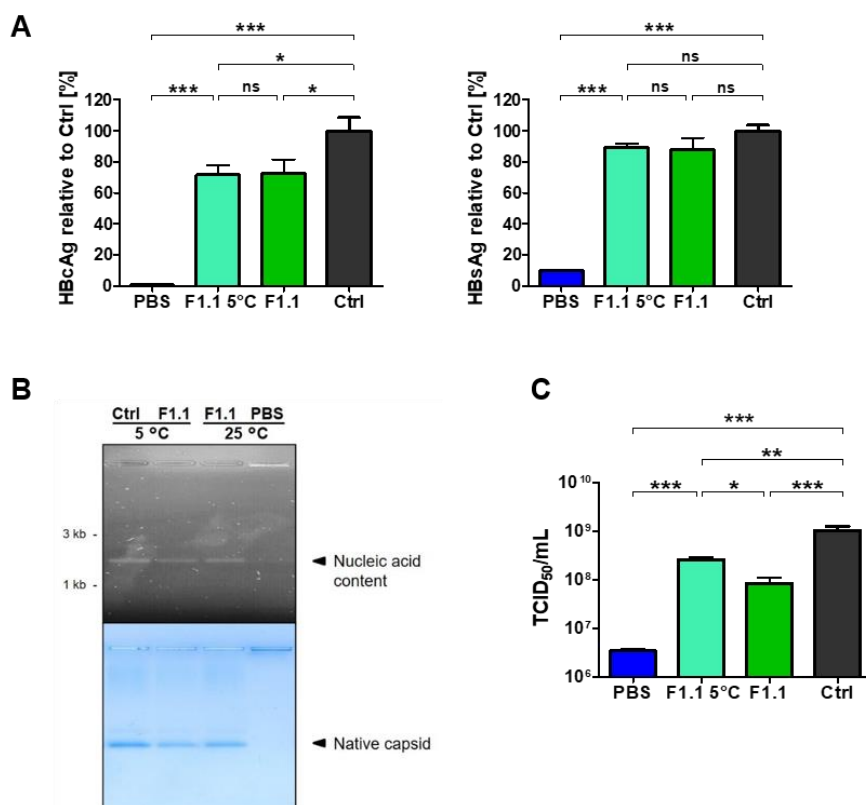


Figure 45. SAAF-stabilized TherVacB components remained stable despite storage at RT for 12 months.

Vaccine potency was analyzed *in vitro* after storage of SAAF-stabilized (F1.1) and non-stabilized (PBS) TherVacB at 25 °C/60 % RH for 12 months. As control SAAF-stabilized and non-stressed (F1.1 5 °C) or TherVacB_{ctrl} without stabilization or stressing (Ctrl) vaccine components were used. (A) HBcAg- and HBsAg-specific ELISA. (B) MVA-S/C titers determined by TCID₅₀. Statistical analysis was performed using unpaired t-test. Asterisks mark statistically significant differences: * $p \leq 0.05$; ** $p \leq 0.01$; *** $p \leq 0.001$; ns - not significant. Modified from [183].

For the *in vivo* part of this experiment, C57BL/6 mice were transduced with AAV-HBV and four weeks later, they were immunized with the SAAF-stabilized or non-stabilized vaccine, which was stored for 1 year at 25 °C/60 % RH according to the TherVacB prime-boost regimen (Figure 47A). HBV-specific parameters in serum and T-cell responses in liver and spleen were studied after sacrificing the mice at week 8, four weeks after the boost. Mice persistently infected with AAV-HBV, but not receiving any vaccine, served as additional controls.

Similar to the results obtained for the mouse experiment described above (chapter 2.6.2), high HBV-specific antibody titers were detected in all vaccinated groups (Figure 47B). In the mice receiving SAAF-stabilized vaccines similar anti-HBc and anti-HBs titers were detected as for TherVacB_{ctrl}, independent of storage at 5 °C or 25 °C. In contrast, in the serum of the mice immunized with non-stabilized vaccine significantly lower anti-HBc titers were measured compared to SAAF-stabilized groups. However, similar anti-HBs titers were detected in SAAF-stabilized, non-stabilized and TherVacB_{ctrl} groups. In consequence, all vaccinated groups efficiently suppressed serum HBsAg. However, the HBsAg decrease was considerably stronger in the SAAF-stabilized group, as compared to the non-stabilized one, and closely resembled TherVacB_{ctrl} despite 1 year of storage at RT.

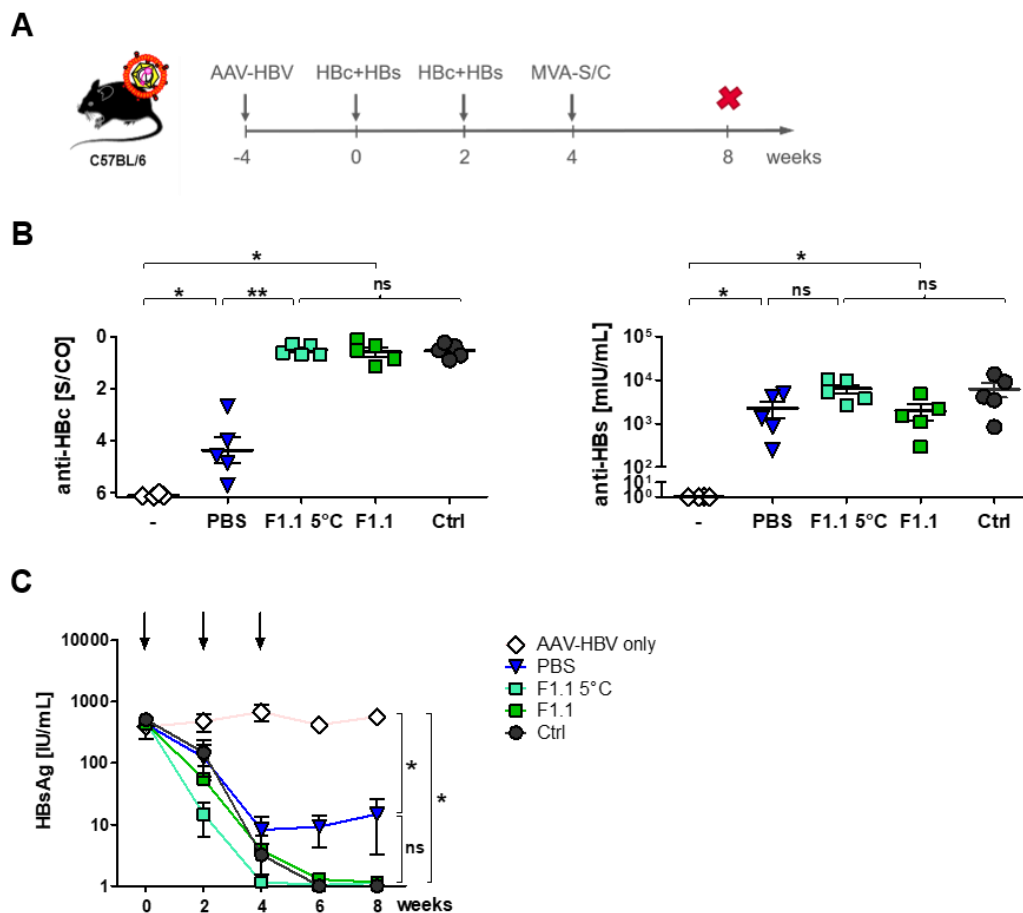


Figure 46. Immunization with SAAF-stabilized TherVacB vaccine led to the induction of high HBV-specific antibodies and suppression of HBsAg levels.

C57BL/6 mice were i.v. injected with AAV-HBV and four weeks later immunized according to the TherVacB regimen (A) with SAAF-stabilized (F1.1) and non-stabilized (PBS) vaccine, which was stored for 12 months at 25 °C/60 % RH. Mice receiving SAAF-stabilized and non-stressed (F1.1 5 °C), TherVacB_{Ctrl} (Ctrl) or no vaccine (-) served as controls. (B) HBV-specific antibody titers were measured in the serum of the mice at week 8, four weeks after the boost. (C) Time kinetics of serum HBsAg levels. Five mice per group were analyzed. Statistical analysis was performed using Mann-Whitney test. Asterisks mark statistically significant differences: * $p \leq 0.05$; ** $p \leq 0.01$; ns - not significant. Modified from [183].

ICS of splenocytes and LALs isolated from immunized mice showed that no positive core-specific IFN- γ ⁺ CD4⁺ T-cell response was detected in any group neither in the livers nor in the spleens at the examined time point (Figure 47A, B). In contrast, immunization with SAAF-stabilized vaccine induced a significantly stronger S-specific CD4⁺ T-cell response in both organs, compared to non-vaccinated AAV-HBV infected mice. However, there was no clear difference detectable between the mice immunized with non-stabilized, SAAF-stabilized or TherVacB_{Ctrl} vaccines.

The ICS analysis of CD8⁺ T cells demonstrated the induction of a strong core-specific CD8⁺ T-cell response in the livers of the mice immunized with SAAF-stabilized TherVacB vaccine in comparison to non-vaccinated AAV-HBV infected mice, independent of storage at 5 °C or 25 °C (Figure 47C). In contrast, mice receiving non-stabilized vaccine showed reduced core-specific CD8⁺ T-cell response, albeit not statistically significant, compared to SAAF-stabilized vaccine. In addition, a significantly stronger core-specific CD8⁺ T-cell

response was measured in the spleens of mice immunized with SAAF-stabilized TherVacB as compared to mice receiving the non-stabilized vaccine (Figure 47D). Without stabilization no CD8⁺ T-cell response was detected, similar to non-vaccinated controls.

The induction of a S-specific CD8⁺ T-cell response in mice receiving 1-year stressed and SAAF-stabilized TherVacB was not as strong as in mice immunized with TherVacB_{Ctrl}. Nevertheless, in mice receiving SAAF-stabilized vaccine significantly stronger S-specific CD8⁺ T-cell responses were measured in liver and spleen as compared to non-vaccinated AAV-HBV infected mice (Figure 47C, D). However, no statistically significant difference between SAAF-stabilized and non-stabilized groups was detected.

After immunization with SAAF-stabilized vaccine, a clear reduction in serum HBeAg was detected suggesting T cell-mediated elimination of AAV-HBV-positive hepatocytes (Figure 47E). The kinetics of HBeAg decreased over time similar to the one measured in mice receiving TherVacB_{Ctrl} vaccine. In contrast, no differences in HBeAg kinetics were detected in the non-stabilized groups as in non-vaccinated AAV-HBV infected mice.

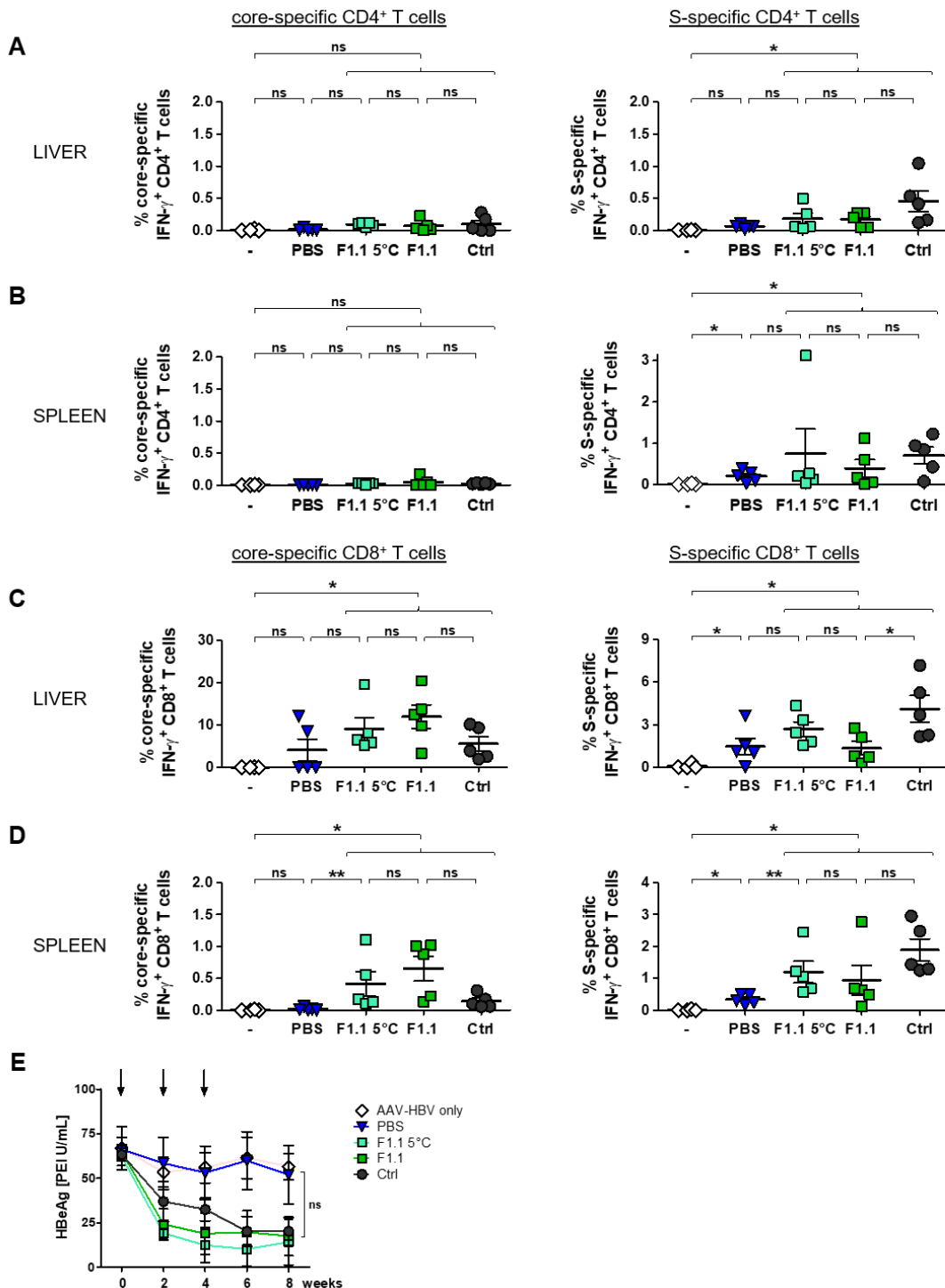


Figure 47. SAAF-stabilized and 1-year at RT-exposed vaccine induced HBV-specific T-cell responses and reduced HBeAg levels in AAV-HBV infected mice.

Four weeks after C57BL/6 mice were transduced with AAV-HBV, mice were immunized according to the TherVacB regimen with SAAF-stabilized (F1.1) and non-stabilized (PBS) vaccine, which was stored for 12 months at 25 °C/60 % RH. Mice receiving SAAF-stabilized non-stressed (F1.1 5 °C) vaccine or TherVacB_{Ctrl} (Ctrl) or non-vaccinated mice (-) served as controls. At week 8, four weeks after boost, HBV-specific parameters in serum and T-cell responses in liver and spleen were analyzed. Core- and S-specific IFN- γ ⁺ CD4⁺ T-cell responses in liver (A) and spleen (B) as well as core- and S-specific IFN- γ ⁺ CD8⁺ T-cell responses in liver (C) and spleen (D) determined by ICS following *ex vivo* stimulation with HBV-specific (C93, S208, C_{pool}, S_{pool}) peptides. (E) Time kinetics of serum HBeAg levels. Five mice per group were analyzed. Statistical analysis was performed using Mann-Whitney test. Asterisks mark statistically significant differences: * $p \leq 0.05$; ** $p \leq 0.01$; ns - not significant. Modified from [183].

In summary, the SAAF-stabilized vaccine proved to be more immunogenic than the non-stabilized one despite temperature stressing. In consequence, SAAF-stabilized TherVacB clearly decreased HBsAg and HBeAg levels, equally efficient as TherVacB_{Ctrl}. These results demonstrated that SAAF-stabilization is successful and allows for 1 year of storage at RT. However, the stabilized vaccine showed higher efficacy after 3 months of heat-exposure as compared to such extreme stressing.

2.7 TherVacB adjuvant, c-di-AMP, remains stable despite storage at higher temperatures

For the prime immunization of TherVacB, HBcAg and HBsAg were formulated with the adjuvant c-di-AMP. Recently, it was shown that use of an appropriate adjuvant is crucial for the prime immunization to induce a satisfactory immune response after vaccination (Su, Kosinska, unpublished data, [73]). C-di-AMP represents a promising candidate for TherVacB clinical trials, as it leads to the induction of a simultaneous T_H1/T_H2-based immune response [96]. The experiments described above clearly demonstrate that an outstanding thermal stability of the TherVacB components was achieved. Therefore, it was of a relevant interest, to test the thermostability of the used adjuvant c-di-AMP. These experiments were performed in cooperation with Prof. Carlos Guzmán and Dr. Thomas Ebensen at HZI Braunschweig.

To test the stability of the adjuvant, lyophilized c-di-AMP was stored at 20 °C, 25 °C or 40 °C. After 3 days, 1, 3 or 12 months of exposure, the activity of c-di-AMP in human monocytic THP-1 cell line was tested. THP-1 Blue™ ISG cells are stable reporter cells which express a reporter gene under the control of an interferon regulatory factors (IRF)-inducible promoter. As c-di-AMP triggers type I IFN production and the induction of interferon stimulated genes (ISG) through IRFs, the c-di-AMP can be evaluated in the THP-1 cell line. As control for the temperature stressing, the non-stressed lyophilized adjuvant, which was stored at -20 °C, was used. In addition, the assay was done in parallel in STING-knockout (KO) cells in which c-di-AMP cannot induce IFN production. As positive control, lipopolysaccharide (LPS) activity was measured, which is induced by Toll-like receptor 4 in both cell lines. To evaluate the background signal, cells without the addition of c-di-AMP or LPS were included.

After 3 days or 1 month of storage at higher temperatures, the c-di-AMP showed a high biological activity (Figure 48A). In addition, no significant difference in c-di-AMP activity was measured between storage periods at 25 °C or 40 °C. Only after 3 months of storage at 40 °C a minor decrease in the detected signal was observed in comparison to the control sample (Figure 48B). Even after storing c-di-AMP for 1-year at 20 °C, comparably high biological activities were determined in the temperature stressed and in the control samples (Figure 48C).

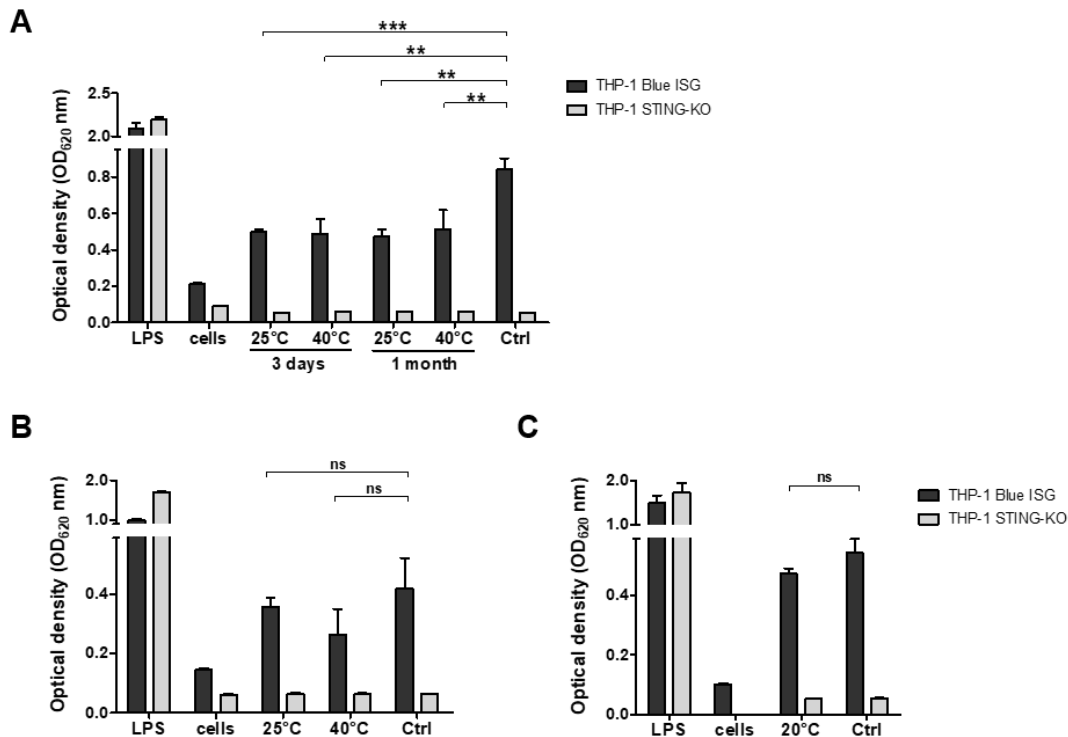


Figure 48. High thermal stability of c-di-AMP despite temperature stressing.

After storing lyophilized c-di-AMP at higher temperatures, biological activity of c-di-AMP was evaluated in THP-1 Blue™ ISG cells. Optimal at -20 °C stored lyophilized c-di-AMP was included as storage control. THP-1 STING-knockout (KO) cells without c-di-AMP activity were used as control. Lipopolysaccharide (LPS) activity can be measured in both cell lines representing the positive control. To evaluate the background signal, cells without c-di-AMP or LPS were used. C-di-AMP was stored for 3 days, 1 month (A) or 3 months (B) at 25 °C or 40 °C or 12 months at 20 °C (C). Statistical analysis was performed using unpaired t-test. Asterisks mark statistically significant differences: ** $p \leq 0.01$; *** $p \leq 0.001$; ns - not significant.

Taken together, these data demonstrate that c-di-AMP showed high biological activity despite prolonged storage at higher temperatures.

3 Discussion

With 257 million infected individuals worldwide, chronic hepatitis B represents one of the major global health problems [69]. Current treatment options are not sufficient as they cannot specifically target or eliminate the persistence form of HBV, the cccDNA [197]. Therefore, therapeutic vaccination is a promising approach to treat chronic hepatitis B, as it aims to reactivate the patient's defective immune system to eliminate HBV-infected hepatocytes and control the virus [71]. However, a major challenge of global vaccine application is the lack of continuous cold chains to prevent loss of vaccine efficacy, due to thermal instability of the vaccine components [133, 134, 136]. To solve this problem, the development of a thermostable, therapeutic vaccine against chronic hepatitis B was described above and is discussed throughout this part of the thesis.

3.1 Effective stabilization of TherVacB vaccine components *in vitro*

Among various therapeutic hepatitis B vaccination concepts, a promising candidate was developed by the Institute of Virology (HMGU/TUM). The heterologous protein prime/MVA vector boost vaccination strategy (TherVacB) was specifically designed to efficiently induce HBV-specific B- and T-cell responses and demonstrated encouraging results in hepatitis B preclinical mouse models [73, 94, 198]. Three components are essential for the success of the TherVacB approach: HBsAg, HBcAg and an MVA vector expressing HBV core and S protein. Previously, it was reported that immunization of chronic hepatitis B patients with HBsAg led to the induction of HBsAg-specific CD4⁺ T-cell response and anti-HBs antibodies [75]. The neutralizing form of these antibodies prevents virus spread to non-infected hepatocytes and the seroconversion from HBsAg to anti-HBs defines the clinical endpoint of HBV-infection [49]. HBcAg is known to be highly immunogenic as the nucleic acids, which are bound to its C-terminal arginine-rich region, activate Toll-like receptor 3 signalling [199] and facilitate priming of T_H1 immunity [200]. In addition, HBcAg can enhance T cell priming by activating B cells to enable their function as potent primary antigen presenting cells [201, 202]. To boost the protein-primed HBV-specific immune response, the recombinant MVA is used, as it mediates strong immune responses against encoded proteins [118-122]. In addition, the safety of MVA immunization was verified in many clinical trials against infectious diseases [123-127]. In this study, the most suitable HBcAg and HBsAg for TherVacB prime immunization were selected from several manufacturers. Within this process methods to analyze the integrity of both antigens were established and optimized (chapter 2.1.3). The chosen HBsAg and HBcAg, were already produced under GMP conditions, which would facilitate the future use in clinical trials as upscaling of the GMP compliant manufacturing process is mandatory for vaccine components [203, 204].

It was shown that the immunization with combined MVA-C and MVA-S induces a stronger immune response than the application of single MVAs during booster immunization [94]. Therefore, in this study a new bicistronic vector MVA-S/C, expressing both HBV core and S protein, was generated and verified in different mouse models. The use of a single MVA vector

for immunization would simplify the approval process of TherVacB vaccine for the future clinical use.

The WHO and many vaccine manufacturers recommend storage at 2-8 °C for the majority of the vaccines to preserve their efficacy [136]. The data obtained within this thesis confirmed that the storage temperature of 4 °C is the most suitable for both HBV antigens in solution (Figure 16, Figure 17). In contrast, MVA-S/C in solution proved to be quite stable within a broader temperature range from -80 °C to 25 °C (Figure 13, Figure 18). Nevertheless, the most optimal MVA-S/C storage condition was the temperature of -80 °C, which supports previously described findings [205]. Interestingly, no significant difference in MVA-S/C infectivity between viral samples stored for 3 months at 4 °C or -80 °C was observed in this study (Figure 13). In addition, long-term experiments showed only a minor decrease in viral titer (less than 1 log) for the lyophilized non-stabilized MVA-S/C after 12 months of storage at 4 °C (Figure 37). Since the results of this study show that the lyophilization process did not influence MVA-S/C infectivity, the results of the long-term study seem to be also valid for a sample in solution, indicating that MVA-S/C remains intact at the WHO recommended storage temperature of 2-8 °C for at least 3 months, but most likely longer. This assumption was substantiated by the results of stability studies of a non-lyophilized recombinant MVA used in a candidate Ebola vaccine, which proved to be stable for 12 months at 2-8 °C [206].

A major challenge of vaccine application worldwide is that most of the vaccine components lose their potency during transport and storage outside the cold chain [133, 136]. The need for continuous cooling was also observed for TherVacB components (Figure 17, Figure 18). The exposure to the temperature of 25 °C for 1 month, the upper limit of RT, led to a significantly reduced stability of HBcAg in solution as compared to SM_{Ctrl} (antigen without lyophilization or storage). For the HBsAg the decrease turned out to be even more drastic as only 20 % remaining ELISA activity was measured (Figure 17). These findings support the need of antigens storage at 2-8 °C, which is already recommended for commercially available HBsAg-based prophylactic hepatitis B vaccines to maintain their efficacy [136]. However, several studies demonstrated that some of the prophylactic hepatitis B vaccines remain quite stable despite storage at higher temperatures [136]. These vaccines contain aluminium salts as adjuvants, which are most likely the reason for their heat-stability and pose a substantial difference to the vaccine components used in this study. In addition, alum-adsorbed prophylactic vaccines are not suitable as therapeutic vaccines, as they do not support the induction of efficient CD8⁺ T-cell responses which are essential to eliminate pre-existing HBV infections [71, 207, 208]. Apart from the benefits of using T helper type one/two (T_H1/T_H2)-biased adjuvants such as c-di-AMP instead of alum, the results of this study demonstrate that lyophilized and SAAF-stabilized TherVacB vaccine displayed a remarkably higher stability concerning the temperature range and storage durations, when compared to HBsAg in solution adjuvanted with alum [136, 209, 210].

In contrast to the strong decrease in the antigen integrities, high stability of MVA-S/C in solution was determined by TCID₅₀ analyses of the virus after stressing at different temperatures and timeframes (Figure 18). Nevertheless, after RT-storage at 28 days a significantly lower MVA-S/C titer was detected than for SM_{Ctrl}. These results confirm previously described data

that poxvirus virions display an excellent stability even after a storage for several months in ambient environment [211].

Many hepatitis B patients are living in countries with high outdoor temperatures [7]. Moreover, the majority of the vaccines are extremely unstable under the climate conditions prevailing in these areas [133, 136]. Therefore, it was expected that the transport and storage of the TherVacB in solution could be challenging. The results obtained in this thesis confirmed this assumption, as the HBcAg in solution showed a severe integrity decrease of around 60 % already after 3 days of storage at 40 °C, whereas HBsAg completely lost its stability (Figure 17). In addition, MVA-S/C in solution demonstrated a significant reduction in viral titer after incubation at 40 °C for 3 days and from day 14 onwards no infectious MVA-S/C particles were detected anymore (Figure 18). These data clearly demonstrate the instability of TherVacB components at higher temperatures. Therefore, an uninterrupted cold chain from the manufacturer to the patient would be essential to ensure effectiveness of the vaccine [133, 134]. However, due to high costs and a low infrastructure in low- and middle income countries a continuous cooling can often not be provided [132].

To prevent stability loss of TherVacB components, the question was addressed how to protect the antigens and the viral vector against heat-mediated damages. To solve this problem, the TherVacB components were stabilized by lyophilization (further discussed in chapter 3.2) in the presence of stabilizing amino acid-based formulations (SAAFs) from LEUKOCARE. Recently, it was described that SAAF can stabilize a broad range of different biological compounds such as therapeutic antibodies, viral vectors (adenovirus type 5) or a split-virion influenza vaccine [178-180]. The results of this thesis clearly demonstrate that lyophilization in the presence of SAAF enabled the successful stabilization of TherVacB components against different heat-challenges over short and long-term storage periods *in vitro* (chapter 2.5). Furthermore, a single optimal SAAF was identified capable of efficiently stabilizing all three TherVacB components (chapter 2.4). This confirms the wide application spectrum of SAAF [178-180]. Moreover, the enhancement of vaccine stability by antigen combination, instead of using single components, and stabilization with one SAAF was demonstrated (Figure 20, Figure 38, Figure 39). These findings could present an additional benefit for the future vaccine application in patients, as only one “ready-to-use” formulation per immunization would be required, thus making the application easier and less strenuous. In addition, the possibility to use one single SAAF for the priming step would simplify the manufacturing process and facilitate the future clinical approval, as only one additional excipient has to be verified by the regulatory authorities. In the context of marketing authorization, it is also useful that SAAF only consist of natural small molecules, which are already approved and accepted by regulators as excipients in various pharmaceuticals [164, 180].

To enable successful global vaccine application and solve the barriers of thermal instability of vaccines and the lack of continuous cold chains, the WHO presented the ECTC guideline which requires the labelling and testing of every vaccine for a storage above 2-8 °C [137] and the CTC program which requests the stability of a vaccine despite a single exposure for a minimum of 3 days at 40 °C [134]. The results of this thesis show that lyophilization and SAAF-stabilization led to the maintenance of HBcAg and HBsAg integrities and improvement

of MVA-S/C heat resistance despite storage at 40 °C for 3 days *in vitro* (chapter 2.5.1). Therefore, TherVacB components fulfill the requested stability of WHO CTC criteria. Moreover, heat-mediated damages were prevented by lyophilization and SAAF-stabilization even after more extreme stressing conditions (chapter 2.5.2, 2.5.3). In contrast, non-stabilized vaccine components showed reduced MVA-S/C titers as well as profound subsequent antigen integrity loss over time during heat-exposure.

Previously published NAGE and DLS analyses demonstrated heat-induced aggregation of HBcAg [212, 213]. The results of the present study (chapter 2.5.2) confirm heat-mediated formation of HBcAg aggregates, as after 1 month of storage at 40 °C non-stabilized HBcAg stuck in the pocket of the agarose gel during NAGE. In addition, DLS analysis showed larger particles for the non-stabilized HBcAg and HBsAg than in SAAF-stabilized samples or SM_{Ctrl}. In addition, non-stabilized and stressed antigens demonstrated an integrity loss of 60-70 % by ELISA. This result indicates that the conformational epitopes of antigens, where ELISA antibodies would bind, were destroyed by 40 °C-exposure. On the contrary, comparable WB signals were detected for all samples indicating that the antigens were not degraded by the heat and WB antibodies could still bind to linear epitopes of the antigens. This observation confirms previously published data, which showed that heat destroyed conformational epitopes, while linear epitopes remained intact [214]. Interestingly, despite many antigen aggregates also a few intact HBcAg and HBsAg particles were detected by TEM, which showed their native structures and sizes independent of SAAF-stabilization and heat-exposure. In addition, also a small peak at a lower size was detected by DLS for the non-stabilized stressed sample which was located at a comparable size as the SAAF-stabilized and SM_{Ctrl} sample. This peak probably represents intact antigens and could be one explanation for the remaining ELISA signal. It was reported that some antibodies could also bind on aggregated antigens if the binding site of the antibodies would be still accessible [215]. However, the small number of stable antigens was not enough to be detected by NAGE, which was expected, as this method is not sensitive enough for samples with very low concentrations. The results clearly demonstrate that SAAF-stabilization significantly improve MVA-S/C heat resistance, even though for non-stabilized MVA-S/C samples infectious viral particles were detected after the temperature stressing. Therefore, it was not astounding that no differences between SAAF-stabilized, non-stabilized and SM_{Ctrl} samples were observed by TEM. These observations were supported by previously reported TEM data displaying intact structures of MVA-C despite heat-stressing [193].

Apart from the WHO CTC criteria, vaccines additionally need to fulfill mandatory guidelines to be approved. In countries with climate zones 1 and 2, EMA, ICH and WHO require vaccine stability despite 12 months of storage at 25 °C [194, 196]. The results of the long-term experiments in this thesis demonstrate the excellent stability of SAAF-stabilized TherVacB *in vitro* at the required conditions (chapter 2.5.3). In contrast, the non-stabilized components did not maintain antigen integrity and showed less infectious MVA-S/C particles after such an extreme stressing.

The development of thermostable vaccines against relevant epidemiological threats for the human population gained significant interest over the past decade [157, 162, 167, 170-173].

To achieve sufficient thermostability, many strategies used various drying methods in the presence of stabilizing excipients. In this context, a spray-dried measles virus vaccine, which was stabilized with several excipients like sugars, proteins or amino acids, demonstrated a thermostability at 37 °C for 8 weeks *in vitro* [157]. The SAAF, used in this study for TherVacB-stabilization, consists of similar components such as amino acids, saponins and sugars. However, the SAAF-stabilized TherVacB demonstrated superior stability to the measles virus vaccine, as the potency of HBV antigens and MVA-S/C was maintained despite storage at 40 °C for 3 months or at 25 °C for 1 year *in vitro*.

3.2 Influence of lyophilization on vaccine components

Lyophilization (freeze-drying) is a common drying method to improve stability of vaccine components during transport and storage [147-149]. Therefore, within this project lyophilization was chosen to protect TherVacB components against damages from higher temperatures. The results demonstrate that even after 3 months of 40 °C-exposure a high MVA-S/C titer was determined in the lyophilized samples without additional SAAF-stabilization (Figure 33). In contrast, no infectious viral particles were detected in the MVA-S/C samples in solution already after 14 days of heat storage (Figure 18), confirming the beneficial impact of lyophilization. Moreover, the protective effect of freeze-drying was proved for non-stabilized single HBsAg. After 3 days of 40 °C-exposure no signal was measured by ELISA for the HBsAg in solution (Figure 17), whereas the lyophilized HBsAg still maintained approximately 50 % of its integrity (Figure 28). Even though, the loss of HBsAg integrity in non-stabilized samples was always observed in the different experiments, the exact values showed small deviations. A reason for this could be that lyophilization in PBS does not present an adequate formulation, such as SAAF-stabilized formulation. Therefore, small differences in terms of freeze-drying derived damages could occur during the various lyophilization runs. Strikingly, after 3 days of 40 °C-storage a complete integrity loss was observed for lyophilized single HBcAg (Figure 28), while HBcAg in solution showed only a decrease of approximately 60 %, which was confirmed by all applied analytical methods (Figure 17). Among many advantages, the negative aspects of the lyophilization process were already reported in the literature, as freeze-drying mediated stress can lead to degradation or destabilization of the components during the different freezing and subsequent drying steps [147, 148, 151, 155].

The lyophilization process described in this thesis was initiated at 20 °C, followed by a freezing step at -50 °C, the sublimation at -50 °C and -35 °C and finalized with a secondary drying at 20 °C. The NAGE results in this thesis showed clear signals despite freezing referring to intact particulate HBcAg structures (Figure 16). However, the ELISA results clearly demonstrated that HBcAg in solution displayed significantly reduced integrity after freezing, independently of storage time. Significant decrease in ELISA signal indicated that several conformational epitopes necessary for ELISA antibody binding were destroyed. These findings show that HBcAg becomes instable during freezing/thawing steps, which explains its stability loss during lyophilization. In contrary, integrity loss of HBsAg was not as pronounced as for the HBcAg. Both antigens in solution showed high stability after storage at RT for a short time. This temperature is comparable to the temperature applied during the drying step of the

lyophilization. However, it needs to be considered that these stability studies were performed in solution, whereas during the lyophilization process the water is removed from the formulation. This may cause the instability of the antigens and could further explain the observed significant reduction of HBsAg integrity and a complete loss of HBcAg stability after lyophilization. This speculation is supported by the reported dehydration-induced degradation, which often occurs as a result of the drying process [147].

Interestingly, the combination of both antigens in one formulation, led to a significant increase of HBcAg (over 80 %) and HBsAg (around 10 %) integrity after lyophilization compared to single components (Figure 20). Despite the positive effect of antigen combination, only a very weak band of the non-stabilized, combined antigens was detected by NAGE compared to SM_{Ctrl}. This observation demonstrates that combined non-stabilized samples still partially maintained particulate structure, in contrast to non-stabilized single HBcAg, which formed large aggregates. These findings were also confirmed by DLS showing much smaller aggregates for the combined antigens or single HBsAg than for the single HBcAg. The observed strong HBcAg-specific ELISA signal of the combined antigens indicates that conformational epitopes of the antigens were mostly preserved and accessible and allowed for antibody binding. Consequently, the results indicate that both antigens can stabilize each other and therefore, partially prevent damages caused by lyophilization, especially for HBcAg. Recently, it was described that Pre-S1 domain of L protein and S domains of HBV surface proteins can interact with the core particle during HBV morphogenesis [216-218]. Therefore, it could be possible that the stabilizing effect of both antigens during lyophilization is based on an unspecific protective interaction of the antigens with each other over their particles' surfaces. As no specific arrangement of the HBcAg and HBsAg to each other was observed by TEM, this interaction was most likely dissolved during reconstitution. A similar mode of action is assumed for SAAF. During lyophilization, the excipients of the SAAF form an amorphous shell embedding the vaccine components, which can be easily dissolved by reconstitution [181, 182].

Stabilizing excipients, such as sugars, polyols or amino acids, are used as cryo- or lyoprotectants during lyophilization. The stabilizers replace hydrogen bonds or form a glassy surrounding matrix around the components protecting the products from freeze-drying derived damages [149, 151, 153-155]. The results of this thesis clearly demonstrate that the addition of SAAF as a stabilizing excipient outstandingly preserved integrity of both antigens after lyophilization (Figure 20). The available literature confirmed this observation for HBsAg, as the advantages of HBsAg freeze-drying in the presence of sugars were already described *in vitro* and *in vivo* [219]. In contrast, despite stabilization the single HBcAg still showed a reduced stability as compared to SM_{Ctrl}. However, by combining both antigens and SAAF in one formulation, the negative effect of lyophilization was completely prevented.

Interestingly, MVA-S/C showed no reduction in viral titer after lyophilization and similar results were observed in samples with and without SAAF-stabilization (Figure 19). However, only for the SAAF-stabilized MVA-S/C a good quality of pharmaceutical cake structure was observed, in contrast to non-stabilized MVA-S/C. The high stability of MVA-S/C despite freezing or RT-storage was demonstrated in this thesis. These results were confirmed by literature, which

in addition reported a superb resistant of MVA against drying [211]. Therefore, lyophilization-mediated decrease of infectious MVA-S/C particles was not expected. However, for the development of good qualities of cake structures, which is mandatory for clinical approval, SAAF-stabilization appears to be essential. Several reports demonstrate that a collapse of the cake has no negative impact on protein stability [220, 221], which substantiated the results obtained in this thesis. However, the reconstitution of the collapsed TherVacB cakes was more difficult and time consuming than for the intact cakes. Collapsed cakes could have very low or high residual moisture, which could have a negative effect on vaccine stability during storage [221]. Previously, it was shown that viral recovery is related to the final moisture content of the dried product [222]. Therefore, further comprehensive analysis of the cake structures after lyophilization and storage regarding residual moisture, reconstitution time or glass transition temperature in relation to the vaccine component stability would be interesting.

3.3 Efficacy of SAAF-stabilized vaccine *in vivo*

Accumulating evidence indicates that for a successful therapeutic vaccination against chronic hepatitis B, the simultaneous induction of HBV-specific B- as well as CD4⁺ and CD8⁺ T-cell responses is required [71, 73, 94, 198]. In the first step of the TherVacB approach, the two prime immunizations with the adjuvanted HBV antigens aim to elicit HBV-specific antibodies, which reduce antigen load, induce seroconversion and prevent virus spread, as well as prime efficient CD4⁺- and CD8⁺ T-cell responses [73, 94]. The second step, consisting of the MVA vector expressing HBV core and S protein, is designed to further activate and expand HBV-specific effector CD8⁺ T cells, which eliminate infected hepatocytes and achieve HBV control. The results of this thesis clearly demonstrate that SAAF-stabilized TherVacB vaccine successfully elicited HBV-specific B- and T-cell responses in HBV-naïve mice despite 3 months of storage at 40 °C with comparable efficacy as TherVacB_{Ctrl}, the control vaccine without lyophilization, SAAF-stabilization and heat-exposure (chapter 2.4.4, 2.6.1). In addition, the immunization with SAAF-stabilized vaccine, which was exposed for 1 month at 40 °C, induced high-titer HBV-specific antibodies and T-cell responses in an AAV-HBV mouse model (chapter 2.6.2), which was used to reflect chronic HBV infection in humans [97]. The results show that both the humoral and the cellular arms of the adaptive immune response, which are essential for HBV control and the elimination of infected cells [71], were efficiently induced by SAAF-stabilized TherVacB. In contrast, mice receiving non-stabilized heat-exposed vaccine showed no core or S-specific CD8⁺ T-cell responses and less pronounced anti-HBc antibody titers compared to the SAAF-stabilized vaccine. Moreover, all performed *in vivo* experiments demonstrated that immunization with SAAF-stabilized TherVacB was safe and well-tolerated.

It is well known that antibodies execute important functions within the immune defence such as neutralization of a pathogen or its toxic product, activation of the complement system or opsonisation of pathogens or foreign particles [215]. During HBV infection, the induction of anti-HBs antibodies is essential to capture circulating antigens and prevent *de novo* infection of non-infected hepatocytes [223]. In contrast to anti-HBs antibodies, anti-HBc antibodies have no neutralising potency [12]. However, it was described that these antibodies can induce natural killer (NK) cells-mediated antibody-dependent cytotoxicity through activation of

FcγRIII/CD16 [224]. Therefore, the induction of HBV-specific antibody responses by TherVacB was examined. The results of this thesis demonstrate that the immunization with SAAF-stabilized vaccine led to the induction of a strong anti-HBc antibody response similar as TherVacB_{Ctrl} in both mouse models despite heat-exposure (chapter 2.4.4, 2.6). In contrary, non-stabilized and at 40 °C stressed vaccine caused significantly lower anti-HBc antibody titers. This observation was expected as *in vitro* results demonstrated a complete loss of HBcAg integrity and the formation of large aggregates in this sample, whereas the SAAF-stabilized and stressed components showed high stability. Surprisingly, the induction of anti-HBs antibodies appeared independently of SAAF-stabilization as similar anti-HBs levels were observed for non-stabilized and stressed vaccine and TherVacB_{Ctrl}. Moreover, experiments in AAV-HBV infected mice demonstrated that serum HBsAg levels were efficiently suppressed in all groups of mice (Figure 43, Figure 46). However, the results of the long-term experiment demonstrate that the decrease in HBsAg was noticeably lower in mice receiving non-stabilized and stressed vaccine compared to SAAF-stabilized and TherVacB_{Ctrl} groups (Figure 46). These data indicate that although similar titers of anti-HBs antibodies were detected in all samples, they could not complex the circulating HBsAg in the same way. This further suggest that non-stabilized and stressed TherVacB might induce different anti-HBs repertoires than SAAF-stabilized and stressed vaccine and TherVacB_{Ctrl}. ELISA data indicate that most of the conformational epitopes of the HBsAg were destroyed during heat-exposure, while linear epitopes remained intact allowing the binding of WB antibodies (chapter 2.5, 2.6). It could be speculated that anti-HBs antibodies elicited by non-stabilized and stressed TherVacB might recognize the linear epitopes, which were unaffected by heat-mediated stress. Since the anti-HBs defines clinical endpoint of HBV infection [49], it would be interesting to further investigate the characteristics of these antibodies. Moreover, as the AAV-HBV mouse model does not support viral spread via infection [97], clinical trial experiments would be necessary to provide more information about the neutralising potential of anti-HBs induced by SAAF-stabilized and non-stabilized vaccine.

Recently, it was proposed that aggregates with a native-like structure are more immunogenic than those consisting of fully degraded proteins [225, 226]. To verify this hypothesis for TherVacB components, the relationship between the level of antigen denaturation and the induction of HBV-specific antibodies was further examined. Therefore, in one of the experiments performed in HBV-naïve mice (chapter 2.4.4), the prime immunization consisted of partially stable antigens (non-stabilized, 5 °C-stored) and was compared to the immunization with intact antigens (TherVacB_{Ctrl}, SAAF-stabilized) or unstable antigens (non-stabilized, 40 °C-stored). Mice receiving non-stabilized and at 5 °C-stored TherVacB vaccine demonstrated comparably strong induction of anti-HBs and anti-HBc antibodies as the TherVacB_{Ctrl}. However, *in vitro* results showed that non-stabilized and at 5 °C-stored antigens displayed more than 50 % reduction in HBsAg and HBcAg integrity and the formation of aggregates. As discussed above, immunization with non-stabilized and at 40 °C-stored vaccine induced similar anti-HBs antibody titers as in the other groups, whereas significantly lower anti-HBc levels were observed in non-stabilized and stressed vaccine groups compared to TherVacB_{Ctrl}. Therefore, it was expected that the only partially stable (non-stabilized and at 5 °C stored) HBcAg would induce lower anti-HBc antibody titers. These findings indicate that aggregated partially instable antigens were sufficient for the efficient induction of both

HBV-specific antibodies, although around 50 % of the conformational epitopes for the ELISA antibodies were unreachable or destroyed. Only completely unstable HBcAg, where large aggregates were detected in the sample did not induce similar anti-HBc antibodies as SAAF-stabilized vaccine and TherVacB_{Ctrl}. In addition, to the above discussed reasons for the differences of anti-HBc and anti-HBs antibody titers, one further explanation could be that HBsAg is more stable and resulted in less and smaller aggregated antigens than the HBcAg after freeze-drying (Figure 20), which was further confirmed by storage experiments of lyophilized single antigens (Figure 38). These findings support the hypothesis that the level of antigen denaturation could affect the efficacy of the HBV-specific immune response.

HBV-specific CD8⁺ T-cell response is crucial to finally achieve HBV clearance and eliminate the virus [51, 227]. Results of this thesis clearly demonstrate that the immunization with SAAF-stabilized TherVacB induced strong HBV-specific T-cell responses in HBV-naïve mice (Figure 27, Figure 41). In contrast, mice receiving non-stabilized and at 40 °C-stressed TherVacB vaccine failed to induce HBV-specific CD8⁺ T-cell response. These findings reflect the *in vitro* results demonstrating that SAAF-stabilized vaccine components were highly stable despite heat-exposure, whereas a complete loss of HBcAg and HBsAg integrity as well as a significantly reduced MVA-S/C titer compared to TherVacB_{Ctrl} were determined in non-stabilized and stressed samples. Immunization with lyophilized, non-stabilized and at 5 °C-stored vaccine induced higher core- and S-specific CD8⁺ T-cell responses compared to non-stabilized samples stored at 40 °C (Figure 27). However, the observed magnitude of HBV-specific CD8⁺ T-cell responses was still significantly lower in groups receiving non-stabilized 5 °C-stored vaccine than in TherVacB_{Ctrl}. Since non-stabilized and at 5 °C-stored MVA-S/C showed similar titers as TherVacB_{Ctrl} these findings were unexpected. To explain these data, two different reasons could be possible. Either the expression of HBV S and core protein by MVA-S/C was not sufficient or the MVA-S/C could not boost the HBV-specific T-cell responses because of inefficient priming of HBV-specific CD4⁺- and CD8⁺ T-cell responses during the protein priming steps. Within this thesis, only the number of infectious MVA-S/C particles was determined and not the amount of proteins expressed per cell. Therefore, the MVA-S/C could remain highly infectious in non-stabilized samples but did not efficiently express HBV core and S protein, which could be responsible for the lower core- and S-specific CD8⁺ T-cell responses. To further investigate in this direction, future studies employing FACS analyses could be performed. These assays would allow to simultaneously quantify the expression of encoded proteins as well as the MVA-S/C titer. Therefore, both parameters could be correlated to each other.

The second explanation could be that the partially instable and aggregated HBcAg and HBsAg could be responsible for the lower CD8⁺ T-cell responses in HBV-naïve mice. This hypothesis could be substantiated by the comparison of *in vitro* (chapter 2.5.3) and *in vivo* (chapter 2.6.3) data during long-term storage experiments in AAV-HBV infected mice. *In vitro* data demonstrate an improved infectivity of SAAF-stabilized MVA-S/C compared to non-stabilized sample despite RT-exposure for 12 months. Therefore, it was expected that the immunization with the SAAF-stabilized MVA-S/C could boost core- and S-specific CD8⁺ T-cell response in equally efficient manner. However, the *in vivo* results clearly show the induction of a strong core-specific CD8⁺ T-cell response, a significantly lower S-specific CD8⁺ T-cell response was detected compared to TherVacB_{Ctrl}. This finding indicates that the improvement of MVA-S/C

infectivity is not the only important key player for a sufficient T-cell response. Already after the first prime immunization, a considerable decrease in HBeAg levels were observed in the groups receiving SAAF-stabilized and TherVacB_{Ctrl} vaccine in contrast to the non-vaccinated and non-stabilized but stressed vaccine groups. These findings indicate that T cell-mediated elimination of HBV-positive hepatocytes could be initiated during the prime immunization phase. Therefore, protein priming plays an important role in the induction of HBV-specific CD4⁺- but also of CD8⁺ T-cell responses, which supports previously published data [73].

To initiate clinical trials of a therapeutic vaccine, first its efficacy has to be investigated in an appropriate chronic hepatitis B animal model. It was previously reported that the TherVacB strategy can break the HBV-specific immune tolerance in AAV-HBV infected mice [95]. The results obtained during this study for the TherVacB_{Ctrl} confirmed these data (chapter 2.6.2, 2.6.3). Moreover, immunization with SAAF-stabilized vaccine induced high-titer HBV-specific antibodies and suppressed HBsAg and HBeAg levels despite storage at 40 °C for 1 month equally efficient as TherVacB_{Ctrl}. In addition, the results demonstrate the elicitation of functional and strong core- and S-specific CD8⁺ T-cell responses. Consequently, SAAF-stabilized vaccine fulfilled WHO CTC criteria [134] not only *in vitro*, but also *in vivo* and proved to be stable even far beyond them.

It was recently demonstrated that CD4⁺ T cells play a crucial role in initiating a vaccine-mediated HBV-specific immune response during the priming phase of TherVacB (Su, personal communication). Experiments in AAV-HBV infected mice demonstrate that SAAF-stabilized vaccine led to the induction of an S-specific CD4⁺ T-cell response similar to TherVacB_{Ctrl} despite 1 month 40 °C-exposure (Figure 44). Strikingly, in all experiments performed in AAV-HBV infected mice no core-specific CD4⁺ T-cell responses were observed in any of the vaccinated groups, also in TherVacB_{Ctrl}, neither in liver nor in spleen (Figure 44, Figure 47). These results seemed to be model specific as similar outcome was previously observed during TherVacB experiments in AAV-HBV infected mice at the Institute of Virology (Kosinska, personal communication). However, it has to be considered that the T cell analysis was performed four weeks after the boost, which might be too late to detect the core-specific CD4⁺ T-cell response. It was reported that effector T_{H1} cells, defined by their secretion of IFN- γ , are short-lived and might be already eliminated via apoptosis before the examined time point [228]. However, the immunization of SAAF-stabilized and stressed TherVacB resulted in the detection of S-specific CD4⁺ T-cell-response four weeks after boost. It is proposed that, the vaccination besides inducing effector T_{H1} cells, can also elicit life-long memory T_{H1} cells [228]. Thus, the results of this study suggest that TherVacB-elicited core- and S-specific CD4⁺ T cells might have different functions. The core-specific CD4⁺ T cells most likely mediate the effector functions, whereas the S-specific CD4⁺ T cells might participate in memory response. To confirm this assumption, the analysis of HBV-specific immune response within a shorter time after the onset of immunization needs to be performed, probably during the priming phase. This time frame, however, would not allow to analyze the immunogenicity and antiviral efficacy of the complete SAAF-stabilized TherVacB regimen. In addition, the detailed phenotypic analysis of core- and S-specific CD4⁺ T cells would require future studies to further investigate these findings.

Comparison of the results obtained in the two mouse models suggest that the TherVacB-elicited HBV-specific CD8⁺ T-cell responses vary between HBV-naïve and AAV-HBV infected mice (chapter 2.4.4, 2.6). The results of this thesis demonstrate that immunization of HBV-naïve mice with TherVacB induced similar core- and S-specific T-cell responses in the spleen. In contrary, a very strong core-specific CD8⁺ but a weaker S-specific CD8⁺ T-cell response were detected in the livers of AAV-HBV infected mice. These results suggest that persistent HBV replication may skew the TherVacB induced CD8⁺ T cells towards different phenotypes as it was shown for the CD4⁺ T cells. These findings are substantiated by literature reporting that core-specific CD8⁺ T cells could have an effector function and stay in the liver as long as infected hepatocytes are present [227, 229]. In the spleens of AAV-HBV infected mice, a low magnitude of core-specific CD8⁺ T cells was detected, whereas a high number of S-specific CD8⁺ T cells was measured. These observations indicate a memory function of these T cells as it seems that they disappear from the liver and return to the spleen, supporting previously published results [229-231]. In addition, as CD4⁺ T cells function as the T_H cells for CD8⁺ T cells similar phenotypes between these cell subsets are not surprising [215]. It would be of interest to further investigate the different phenotypes of CD8⁺ T cells induced by TherVacB vaccination using the multimer staining and detailed analysis of phenotypic markers.

Results of long-term experiment in a persistent infection model (AAV-HBV) demonstrated that SAAF-stabilized TherVacB vaccine remained immunogenic, induced high-titer HBV-specific antibodies and led to a remarkable reduction of HBV-specific parameters even after 1 year of storage at RT (chapter 2.6.3). Thereby, SAAF-stabilized TherVacB fulfilled the requirements of EMA, ICH and WHO for long-term stability of vaccines at 25 °C/60 % RH [194, 196]. Although, the results clearly demonstrate that SAAF-stabilization was proven successful and overall vaccination efficacy was comparable to TherVacB_{Ctrl}, a lower stabilization effect concerning S-specific CD8⁺ T-cell responses was observed after 12 months of storage as compared to shorter exposure periods. In contrast, the very strong induction of core-specific CD8⁺ T-cell responses was detected in the livers of the mice receiving SAAF-stabilized vaccine and HBeAg levels were remarkably suppressed indicating elimination of HBV-infected hepatocytes. These responses are crucial for any successful therapeutic vaccination as it is associated with immune-mediated HBV control [58]. As discussed above, explanations for the lower S-specific CD8⁺ T-cell response could be either that the SAAF-stabilization of the antigens for prime immunization or MVA-S/C was not as efficient as in other experiments. Although, the SAAF-stabilized MVA-S/C showed lower titer than TherVacB_{Ctrl} *in vitro*, similar findings were also observed in short-term experiments, which however, did not cause a lower S-specific CD8⁺ T-cell response (chapter 2.6.1, 2.6.2). Therefore, to finally determine whether insufficient MVA-S/C stabilization was responsible for the lower S-specific CD8⁺ T-cell response in this experiment, the quantification of protein expression by MVA-S/C needs to be performed.

The detection of a low S-specific, but a high core-specific CD8⁺ T-cell response in SAAF-stabilized groups indicated that priming with HBsAg was less immunogenic than with HBcAg. However, this was unexpected as *in vitro* analysis of antigens demonstrated that SAAF-stabilized HBsAg maintained antigen integrity despite the long-term stressing. A significant difference within the long-term storage experiment was that the applied HBcAg and

HBsAg were lyophilized and stored independently, in contrast to all other *in vivo* experiments, in which the antigens combination was used. The presented results demonstrate that single antigens showed lower integrity than the combined antigens *in vitro*. As it was reported that the level of destruction of antigens in aggregates might influence the immunogenicity [225, 226], the lower stability of single antigens could be an explanation for the lower S-specific CD8⁺ T-cell response. However, the *in vitro* results showed that the lyophilization and storage-mediated stability reduction of single antigens was more pronounced for the HBcAg than for the HBsAg, which would argue for a lower core-specific CD8⁺ T-cell response. Hereby, it has to be considered that the testing conditions *in vivo* are more complex than *in vitro*, which makes a translation from *in vitro* to *in vivo* data difficult [232], especially after such an extreme stressing. Therefore, for *in vivo* application the antigen combination could be more beneficial for HBsAg stability.

Adjuvants are used in many vaccines to accelerate, enhance and prolong the immunogenicity of highly purified antigens [233]. It was shown that the use of a potent adjuvant enhanced immunogenicity of the TherVacB regimen [94]. In recent years, c-di-AMP has gained considerable interest as a vaccine adjuvant since it induces a balanced T_H1/T_H2 immune response [96]. c-di-AMP is available in lyophilized form and is routinely stored at -20 °C. Recently, it was reported that TherVacB prime immunization with c-di-AMP adjuvanted HBV antigens led to the induction of strong HBV-specific B- and T-cell responses [234]. The results of this thesis confirmed these findings (chapter 2.4.4, 2.6). However, during the experiments c-di-AMP was always used without temperature stressing, which raised the question, whether this adjuvant could remain active after exposure to higher temperatures. The *in vitro* results of this thesis demonstrated that even without additional stabilization c-di-AMP proved biologically active after prolonged heat stressing (Figure 48). Experiments performed in mice by our cooperation partner showed that the slight reduction in c-di-AMP activity after 12 months of storage, did not have a negative influence on the immune response (Guzmán and Ebensen, personal communication). Despite the high storage stability of c-di-AMP at higher temperatures, it was shown that c-di-AMP is degraded in the body within 30 min by phosphodiesterases 1 and 2 (Ebensen, personal communication).

The two priming steps of the thermostable TherVacB approach consist of one formulation containing SAAF-stabilized HBcAg and HBsAg. In order not to change the concept of using one “ready-to-use” formulation for priming, it would be of significant interest, whether c-di-AMP could be additionally included in the already existing formulation. The lyophilization of TherVacB components together with c-di-AMP should not cause a problem, as c-di-AMP is already available in freeze-dried form. Future experiments *in vitro* and *in vivo* shall evaluate the impact of SAAF on c-di-AMP by formulating all four components together. According to previous knowledge about SAAF and c-di-AMP [96, 178], no negative effect of combining these two biological compounds is expected. Moreover, a stabilizing effect of SAAF on c-di-AMP during heat-stressing could be possible.

The results obtained *in vivo* experiments confirm the excellent thermostability of TherVacB formulated with SAAF. Several air-dried, freeze-dried or spray-dried vaccines against influenza or herpes simplex virus, which were stabilized with various excipients like sugars (such as trehalose), amino acids (such as methionine) or different proteins, were tested in naïve

C57BL/6 mice or BALB/c mice [157, 162, 167]. They reached heat-stability for 8 or 12 weeks at 37 °C or for 2 or 3 months at 40 °C. Further approaches used stabilizing adjuvants such as PEG or aluminium hydroxide resulted in stable adenoviral vaccine formulation or lyophilized ricin A toxin, anthrax or Ebola vaccine for 10 days at 37 °C, 1, 3 or 4 months at 40 °C [170-173]. The results of this thesis demonstrate that SAAF-stabilized TherVacB vaccine easily withstand the international comparison, by reaching excellent stability of a highly functional and immunogenic vaccine for at least 3 months at 40 °C in HBV-naïve mice. In addition, despite extensive heat-exposure SAAF-stabilized TherVacB induced a strong HBV-specific immune response, which efficiently control HBV replication, even in a persistent infection mouse model.

3.4 Future perspectives of thermostable TherVacB and implications for other vaccines

As continuous cold chains can often not be provided in low- and middle-income countries with high outdoor temperatures, the use of heat-stable vaccines gained rising interest over the last years. A recent study highlighted the benefits of introducing thermostable vaccines into immunization programmes in six low- and middle-income countries, which was recognized by stakeholders [139]. Moreover, replacing existing WHO Expanded Program on Immunization (EPI) vaccines with thermostable vaccines could potentially relieve the bottlenecks during distribution, as it was shown for Niger's vaccine supply chain [235]. Therefore, thermostable TherVacB developed within this study could in the future facilitate the distribution and application of the vaccine, especially in countries with high outdoor temperatures where adequate cooling cannot be provided. Nevertheless, remarkably high costs are linked with the development and manufacturing of thermostable formulations, which raises the question whether the use of thermostable vaccines is practicable after all [147, 236]. The answer was already evaluated based on different models showing the positive economic impact of thermostable vaccines. Despite the high costs for production of thermostable formulations, the clear benefits were determined by mathematic models for the meningitis A vaccine in Chad and Highly Extensible Resource for Modelling Event-Driven Supply Chains (HERMES) software for vaccine supply chains in Benin, Bihar, India, and Niger [138, 141, 235].

The recombinant MVA was already proven to be safe, immunogenic and protective in animal models and humans [118-122]. In addition, it was shown that MVA facilitates the induction of excellent T-cell responses against encoded antigens [237]. Therefore, the MVA vector gradually gained more interest as an excellent candidate for vaccine development in the last years. The results of this thesis clearly demonstrate that formulation with SAAF outstandingly retained the immunogenicity of MVA-S/C and allowed for elicitation of highly functional HBV-specific CD8⁺ T cells, even after extreme temperature stressing. The induction of virus-specific B- and T-cell responses is highly desirable for the development of vaccines against several challenging infectious diseases such as malaria, tuberculosis or HIV infection, which are also prevalent in countries with high outdoor temperatures [188]. As many of these MVA-based prophylactic and therapeutic vaccines are currently in clinical trials [188], the heat-stabilization with SAAF could significantly improve their performance.

In line with this, the non-stabilized TherVacB vaccine is entering clinical trials in the very near future. To this purpose, a very similar but larger MVA construct, which contains sequences of HBV S (genotype A) and L protein (genotype C), core full-length (genotype D) and truncated protein (genotype C) and RT domain of the HBV polymerase, was generated [184]. This MVA construct was designed to elicit broader HBV-specific immune responses directed against several HBV serotypes and genotypes, thereby, increasing the chances of treatment success for more hepatitis B patients. As the results of this thesis demonstrate that SAAF can efficiently heat-stabilize MVA-S/C, a successful stabilization of the MVA with a larger insert seems most likely possible and would remarkably improve the TherVacB regimen.

3.5 Summary and conclusion

This thesis describes the process of developing a lyophilized, thermostable, therapeutic protein prime/MVA vector boost hepatitis B vaccine employing SAAFs from LEUKOCARE. The obtained results demonstrate that lyophilization in the presence of one single SAAF efficiently stabilized the TherVacB components despite freeze-drying and heat-challenges according to WHO CTC criteria (storage at 40 °C for 3 days). Moreover, the formulation with SAAF maintained antigen integrity and MVA-S/C infectivity over prolonged storage at higher temperatures, far exceeding the WHO recommendations. In addition, SAAF-stabilized TherVacB vaccine was proven to be safe, well-tolerated and induced a strong HBV-specific immune response in HBV-naïve and AAV-HBV infected mice despite a temperature stressing at 25 °C or 40 °C for 3 months. Even after 1 year of storage at RT SAAF-stabilized TherVacB remained immunogenic and resulted in high HBV-specific antibody titers and reduced serum HBsAg and HBeAg as efficient as optimally stored TherVacB_{Ctrl}.

In conclusion, this thesis demonstrates the successful generation of a thermostable, highly immunogenic therapeutic vaccine for the treatment of chronic hepatitis B. The excellent thermostability of TherVacB vaccine could be especially important for the storage and distribution of the vaccine to patients in the future, as chronic hepatitis B is predominantly endemic in countries with high outdoor temperatures lacking continuous cold chains.

4 Materials and Methods

In the following chapters used materials and applied methods are described. Parts of these methods will be published in Sacherl and Kosinska et al [183].

4.1 Materials

4.1.1 Antigens

Name	Supplier
HBcAg, genotype D	Dr. Dišlers, APP Latvijas Biomedicīnas (Rīga, Latvia)
HBcAg, genotype A	Dr. Geerlof, HMGU
HBcAg, genotype A	Centro de Ingeniería Genética y Biotecnología de Cuba (CIBG)
HBsAg, genotype A	Biovac (South Africa)
HBsAg, genotype A	Dynavax
HBsAg, genotype A	Centro de Ingeniería Genética y Biotecnología de Cuba (CIBG)
HBsAg	Roche
HBcAg+HBsAg, genotype A	Centro de Ingeniería Genética y Biotecnología de Cuba (CIBG)

Table 7. Antigens.

4.1.2 Viral vectors

Name	Supplier
AAV-HBV 1.2	Plateforme de Thérapie Génique in Nantes, France (INSERM U1089)
MVA-S/C, genotype A (HBsAg), D (HBcAg)	Institute of Virology TUM/HMGU
MVA-WT (F6)	Prof. Sutter, LMU

Table 8. Viral vectors.

4.1.3 Cell lines and bacterial strains

Name	Description
BHK-21	Baby hamster kidney cells [238]
CEF	Chicken embryo fibroblasts [239]
DF-1	Chicken fibroblast cell line [240]
HEK293	Human embryonic kidney cells, transformed with fragments of adenovirus type 5 DNA [241]

THP1-Dual™	Human THP-1 monocyte cell line with two stable integrated inducible reporter constructs (InvivoGen)
THP1-Dual™ KO-STING	STING knockout dual reporter monocytes (InvivoGen)
<i>E. coli</i> XL1-blue	Chemically competent <i>E. coli</i> strain

Table 9. Cell lines and bacterial strains.

4.1.4 Primers

Primers were purchased from Microsynth AG.

Name	Sequence (5' to 3')
Del I-F	CTT TCG CAG CAT AAG TAG TAT GTC
Del I-R	CAT TAC CGC TTC ATT CTT ATA TTC
Del II-F	GGGTAAAATTGTAGCATCATATACC
Del II-R	AAAGCTTTCTCTCTAGCAAAGATG
Del III-F	GAT GAG TGT AGA TGC TGT TAT TTT G
Del III-R	GCA GCT AAA AGA ATA ATG GAA TTG
Del IV-F	AGATAGTGGAAGATACAACCTGTTACG
Del IV-R	TCTCTATCGGTGAGATACAAATACC
Del V-F	CGTGTATAACATCTTTGATAGAATCAG
Del V-R	AACATAGCGGTGTACTAATTGATTT
Del VI-F	CGTCATCGATAACTGTAGTCTTG
Del VI-R	TACCCTTCGAATAAATAAAGACG

Table 10. Primers.

4.1.5 Antibodies

4.1.5.1 Plaque Assay

Name	Dilution	Supplier
Anti-Vaccinia Lister strain, rabbit [#BP1076]	1:2000	Acris Antibodies GmbH
AffiniPure anti-human IgG (H+L), goat, HRP labeled [#111-035-144]	1:5000	Jackson Immuno Research

Table 11. Antibodies for plaque assay.

4.1.5.2 Western blot

Name	Dilution	Specificity	Supplier
8C9	1:1	HBcAg	Core Facilities HMGU

HB1	1:1000	HBsAg	Prof. Glebe
anti-mouse IgG, (whole molecule), goat, HRP labeled [#A4416]	1:10000		Sigma-Aldrich

Table 12. Antibodies for Western blot.

4.1.5.3 ELISA

Name	Dilution	Specificity	Supplier
Anti IFA HepBCore	1 µg/mL (100 µL/well)	HBcAg	Centro de Ingeniería Genética y Biotecnología de Cuba (CIBG)
Anti HepBcore, HRP labeled	1:7000	HBcAg	Centro de Ingeniería Genética y Biotecnología de Cuba (CIBG)
scFv C8	1 µg/mL (100 µL/well)	HBsAg	Institute of Virology TUM/HMGU
5F9	5 µg/mL (100 µL/well)	HBsAg	Institute of Virology TUM/HMGU
anti-Human IgG Fc, goat, HRP labeled [#ab97225]	1:1000	HBsAg	Abcam
anti-Human IgG (whole molecule), goat, HRP labeled [#A8667]	1:1000	5F9	Sigma-Aldrich

Table 13. Antibodies for ELISA.

4.1.5.4 Flow cytometry

Name	Dilution	Supplier
anti-mouse CD4 APC (clone GK1.5) [#17-0041-83]	1:100	eBioscience
Pacific blue™, Rat, anti-mouse, CD8a (clone 53-6.7) [#558106]	1:100	BD Pharmingen
FITC, Rat, anti-mouse, IFN-γ (clone XMG1.2) [#554411]	1:300	BD Pharmingen

Table 14. Antibodies for flow cytometry.

4.1.6 Peptides

4.1.6.1 Cytotoxic T lymphocytes epitopes

Name	Specificity	Amino acid sequence
B8R	MVA	TSYKFESV
C ₉₃	HBcAg	MGLKFRQL
OVA _{S8L}	ovalbumin	SIINFEKL
S ₂₀₈	HBsAg	IVSPFIPL

Table 15. Cytotoxic T lymphocytes epitopes.

4.1.6.2 HBcAg-derived peptide pools

Name	Amino acid position	Amino acid sequence
Cp2-188	70-87	TWVGGNLEDPISRDLVVS
Cp2-189	77-94	EDPISRDLVVS YVNTNMG
Cp2-190	84-101	LVVSYVNTNMGLKFRQLL
Cp2-191	91-108	TNMGLKFRQLLWFHISCL
Cp2-192	98-115	RQLLWFHISCLTFGRET V
Cp2-193	105-122	ISCLTFGRET VIEYLVSF
Cp2-194	112-129	RET VIEYLVSF GVVIRTP
Cp2-195	119-136	LVSFGVVIRTPPAYRPPN
Cp2-196	126-143	IRTPPAYRPPNAPILSTL
Cp2-197	133-150	RPPNAPILSTLPETT VVR
Cp2-198	140-157	LSTLPETT VVRRRGRSPR

Table 16. HBcAg-derived peptide pool, genotype D.

4.1.6.3 HBsAg-derived peptide pools

Name	Amino acid position	Amino acid sequence
Sp3-37	145-159	GNCTCIPIPSSWAF A
Sp3-38	149-163	CIPIPSSWAF AKYLW
Sp3-39	153-167	PSSWAF AKYLWEWAS
Sp3-40	157-171	AF AKYLWEWASARFS
Sp3-41	161-175	YLWEWASARFSWLSL
Sp3-42	165-179	WASARFSWLSLLVPF
Sp3-43	169-183	RFSWLSLLVPFVQWF
Sp3-44	173-187	LSLLVPFVQW FVGLS
Sp3-45	177-191	VPFVQW FVGLSPTVW
Sp3-46	181-195	QW FVGLSPTVWLSAI
Sp3-47	185-199	GLSPTVWLSAIWMMW

Sp3-48	189-203	TVWLSAIWMMWYWGP
Sp3-49	193-207	SAIWMMWYWGPSLYS
Sp3-50	197-211	MMWYWGPSLYSIVSP
Sp3-51	201-215	WGPSLYSIVSPFIPL
Sp3-52	205-219	LYSIVSPFIPLLPFI
Sp3-53	209-223	VSPFIPLLPFIFFCLW
Sp3-54	213-226	IPLLPFIFFCLWVYI

Table 17. HBsAg-derived peptide pool, genotype D.

4.1.7 Enzymes

Name	Supplier
Benzonase	Merck
Collagenase type IV	Sigma-Aldrich
Lysozyme	Thermo Fisher Scientific
Phusion Hot Start Flex 2x Master Mix	New England Biolabs
Trypsin	Gibco

Table 18. Enzymes.

4.1.8 Plasmids and Markers

Name	Supplier
5F9 heavy chain	Institute of Virology TUM/HMGU
5F9 light chain	Institute of Virology TUM/HMGU
scFv C8-encoding pHOG21	Institute of Virology TUM/HMGU
10 kB DNA ladder	Eurogentec
PageRuler Plus Prestained Protein Ladder	Thermo Fischer Scientific
Triple Color Protein Standard III	Serva

Table 19. Plasmids and Markers.

4.1.9 Kits

Name	Supplier
Architect™ anti-HBsAg Reagent Kit	Abbott
Architect™ HBeAg Reagent Kit	Abbott
Architect™ HBsAg Reagent Kit	Abbott
Cytofix/Cytoperm™ Kit	BD Biosciences
NucleoSpin® Blood QuickPure	Macherey Nagel GmbH & Co. KG
Enzygnost® HBe monoclonal Kit	Siemens
Enzygnost® Anti-HBc monoclonal Kit	Siemens

Table 20. Kits.

4.1.10 Mouse strains

For *in vivo* experiments, 9 weeks old wild-type C57BL/6J male mice (haplotype H-2^{b/b}) were purchased from JANVIER LABS.

4.1.11 Cell culture media

Name	Cells/application	Ingredients
DMEM (10 % FCS)	HEK293 cells	10 % FCS 1 % penicillin-streptomycin 1 % L-Glutamine 1 % NEAA 1 % sodium pyruvate
DMEM+GlutaMAX™ (2 % or 10 % FCS)	DF-1 cells	2 % or 10 % FCS 1 % penicillin-streptomycin 1 % NEAA 1 % sodium pyruvate
RPMI (2 % or 10 % FCS)	BHK-21 cells, mouse experiments	2 % or 10 % FCS 1 % penicillin-streptomycin 1 % L-Glutamine 1 % NEAA 1 % sodium pyruvate

Table 21. Cell culture media.

4.1.12 Buffers and solutions

If not noted otherwise, the 1x buffers were diluted with H₂O from the stock buffers.

Name	Ingredients
1 % phosphotungstic acid (PTA)	1 % PTA (w/v) solved in H ₂ O, pH 7.1-7.2
1x trypsin	50x trypsin diluted in 1x PBS
2 % glutaraldehyde	25 % glutaraldehyde diluted in 1x PBS
2 % paraformaldehyde (PFA)	20 % PFA diluted in 1x PBS
2x yeast extract tryptone (YT) medium	17 g Tryptone 10 g yeast extract 5 g NaCl Adding H ₂ O to 1 L
36 % sucrose buffer	36 % (w/v) sucrose solved in 10 mM Tris, pH 9.0
40 % Percoll solution	50 ml 80 % Percoll solution 50 ml 1x PBS 100 IU/ml heparin

80 % Percoll solution	72 ml pure Percoll 8 ml 10x PBS 20 ml 1x PBS
5F9 binding buffer	0.02 M NaH ₂ PO ₄ x 1 H ₂ O 0.02 M NaH ₂ PO ₄ pH 7.0, in H ₂ O
5F9 elution buffer	0.1 M Glycine-HCl pH 2.7, in H ₂ O
5F9 neutralization buffer	1 M Tris-HCl pH 9.0, in H ₂ O
ACK lysis buffer	150 mM NH ₄ Cl 10 mM KHCO ₃ 0.1 mM Na ₂ EDTA pH 7.2 – 7.4, in H ₂ O
ÄKTA binding buffer	20 mM Na ₂ HPO ₄ 500 mM NaCl 20 mM imidazole pH 7.4, in H ₂ O
ÄKTA elution buffer	20 mM Na ₂ HPO ₄ 500 mM NaCl 500 mM imidazole pH 7.4, in H ₂ O
Coomassie staining solution	0.1 % (w/v) CDD-R250 40 % (v/v) MeOH 10 % (v/v) acetic acid 50 % (v/v) H ₂ O
Destain solution	40 % (v/v) MeOH 10 % (v/v) acetic acid 50 % (v/v) H ₂ O
ELISA blocking buffer	5 % (w/v) BSA solved in 1x PBS
ELISA washing buffer PBS-T	1x PBS containing 0.05 % Tween20
FACS buffer	1 % (v/v) diluted in 1x PBS
Freezing medium	90 % (v/v) FCS 10 % (v/v) DMSO
Lysogeny broth (LB) medium	10 g Tryptone 5 g yeast extract 10 g NaCl Adding H ₂ O to 1 L
scFv C8 storage buffer	25 mM Tris-HCl 100 mM KCl 1 mM EDTA 1 mM MgCl ₂ 10 % (v/v) Glycerol pH 7.4, in H ₂ O

SDS-PAGE loading buffer (4x SEB)	10 mL Glycerin 12 mL 0.5 M Tris pH 6.8 (HCl) 20 mL 10 % SDS 0.1 g Bromophenol blue + 40 μ L β -Mercaptoethanol/mL
SDS-Page running buffer (10x)	250 mM Tris base 2 M Glycine 1 % (w/v) SDS Adding H ₂ O to 1 L
TAE-buffer (50x)	2 M Tris-HCl 1 M Acetic acid 50 mM EDTA pH 8.0, in H ₂ O
Tris buffer (MVA)	10 mM Tris base pH 9.0, in H ₂ O
WB blocking buffer	5 % (w/v) milk powder solved in 1x TBS-T
WB TBS-T (10x)	200 mM Tris base 1.4 M NaCl 10 mL Tween20 Adding H ₂ O to 1 L, pH 7.4
WB transfer buffer (10x)	39.4 g Tris-HCl or 30.3 g Tris base 144.1 g Glycine Adding H ₂ O to 1 L
WB transfer buffer (1x)	100 mL 10x Transfer buffer 200 mL MeOH Adding H ₂ O to 1 L

Table 22. Buffers and solutions.

4.1.13 Chemicals and reagents

Product	Supplier
3,3',5,5'-tetramethylbenzidine	Invitrogen
Acetic acid	Roth
Acetone	Roth
Acrylamide (40 %)	Roth
Activated carbon	Roth
Agar-agar	Roth
Agarose	Peqlab
Amersham ECL Prime Western Blotting Detection Reagent	GE Healthcare
Ammonium chloride (NH ₄ Cl)	Roth
Ammonium persulfate (APS)	Roth
Ampicillin	Roth

Bovine serum albumin (BSA)	Roth
Bradford Reagent	Sigma-Aldrich
Brefeldin A (BFA)	Sigma-Aldrich
bis-(3',5')-cyclic dimeric adenosine monophosphate (c-di-AMP)	InvivoGen (<i>in vivo</i> experiments) or Biolog
Coomassie Brilliant Blue R250	Roth
Dimethyl sulfoxide (DMSO)	Sigma-Aldrich
Disodium phosphate (Na ₂ HPO ₄)	Roth
DNA Loading Dye (6x)	Thermo Fisher Scientific
Dulbecco's Modified Eagle's Medium (DMEM)	Gibco
Dulbecco's Modified Eagle's Medium (DMEM)-GlutaMAX™	Gibco
EDTA di-sodium salt (Na ₂ EDTA)	Roth
Ethylenediaminetetraacetic acid (EDTA)	Roth
Ethanol (EtOH)	Roth
Fetal calf serum (FCS), heat-inactivated	Gibco
Fixable Viability Dye eFluor™ 780	eBioscience
Formaldehyde	Roth
Fugene® HD transfection reagent	Promega
Glutaraldehyde (25 %)	Agar Scientific
Glycerol	Roth
Heparin-Natrium-25000	ratiopharm
Hepes 1 M	Gibco
Hydrochloric acid (HCl)	Roth
Imidazole	Sigma-Aldrich
Isoflurane	Henry Schein
Isopropanol	Roth
Isopropyl b-D-1-thiogalactopyranoside (IPTG)	Roth
KPL True Blue™	Sera care
L-Glutamine, 200 mM	Gibco
Magnesium chloride (MgCl ₂)	Sigma-Aldrich
Methanol (MeOH)	Roth
Milk powder	Roth
MilliQ H ₂ O	Merck-Millipore
N,N,N',N'-tetramethylethylenediamine (TEMED)	Roth
Non-essential amino acids (NEAA), 100x	Gibco
OptiMEM	Gibco
Paraformaldehyde (PFA), 20 %	Science Services
Penicillin-Streptomycin, 10,000 U/mL (100x)	Gibco
Percoll	GE Healthcare

Phosphate buffered saline (PBS), 10x	Gibco
Phosphotungstic acid hydrate (PTA)	Sigma-Aldrich
Potassium bicarbonate (KHCO ₃)	Roth
Potassium chloride (KCl)	Roth
Roswell Park Memorial Institute (RPMI) 1640	Gibco
Roti [®] -Safe GelStain	Roth
Sodium chloride (NaCl)	Sigma-Aldrich
sodium dihydrogen phosphate (NaH ₂ PO ₄)	Roth
sodium dodecyl sulfate (SDS)	Roth
Sodium hydroxide (NaOH)	Roth
Sodium pyruvate, 100 mM	Gibco
Sucrose	Roth
Sulfuric acid, 1 M	Roth
Tris base	Roth
Tris HCl	Roth
Trypan Blue	Gibco
Tryptone	Roth
Tween20	Roth
Vi-CELL Reagent Pak	Beckman Coulter
Yeast extract	Roth
β-Mercaptoethanol, 50 mM	Gibco

Table 23. Chemicals and reagents.

4.1.14 Consumables

Product	Supplier
1.1 mL Z-Gel Micro tubes	Sarstedt
2R Lyophilization vials	Schott
Amersham Hybond PVDF membrane	GE Healthcare
Amicon Ultra-4 Centrifugal filters	Merck Millipore
Cell culture flask, dishes, plates	Techno Plastic Products AG (TPP)
Cell scraper	Techno Plastic Products AG (TPP)
Cell strainer 100 µM	Falcon
Centrifugation Tubes	Beckman Coulter
Cryovials	Greiner Bio One
Cuvettes	Sarstedt
ELISA 96-well plates NUNC MaxiSorp™	Thermo Fisher Scientific
FACS 96-well V-bottom plates	Roth
Falcon Tubes (15 mL, 50 mL)	Greiner Bio One
Grids FF400-Cu	Electron Microscopy Science
“Haftplatten“ Ø 85 mm	Plano

Needles	Braun
Open-Top Polyclear Centrifuge Tubes (14x89 mm, 25x89mm)	Seton Scientific
Parafilm M	Pechiney Plastic Packaging
PCR tubes	Thermo Fisher Scientific
Pipette tips (filtered/unfiltered)	Starlab, Greiner Bio One
Pipettes (disposable) (2 mL, 5 mL, 10 mL, 25 mL, 50 mL)	Greiner Bio One
Protein LoBind tubes (1.5 mL)	Eppendorf
Reaction tubes (1.5 mL, 2 mL)	Greiner Bio One
Reflotron ALT (GPT) stripes	Roche Diagnostics
Siliconized bromobutyl stoppers	West
Sterile filters 0.45 µm or 0.2 µm	Sarstedt
Surgical Disposable Scalpels	Braun
Syringes	Braun
Vase-vials	Glastechnik Gräfenroda GmbH (GTG)
Whatman® High quality filter paper, grade 1 Ø 90 mm	Sigma-Aldrich

Table 24. Consumables.

4.1.15 Laboratory equipment

Product	Supplier
Accu-jet® pro	Brand
ÄKTA avant chromatography system	GE Healthcare
Architect™ platform	Abbott
Axiovert 40 C (light microscope)	Zeiss
BEP III platform	Siemens
Big centrifuge 5920R	Eppendorf
Centrifuge 5417R	Eppendorf
Centrifuge 5430	Eppendorf
Centrifuge 5920R	Eppendorf
Centrifuge Avanti J-26 XP	Beckman Coulter
Centrifuge Heraeus Multifuge 4KR	Thermo Fisher Scientific
Cover glasses (20x26 mm)	Menzel
CytoFLEX S	Beckman Coulter
Digital lab scale balance analytical PC440	Mettler-Toledo
Epsilon 2-6D freeze dryer	Martin Christ
ErgoOne® 8-channel Pipette (30-300 µl)	Starlab
FiveEasyPlus™ pH Meters	Mettler-Toledo
Freezing container	Thermo Fisher Scientific
Fusion Fx7 imaging system	Peqlab

Gel chambers (agarose gel electrophoresis)	Peqlab
Gel chambers (SDS-PAGE)	Bio-Rad
Heating block	Eppendorf
HisTrap™ FF crude 5 mL colum	GE Healthcare
HisTrap™ protein G HP	GE Healthcare
Incubator HERAcell 150i	Thermo Fisher Scientific
Libra 120 (TEM)	Zeiss
Malvern Zetasizer Nano ZS	Malvern Panalytical
Masterflex® L/S™, Easy-load® II	Cole-Parmer Instrument Company
Maxi blu, max. 180 VDC, 60 W	b _s b11 biotech service blue
Mini Centrifuge	Labnet
MS 3 basic Vortex Mixer	IKA-Werke
NanoDrop One	Thermo Fisher Scientific
Nanophotometer OD600	IMPLEN GmbH
Neubauer improved hemocytometer	Brand
Optima L-90K (ultracentrifuge)	Beckman Coulter
Power Supply PowerPac 200	Bio-Rad
PowerPac Basic	Bio-Rad
PowerPac HC	Bio-Rad
Reagent Reservoir (50 mL)	Corning
Reflotron® Reflovet Plus	Roche Diagnostics
Shaker and incubator for bacteria	INFORS HT
Size-exclusion column TSK-gel® G5000 SWXL 300 mm x 7.8 I.D. column, 100 nm pore size	Tosoh Bioscience
Sterile hood HERASafe KS 9/KS18	Thermo Fisher Scientific
T professional Trio Thermocycler	Analytik Jena
Infinite F200 plate reader	Tecan
Thermo Mixer F1.5	Eppendorf
Thermocycler T3000	Biometra
Thermomixer <i>comfort</i> 535	Eppendorf
UHPLC system UltiMate3000	Thermo Fisher Scientific
Ultracentrifuge SW 23 Ti Rotor Beckman Coulter	Beckman Coulter
Ultracentrifuge SW 41 Ti Rotor Beckman Coulter	Beckman Coulter
Ultrasonic generator GM 200	Brandelin
Ultrasonic needle UW 200	Brandelin
UV-280 nm detector	Thermo Fisher Scientific
Vi-CELL® XR cell viability analyzer	Beckman Coulter
Western Blotting Chamber (Wet Blot)	Bio-Rad

Table 25. Laboratory equipment.

4.1.16 Software

Name	Supplier
Chromeleon 7 Chromatography Data Software	Thermo Fisher Scientific
FlowJo 10.4	BD Biosciences
Fusion-Capt Advance FX7 imaging system	Peqlab
GrpH Pad Prism 5.01	GrpH Pad
i-control™ software	Tecan
Image J	National Institute of Health (NIH)
ImageSP	TRS image SysProg
Serial Cloner 2.6.1	Serial Basics
Windows 10, Microsoft Office 2010	Microsoft
WinTEM	Zeiss
Zetasizer Software 7.11.	Malvern Panalytical

Table 26. Software.

4.2 Methods

4.2.1 Cell culture

All cells were cultured under standard cell culture conditions (37 °C, 5 % CO₂) and the corresponding experiments were performed under sterile conditions with mycoplasma-negative cells.

Baby hamster kidney cells (BHK-21) were cultured in Roswell Park Memorial Institute (RPMI) medium and human embryonic kidney (HEK) 293 cells in Dulbecco's Modified Eagle's Medium (DMEM) supplemented with 10 % fetal calf serum (FCS), 1 % penicillin-streptomycin, 1 % non-essential amino acids, 1 % sodium pyruvate and 2 mmol/L L-Glutamine. Chicken fibroblast cell lines (DF-1) were cultured in DMEM+GlutaMAX™ medium containing the same supplements as described above without L-Glutamine. For passaging, cells were washed with 1x phosphate buffered saline (PBS) and detached from the cell culture flask by the addition of 1x trypsin followed by incubation for approximately 5 to 10 min at 37 °C. Cells were resuspended in cell culture medium to obtain single-cell suspension. DF-1 and HEK293 cells were passaged 1:10 twice a week and BHK-21 cells 1:5 three times per week.

To freeze cells, cell suspension was centrifuged at 500 x g for 5 min at RT. The cell pellet was resuspended in 1 mL freezing medium (90 % FCS, 10 % DMSO) per cryovial. The cells were put in a freezing container and stored at -80 °C. At least one day later, cells were transferred to the liquid nitrogen tank.

To thaw cells, a cryovial of cells was taken out of the liquid nitrogen tank and shortly heated at 37 °C. The cell suspension was resuspended, transferred to a new falcon tube containing cell culture medium and centrifuged at 500 x g for 5 min at 4 °C. The cell pellet was resuspended in fresh medium and put into an appropriate cell culture flask.

To seed a defined number of cells, single-cell suspension was diluted 1:1 with trypan blue. The cell number was determined by using a Neubauer improved counting chamber. The number of living cells/mL was obtained by calculating the mean value of the four corner squares and multiplication with the factor 10⁴ and the dilution factor 2.

4.2.2 Generation of MVA-S/C

The MVA-S/C was generated by homologous recombination according to the previously published protocol [205] as described in detail in the Results section (chapter 2.1.1).

4.2.3 Amplification of MVA-S/C

Amplification and purification of the MVA-S/C was performed according to Kremer et al. [205] with some modifications.

First, a MVA preculture was prepared, which was later used to infect the main culture of DF-1 cells. For this purpose, DF-1 cells were seeded in one T150 cell culture flask to obtain around 95 % confluency on the day of infection. The cell monolayer was inoculated with 10 μ L of purified MVA stock ($1:10^9$ TCID₅₀/mL) diluted in 3 mL of 10 % DMEM+GlutaMAX™ medium. After incubation for 2 h at 37 °C, 27 ml 10 % DMEM+GlutaMAX™ medium was added and the cells were incubated at 37 °C until the virus induced cytopathic effect (CPE) was observed. The supernatant and the cells of the MVA preculture were stored at -80 °C until further use. DF-1 cells were seeded in 30 T150 cell culture flasks to obtain approximately 95 % confluency on the day of infection. The MVA preculture was thawed and diluted in the corresponding volume of 10 % DMEM+GlutaMAX™ medium. Cells were inoculated with 5 mL/flask of MVA preculture suspension. Following virus adsorption for 1 h at 37 °C, 25 mL/flask of 10 % DMEM+GlutaMAX™ medium was added and cells were incubated until CPE could be clearly seen. The infected cells were harvested by scraping the cells and subsequent centrifugation at 3850 x g for 5 min at 4 °C. The cell pellets were resuspended in 30 mL Tris buffer (10 mM) and stored at -80 °C. After three freeze-thaw cycles, the virus/cell suspension was sonicated three times, each 30 seconds long, and centrifuged at 3850 x g for 5 min at 4 °C. The supernatant was collected and the pellet was resuspended in Tris buffer (10 mM). After repeating these steps three times, purification of the virus suspension was performed on a 36 % sucrose cushion by ultracentrifugation (Optima L-90K Beckman Coulter GmbH) using SW32 Ti rotor at 13500 rpm for 1.5 h at 4 °C with a virus suspension to sucrose ratio of 1:2. The pellet was resuspended in 12 mL Tris buffer (10 mM). The second purification step was performed by ultracentrifugation using SW41 Ti rotor at 13500 rpm for 1.5 h at 4 °C with a virus suspension to sucrose ratio of 1:6. The viral pellet was resuspended in 300 μ L Tris buffer (10 mM) and the virus stock was stored at -80 °C.

4.2.4 Determination of MVA-S/C titer by TCID₅₀

The MVA-S/C titer was determined by TCID₅₀ as previously described [205] with some modifications. Confluent BHK-21 cells were seeded one day prior to infection in a flat-bottom 96-well plate. On the next day, the cell monolayers were infected with 200 μ L/well of 10-fold serial dilution of virus suspension in 2 % RPMI medium. Per dilution 16 wells were infected. Additional 8 wells incubated with 200 μ L/well of 2 % RPMI medium served as controls. At day 7 post-infection, cells were analyzed by light microscopy for the formation of CPE induced by MVA-S/C. The wells in which CPE was observed were counted positive. To determine the viral titer in TCID₅₀/mL, the following formula was used according to the method of Kaerber [242]:

$$\log_{10} 50 \% \text{ end-point dilution} = x - d/2 + (d \sum r/n)$$

In this formula **x** represents the highest dilution in which all wells are counted positive, **d** is the log₁₀ of the dilution factor (**d** = 1 if 10-fold serial dilutions are used), **r** serves as the number of positive wells per dilution and **n** indicates the total number of wells per dilution.

All viral titers in this thesis were calculated from two independent experiments.

4.2.5 Determination of MVA-S/C titer by plaque assay

Plaque assay was performed as previously described [205] with some modifications. One day prior to infection 2×10^6 DF-1 cells/well were seeded in a 6-well plate and incubated overnight at 37 °C. Ten-fold serial dilutions of virus material were prepared in 2 % DMEM+GlutaMAX™ medium. Cells were infected with 1 mL/well of virus suspension in duplicates for 2 h at 37 °C. After washing the cells once with 1x PBS, inoculum was replaced with 2 mL/well 10 % DMEM+GlutaMAX™ medium and incubated for 48 h at 37 °C. Next, medium was removed and cells were fixed with 1 mL/well of 1:1 mixture of acetone/methanol for 5 min at RT followed by air-drying. The blocking was performed with 2 mL/well of 1x PBS containing 3 % FCS for 1 h at RT or overnight at 4 °C. Afterwards, 1 mL/well primary antibody solution (anti-Vaccinia Lister strain) diluted 1:2000 in 1x PBS containing 3 % FCS was added and cells were incubated for 1 h at RT. After three washing steps with 1x PBS, 1 mL/well of horseradish peroxidase (HRP) labeled AffiniPure goat anti-human IgG (diluted 1:5000 in 1x PBS with 3 % FCS) antibody solution was added and cells were incubated for 1 h at RT. Cells were washed three times and viral plaques were visualized with 0.5 mL/well TrueBlue substrate solution at RT. To determine the titer in PFU/mL, stained viral plaques were counted, the mean value of the duplicates was calculated and multiplied by their dilution factor.

4.2.6 Infection assay

One day prior to infection DF-1 cells were seeded in a 12-well plate to obtain approximately 80 % confluency on the next day. Cells were infected with MVA-S/C or MVA-WT with an MOI of 0.1. At the examined time points either the supernatant was collected (HBeAg/HBsAg determination) or the supernatant and the cells were harvested (MVA growth curve) or the cells were lysed (WB analysis). The material was stored at -20 °C until further analysis.

4.2.7 HBeAg and HBsAg measurements of *in vitro* samples

HBeAg and HBsAg levels in the supernatant of MVA infected cells were measured in the appropriate dilution using Enzygnost® HBe monoclonal kit on the BEP III platform or Architect™ HBsAg Reagent Kit on the Architect™ platform. The results of HBeAg analyses are presented as sample/cut-off (S/CO) values using the internal cut-off value of the measurement.

4.2.8 Purification of viral DNA

Viral DNA was extracted from purified MVA-S/C stock solution using the NucleoSpin® Blood QuickPure by Macherey Nagel following the manufacturer's protocol.

4.2.9 Polymerase chain reaction

Polymerase chain reactions (PCRs) were performed using the Phusion Hot Start Flex 2x Master Mix following the manufacturer's instructions. In detail, 2.5 μL of each primer (10 μM , Table 10), and 2 μL purified DNA was mixed with 25 μL of Master Mix and sterile H_2O was added to a total volume of 50 μL . As negative control sterile H_2O was used. Amplification of the gene of interest was performed according to PCR conditions presented in Table 27.

Phase	Temperature [$^{\circ}\text{C}$]	Time [s]	Cycles
Initial denaturation	95	30	1
Denaturation	95	30	
Primer annealing	63	40	34
Elongation	72	180	
Final elongation	72	420	1
Cooling	4	∞	

Table 27. PCR program for MVA-S/C and MVA-WT using Del I-VI primers.

4.2.10 Agarose gel electrophoresis

PCR products were loaded on a 1 % agarose gel containing Roti[®]-Safe stain. To estimate the size of the PCR products, 10 kB DNA ladder was used. The samples were separated at 100 V until desired separation of the fragments had been reached. To visualize the bands, the gel was analyzed by UV-light using Fusion FX7 imaging system.

4.2.11 Sequencing

Samples were diluted to a concentration of 30-100 ng/ μL in 20 μL total volume and 20 μL primer solution were sent for Sanger sequencing to the external provider Eurofins Genomics GmbH. Sequencing results were downloaded and subsequently analyzed using Serial Cloner software.

4.2.12 Determination of DNA, RNA or protein concentrations

The concentration of plasmid or genomic DNA or RNA was measured on a NanoDrop One using the appropriate buffer solution as blank. Protein concentration was determined via Bradford assay following the manufacturer's instructions. For quantification, BSA or bovine gamma globulin protein standard (in case of 5F9), serial 1:1 diluted in H_2O from 2 mg/mL to 0 mg/mL was used. The protein concentration was determined by measuring absorbance at OD₅₉₅ with Infinite F200 plate reader and calculated by linear regression.

4.2.13 Production of recombinant single-chain variable fragment C8

The recombinant HBV-specific single-chain variable fragment (scFv) C8 was produced as previously reported [243].

The chemically competent *E. coli* strain XL1-blue was transformed with scFv C8-encoding pHOG21 plasmid. As preculture, 5 mL of lysogeny broth (LB) medium containing Ampicillin (1:1000) was inoculated with one single-clone colony and incubated overnight at 37 °C. As a main culture, 6 L of 2x yeast extract tryptone (YT) medium containing Ampicillin (1:1000) was inoculated with the overnight culture and grown at 37 °C until reaching the optical density (OD)₆₀₀ of 0.6. The induction of protein expression was performed with 0.1 mM isopropyl b-D-1-thiogalactopyranoside (IPTG) overnight at 18 °C.

Large-scale protein purification was performed by fast protein liquid chromatography under native conditions using ÄKTA avant chromatography system. Cells of the main culture were harvested at 5000 x g for 15 min at RT. The cell pellets were resuspended in 10 mL ÄKTA binding buffer per gram bacterial pellet. After adding 3 U/mL benzonase and 0.2 mg/mL lysozyme, samples were incubated for 20 min on ice followed by five cycles of sonication at high power, each 1 min long. Samples were centrifuged at 15000 x g for 30 min at RT and supernatants were collected. For purification, a HisTrap™ FF crude 5 mL column was connected to the ÄKTA avant chromatography system and loaded with the lysate. Samples were eluted by gradually increasing the proportion of elution buffer with a flow rate of 5 mL/min and 1 mL fractions were collected. The protein content of the eluent was monitored by UV at OD₂₈₀ and plotted as absorbance units against eluent time. To confirm protein presence, respective fractions were selected according to the chromatographic peaks and analyzed by SDS-PAGE and Coomassie staining. After pooling the positive fractions, samples were dialyzed to scFv C8 storage buffer overnight at 4 °C. After sterile filtration (0.45 µm), the final sample was stored in Protein LoBind tubes at 4 °C.

4.2.14 Production and purification of 5F9 antibody

HEK293 cells were seeded two days prior to infection in a T150 cell culture flask to obtain approximately 80 % confluency on the day of transfection. First, 1 mL OptiMEM, 25 µg of 5F9 heavy chain plasmid DNA, 25 µg 5F9 light chain plasmid DNA and 150 µL Fugene® HD transfection reagent was mixed and incubated for 10 min at RT. Meanwhile, the cell medium was replaced with fresh 10 % DMEM medium. Cells were transfected by the addition of the transfection solution, followed by incubation for 9 days at 37 °C. Every second day the antibody-containing supernatant was collected and 25 mL fresh 10 % DMEM medium was added to the cells. After sterile filtration (0.45 µm), supernatants were stored at 4 °C until purification.

The 5F9 antibody was purified by G column affinity chromatography. For the purification a peristaltic pump and a protein G column connected to a 1.6 mm tube were used. In a first step, the column was washed with 5 column volumes (CVs) of H₂O and equilibrated with 5 CVs of binding buffer at a flow rate of 1 mL/min. Afterwards, the antibody-containing supernatant was loaded on the column with a flow rate of 1.5 mL/min. The column was washed with 10 CVs of

binding buffer. Meanwhile, Protein LoBind tubes were prepared with 75 μL /tube neutralization buffer. The elution was performed in 1 mL fractions with a flow rate of 1 mL/min and 12 CVs of elution buffer. After re-equilibration with 10 CVs of binding buffer, the column was stored in 20 % EtOH at 4 °C. The elution fractions were stored at 4 °C.

The eluted fractions were analyzed by enzyme linked immunosorbent assay (ELISA). For this purpose, a NUNC MaxiSorp™ 96-well plate was coated with 50 μL /well HBsAg from Roche (diluted 1:1000 in 1x PBS) for 30 min at 37 °C. After four washing steps (PBS-T), the blocking with 200 μL /well of bovine serum albumin (BSA; 5 %) for 1 h at RT was performed. Afterwards, 50 μL /well of eluted fractions were added and incubated for 1.5 h at RT. Following four washing steps, the bound antibodies were detected with 50 μL /well HRP labeled goat anti-human IgG antibody (diluted 1:1000 in 1x PBS). 3,3',5,5'-tetramethylbenzidine (TMB) substrate conversion (OD_{450} to OD_{560}) was measured on an Infinite F200 plate reader.

The antibody-containing fractions were pooled and concentrated with Amicon Ultra centrifugal filters. After Amicon filters were wetted with 1x PBS via centrifugation at 3200 x g for 2 min at RT, pooled fractions were added. The samples were concentrated to a total volume of 1 mL via centrifugation at 3200 x g for approximately 20 min at RT. Before storing the samples at 4 °C in Protein LoBind tubes, the buffer of the antibody solution was exchanged. For this purpose, 1x PBS was added twice to the concentrated sample in the Amicon filters following centrifugation until 1 mL antibody solution remained. After the sample was recovered according to manufacturer's instructions, the final concentration was analyzed by Bradford assay.

4.2.15 Stabilization, lyophilization, temperature exposure and reconstitution

To thermally stabilize HBV antigens and MVA-S/C, SAAFs from LEUKORE database were used. The LEUKOCARE library contains information about particular physicochemical and structural properties of different kinds of biological compounds, formulations and more than 100 excipients previously identified to be effective in stabilization of this biologics together with literature-known characteristic stabilization data.

Stabilizing formulations were prepared by dilution of concentrated stock solutions of the HBV antigens and MVA-S/C with the selected SAAF. As a negative control the vaccine components were diluted in PBS. For experiments, the HBV antigens were formulated separately or in combination as it is mentioned in each chapter of Results section. The MVA-S/C was formulated in a separate vial with the same SAAF as the antigens for *in vitro* and *in vivo* experiments.

The lyophilization of the samples was performed using the protocol which is described in Table 28.

Step	Target temperature [°C]	Slope [h]	Hold [h]	Pressure [mbar]
Introduction	20	0	0	1000
Freezing	-50	2:00	2:00	1000
Sublimation	-50	0:01	0:30	0.045
	-35	3:00	30:00	0.045
Secondary Drying	20	3:00	7:00	0.009

Table 28. Different steps of the lyophilization process.

After lyophilization, the samples were stored under ICH-conditions at 40 °C/75 % relative humidity (RH), 25 °C/60 % RH or 5 °C in the refrigerator. The stabilization, lyophilization and temperature exposure was kindly performed by Dr. Kristina Kemter at LEUKOCARE.

The samples were reconstituted with the required volume of H₂O (*in vitro*) or PBS (*in vivo*) directly before *in vitro* analysis or immunization of the mice.

4.2.16 Sandwich enzyme linked immunosorbent assay

To analyze the integrity of HBV antigens, sandwich ELISA was performed using NUNC MaxiSorp™ 96-well plates. For HBsAg analysis the plate was coated with 100 µL/well scFv C8 antibody (1 µg/mL diluted in 1x PBS) overnight at 4 °C. After four washing steps (PBS-T), the blocking with 250 µL/well BSA (5 %) for 1 h at RT was performed. After the washing of the plate, 100 µL/well of sample (30 ng/mL, diluted in 1 % BSA) was added and incubated for 2 h at RT. To further determine the antigen concentration, 1:1 serial dilutions of optimal stored antigens (SM_{Ctrl}) from 80 ng/mL to 0 ng/mL were additionally analyzed. Following four washing steps, the plate was incubated with 5 µg/well of the primary antibody 5F9 (diluted in 1 % BSA) for 1 h at RT. After washing, the bound antibodies were detected with a secondary HRP labeled goat pAb to Hu IgG antibody (100 µL/well; diluted 1:1000 in 1 % BSA). After incubation for 30 min at RT and final washing, 100 µL/well of TMP was added. To stop the reaction 100 µL/well of 1 M sulphuric acid was used. The absorbance was measured by Infinite F200 plate reader at OD₄₅₀ and the antigen concentration was calculated by linear regression.

HBcAg was analyzed according to a similar protocol using 1 µg/mL anti IFA HepBCore for coating and anti HepBcore-HRP antibody (diluted 1:7000 in 1 % BSA) for detection. HBcAg samples were used in a concentration of 15 ng/mL.

4.2.17 Native agarose gel electrophoresis

To analyze native HBcAg capsids, native agarose gel electrophoresis (NAGE) was performed. HBcAg samples were diluted in H₂O to a concentration of 2.5 µg/lane. The samples were mixed with an appropriate volume of 4x DNA loading Dye and loaded on a 1 % agarose gel containing Roti®-Safe. To estimate the size, 10 kDa DNA ladder was additionally loaded on the

gel. The samples were separated for 90 min at 150 V. The nucleic acid content was analyzed by UV-light using Fusion FX7 imaging system. Afterwards, the gel was stained with Coomassie Staining Solution for 20 min at RT. To visualize the protein content, the gel was destained at RT using destain solution. The NAGE was routinely performed twice to verify the results.

4.2.18 Transmission electron microscopy

The morphology of HBV antigens and MVA-S/C was analyzed by transmission electron microscopy (TEM). The purified MVA-S/C was inactivated with 2 % paraformaldehyde (PFA). The absorption of the vaccine components onto a copper grid with a formvar/carbon film (400 mesh) was performed at RT for 5 min (antigens) or 15 min (MVA). The grid was negatively stained with 1 % phosphotungstic acid (PTA). Images were examined using a Libra 120 transmission electron microscope with a magnification of 40000x.

4.2.19 Dynamic light scattering

To examine purity and particle size of antigen formulations dynamic light scattering (DLS) was performed using a Malvern Zetasizer Nano ZS. The samples were analyzed at a concentration of 5 µg diluted in 10 mL NaCl. Per measurement 50 individual scans, each 10 seconds long, were performed. To verify the results, the hydrodynamic radius was additionally measured using DynaPro Nanostar DLS instrument by Dr. Kristina Kemter at LEUKOCARE.

4.2.20 Size exclusion-high performance liquid chromatography

The structural integrity of HBV antigens was additionally analyzed by size-exclusion high-performance liquid chromatography (SE-HPLC). SE-HPLC was performed using a size-exclusion column TSK-gel® G5000 SW_{XL} 300 mm x 7.8 I.D. column (100 nm pore size) at 25 °C with a flow rate of 0.6 mL/min and an injection volume of 100 µL for each undiluted sample. The mobile phase was a 50 mM phosphate buffer pH 7.0. The chromatograms were analyzed using Chromeleon 7 Chromatography Data software. The analyses were kindly performed by Dr. Kristina Kemter at LEUKOCARE.

4.2.21 Sodium dodecyl sulphate polyacrylamide gel electrophoresis and Western blot analysis

To analyze the antigens by sodium dodecyl sulphate polyacrylamide gel electrophoresis (SDS-PAGE) and subsequent Western blotting (WB), 70 ng HBcAg and 10 ng HBsAg was diluted with H₂O and mixed with loading dye 4x SEB (diluted sample and loading dye ratio 1:3). The samples were heated for 10 min at 95 °C, 300 rpm. After cooling and short centrifugation, 10 µL sample were loaded into each pocket of the SDS-PAGE gel, which was prepared

according to Table 29. To verify the size of the separated samples, pre-stained protein ladder (Serva Triple color III) was used.

Reagent	Separation gel (12.5 %) Volume [μ L]	Collection gel (5 %) Volume [μ L]
Acrylamide (40 %)	2500	240
Tris (1 M, pH 8.8)	3000	500
SDS (10 %)	80	20
H ₂ O	2500	1250
TEMED	7	2
APS (10 %)	40	15

Table 29. Volume of reagents for separating and collection gel.

Protein separation was performed in 1x SDS-PAGE running buffer for approximately 1.5 h at 15 mA per gel. Proteins were blotted onto a methanol-activated 0.2 μ M PVDF membrane using wet blot technique with 1x WB transfer buffer for 2 h at 300 mA. The following blocking was performed in 5 % milk for 1 h at RT. The membrane was incubated overnight at 4 °C with appropriate primary antibodies. For HBcAg the 8C9 antibody diluted 1:1 in 3 % milk and for HBsAg the polyclonal mouse antibody HB1 diluted 1:1000 in 1 % milk was used. After the washing steps with 1x TBS-T, membranes were incubated in the secondary antibody goat anti-mouse (HRP labeled; diluted 1:10000 in 1 % milk) for at least 2 h at 4 °C. Following three washing steps, the detection was performed using Amersham ECL Prime Western Blotting Detection Reagent in a Fusion FX7 imaging system. The WB analysis presented in this thesis were routinely performed twice to verify the results.

4.2.22 Determination of biological activity of c-di-AMP

The analyses were kindly performed by the group of Prof. Carlos Guzmán at HZI Braunschweig. Briefly, the biological activity of c-di-AMP was determined via the reporter gene cell lines THP-1 BlueTM ISG and THP-1 STING-knockout (KO) following the manufacturer's instructions (InvivoGen). c-di-AMP and LPS were used in a concentration of 10 μ g/mL. Measurements at OD₆₂₀ were performed after 1 or 3 h of stimulation with the appropriate reagents as it is described in the manufacturer's protocol. Presented data show representative results after 3 h.

4.2.23 Mouse experiments

Mouse experiments were performed in cooperation with Dr. Anna Kosinska.

4.2.23.1 Ethical statement

Mouse experiments were strictly performed according to the German regulations of the Society for Laboratory Animal Science (GV-SOLAS), the European Health Law of the Federation of Laboratory Animal Science Associations (FELASA) and the 3Rs. The local Animal Care and Use Committee of Upper Bavaria (permission number: ROB-55.2-2532. Vet_02-18-24) approved the experiments and the study protocols according to the institution's guidelines. Animals were kept in a specific pathogen free animal facility at TUM and all experiments were performed during the light phase of the day.

4.2.23.2 Mice and AAV-HBV transduction

To establish persistent HBV replication, C57BL/6 male mice were intravenously (i.v.) infected with 4×10^9 genome equivalents of the AAV-HBV1.2 vector encoding 1.2-fold overlength HBV genome of genotype D through the tail vein of the mice, as previously described [97]. The vaccination was initiated four weeks after AAV-HBV transduction. One day prior to the onset of the vaccination, animals were bled and allocated into groups with comparable HBsAg and HBeAg levels.

4.2.23.3 Heterologous protein prime/MVA boost vaccination strategy

Mice were immunized intramuscularly (i.m.) using the heterologous protein prime/MVA boost vaccination strategy as previously reported [94]. The vaccine was injected in the quadriceps muscles of both hind limbs, each with the same volume. Mice were immunized twice with 10 µg HBcAg and 10 µg HBsAg adjuvanted with 10 µg c-di-AMP at two weeks intervals. Two weeks after the second prime immunization, mice received a boost with 5×10^7 TCID₅₀ of recombinant MVA-S/C. The experiments were terminated one week (HBV-naïve mice) or four weeks (AAV-HBV infected mice) after booster immunization.

4.2.23.4 Blood withdrawal

Mice were bled from the submandibular vein (cheek pouch). Blood was collected in 1.1 mL Z-Gel Micro tubes. To obtain sera, the blood samples were centrifuged at 10 000 x g for 5 min at RT. The sera were transferred into new reaction tubes and the samples were stored at -20 °C for further analyses.

4.2.23.5 Dissection and organ removal

Mice were sacrificed on the day of analysis by cervical dislocation. Afterwards, the abdominal cavity was open via one midline incision. Liver perfusion was performed with 1x PBS through

the portal vein to remove non-liver associated lymphocytes. The liver and spleen were resected and both organs were stored in 10 % RPMI medium on ice until further processing.

4.2.23.6 Isolation of splenocytes

To isolate the splenocytes, spleens were forced through 100 μ m cell strainers and washed with RPMI medium. After centrifugation at 450 x g for 5 min at 4 °C and discarding the supernatant, erythrocytes were lysed in 2 mL of ammonium-chloride-potassium (ACK) lysis buffer for 1.5 min at RT. The reaction was stopped by the addition of RPMI medium followed by centrifugation at 450 x g for 5 min at 4 °C. The cell pellet was resuspended in 5 mL 10 % RPMI medium and sieved through a 100 μ m cell strainer to obtain single-cell suspension. Until seeding, the cells were kept on ice. Cell viability and cell numbers were determined using Vi-CELL® XR cell viability analyzer and Vi-CELL Reagent Pak following the manufacturer's instructions.

4.2.23.7 Isolation of liver associated lymphocytes

Liver associated lymphocytes (LALs) were isolated as previously described with some modifications [95, 244]. For this purpose, the PBS-perfused mouse liver was forced through a 100 μ m cell strainer. After washing with RPMI medium, cell pellets were resuspended in 8 mL collagenase type IV solution (0.02 gram/mouse diluted in 10 % RPMI medium) and digested for 25 min at 37 °C. The reaction was stopped by the addition of RPMI medium and centrifugation at 450 x g for 5 min at 4 °C. LALs were isolated by density gradient centrifugation. The cells were resuspended in 3 mL 40 % of Percoll solution containing 100 IU/ml heparin, layered on 3 mL of 80 % Percoll solution and centrifuged at 1200 x g for 20 min at RT without breaks. The lymphocytes containing fraction was collected followed by a washing step with RPMI medium. The cell pellets were resuspended in the minimal volume of 10 % RPMI medium needed for further analyses. Cells were kept on ice until seeding.

4.2.23.8 Intracellular cytokine staining

For intracellular cytokine staining (ICS) murine splenocytes and LALs were stimulated *ex vivo*. Up to 2×10^6 /well splenocytes or LALs were seeded on a U-bottom 96-well plate in a total volume of 200 μ L/well. Cells were stimulated with 50 μ L/well peptides B8R, S₂₈₀, C₉₃ or peptide pools covering HBV S (genotype D, aa 145-226) or core (genotype D, aa 70-157) containing the dominant CD8 as well as CD4 T-cell epitopes (1 μ g/mL). The amino acid sequences of the peptides were listed in Table 15-16. As a negative control ovalbumin-derived peptide (OVA_{S8L}) was used. After 1 h stimulation at 37 °C, 20 μ L/well brefeldin A (1 μ g/mL) was added and cells were stimulated for additional 14 h at 37 °C until subsequent ICS was performed.

Stimulated lymphocytes were transferred to a V-bottom 96-well plate and centrifuged at 450 x g for 2.5 min at 4 °C. All the incubation steps were performed on ice in the dark. Cell

surface was stained with anti-CD4 APC and anti-CD8a Pacific blue antibodies (both diluted 1:100 in FACS buffer) with a volume of 50 μ L/well for 20 min. Death cells were excluded from analysis by staining with Fixable Viability Dye eFluor™ 780 (diluted 1:3000 in FACS buffer). After one washing step with 200 μ L/well FACS buffer, the cells were fixed and permeabilised using Cytofix/Cytoperm Kit according to manufacturer's protocol. For ICS, cells were stained with 50 μ L/well anti-IFN- γ (diluted 1:300 in 1x Perm/Wash buffer) and incubated for 25 min. Afterwards, cells were washed once with 1x Perm/Wash buffer and once with FACS buffer and resuspended in 200 μ L/well FACS buffer until analyses. Samples were measured on a CytoFLEX S flow cytometer. Analysis was performed using FlowJo software. Presented data are shown as relative values after subtraction of background using OVA_{S8L} peptide.

In HBV-specific CD4⁺ T cells graphs, the results of cells stimulated with peptide pools were shown. In HBV-specific CD8⁺ T cells graphs, the data of cells stimulated with single peptides or peptide pools are presented. Five mice per group were analyzed. In the presented graphs of HBV-specific antibodies and CD4⁺ and CD8⁺ T cells values of individual mice are shown, horizontal lines indicate median.

4.2.23.9 Serological analysis

ALT activity was determined in the fresh serum samples diluted 1:4 in 1x PBS using Reflotron® GPT/ALT tests according to manufacturer's instructions. Serum HBeAg, HBsAg and anti-HBs levels were analyzed by Architect™ platform. Anti-HBc levels were quantified using the Enzygnost® Anti-HBc monoclonal test on the BEP III platform. Sera were diluted 1:20 with 1x PBS for HBeAg and HBsAg and 1:50 to 1:100 for anti-HBs and anti-HBc antibodies. Time kinetics of HBeAg, HBsAg and ALT levels display the mean value of each experimental group.

4.2.24 Statistical analysis

Data were analysed using GraphPad Prism version 5.01. Data are presented as mean values with standard deviation (SD; *in vitro* data) or standard error of mean (SEM; *in vivo* data). Statistical differences were calculated according to Mann-Whitney test and Students unpaired t-test. *P*-values <0.05 were considered as significant.

5 Figures and Tables

5.1 Figures

Figure 1. Global distribution of different HBV genotypes.....	8
Figure 2. Virion and subviral particle structures of HBV.....	10
Figure 3. Genome organization of HBV.....	11
Figure 4. Schematic illustration of HBV life cycle.....	12
Figure 5. Distribution of global chronic HBV infections worldwide.....	13
Figure 6. Heterologous protein prime/MVA boost vaccination strategy.....	17
Figure 7. Schematic structure of MVA particle.....	19
Figure 8. Appearance comparison of lyophilized (freeze-dried), spray-dried and foam-dried live attenuated influenza samples.....	22
Figure 9. Assumed mode of action of SAAF.....	25
Figure 10. MVA-S/C construct and possible protein products.....	28
Figure 11. Generation of MVA-S/C.....	29
Figure 12. Verification of the S/C insert.....	31
Figure 13. Characterization of MVA-S/C.....	32
Figure 14. Comparison of HBcAg from different providers.....	35
Figure 15. Comparison of HBsAg from different providers.....	36
Figure 16. HBcAg and HBsAg demonstrated highest stability after storage at 4 °C.....	37
Figure 17. Heat-exposure led to antigen instability.....	39
Figure 18. Heat-exposure resulted in reduction of MVA-S/C infectivity.....	40
Figure 19. Lyophilization did not cause MVA-S/C infectivity reduction.....	41
Figure 20. Negative impact of lyophilization on antigen integrity.....	43
Figure 21. Antigen integrity of reconstituted samples decreased after 1 day of storage.....	44
Figure 22. No influence on MVA-S/C infectivity after storage of reconstituted samples for 3 months.....	45
Figure 23. SAAF I A and B stabilized HBcAg during lyophilization and storage at 45 °C for 28 days.....	47
Figure 24. Selected SAAFs efficiently stabilized HBsAg.....	50
Figure 25. All selected SAAFs stabilized antigen combinations during lyophilization.....	52
Figure 26. SAAFs 1-4 stabilized vaccine components during storage at 40 °C for 1 month.....	54
Figure 27. Stabilization with SAAFs induced HBV-specific immune response in HBV-naïve mice despite heat-exposure.....	56
Figure 28. SAAF-stabilized antigens remained stable after 40 °C-exposure for 3 days.....	58
Figure 29. SAAF-stabilized MVA-S/C remained stable after 40 °C-exposure for 3 days.....	59
Figure 30. SAAF-stabilization led to intact antigens and high infectious MVA-S/C titer despite storage at 40 °C for 14 days.....	60
Figure 31. Formulation with SAAF led to stable antigens despite 1 month of heat-exposure.	61
Figure 32. Stabilization with SAAF maintained antigen integrity despite 3 months of storage at 25 °C or 40 °C.....	62

Figure 33. Formulation with SAAF improved MVA-S/C infectivity after 1 and 3 months of storage at 25 °C or 40 °C.....63

Figure 34. Heat-exposure did not cause structural differences of vaccine components.....64

Figure 35. SAAF-stabilization of antigens retained their integrities after storage at RT up to 12 months.....66

Figure 36. Formulation with SAAF led to stable antigens after 25 °C-exposure for up to 12 months.....67

Figure 37. Formulation with SAAF improved MVA-S/C infectivity after a storage at RT for up to 12 months.....67

Figure 38. Formulation with SAAF led to stable antigens either in antigen combination or as single components after 40 °C-exposure for 3 days and 3 months.69

Figure 39. SAAF-stabilization remained antigen integrity after a storage at RT for 6 and 12 months.70

Figure 40. SAAF-stabilization maintained vaccine potency despite heat-exposure for 1 and 3 months.....72

Figure 41. SAAF-stabilized vaccine induced strong HBV-specific immune response in HBV-naïve mice despite storage at 25 °C or 40 °C.....74

Figure 42. SAAF-stabilization maintained vaccine potency despite 40 °C-exposure for 1 month.....75

Figure 43. SAAF-stabilized TherVacB vaccine induced high HBV-specific antibody titers and reduced serum HBsAg levels despite 1 month of storage at 40 °C.....76

Figure 44. Formulation with SAAF led to the induction of a strong HBV-specific immune response in AAV-HBV infected mice despite 40 °C-exposure for 1 month.....78

Figure 45. SAAF-stabilized TherVacB components remained stable despite storage at RT for 12 months.....80

Figure 46. Immunization with SAAF-stabilized TherVacB vaccine led to the induction of high HBV-specific antibodies and suppression of HBsAg levels.81

Figure 47. SAAF-stabilized and 1-year at RT-exposed vaccine induced HBV-specific T-cell responses and reduced HBeAg levels in AAV-HBV infected mice.....83

Figure 48. High thermal stability of c-di-AMP despite temperature stressing.85

5.2 Tables

Table 1. Various GRAS excipients used for stabilization in licensed viral vaccines.....23

Table 2. PCR product sizes of MVA Del I-IV region and MVA-S/C insert... ..30

Table 3. Different analytical methods for characterization of HBcAg and HBsAg... ..34

Table 4. Characteristics of investigated HBcAg from various providers.34

Table 5. Characteristics of investigated HBsAg from various manufacturers.35

Table 6. Excipients of the SAAFs F1.1-F1.4.....53

Table 7. Antigens.100

Table 8. Viral vectors.....100

Table 9. Cell lines and bacterial strains.101

Table 10. Primers... ..101

Table 11. Antibodies for plaque assay	101
Table 12. Antibodies for Western blot.....	102
Table 13. Antibodies for ELISA.....	102
Table 14. Antibodies for flow cytometry.....	102
Table 15. Cytotoxic T lymphocytes epitopes.....	103
Table 16. HBcAg-derived peptide pool, genotype D.....	103
Table 17. HBsAg-derived peptide pool, genotype D.....	104
Table 18. Enzymes.....	104
Table 19. Plasmids and Markers.....	104
Table 20. Kits.....	104
Table 21. Cell culture media.....	105
Table 22. Buffers and solutions.....	107
Table 23. Chemicals and reagents.....	109
Table 24. Consumables.....	110
Table 25. Laboratory equipment.....	111
Table 26. Software.....	112
Table 27. PCR program for MVA-S/C and MVA-WT using Del I-VI primers.....	116
Table 28. Different steps of the lyophilization process.....	119
Table 29. Volume of reagents for separating and collection gel.....	121

6 References

- [1] Blumberg BS, Melartin L, et al. Family studies of a human serum isoantigen system (Australia antigen). *Am J Hum Genet* 1966;18:594-608.
- [2] Dane DS, Cameron CH, et al. VIRUS-LIKE PARTICLES IN SERUM OF PATIENTS WITH AUSTRALIA-ANTIGEN-ASSOCIATED HEPATITIS. *The Lancet* 1970;295:695-698.
- [3] WHO. Hepatitis B, Fact sheet, Updated July 2019, Available: <https://www.who.int/en/news-room/fact-sheets/detail/hepatitis-b> [Accessed 02.07.2020].
- [4] Modrow S, Falke D, et al. *Molekulare Virologie: Spektrum Akademischer Verlag*; 2010.
- [5] Hu J, Liu K. Complete and Incomplete Hepatitis B Virus Particles: Formation, Function, and Application. *Viruses* 2017;9:56.
- [6] Kramvis A, Arakawa K, et al. Relationship of serological subtype, basic core promoter and precore mutations to genotypes/subgenotypes of hepatitis B virus. *Journal of Medical Virology* 2008;80:27-46.
- [7] Velkov S, Ott J, et al. The Global Hepatitis B Virus Genotype Distribution Approximated from Available Genotyping Data. *Genes* 2018;9:495.
- [8] Tatematsu K, Tanaka Y, et al. A Genetic Variant of Hepatitis B Virus Divergent from Known Human and Ape Genotypes Isolated from a Japanese Patient and Provisionally Assigned to New Genotype J. *Journal of Virology* 2009;83:10538-10547.
- [9] Locarnini S, Littlejohn M, et al. Possible origins and evolution of the hepatitis B virus (HBV). *Semin Cancer Biol* 2013;23:561-575.
- [10] Dane DS, Cameron CH, et al. Virus-like particles in serum of patients with Australia-antigen-associated hepatitis. *Lancet* 1970;1:695-698.
- [11] Blumberg B. Australia antigen and the biology of hepatitis B. *Science* 1977;197:17-25.
- [12] Gerlich WH. Medical virology of hepatitis B: how it began and where we are now. *Virol J* 2013;10:239.
- [13] Mangold CM, Streeck RE. Mutational analysis of the cysteine residues in the hepatitis B virus small envelope protein. *J Virol* 1993;67:4588-4597.
- [14] Wang J, Shen T, et al. Serum hepatitis B virus RNA is encapsidated pregenome RNA that may be associated with persistence of viral infection and rebound. *Journal of Hepatology* 2016;65:700-710.
- [15] Van Bömmel F, Bartens A, et al. Serum hepatitis B virus RNA levels as an early predictor of hepatitis B envelope antigen seroconversion during treatment with polymerase inhibitors. 2015;61:66-76.
- [16] Rokuhara A, Matsumoto A, et al. Hepatitis B virus RNA is measurable in serum and can be a new marker for monitoring lamivudine therapy. *Journal of Gastroenterology* 2006;41:785-790.
- [17] Ning X, Nguyen D, et al. Secretion of Genome-Free Hepatitis B Virus – Single Strand Blocking Model for Virion Morphogenesis of Para-retrovirus. *PLoS Pathogens* 2011;7:e1002255.

-
- [18] Luckenbaugh L, Kitrinou KM, et al. Genome-free hepatitis B virion levels in patient sera as a potential marker to monitor response to antiviral therapy. *Journal of Viral Hepatitis* 2015;22:561-570.
- [19] Wynne SA, Crowther RA, et al. The Crystal Structure of the Human Hepatitis B Virus Capsid. *Molecular Cell* 1999;3:771-780.
- [20] Crowther R. Three-dimensional structure of hepatitis B virus core particles determined by electron cryomicroscopy. 1994;77:943-950.
- [21] Seifer M, Standing DN. Assembly and antigenicity of hepatitis B virus core particles. *Intervirology* 1995;38:47-62.
- [22] Zlotnick A, Johnson JM, et al. A Theoretical Model Successfully Identifies Features of Hepatitis B Virus Capsid Assembly†. *Biochemistry* 1999;38:14644-14652.
- [23] Nassal M. HBV cccDNA: viral persistence reservoir and key obstacle for a cure of chronic hepatitis B. *Gut* 2015;64:1972-1984.
- [24] Seeger C, Mason WS. Molecular biology of hepatitis B virus infection. *Virology* 2015;479-480:672-686.
- [25] Chen MT, Billaud JN, et al. A function of the hepatitis B virus precore protein is to regulate the immune response to the core antigen. *Proceedings of the National Academy of Sciences* 2004;101:14913-14918.
- [26] Chen M, Sallberg M, et al. Immune Tolerance Split between Hepatitis B Virus Precore and Core Proteins. 2005;79:3016-3027.
- [27] Milich D. Exploring the biological basis of hepatitis B e antigen in hepatitis B virus infection. *Hepatology* 2003;38:1075-1086.
- [28] Ganem D, Prince AM. Hepatitis B virus infection--natural history and clinical consequences. *N Engl J Med* 2004;350:1118-1129.
- [29] Lucifora J, Arzberger S, et al. Hepatitis B virus X protein is essential to initiate and maintain virus replication after infection. *J Hepatol* 2011;55:996-1003.
- [30] Bouchard MJ, Schneider RJ. The Enigmatic X Gene of Hepatitis B Virus. 2004;78:12725-12734.
- [31] Rivière L, Gerossier L, et al. HBx relieves chromatin-mediated transcriptional repression of hepatitis B viral cccDNA involving SETDB1 histone methyltransferase. *Journal of Hepatology* 2015;63:1093-1102.
- [32] Schulze A, Gripon P, et al. Hepatitis B virus infection initiates with a large surface protein-dependent binding to heparan sulfate proteoglycans. *Hepatology* 2007;46:1759-1768.
- [33] Yan H, Zhong G, et al. Sodium taurocholate cotransporting polypeptide is a functional receptor for human hepatitis B and D virus. *eLife* 2012;1.
- [34] Huang HC, Chen CC, et al. Entry of Hepatitis B Virus into Immortalized Human Primary Hepatocytes by Clathrin-Dependent Endocytosis. *Journal of Virology* 2012;86:9443-9453.
- [35] Schmitz A, Schwarz A, et al. Nucleoporin 153 Arrests the Nuclear Import of Hepatitis B Virus Capsids in the Nuclear Basket. *PLoS Pathogens* 2010;6:e1000741.
- [36] Watanabe T, Sorensen EM, et al. Involvement of host cellular multivesicular body functions in hepatitis B virus budding. *Proceedings of the National Academy of Sciences* 2007;104:10205-10210.

- [37] Jiang B, Himmelsbach K, et al. Subviral Hepatitis B Virus Filaments, like Infectious Viral Particles, Are Released via Multivesicular Bodies. *J Virol* 2015;90:3330-3341.
- [38] Patient R, Hourieux C, et al. Hepatitis B Virus Subviral Envelope Particle Morphogenesis and Intracellular Trafficking. *Journal of Virology* 2007;81:3842-3851.
- [39] Ko C, Michler T, et al. Novel viral and host targets to cure hepatitis B. *Current Opinion in Virology* 2017;24:38-45.
- [40] Virushepatitis B und D im Jahr 2019. *Epidemiologisches Bulletin, Aktuelle Daten und Informationen zu Infektionskrankheiten und Public Health*, Robert Koch-Institut (Hrsg.), 23.07.2020.
- [41] Peeridogaheh H, Meshkat Z, et al. Current concepts on immunopathogenesis of hepatitis B virus infection. *Virus Research* 2018;245:29-43.
- [42] McMahon BJ, Alward WL, et al. Acute hepatitis B virus infection: relation of age to the clinical expression of disease and subsequent development of the carrier state. *J Infect Dis* 1985;151:599-603.
- [43] Guidotti LG, Chisari FV. IMMUNOBIOLOGY AND PATHOGENESIS OF VIRAL HEPATITIS. *Annual Review of Pathology: Mechanisms of Disease* 2006;1:23-61.
- [44] Hoofnagle JH. Serologic Markers of Hepatitis B Virus Infection. 1981;32:1-11.
- [45] Cohen BJ. The IgM antibody responses to the core antigen of hepatitis B virus. 1978;3:141-149.
- [46] Gerlich WH, Uy A, et al. Cutoff levels of immunoglobulin M antibody against viral core antigen for differentiation of acute, chronic, and past hepatitis B virus infections. *J Clin Microbiol* 1986;24:288-293.
- [47] Liaw Y-F, Pao CC, et al. Changes of serum hepatitis B virus DNA in two types of clinical events preceding spontaneous hepatitis B e antigen seroconversion in chronic type B hepatitis. 1987;7:1-3.
- [48] Cornberg M, Protzer U, et al. Aktualisierung der S 3-Leitlinie zur Prophylaxe, Diagnostik und Therapie der Hepatitis-B-Virusinfektion. *Zeitschrift für Gastroenterologie* 2011;49:871-930.
- [49] Rehmann B, Nascimbeni M. Immunology of hepatitis B virus and hepatitis C virus infection. *Nat Rev Immunol* 2005;5:215-229.
- [50] Murphy KM, Travers P, et al. *Janeway Immunologie*: Springer Berlin Heidelberg; 2014.
- [51] Maini MK, Boni C, et al. Direct ex vivo analysis of hepatitis B virus-specific CD8+ T cells associated with the control of infection. *Gastroenterology* 1999;117:1386-1396.
- [52] Chisari FV, Ferrari C. Hepatitis B virus immunopathogenesis. *Annu Rev Immunol* 1995;13:29-60.
- [53] Guidotti LG, Ishikawa T, et al. Intracellular Inactivation of the Hepatitis B Virus by Cytotoxic T Lymphocytes. 1996;4:25-36.
- [54] McClary H, Koch R, et al. Relative Sensitivity of Hepatitis B Virus and Other Hepatotropic Viruses to the Antiviral Effects of Cytokines. 2000;74:2255-2264.
- [55] Trapani JA, Smyth MJ. Functional significance of the perforin/granzyme cell death pathway. *Nat Rev Immunol* 2002;2:735-747.
- [56] Maini MK, Boni C, et al. The Role of Virus-Specific Cd8+ Cells in Liver Damage and Viral Control during Persistent Hepatitis B Virus Infection. *The Journal of Experimental Medicine* 2000;191:1269-1280.

- [57] Bertoletti A. Cytotoxic T lymphocyte response to a wild type hepatitis B virus epitope in patients chronically infected by variant viruses carrying substitutions within the epitope. 1994;180:933-943.
- [58] Webster GJM, Reignat S, et al. Longitudinal Analysis of CD8+ T Cells Specific for Structural and Nonstructural Hepatitis B Virus Proteins in Patients with Chronic Hepatitis B: Implications for Immunotherapy. *Journal of Virology* 2004;78:5707-5719.
- [59] Tan A, Koh S, et al. Immune Response in Hepatitis B Virus Infection. *Cold Spring Harbor Perspectives in Medicine* 2015;5:a021428.
- [60] Emini EA, Ellis RW, et al. Production and immunological analysis of recombinant hepatitis B vaccine. *J Infect* 1986;13 Suppl A:3-9.
- [61] Gerlich WH. Prophylactic vaccination against hepatitis B: achievements, challenges and perspectives. *Medical Microbiology and Immunology* 2015;204:39-55.
- [62] Hepatitis B vaccines: WHO position paper--recommendations. *Vaccine* 2010;28:589-590.
- [63] Rothstein SS, Goldman HS, et al. Passive immunization for hepatitis B. *Journal of Oral and Maxillofacial Surgery* 1982;40:34-37.
- [64] Janssen HL, Van Zonneveld M, et al. Pegylated interferon alfa-2b alone or in combination with lamivudine for HBeAg-positive chronic hepatitis B: a randomised trial. 2005;365:123-129.
- [65] Yoo J, Hann H-W, et al. Update Treatment for HBV Infection and Persistent Risk for Hepatocellular Carcinoma: Prospect for an HBV Cure. *Diseases* 2018;6:27.
- [66] Wang L, Zou ZQ, et al. Immunotherapeutic interventions in chronic hepatitis B virus infection: a review. *J Immunol Methods* 2014;407:1-8.
- [67] Van Bömmel F, Berg T. Antiviral Therapy of Chronic Hepatitis B. *Intervirol* 2014;57:171-180.
- [68] Gehring AJ, Protzer U. Targeting Innate and Adaptive Immune Responses to Cure Chronic HBV Infection. *Gastroenterology* 2019;156:325-337.
- [69] WHO. Global Hepatitis Report 2017. Geneva 2017. Licence: CC BY-NC-SA 3.0 IGO.
- [70] Revill P, Testoni B, et al. Global strategies are required to cure and eliminate HBV infection. *Nat Rev Gastroenterol Hepatol* 2016;13:239-248.
- [71] Kutscher S, Bauer T, et al. Design of therapeutic vaccines: hepatitis B as an example. *Microb Biotechnol* 2012;5:270-282.
- [72] Lobaina Y, Michel ML. Chronic hepatitis B: Immunological profile and current therapeutic vaccines in clinical trials. *Vaccine* 2017;35:2308-2314.
- [73] Kosinska AD, Bauer T, et al. Therapeutic vaccination for chronic hepatitis B. *Curr Opin Virol* 2017;23:75-81.
- [74] Pol S, Nalpas B, et al. Efficacy and limitations of a specific immunotherapy in chronic hepatitis B. *Journal of Hepatology* 2001;34:917-921.
- [75] Vandepapelière P, Lau GKK, et al. Therapeutic vaccination of chronic hepatitis B patients with virus suppression by antiviral therapy: A randomized, controlled study of co-administration of HBsAg/AS02 candidate vaccine and lamivudine. *Vaccine* 2007;25:8585-8597.
- [76] Xu D-Z, Zhao K, et al. A Randomized Controlled Phase IIb Trial of Antigen-Antibody Immunogenic Complex Therapeutic Vaccine in Chronic Hepatitis B Patients. *PLoS ONE* 2008;3:e2565.

- [77] Xu DZ, Wang XY, et al. Results of a phase III clinical trial with an HBsAg-HBIG immunogenic complex therapeutic vaccine for chronic hepatitis B patients: experiences and findings. *J Hepatol* 2013;59:450-456.
- [78] Gaggar A, Coeshott C, et al. Safety, tolerability and immunogenicity of GS-4774, a hepatitis B virus-specific therapeutic vaccine, in healthy subjects: A randomized study. *Vaccine* 2014;32:4925-4931.
- [79] Lok AS, Pan CQ, et al. Randomized phase II study of GS-4774 as a therapeutic vaccine in virally suppressed patients with chronic hepatitis B. *J Hepatol* 2016;65:509-516.
- [80] Boni C, Janssen HLA, et al. Combined GS-4774 and Tenofovir Therapy Can Improve HBV-Specific T-Cell Responses in Patients With Chronic Hepatitis. *Gastroenterology* 2019;157:227-241.e227.
- [81] Betancourt AA, Delgado CAG, et al. Phase I clinical trial in healthy adults of a nasal vaccine candidate containing recombinant hepatitis B surface and core antigens. *International Journal of Infectious Diseases* 2007;11:394-401.
- [82] Fernández G, A LS, et al. Five-year Follow-up of Chronic Hepatitis B Patients Immunized by Nasal Route with the Therapeutic Vaccine HeberNasvac. *Euroasian J Hepatogastroenterol* 2018;8:133-139.
- [83] Al-Mahtab M, Akbar SMF, et al. Therapeutic potential of a combined hepatitis B virus surface and core antigen vaccine in patients with chronic hepatitis B. *Hepatology International* 2013;7:981-989.
- [84] Al Mahtab M, Akbar SMF, et al. Treatment of chronic hepatitis B naïve patients with a therapeutic vaccine containing HBs and HBc antigens (a randomized, open and treatment controlled phase III clinical trial). *PLOS ONE* 2018;13:e0201236.
- [85] Bourguine M, Crabe S, et al. Nasal route favors the induction of CD4(+) T cell responses in the liver of HBV-carrier mice immunized with a recombinant hepatitis B surface- and core-based therapeutic vaccine. *Antiviral Res* 2018;153:23-32.
- [86] Mancini-Bourguine M, Fontaine H, et al. Induction or expansion of T-cell responses by a hepatitis B DNA vaccine administered to chronic HBV carriers. 2004;40:874-882.
- [87] Godon O, Fontaine H, et al. Immunological and Antiviral Responses After Therapeutic DNA Immunization in Chronic Hepatitis B Patients Efficiently Treated by Analogues. 2014;22:675-684.
- [88] Fontaine H, Kahi S, et al. Anti-HBV DNA vaccination does not prevent relapse after discontinuation of analogues in the treatment of chronic hepatitis B: a randomised trial—ANRS HB02 VAC-ADN. *Gut* 2015;64:139-147.
- [89] Pancholi P. DNA prime/canarypox boost—based immunotherapy of chronic hepatitis B virus infection in a chimpanzee. 2001;33:448-454.
- [90] Cavanaugh JS, Awi D, et al. Partially Randomized, Non-Blinded Trial of DNA and MVA Therapeutic Vaccines Based on Hepatitis B Virus Surface Protein for Chronic HBV Infection. 2011;6:e14626.
- [91] Roche (2013) Roche and Inovio Pharmaceuticals partner on Inovio's prostate cancer and hepatitis B immunotherapy products, Available: <https://www.roche.com/media/releases/med-cor-2013-09-10p.htm> [Accessed 03.09.2020]

- [92] Martin P, Dubois C, et al. TG1050, an immunotherapeutic to treat chronic hepatitis B, induces robust T cells and exerts an antiviral effect in HBV-persistent mice. *Gut* 2015;64:1961-1971.
- [93] Zoulim F, Fournier C, et al. Safety and immunogenicity of the therapeutic vaccine TG1050 in chronic hepatitis B patients: a phase 1b placebo-controlled trial. *Human Vaccines & Immunotherapeutics* 2020;16:388-399.
- [94] Backes S, Jäger C, et al. Protein-prime/modified vaccinia virus Ankara vector-boost vaccination overcomes tolerance in high-antigenemic HBV-transgenic mice. 2016;34:923-932.
- [95] Kosinska AD, Moeed A, et al. Synergy of therapeutic heterologous prime-boost hepatitis B vaccination with CpG-application to improve immune control of persistent HBV infection. *Sci Rep* 2019;9:10808.
- [96] Ebensen T, Libanova R, et al. Bis-(3',5')-cyclic dimeric adenosine monophosphate: strong Th1/Th2/Th17 promoting mucosal adjuvant. *Vaccine* 2011;29:5210-5220.
- [97] Dion S, Bourguine M, et al. Adeno-Associated Virus-Mediated Gene Transfer Leads to Persistent Hepatitis B Virus Replication in Mice Expressing HLA-A2 and HLA-DR1 Molecules. *Journal of Virology* 2013;87:5554-5563.
- [98] Lucifora J, Salvetti A, et al. Detection of the hepatitis B virus (HBV) covalently-closed-circular DNA (cccDNA) in mice transduced with a recombinant AAV-HBV vector. *Antiviral Res* 2017;145:14-19.
- [99] Chen H-B. A novel hepatitis B virus mutant with A-to-G at nt551 in the surface antigen gene. 2003;9:304.
- [100] Khan N, Guarnieri M, et al. Modulation of Hepatitis B Virus Secretion by Naturally Occurring Mutations in the S Gene. *Journal of Virology* 2004;78:3262-3270.
- [101] Ashton-Rickardt PG, Murray K. Mutants of the hepatitis B virus surface antigen that define some antigenically essential residues in the immunodominant a region. *J Med Virol* 1989;29:196-203.
- [102] Berkower I, Spadaccini A, et al. Hepatitis B Virus Surface Antigen Assembly Function Persists when Entire Transmembrane Domains 1 and 3 Are Replaced by a Heterologous Transmembrane Sequence. *Journal of Virology* 2011;85:2439-2448.
- [103] Pasek M, Goto T, et al. Hepatitis B virus genes and their expression in *E. coli*. *Nature* 1979;282:575-579.
- [104] Cohen BJ, Richmond JE. Electron microscopy of hepatitis B core antigen synthesized in *E. coli*. 1982;296:677-678.
- [105] Porterfield JZ, Dhason MS, et al. Full-Length Hepatitis B Virus Core Protein Packages Viral and Heterologous RNA with Similarly High Levels of Cooperativity. 2010;84:7174-7184.
- [106] Chain BM, Myers R. *BMC Microbiology* 2005;5:33.
- [107] Birnbaum F, Nassal M. Hepatitis B virus nucleocapsid assembly: primary structure requirements in the core protein. *J Virol* 1990;64:3319-3330.
- [108] Watts NR. The morphogenic linker peptide of HBV capsid protein forms a mobile array on the interior surface. 2002;21:876-884.
- [109] Seifer M, Standing DN. A protease-sensitive hinge linking the two domains of the hepatitis B virus core protein is exposed on the viral capsid surface. *J Virol* 1994;68:5548-5555.

- [110] Doane FW, Anderson N. *Electron Microscopy in Diagnostic Virology: A Practical Guide and Atlas*: Cambridge University Press; 1987.
- [111] Flint SJ. *Principles of Virology: Molecular Biology, Pathogenesis, and Control of Animal Viruses*: ASM Press; 2004.
- [112] McFadden G. Poxvirus tropism. *Nat Rev Microbiol* 2005;3:201-213.
- [113] Sakwa. Characterization of orthopox ankyrin repeat proteins in the modified vaccinia virus Ankara background. 2013. Available: <https://dx.doi.org/10.17169/refubium-15232>.
- [114] Mayr A, Hochstein-Mintzel V, et al. Abstammung, Eigenschaften und Verwendung des attenuierten Vaccinia-Stammes MVA. *Infection* 1975;3:6-14.
- [115] Meyer H, Sutter G, et al. Mapping of deletions in the genome of the highly attenuated vaccinia virus MVA and their influence on virulence. *Journal of General Virology* 1991;72:1031-1038.
- [116] Antoine G, Scheiflinger F, et al. The complete genomic sequence of the modified vaccinia Ankara strain: comparison with other orthopoxviruses. *Virology* 1998;244:365-396.
- [117] Wyatt LS, Carroll MW, et al. Marker rescue of the host range restriction defects of modified vaccinia virus Ankara. *Virology* 1998;251:334-342.
- [118] Wyatt LS, Earl PL, et al. Highly attenuated smallpox vaccine protects mice with and without immune deficiencies against pathogenic vaccinia virus challenge. *Proc Natl Acad Sci U S A* 2004;101:4590-4595.
- [119] Mayr A, Stickl H, et al. [The smallpox vaccination strain MVA: marker, genetic structure, experience gained with the parenteral vaccination and behavior in organisms with a debilitated defence mechanism (author's transl)]. *Zentralbl Bakteriol B* 1978;167:375-390.
- [120] Stittelaar KJ, Kuiken T, et al. Safety of modified vaccinia virus Ankara (MVA) in immune-suppressed macaques. *Vaccine* 2001;19:3700-3709.
- [121] Werner GT, Jentsch U, et al. Studies on poxvirus infections in irradiated animals. *Arch Virol* 1980;64:247-256.
- [122] Vollmar J, Arndtz N, et al. Safety and immunogenicity of IMVAMUNE, a promising candidate as a third generation smallpox vaccine. *Vaccine* 2006;24:2065-2070.
- [123] Bejon P, Kai OK, et al. Alternating vector immunizations encoding pre-erythrocytic malaria antigens enhance memory responses in a malaria endemic area. *Eur J Immunol* 2006;36:2264-2272.
- [124] Dorrell L, Yang H, et al. Expansion and diversification of virus-specific T cells following immunization of human immunodeficiency virus type 1 (HIV-1)-infected individuals with a recombinant modified vaccinia virus Ankara/HIV-1 Gag vaccine. *J Virol* 2006;80:4705-4716.
- [125] Goonetilleke N, Moore S, et al. Induction of multifunctional human immunodeficiency virus type 1 (HIV-1)-specific T cells capable of proliferation in healthy subjects by using a prime-boost regimen of DNA- and modified vaccinia virus Ankara-vectored vaccines expressing HIV-1 Gag coupled to CD8+ T-cell epitopes. *J Virol* 2006;80:4717-4728.
- [126] Scriba TJ, Tameris M, et al. Modified vaccinia Ankara-expressing Ag85A, a novel tuberculosis vaccine, is safe in adolescents and children, and induces polyfunctional CD4+ T cells. *Eur J Immunol* 2010;40:279-290.

- [127] Sutter G, Wyatt LS, et al. A recombinant vector derived from the host range-restricted and highly attenuated MVA strain of vaccinia virus stimulates protective immunity in mice to influenza virus. *Vaccine* 1994;12:1032-1040.
- [128] Corona Gutierrez CM, Tinoco A, et al. Clinical protocol. A phase II study: efficacy of the gene therapy of the MVA E2 recombinant virus in the treatment of precancerous lesions (NIC I and NIC II) associated with infection of oncogenic human papillomavirus. *Hum Gene Ther* 2002;13:1127-1140.
- [129] Meyer RG, Britten CM, et al. A phase I vaccination study with tyrosinase in patients with stage II melanoma using recombinant modified vaccinia virus Ankara (MVA-hTyr). *Cancer Immunol Immunother* 2005;54:453-467.
- [130] Dreicer R, Stadler WM, et al. MVA-MUC1-IL2 vaccine immunotherapy (TG4010) improves PSA doubling time in patients with prostate cancer with biochemical failure. *Invest New Drugs* 2009;27:379-386.
- [131] Ramlau R, Quoix E, et al. A phase II study of Tg4010 (Mva-Muc1-II2) in association with chemotherapy in patients with stage III/IV Non-small cell lung cancer. *J Thorac Oncol* 2008;3:735-744.
- [132] Levin A, Wang SA, et al. Costs of Introducing and Delivering HPV Vaccines in Low and Lower Middle Income Countries: Inputs for GAVI Policy on Introduction Grant Support to Countries. 2014;9:e101114.
- [133] Chen D, Kristensen D. Opportunities and challenges of developing thermostable vaccines. *Expert Review of Vaccines* 2009;8:547-557.
- [134] WHO. Meeting report. WHO/Paul-Ehrlich-Institut Informal Consultation on Scientific and Regulatory Considerations on the Stability Evaluation of Vaccines under Controlled Temperature Chain (CTC). Langen 2013.
- [135] Zaffran M, Vandelaer J, et al. The imperative for stronger vaccine supply and logistics systems. *Vaccine* 2013;31:B73-B80.
- [136] WHO. Temperature sensitivity of vaccines. Geneva 2006. Ordering code: WHO/IVB/06.10
- [137] WHO. Annex 5. Guidelines on the stability evaluation of vaccines for use under extended controlled temperature conditions. 2006. Technical report series No 999.
- [138] Lee BY, Wedlock PT, et al. Economic impact of thermostable vaccines. *Vaccine* 2017;35:3135-3142.
- [139] Kristensen DD, Lorenson T, et al. Can thermostable vaccines help address cold-chain challenges? Results from stakeholder interviews in six low- and middle-income countries. *Vaccine* 2016;34:899-904.
- [140] WHO. Use of MenAfriVac™ (meningitis A vaccine) in a controlled temperature chain (CTC) during campaigns. Guidance for immunization programme decision-makers and managers. Geneva 2013. Ordering code: WHO/IVB/13.04.
- [141] Lydon P, Zipursky S, et al. Economic benefits of keeping vaccines at ambient temperature during mass vaccination: the case of meningitis A vaccine in Chad. *Bulletin of the World Health Organization* 2014;92:86-92.
- [142] Zipursky S, Djingarey MH, et al. Benefits of using vaccines out of the cold chain: Delivering Meningitis A vaccine in a controlled temperature chain during the mass immunization campaign in Benin. *Vaccine* 2014;32:1431-1435.

-
- [143] Trotter CL, Lingani C, et al. Impact of MenAfriVac in nine countries of the African meningitis belt, 2010–15: an analysis of surveillance data. *The Lancet Infectious Diseases* 2017;17:867-872.
- [144] Rossi R, Konar M, et al. Meningococcal Factor H Binding Protein Vaccine Antigens with Increased Thermal Stability and Decreased Binding of Human Factor H. 2016;84:1735-1742.
- [145] Konar M, Pajon R, et al. A meningococcal vaccine antigen engineered to increase thermal stability and stabilize protective epitopes. 2015;112:14823-14828.
- [146] Campeotto I, Goldenzweig A, et al. One-step design of a stable variant of the malaria invasion protein RH5 for use as a vaccine immunogen. *Proceedings of the National Academy of Sciences* 2017;114:998-1002.
- [147] Manning MC, Chou DK, et al. Stability of Protein Pharmaceuticals: An Update. *Pharmaceutical Research* 2010;27:544-575.
- [148] Carpenter JF, Pikal MJ, et al. Rational design of stable lyophilized protein formulations: some practical advice. *Pharm Res* 1997;14:969-975.
- [149] Carpenter JF, Chang BS, et al. Rational design of stable lyophilized protein formulations: theory and practice. *Pharm Biotechnol* 2002;13:109-133.
- [150] Manning MC, Patel K, et al. Stability of protein pharmaceuticals. *Pharm Res* 1989;6:903-918.
- [151] Arakawa T, Prestrelski SJ, et al. Factors affecting short-term and long-term stabilities of proteins. *Adv Drug Deliv Rev* 2001;46:307-326.
- [152] Patel SM, Nail SL, et al. Lyophilized Drug Product Cake Appearance: What Is Acceptable? *J Pharm Sci* 2017;106:1706-1721.
- [153] Carpenter JF, Hand SC, et al. Cryoprotection of phosphofructokinase with organic solutes: characterization of enhanced protection in the presence of divalent cations. *Arch Biochem Biophys* 1986;250:505-512.
- [154] Crowe JH, Hoekstra FA, et al. Anhydrobiosis. *Annual Review of Physiology* 1992;54:579-599.
- [155] Wang W. Lyophilization and development of solid protein pharmaceuticals. *International Journal of Pharmaceutics* 2000;203:1-60.
- [156] Lovalenti PM, Anderl J, et al. Stabilization of Live Attenuated Influenza Vaccines by Freeze Drying, Spray Drying, and Foam Drying. *Pharmaceutical Research* 2016;33:1144-1160.
- [157] Ohtake S, Martin RA, et al. Heat-stable measles vaccine produced by spray drying. *Vaccine* 2010;28:1275-1284.
- [158] Walters RH, Bhatnagar B, et al. Next Generation Drying Technologies for Pharmaceutical Applications. *Journal of Pharmaceutical Sciences* 2014;103:2673-2695.
- [159] Abdul-Fattah AM, Truong-Le V, et al. Drying-Induced Variations in Physico-Chemical Properties of Amorphous Pharmaceuticals and Their Impact on Stability (I): Stability of a Monoclonal Antibody**Official contribution of NIST; not subject to copyright in the U.S. Certain commercial equipment. *Journal of Pharmaceutical Sciences* 2007;96:1983-2008.

- [160] Abdul-Fattah AM, Truong-Le V, et al. Drying-induced variations in physico-chemical properties of amorphous pharmaceuticals and their impact on Stability II: stability of a vaccine. *Pharm Res* 2007;24:715-727.
- [161] Ohtake S, Martin RA, et al. Formulation and Stabilization of Francisella tularensis Live Vaccine Strain. *Journal of Pharmaceutical Sciences* 2011;100:3076-3087.
- [162] Ohtake S, Martin R, et al. Room temperature stabilization of oral, live attenuated Salmonella enterica serovar Typhi-vectored vaccines. *Vaccine* 2011;29:2761-2771.
- [163] Emily P. Wen RE, Narahari S. Pujar. *Vaccine Development and Manufacturing*.
- [164] F, Petrovajová D, et al. Viral vaccine stabilizers: status and trends. *Acta virologica* 2017;61:231-239.
- [165] Cicerone MT, Douglas JF. β -Relaxation governs protein stability in sugar-glass matrices. *Soft Matter* 2012;8:2983.
- [166] Kaushik JK, Bhat R. Why is trehalose an exceptional protein stabilizer? An analysis of the thermal stability of proteins in the presence of the compatible osmolyte trehalose. *J Biol Chem* 2003;278:26458-26465.
- [167] Leung V, Mapletoft J, et al. Thermal Stabilization of Viral Vaccines in Low-Cost Sugar Films. *Scientific Reports* 2019;9.
- [168] Naik SP, Zade JK, et al. Stability of heat stable, live attenuated Rotavirus vaccine (ROTASIIIL(R)). *Vaccine* 2017;35:2962-2969.
- [169] Chen D, Kapre S, et al. Thermostable formulations of a hepatitis B vaccine and a meningitis A polysaccharide conjugate vaccine produced by a spray drying method. 2010;28:5093-5099.
- [170] Pelliccia M, Andreozzi P, et al. Additives for vaccine storage to improve thermal stability of adenoviruses from hours to months. 2016;7:13520.
- [171] Hassett KJ, Vance DJ, et al. Glassy-State Stabilization of a Dominant Negative Inhibitor Anthrax Vaccine Containing Aluminum Hydroxide and Glycopyranoside Lipid A Adjuvants. *Journal of Pharmaceutical Sciences* 2015;104:627-639.
- [172] Hassett KJ, Cousins MC, et al. Stabilization of a recombinant ricin toxin A subunit vaccine through lyophilization. 2013;85:279-286.
- [173] Chisholm CF, Kang TJ, et al. Thermostable Ebola virus vaccine formulations lyophilized in the presence of aluminum hydroxide. *Eur J Pharm Biopharm* 2019;136:213-220.
- [174] Mistilis MJ, Joyce JC, et al. Long-term stability of influenza vaccine in a dissolving microneedle patch. *Drug Delivery and Translational Research* 2017;7:195-205.
- [175] Chu LY, Ye L, et al. Enhanced Stability of Inactivated Influenza Vaccine Encapsulated in Dissolving Microneedle Patches. *Pharmaceutical Research* 2016;33:868-878.
- [176] Choi H-J, Yoo D-G, et al. Stability of influenza vaccine coated onto microneedles. *Biomaterials* 2012;33:3756-3769.
- [177] Alcock R, Cottingham MG, et al. Long-term thermostabilization of live poxviral and adenoviral vaccine vectors at suprphysiological temperatures in carbohydrate glass. *Sci Transl Med* 2010;2:19ra12.
- [178] Scherliess R, Ajmera A, et al. Induction of protective immunity against H1N1 influenza A(H1N1)pdm09 with spray-dried and electron-beam sterilised vaccines in non-human primates. *Vaccine* 2014;32:2231-2240.

- [179] Kemter K, Altrichter J, et al. Amino Acid-Based Advanced Liquid Formulation Development for Highly Concentrated Therapeutic Antibodies Balances Physical and Chemical Stability and Low Viscosity. *Biotechnology Journal* 2018;13:1700523.
- [180] Reinauer EB, Grosso SS, et al. Algorithm-Based Liquid Formulation Development Including a DoE Concept Predicts Long-Term Viral Vector Stability. *J Pharm Sci* 2020;109:818-829.
- [181] LEUKOCARE. Mode of action SPS. Available: <https://www.leukocare.com/mode-of-action.html> [Accessed 06.07.2020].
- [182] Tscheliessnig R, Zörnig M, et al. Nano-coating protects biofunctional materials. *Materials Today* 2012;15:394-404.
- [183] Sacherl, Kosinska, et al. Highly efficient thermostable, therapeutic protein prime/ MVA boost vaccine against chronic hepatitis B. *Journal of Hepatology* (prepared manuscript)
- [184] Protzer, Bauer et al. Means and methods for treating HBV. WO2017121791, 2017.
- [185] Luke GA, De Felipe P, et al. Occurrence, function and evolutionary origins of '2A-like' sequences in virus genomes. *Journal of General Virology* 2008;89:1036-1042.
- [186] Donnelly MLL, Ryan MD, et al. Analysis of the aphthovirus 2A/2B polyprotein 'cleavage' mechanism indicates not a proteolytic reaction, but a novel translational effect: a putative ribosomal 'skip'. *Journal of General Virology* 2001;82:1013-1025.
- [187] Song F, Fux R, et al. Middle East Respiratory Syndrome Coronavirus Spike Protein Delivered by Modified Vaccinia Virus Ankara Efficiently Induces Virus-Neutralizing Antibodies. *Journal of Virology* 2013;87:11950-11954.
- [188] Verheust C, Goossens M, et al. Biosafety aspects of modified vaccinia virus Ankara (MVA)-based vectors used for gene therapy or vaccination. *Vaccine* 2012;30:2623-2632.
- [189] Carroll MW, Moss B. Host range and cytopathogenicity of the highly attenuated MVA strain of vaccinia virus: propagation and generation of recombinant viruses in a nonhuman mammalian cell line. *Virology* 1997;238:198-211.
- [190] Drexler I, Wahren B, et al. Highly attenuated modified vaccinia virus Ankara replicates in baby hamster kidney cells, a potential host for virus propagation, but not in various human transformed and primary cells. 1998;79:347-352.
- [191] ATCC. Available: https://www.lgcstandards-atcc.org/support/faqs/48802/Converting+TCID50+to+plaque+forming+units+PFU-124.aspx?geo_country=de# [Accessed 20.08.2020]
- [192] Kratz PA, Böttcher B, et al. Native display of complete foreign protein domains on the surface of hepatitis B virus capsids. *Proc Natl Acad Sci U S A* 1999;96:1915-1920.
- [193] Sacherl J. Influence of the treatment with stabilizing and protecting solutions on the morphology of vaccine antigens and Poxvirus particles. Unpublished master thesis, Technische Universität München, 2016.
- [194] ICH. ICH Harmonised Tripartite Guideline. Stability testing of new drug substances and products Q1A(R2). step 4 version. 2003.
- [195] ICH. Available: <https://www.ich.org/> [Accessed 03.09.2020].
- [196] WHO. WHO expert committee on specifications for pharmaceutical preparations. Geneva 2009. Technical report series 953.
- [197] Lucifora J, Protzer U. Attacking hepatitis B virus cccDNA – The holy grail to hepatitis B cure. *Journal of Hepatology* 2016;64:S41-S48.

- [198] Boni C, Barili V, et al. HBV Immune-Therapy: From Molecular Mechanisms to Clinical Applications. *Int J Mol Sci* 2019;20.
- [199] Aguilar J, Lobaina Y, et al. Development of a nasal vaccine for chronic hepatitis B infection that uses the ability of hepatitis B core antigen to stimulate a strong Th1 response against hepatitis B surface antigen. *2004*;82:539-546.
- [200] Riedl P, Stober D, et al. Priming Th1 immunity to viral core particles is facilitated by trace amounts of RNA bound to its arginine-rich domain. *J Immunol* 2002;168:4951-4959.
- [201] Milich DR, Chen M, et al. Role of B cells in antigen presentation of the hepatitis B core. *Proc Natl Acad Sci U S A* 1997;94:14648-14653.
- [202] Lazdina U, Cao T, et al. Molecular Basis for the Interaction of the Hepatitis B Virus Core Antigen with the Surface Immunoglobulin Receptor on Naive B Cells. *Journal of Virology* 2001;75:6367-6374.
- [203] WHO. Annex 2. WHO good manufacturing practices for biological products. 2016. Technical report series No 999.
- [204] Gomez PL, Robinson JM. Vaccine Manufacturing. *Plotkin's Vaccines* 2018:51-60.e51.
- [205] Kremer M, Volz A, et al. Easy and efficient protocols for working with recombinant vaccinia virus MVA. *Methods Mol Biol* 2012;890:59-92.
- [206] Capelle MAH, Babich L, et al. Stability and suitability for storage and distribution of Ad26.ZEBOV/MVA-BN®-Filo heterologous prime-boost Ebola vaccine. *Eur J Pharm Biopharm* 2018;129:215-221.
- [207] Jung M-C, Grüner N, et al. Immunological monitoring during therapeutic vaccination as a prerequisite for the design of new effective therapies: induction of a vaccine-specific CD4+ T-cell proliferative response in chronic hepatitis B carriers. *Vaccine* 2002;20:3598-3612.
- [208] Ren F, Hino K, et al. Cytokine-dependent anti-viral role of CD4-positive T cells in therapeutic vaccination against chronic hepatitis B viral infection. *Journal of Medical Virology* 2003;71:376-384.
- [209] Just M, Berger R. Immunogenicity of a heat-treated recombinant DNA hepatitis B vaccine. *Vaccine* 1988;6:399-400.
- [210] Van Damme P, Cramm M, et al. Heat stability of a recombinant DNA hepatitis B vaccine. *Vaccine* 1992;10:366-367.
- [211] Rheinbaben Fv, Gebel J, et al. Environmental resistance, disinfection, and sterilization of poxviruses. In: Mercer AA, Schmidt A, Weber O, editors. *Poxviruses*. Basel: Birkhäuser Basel; 2007. p. 397-405.
- [212] Schumacher J, Bacic T, et al. Enhanced stability of a chimeric hepatitis B core antigen virus-like-particle (HBcAg-VLP) by a C-terminal linker-hexahistidine-peptide. *Journal of Nanobiotechnology* 2018;16.
- [213] Newman M, Suk F-M, et al. Stability and Morphology Comparisons of Self-Assembled Virus-Like Particles from Wild-Type and Mutant Human Hepatitis B Virus Capsid Proteins. *Journal of Virology* 2003;77:12950-12960.
- [214] Davis PJ, Williams SC. Protein modification by thermal processing. *Allergy* 1998;53:102-105.
- [215] Janeway C, Travers P, et al. *Immunobiology 5 : the Immune System in Health and Disease*: Garland Pub.; 2001.

- [216] Bruss V. Hepatitis B virus morphogenesis. *World Journal of Gastroenterology* 2007;13:65.
- [217] Pastor F, Herrscher C, et al. Direct interaction between the hepatitis B virus core and envelope proteins analyzed in a cellular context. *Scientific Reports* 2019;9.
- [218] Poisson F, Severac A, et al. Both Pre-S1 and S Domains of Hepatitis B Virus Envelope Proteins Interact with the Core Particle. *Virology* 1997;228:115-120.
- [219] Tonnis WF, Amorij JP, et al. Improved storage stability and immunogenicity of hepatitis B vaccine after spray-freeze drying in presence of sugars. *Eur J Pharm Sci* 2014;55:36-45.
- [220] Schersch K, Betz O, et al. Systematic investigation of the effect of lyophilizate collapse on pharmaceutically relevant proteins I: stability after freeze-drying. *J Pharm Sci* 2010;99:2256-2278.
- [221] Schersch K, Betz O, et al. Systematic investigation of the effect of lyophilizate collapse on pharmaceutically relevant proteins, part 2: stability during storage at elevated temperatures. *J Pharm Sci* 2012;101:2288-2306.
- [222] Croyle MA, Cheng X, et al. Development of formulations that enhance physical stability of viral vectors for gene therapy. *Gene Ther* 2001;8:1281-1290.
- [223] Warner N, Locarnini S, et al. The role of hepatitis B surface antibodies in HBV infection, disease and clearance. *Future Virology* 2020;15:293-306.
- [224] GfV. 29th Annual Meeting of the Society of Virology. 2019. Abstract book.
- [225] Rosenberg AS. Effects of protein aggregates: An immunologic perspective. *The AAPS Journal* 2006;8:E501-E507.
- [226] Moussa EM, Panchal JP, et al. Immunogenicity of Therapeutic Protein Aggregates. *Journal of Pharmaceutical Sciences* 2016;105:417-430.
- [227] Thimme R, Wieland S, et al. CD8+ T Cells Mediate Viral Clearance and Disease Pathogenesis during Acute Hepatitis B Virus Infection. *Journal of Virology* 2003;77:68-76.
- [228] Wu C-Y, Kirman JR, et al. Distinct lineages of TH1 cells have differential capacities for memory cell generation in vivo. *Nature Immunology* 2002;3:852-858.
- [229] Cui W, Kaech SM. Generation of effector CD8+ T cells and their conversion to memory T cells. *Immunol Rev* 2010;236:151-166.
- [230] Penna A, Artini M, et al. Long-lasting memory T cell responses following self-limited acute hepatitis B. *Journal of Clinical Investigation* 1996;98:1185-1194.
- [231] Wherry EJ, Ahmed R. Memory CD8 T-Cell Differentiation during Viral Infection. *Journal of Virology* 2004;78:5535-5545.
- [232] Steger-Hartmann T, Raschke M. Translating in vitro to in vivo and animal to human. *Current Opinion in Toxicology* 2020;23-24:6-10.
- [233] Di Pasquale A, Preiss S, et al. Vaccine Adjuvants: from 1920 to 2015 and Beyond. *Vaccines (Basel)* 2015;3:320-343.
- [234] Michler T, Kosinska AD, et al. Knockdown of Virus Antigen Expression Increases Therapeutic Vaccine Efficacy in High-Titer Hepatitis B Virus Carrier Mice. *Gastroenterology* 2020.
- [235] Lee BY, Cakouros BE, et al. The impact of making vaccines thermostable in Niger's vaccine supply chain. *Vaccine* 2012;30:5637-5643.

-
- [236] FDA. Lyophilization of Parenteral (7/93). GUIDE TO INSPECTIONS OF LYOPHILIZATION OF PARENTERALS. Available: <https://www.fda.gov/inspections-compliance-enforcement-and-criminal-investigations/inspection-guides/lyophilization-parenteral-793> [Accessed 23.07.2020].
- [237] Volz A, Sutter G. Modified Vaccinia Virus Ankara. Elsevier; 2017. p. 187-243.
- [238] Stoker M, Macpherson I. Syrian Hamster Fibroblast Cell Line BHK21 and its Derivatives. 1964;203:1355-1357.
- [239] Henle G. STUDIES ON PERSISTENT INFECTIONS OF TISSUE CULTURES: I. GENERAL ASPECTS OF THE SYSTEM. 1958;108:537-560.
- [240] Himly M, Foster DN, et al. The DF-1 chicken fibroblast cell line: transformation induced by diverse oncogenes and cell death resulting from infection by avian leukosis viruses. *Virology* 1998;248:295-304.
- [241] Graham FL, Russell WC, et al. Characteristics of a Human Cell Line Transformed by DNA from Human Adenovirus Type 5. *Journal of General Virology* 1977;36:59-72.
- [242] Kärber G. Beitrag zur kollektiven Behandlung pharmakologischer Reihenversuche. *Naunyn-Schmiedebergs Archiv für experimentelle pathologie und pharmakologie* 1931;162:480-483.
- [243] Festag MM, Festag J, et al. Evaluation of a Fully Human, Hepatitis B Virus-Specific Chimeric Antigen Receptor in an Immunocompetent Mouse Model. *Mol Ther* 2019;27:947-959.
- [244] Stross L, Günther J, et al. Foxp3+ regulatory T cells protect the liver from immune damage and compromise virus control during acute experimental hepatitis B virus infection in mice. *Hepatology* 2012;56:873-883.

7 Publications and Meetings

a) Publications

Ko C, Bester R, Zhou X, Xu Z, Blossey C, **Sacherl J**, et al. A New Role for Capsid Assembly Modulators To Target Mature Hepatitis B Virus Capsids and Prevent Virus Infection. *Antimicrob Agents Chemother* 2019;64.

Festag MM, Festag J, Fräßle SP, Asen T, **Sacherl J**, et al. Evaluation of a Fully Human, Hepatitis B Virus-Specific Chimeric Antigen Receptor in an Immunocompetent Mouse Model. *Mol Ther* 2019;27:947-959.

Svilenov HL[#], **Sacherl J**[#], Reiter A[#], et al. Picomolar inhibition of SARS-CoV-2 variants of concern by an engineered ACE2-IgG4-Fc fusion protein. *Antiviral Research*, *submitted*. (<https://www.biorxiv.org/content/10.1101/2020.12.06.413443v1>)

Sacherl J[#], Kosinska AD[#], et al. Highly efficient thermostable, therapeutic protein prime/MVA boost vaccine against chronic hepatitis B. *Journal of Hepatology*, *prepared manuscript*.

Su J, Brunner L, **Sacherl J**, et al. Protein prime with novel adjuvant activates CD4 T cells to initiate therapeutic vaccine-mediated efficacy against chronic hepatitis B. *Journal of Hepatology*, *prepared manuscript*.

Kosinska AD[#], Kächele M[#], Mück-Häusl M, **Sacherl J**, et al. MVA-HBVac – a novel therapeutic vaccine vector for targeting chronic hepatitis B. *EMBO Molecular Medicine*, *prepared manuscript*.

Ko C, Cheng C, Ambike S, **Sacherl J** et al. SARS-CoV-2 exploits ACE2 and TMPRSS2 for infecting human hepatocytes and causes infected hepatocyte death. *Journal of Hepatology*, *prepared manuscript*.

Chou WM, Ko C, Chakraborty A, **Sacherl J**, et al. A novel genome-editing based reporter system for tracking HBV infection. *Antiviral Research*, *prepared manuscript*.

Singethan K, Gaber H, **Sacherl J**, et al. Acid lipase activity is essential in early HCV infection. *prepared manuscript*.

Singethan K[#], **Sacherl J**[#], et al. Stabilization with amino acid-based formulations results in heat-stable MVA-based vaccine to combat chronic hepatitis B. *manuscript in preparation*.

shared first-authorship

b) International conferences

Innovative vaccine approaches (Keystone symposia EK50)

June 28-30, 2021

ePoster presentation: Solving the cold chain problem – development of a highly efficient thermostable, therapeutic vaccine against hepatitis B

30th Annual Meeting of the Society of Virology

March 24-26, 2021

Oral presentation: Singular ACE2-IgG4-Fc fusion protein efficiently inhibits SARS-CoV-2 entry

Oral presentation: Highly efficient thermostable, therapeutic protein prime/MVA boost vaccine to combat hepatitis B

Antibodies and Vaccines as Drugs for COVID-19 (Keystone symposia EK31)

January 13-14, 2021

ePoster presentation: Highly efficient inhibition of SARS-CoV-2 entry by a biologically unique ACE2-IgG4-Fc fusion protein with a stabilized hinge region

The Digital International Liver Congress™

August 27-29, 2020

ePoster presentation: Solving the cold chain problem - development of a heat-stable therapeutic vaccine to combat chronic hepatitis b

Travel grant by DZIF, Registration bursary by EASL

2019 International HBV meeting

October 1-5, 2019, Melbourne, Australia

Oral presentation: Development of a heat-stable therapeutic protein-prime, MVA-boost vaccine against chronic hepatitis B

Travel grant by International HBV Meeting Organizing Committee

29th Annual Meeting of the Society of Virology

March 20-23, 2019, Düsseldorf, Germany

Poster presentation: Development of a heat-stable therapeutic MVA-based prime/boost vaccine to combat chronic hepatitis B

16th Medical Biodefence Conference

October 28-31, 2018, Munich, Germany

Poster presentation: Development of a heat-stable therapeutic MVA-based prime/boost vaccine against chronic hepatitis B

12th Vaccine Congress

September 16-19, 2018, Budapest, Hungary

Poster presentation: Development of a heat-stable therapeutic MVA-based prime/boost vaccine against chronic hepatitis B

8 Acknowledgments

First of all, I thank Prof. Ulrike Protzer for welcoming me in your research group and giving me the opportunity to work on my desired topic - it was a fascinating and challenging project. I am especially grateful for your valuable scientific advice, the fruitful discussions and that you always found time for urgent questions.

I am thankful to my second supervisor Prof. Jörg Durner for your time and your valuable input during my thesis committee meetings.

Many thanks also go to Dr. Katrin Singethan who first introduced me to the world of viruses and trained me in different virological techniques during her time at the Institute.

I am particularly grateful to Dr. Anna Kosinska who took over the role of my mentor. Thank you so much for always having time for me, even on stressful days, and for supporting me in various ways over the past years. Without you, the mouse experiments for the successful completion of the project would not have been possible. Finally, many thanks for taking the time to proofread my thesis and your valuable advice.

I am deeply thankful to all my cooperation partners:

The team of LEUKOCARE, especially Dr. Kristina Kemter. Many thanks for the great cooperation over the past years and the interesting discussions. I am very grateful for the data and the feedback I received from you for my thesis.

The ELMI team at the Institute for Microbiology at the Bundeswehr, especially Dr. Sandra Eßbauer and Claudia Kahlhofer who trained me and enabled me to use transmission electron microscopy. I always enjoyed the time I spend at your lab.

In addition, I am thankful to Dr. Behnam Naderi Kalali and Ahmed Sadek for your support with antibody production and Dr. Regina Feederle and Dr. Andris Dišlers for providing antibodies and HBcAg. Moreover, I thank the Center for Genetic Engineering and Biotechnology in Cuba, especially Dr. Julio Cesar Aguilar, for providing antibodies and antigens.

I thank the group of Prof. Carlos Guzmán at the HZI in Braunschweig, especially Dr. Thomas Ebensen and Elena Reinhard, who conducted the c-di-AMP stability studies for me.

Without great colleagues, the daily lab life would not be the same. Thanks a lot, to all current and former members of the 3rd floor lab for the great time! Many thanks also to Daniela for proofreading my thesis. A special thank goes to Romina - without you our daily lab life would not be so convenient and thank you especially for supporting me during my large MVA production. And last but not least, I am very thankful to Martin – in the last few years you have always provided me valuable advice and support. Furthermore, thanks a lot for your proofreading of my thesis.

Of course, many thanks also go to all other members of the Institute of Virology, including former ones, for the great working atmosphere. Over the past years, many of you (too many to name you all) have supported my work in various ways - I am happy to have you as my colleagues. In addition, I want to acknowledge the help of our mouse team who supported Anna and me when necessary. Especially, I thank Philipp who facilitated my lab work and supported me on stressful days. Thank you Marinka and Raza for making our lab life so comfortable. I am grateful to the team of the fourth floor for your support regarding experiment approvals and other office work.

Thank you, Sabine, for your valuable contribution to my project during your bachelor thesis and your HiWi time.

Additionally, I am thankful for the financial support of the "Stiftung der deutschen Wirtschaft" (sdw, German industrial foundation) and the opportunity to be part of such a great foundation.

Many thanks also to all my friends who are always at my side.

Zu guter Letzt, möchte ich mich bei meiner Familie bedanken, die mir stets den Rücken freihält und mich wann immer nötig motiviert. Vielen Dank, dass ihr mich immer in allen Lebenssituationen unterstützt und jederzeit für mich da seid!